

5-6-2017

Novel One-Pot Syntheses of Uracils and Arylidenehydantoins, and Analysis of Xylitol in Chewing Gum by Gc-Ms

RM Suranga Mahesh Rajapaksha

Follow this and additional works at: <https://scholarsjunction.msstate.edu/td>

Recommended Citation

Rajapaksha, RM Suranga Mahesh, "Novel One-Pot Syntheses of Uracils and Arylidenehydantoins, and Analysis of Xylitol in Chewing Gum by Gc-Ms" (2017). *Theses and Dissertations*. 3316.
<https://scholarsjunction.msstate.edu/td/3316>

This Dissertation - Open Access is brought to you for free and open access by the Theses and Dissertations at Scholars Junction. It has been accepted for inclusion in Theses and Dissertations by an authorized administrator of Scholars Junction. For more information, please contact scholcomm@msstate.libanswers.com.

Novel one-pot syntheses of uracils and arylidenehydantoins, and
analysis of xylitol in chewing gum by GC-MS

By

R.M. Suranga Mahesh Rajapaksha

A Dissertation
Submitted to the Faculty of
Mississippi State University
in Partial Fulfillment of the Requirements
for the Degree of Doctor of Philosophy
in Chemistry
in the Department of Chemistry

Mississippi State, Mississippi

May 2017

Copyright by

R.M. Suranga Mahesh Rajapaksha

2017

Novel one-pot syntheses of uracils and arylidenehydantoins, and
analysis of xylitol in chewing gum by GC-MS

By

R.M. Suranga Mahesh Rajapaksha

Approved:

Todd E. Mlsna
(Major Professor)

Charles U. Pittman, Jr
(Co-Major Professor)

Andrzej Sygula
(Committee Member)

David O. Wipf
(Committee Member)

Colleen N. Scott
(Committee Member)

Joseph P. Emerson
(Graduate Coordinator)

Rick Travis
Interim Dean
College of Arts & Sciences

Name: R.M. Suranga Mahesh Rajapaksha

Date of Degree: May 6, 2017

Institution: Mississippi State University

Major Field: Chemistry

Major Professor: Todd E. Mlsna

Title of Study: Novel one-pot syntheses of uracils and arylidenehydantoins, and analysis of xylitol in chewing gum by GC-MS

Pages in Study 167

Candidate for Degree of Doctor of Philosophy

The first section of this dissertation (Chapter I-III) describes the development of new methodologies to prepare uracil and arylidenehydantoin derivatives. A regioselective synthesis of 6-alkyl- and 6-aryloracils was developed by the dimerization of 3-alkyl- and 3-aryl-2-propynamides promoted by either Cs_2CO_3 or K_3PO_4 . A range of 3-aryl-2-propynamides, with both electron-deficient and electron-rich 3-aryl substituents, were successfully reacted in high yields. A synthetic route to prepare arylidenehydantoins was developed using the Pd-catalyzed dimerization of 3-aryl-2-propynamides. Both electron rich and electron deficient 3-aryl-2-propynamides were dimerized successfully to produce the desired arylidenehydantoins in moderate to excellent yields.

The second section of this dissertation (Chapter IV and V) describes the development of a reliable low-cost method to determine amounts of xylitol in sugar free gum samples to predict dangerous exposure levels for dogs. Xylitol is generally considered safe for human consumption and is frequently used in sugar free gum, however, it is extremely toxic to dogs. It is unknown if partially consumed chewing gum is also dangerous. A method to determine xylitol content of these sugar free gum samples

employing GC-MS with direct aqueous injection (DAI) is presented. This method was successfully applied to over 120 samples including, fresh gum, 5 min, 15 min, and 30 min chewed gum samples. Further extension of this work resulted in the development of an undergraduate laboratory experiment for upper-level undergraduate chemistry students which teaches calibration methods, xylitol extraction, sample preparation for GC-MS analysis, and data analysis.

DEDICATION

To my parents, Anula and Tikiribanda, my wife (Piumi), sister (Eranga), and Dr. Madurani for their continual love, support and encouragement.

ACKNOWLEDGEMENTS

I would like to express my sincerest gratitude to my advisors Dr. Todd E. Mlsna and Dr. Charles U. Pittman, Jr. for their continuous support, tremendous guidance, patience, and strong encouragement. Most of all, I truly appreciate the friendship that we have developed.

I would also like to thank Dr. Debra A. Mlsna for her immense help and guidance. I also would like thank Dr. Gerald Rowland, my former supervisor for his help and guidance.

I am heartily thankful to my committee members, Dr. Andrzej Sygula, Dr. David O. Wipf, and Dr. Colleen Scott for their great teaching, ideas, and directions throughout my graduate studies.

I sincerely thank all the faculty and staff of Department of Chemistry for helping me throughout my graduate career.

TABLE OF CONTENTS

DEDICATION	ii
ACKNOWLEDGEMENTS	iii
LIST OF TABLES	vii
LIST OF FIGURES	viii
LIST OF SCHEMES	x
CHAPTER	
I. A REGIOSELECTIVE SYNTHESIS OF 6-ALKYL- AND 6-ARYLURACILS BY CS ₂ CO ₃ - OR K ₃ PO ₄ -PROMOTED DIMERIZATION OF 3-ALKYL- AND 3-ARYL-2-PROPYNAMIDES.....	1
1.1 Abstract.....	1
1.2 Introduction	2
1.3 Results and discussion	4
1.3.1 Insights into the dimerization mechanism:.....	14
1.3.1.1 Evidence to support the proposed reaction mechanism (Scheme 1.4a).....	15
1.4 Conclusions	22
1.5 References	24
II. A SYNTHESIS OF ARYLIDENEHYDANTOINS BY PALLADIUM-CATALYZED DIMERIZATION OF 3-ARYL-2-PROPYNAMIDES.....	28
2.1 Abstract.....	28
2.2 Introduction	29
2.3 Results and discussion	30
2.4 Conclusion.....	42
2.5 References	43
III. ONE POT SYNTHESIS OF URACILS AND HYDANTOINS: EXPERIMENTAL	46
3.1 General Information	46

3.2	General Procedure for the Cs ₂ CO ₃ -promoted dimerizations of 1a-h, m to 6-substituted-uracils	47
3.3	General Procedure for the K ₃ PO ₄ -promoted dimerizations of 1a-m to 6-substituted-uracils.	53
3.4	General procedure for Pd(OAc) ₂ /tBuXPhos-catalyzed dimerization of <i>N</i> -methyl- and <i>N</i> -ethyl-3-aryl-2-propynamides promoted by either Cs ₂ CO ₃ or K ₃ PO ₄	54
3.5	General procedure for Pd(OAc) ₂ /tBuXPhos-catalyzed dimerization of <i>N</i> -methyl- and <i>N</i> -ethyl-3-aryl-2-propynamides promoted by K ₂ CO ₃	59
3.6	General procedure for the dimerization of 1a in ethanol.....	64
3.7	General procedure for the synthesis of intermediate 23	66
3.8	Determination of concentration of the K ₃ PO ₄ in toluene at 115 °C.....	67
3.9	References	68
IV.	EXTRACTION AND QUANTIFICATION OF XYLITOL IN SUGAR FREE GUM SAMPLES BY DIRECT AQUEOUS INJECTION GC-MS	69
4.1	Abstract.....	69
4.2	Introduction	70
4.3	Materials and Method.....	74
4.3.1	Reagents and Materials.....	74
4.3.2	GC-MS Analysis	74
4.3.3	Method overview	75
4.3.3.1	Extraction of xylitol from Fresh Gum samples	76
4.3.3.2	Extraction of xylitol from 5 min chewed gum samples	77
4.3.3.3	Extraction of xylitol from 15 min chewed gum samples	78
4.3.3.4	Extraction of xylitol from 30 min chewed gum samples	79
4.4	Results and Discussion	79
4.4.1	GC-MS method development.....	79
4.4.2	Selection of internal standard	82
4.4.3	Recovery.....	84
4.4.4	Detection limit	85
4.4.5	Statistical analysis	85
4.4.6	Determination effect of chewing rate on xylitol release from gum base.....	86
4.4.7	Sample analysis	87
4.5	Conclusions	91
4.6	References	93
V.	ANALYSIS OF XYLITOL IN SUGAR FREE GUM BY GC-MS WITH DIRECT AQUEOUS INJECTION: A LABORATORY EXPERIMENT FOR CHEMISTRY STUDENTS	95
5.1	Abstract.....	95

5.2	Introduction	96
5.3	Experimental overview.....	98
5.4	Safety hazards.....	99
5.5	Results and discussion.....	100
5.6	Evaluation of learning outcomes	104
5.7	Conclusions	105
5.8	References	106

APPENDIX

A.	¹ H NMR, ¹³ C NMR AND 2D-NOESY OF ALL NEW COMPOUNDS	108
B.	X-RAY CRYSTAL STRUCTURES.....	155

LIST OF TABLES

1.1	Optimization of reaction conditions for the dimerization of <i>N</i> -methyl-3-phenyl-2-propynamide to <i>N, N</i> -dimethyl-6-phenyluracil. ^a8
1.2	Cs ₂ CO ₃ -promoted dimerizations of 1a-m under optimized conditions ^a11
1.3	K ₃ PO ₄ -promoted dimerizations of 1a-m under optimized conditions ^a13
2.1	Screening palladium sources, ligands, and bases for the synthesis of hydantoin derivatives (<i>Z</i>)- 2a and (<i>E</i>)- 2a34
2.2	Pd(OAc) ₂ /L ₄ -catalyzed dimerization of <i>N</i> -methyl- and <i>N</i> -ethyl-3-aryl-2-propynamides promoted by either Cs ₂ CO ₃ or K ₃ PO ₄36
2.3	Pd(OAc) ₂ /L ₄ -catalyzed dimerization of <i>N</i> -methyl- and <i>N</i> -ethyl-3-aryl-2-propynamides promoted by K ₂ CO ₃37
2.4	Pd-catalyzed self-dimerization of primary 3-aryl-2-propynamides38
4.1	The amount of xylitol and number of fresh gum sticks that can cause hypoglycemia in dogs. ^{15,17,18}72
4.2	Precision and recovery of fresh gum analysis method (<i>n</i> = 3)85
4.3	Determination xylitol content of Trident spearmint gum flavor (regular care)88
4.4	Statistical analysis of xylitol content of chewed gum samples90
4.5	Amount of gum sticks required to supply toxic dose to make a dog sick.....91
5.1	Amounts of xylitol required to cause hypoglycemia in dogs.97

LIST OF FIGURES

1.1	Cs ₂ CO ₃ or K ₃ PO ₄ promoted dimerization of 3-alkyl- and 3-aryl-2-propynamides.	1
1.2	Molecular structure of 1,3-dimethyl-6-phenylpyrimidine-2,4(1H,3H)-dione, 3a . Thermal ellipsoids are shown at 50% probability.	5
1.3	Reaction composition verses time in THF and toluene. ^a	9
2.1	Pd-catalyzed dimerizations of 3-aryl-2-propynamides	28
2.2	Molecular structure of (Z)-5-(4-methoxybenzylidene)-1,3-dimethylimidazolidine-2,4-dione, (Z)- 2b	31
2.3	Phosphine ligands employed	33
2.4	Product distribution in the dimerization of 1a catalyzed by Pd(OAc) ₂ /L ₄ system in toluene at 115 °C with (A). Cs ₂ CO ₃ , (B). K ₃ PO ₄ and (C). K ₂ CO ₃	35
4.1	Commercial production of xylitol	70
4.2	A flow diagram of xylitol analysis method.	76
4.3	Amount of xylitol extracted after each extraction.	77
4.4	Laminar cup splitter design	80
4.5	GC oven program	81
4.6	Effect of injection temperature on xylitol peak area. Note: Error bars indicate standard deviation (<i>n</i> = 3).	82
4.7	Total ion chromatogram (TIC) of Trident gum extract.	83
4.8	Total ion chromatogram (TIC) of Trident gum extract with internal standard.	84
4.9	Amount of xylitol remaining in a gum piece chewed by four participants at three different rates.	87

4.10	Determination of xylitol content in 5 min chewed gum samples	89
4.11	Determination of xylitol content in 15 min chewed gum samples	89
5.1	Xylitol	96
5.2	Overview of xylitol analysis laboratory procedure	98
5.3	Total ion chromatogram (TIC) of Trident gum extraction with internal standard.....	100
5.4	Low resolution mass spectrum collected from GC-MS for the xylitol peak.....	101
5.5	Calibration plot with internal standard.	103
5.6	Calibration plot without internal standard.....	103

LIST OF SCHEMES

1.1	(a) Palladium-catalyzed, (b) Cs ₂ CO ₃ -promoted dimerization of 1a	4
1.2	Dimerization of 1a with CsOH. ^a GC yield.....	7
1.3	Unsuccessful attempt to synthesize of 8 . ^a Isolated yield.....	12
1.4	Proposed mechanism for the regioselective synthesis of (a) 6-alkyl and 6-arylracils and (b) (<i>Z</i>)-5-benzylidene-hydantoins promoted by Cs ₂ CO ₃	15
1.5	Conversion of 1a to (<i>Z</i>)- 21 and (<i>E</i>)- 21 in ethanol.....	16
1.6	Proposed synthesis of 3d via intermediates.....	17
1.7	Synthesis of intermediate 23 . ^a Isolated yield.....	18
1.8	Attempted synthesis of 11d via intermediate 23	19
1.9	Possible rate determining steps for dimerization of secondary 3-alkyl- and 3-aryl-2-propynamides, (a) to 3 , and (b) to (<i>Z</i>)- 2	20
1.10	Dimerization of 1a with, (a) granular K ₃ PO ₄ , (b) powdered K ₃ PO ₄	21
1.11	Attempted interconversion of, (<i>Z</i>)- 2a to 3a and 3a to (<i>Z</i>)- 2a	22
2.1	Unsuccessful attempt to prepare oxindole derivative 24	31
2.2	Cs ₂ CO ₃ promoted dimerization of 1a to prepare uracil 3a	39
2.3	Proposed mechanism for palladium-catalyzed dimerization of <i>N</i> -methyl- and <i>N</i> -ethyl-3-aryl-2-propynamides to produce hydantoins with (<i>Z</i>)-selectivity in the presence of Cs ₂ CO ₃	41
2.4	Possible mechanism for palladium-catalyzed dimerization of <i>N</i> -methyl- and <i>N</i> -ethyl-3-aryl-2-propynamides to produce with <i>E</i> -selectivity.....	42
3.1	Synthesis of 1,3-dimethyl-6-phenylpyrimidine-2,4(1H,3H)-dione (3a).....	48

3.2	Synthesis of 6-(4-methoxyphenyl)-1,3-dimethylpyrimidine-2,4 (1H,3H)-dione (3b).....	48
3.3	Synthesis of 6-(4-methylphenyl)-1,3-dimethylpyrimidine-2,4(1H,3H)- dione (3c).....	49
3.4	Synthesis of 6-(3,5-dimethylphenyl)-1,3-dimethylpyrimidine- 2,4(1H,3H)-dione (3d).....	50
3.5	Synthesis of 6-(3,4-dimethylphenyl)-1,3-dimethylpyrimidine- 2,4(1H,3H)-dione (3e).....	50
3.6	Synthesis of 1,3-dimethyl-6-(3-nitrophenyl)pyrimidine-2,4(1H,3H)- dione (3f).....	51
3.7	Synthesis of 1,3-diethyl-6-phenylpyrimidine-2,4(1H,3H)-dione (3g).....	52
3.8	Synthesis of 1,3-diethyl-6-(4-methoxyphenyl)pyrimidine-2,4(1H,3H)- dione (3h).....	52
3.9	Synthesis of 1,3-dimethyl-6-propylpyrimidine-2,4(1H,3H)-dione (3m).....	53
3.10	Synthesis of (Z)-5-benzylidene-1,3-dimethylimidazolidine-2,4-dione [(Z)- 2a].....	55
3.11	Synthesis of (Z)-5-(4-methoxybenzylidene)-1,3- dimethylimidazolidine-2,4-dione [(Z)- 2b].....	55
3.12	Synthesis of (Z)-5-(4-methylbenzylidene)-1,3-dimethylimidazolidine- 2,4-dione [(Z)- 2c].....	56
3.13	Synthesis of (Z)-5-(3,5-dimethylbenzylidene)-1,3- dimethylimidazolidine-2,4-dione [(Z)- 2d].....	56
3.14	Synthesis of (Z)-5-(3,4-dimethylbenzylidene)-1,3- dimethylimidazolidine-2,4-dione [(Z)- 2e].....	57
3.15	Synthesis of (Z)-5-(3-nitrophenyl)-1,3-dimethylimidazolidine-2,4- dione [(Z)- 2f].....	57
3.16	Synthesis of (Z)-5-benzylidene-1,3-diethylimidazolidine-2,4-dione [(Z)- 2g].....	58
3.17	Synthesis of (Z)-5-(4-methoxybenzylidene)-1,3-diethylimidazolidine- 2,4 dione [(Z)- 2h].....	59

3.18	Synthesis of (<i>E</i>)-5-benzylidene-1,3-dimethylimidazolidine-2,4-dione [(<i>E</i>)- 2a].....	60
3.19	Synthesis of (<i>E</i>)-5-(4-methoxybenzylidene)-1,3-dimethylimidazolidine-2,4-dione [(<i>E</i>)- 2b].....	60
3.20	Synthesis of (<i>E</i>)-5-(4-methylbenzylidene)-1,3-dimethylimidazolidine-2,4-dione [(<i>E</i>)- 2c].....	61
3.21	Synthesis of (<i>E</i>)-5-(3,5-dimethylbenzylidene)-1,3-dimethylimidazolidine-2,4-dione [(<i>Z</i>)- 2d].....	61
3.22	Synthesis of (<i>E</i>)-5-(3,4-dimethylbenzylidene)-1,3-dimethylimidazolidine-2,4-dione [(<i>E</i>)- 2e].....	62
3.23	Synthesis of (<i>E</i>)-5-(3-nitrophenyl)-1,3-dimethylimidazolidine-2,4-dione [(<i>E</i>)- 2f].....	63
3.24	Synthesis of (<i>E</i>)-5-benzylidene-1,3-diethylimidazolidine-2,4-dione [(<i>E</i>)- 2g].....	63
3.25	Synthesis of (<i>E</i>)-5-(4-methoxybenzylidene)-1,3-diethylimidazolidine-2,4 dione [(<i>E</i>)- 2h].....	64
3.26	Synthesis of (<i>Z</i>)-3-ethoxy- <i>N</i> -methyl-3-phenyl-2-propenamide [(<i>Z</i>)- 21].	65
3.27	Synthesis of (<i>E</i>)-3-ethoxy- <i>N</i> -methyl-3-phenyl-2-propenamide [(<i>E</i>)- 21].	65
3.28	(<i>Z</i>)-Methyl 3-(3,5-dimethylphenyl)-3-(<i>N</i> -methyl-3-phenyl-2-propynamido)acrylate, 23	66

CHAPTER I

A REGIOSELECTIVE SYNTHESIS OF 6-ALKYL- AND 6-ARYLURACILS BY CS₂CO₃- OR K₃PO₄-PROMOTED DIMERIZATION OF 3-ALKYL- AND 3-ARYL-2-PROPYNAMIDES.

1.1 Abstract

A regioselective synthesis of 6-alkyl- and 6-arylracils was developed by the dimerization of 3-alkyl- and 3-aryl-2-propynamides promoted by either Cs₂CO₃ or K₃PO₄. A range of 3-aryl-2-propynamides, with both electron-deficient and electron-rich 3-aryl substituents, were successfully reacted in high yields. Cs⁺ acts as a soft Lewis acid to polarize the carbon-carbon triple bond and solid K₃PO₄ interacts with carbonyl oxygen promoting intermolecular nucleophilic attack by the only weakly nucleophilic amide nitrogen. Experiments were conducted to support the proposed mechanism.

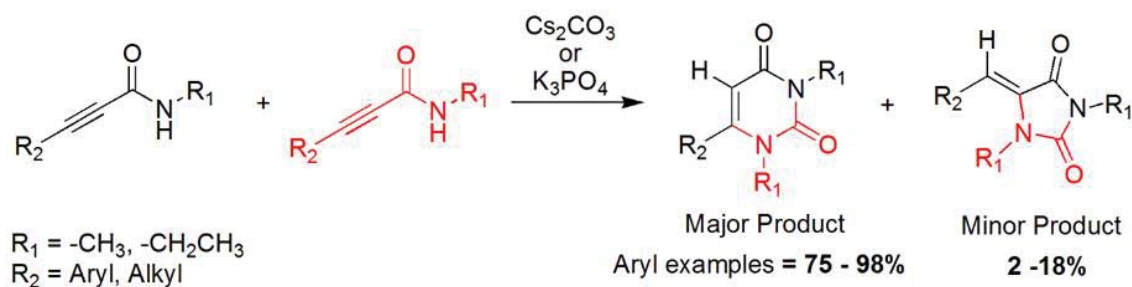


Figure 1.1 Cs₂CO₃ or K₃PO₄ promoted dimerization of 3-alkyl- and 3-aryl-2-propynamides.

1.2 Introduction

Nitrogen heterocycles with the pyrimidinone motif have long been known as important scaffolds in drug discovery exhibiting a wide range of biological activities.¹⁻³ C-aryl-substituted uracils, a class of pyrimidinones, have gained significant attention.⁴⁻²⁰ Recently, 6-arylluracils have been widely studied as hepatitis C viral NS5B inhibitors,¹⁴ GnRH antagonists,^{5,6} sirtuin inhibitors,⁷ dipeptidyl peptidase IV inhibitors,⁸ Epstein-Barr virus early antigen inhibitors,²¹ HIV-1 reverse transcriptase inhibitors,⁹ and also as antimicrobial and anticancer agents.¹⁰ Herein, we report a new and unexpected route to 6-alkyl- and 6-arylluracils from readily prepared secondary propynylamide.

The C5- and C6-aryl-substituted uracils are usually prepared by palladium-promoted cross-coupling reactions from the corresponding C-halouracils.^{2,19,20,22-28} However, the syntheses of C-halouracils are challenging due to such limitations as harsh conditions and lower yields.²⁸⁻³⁰ Direct C-H³¹⁻³⁶ and C-O³⁷ bond activation have also been reported to prepare 6-arylluracils. Both cross-coupling and many direct arylation reactions use transition metals catalysis. The Stille cross coupling^{20,22,25} uses arylstannanes with C-halouracils. Trace amounts of these toxic stannane and palladium impurities should be avoided in biological and pharmacological applications. Photochemical³⁸ and heterocyclization reactions (HCRs)³⁹⁻⁴⁷ have also been reported as tools to construct C-substituted uracils. Classic heterocyclization condensation reactions by Davidson et al³⁹ and Schwartz et al⁴⁰ have long been used to construct certain uracil skeletons.

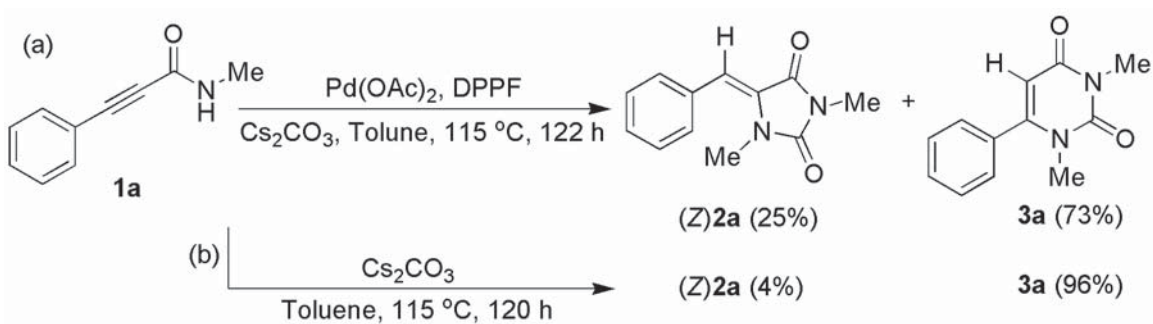
C-alkyl-substituted uracil syntheses have continually been pursued for potential biological and pharmacological applications.⁴⁸⁻⁵² The following methods have been used

to synthesize 6-alkyl-substituted uracils: (1) lithiation followed by reaction with an electrophile,^{30,52,53} (2) heterocyclization reactions,^{41,43,46,47,49} and (3) direct nucleophilic substitution with alkyl Grignard reagents⁵⁴ on 6-cyanouracil, derived from 6-halouracil.⁵⁵ However, 6-alkyluracil syntheses are often limited by low yields and harsh reaction conditions. Thus, this proposed new synthetic approach should be of interest.

In this study, a simple and efficient method for the regioselective synthesis of 6-alkyl- and 6-aryloracil derivatives was discovered employing the Cs₂CO₃- or K₃PO₄-promoted dimerization of secondary 3-alkyl- and 3-aryl-2-propynamides. The “Cesium Effect” is known to produce advantageous yields and improved reaction conditions compared to analogous routes without cesium ion.^{56,57} Various cesium bases have previously been reported to catalyze syntheses with alkynes.⁵⁸⁻⁶² On the other hand, successful use of the less expensive K₃PO₄ in place of Cs₂CO₃ in Buchwald’s amination and amidation reactions⁶³ inspired us to also test scope of the regioselective dimerization of 3-substituted-2-propynamides using K₃PO₄ as a dimerization catalyst. To the best of our knowledge, the first dimerization reactions of 3-alkyl- and 3-aryl-2-propynamides to 6-alkyl- and 6-aryloracils are demonstrated herein. This reaction is promoted by either Cs₂CO₃ or K₃PO₄.

1.3 Results and discussion

While attempting to construct the oxindole skeleton using sequential reactions in a one-pot process that employed a $[\text{Pd}(\text{allyl})\text{Cl}]_2$ and JackiePhos catalyst for N-arylation⁶⁴ followed by $\text{Pd}(\text{OAc})_2$ and bis-1,1'-diphenylphosphinoferrocene (DPPF) to catalyze ring closure,⁶⁵ the dimerization of **1a** was observed. Although this oxindole synthesis failed, further investigation of this palladium catalyzed dimerization of **1a**, surprisingly found that a 73% yield of **3a** and a 25% yield of (Z)-**2a** were produced (Scheme 1.1). While we were extending these findings to a novel synthetic route to arylidenehydantoins by the palladium-catalyzed dimerization of N-alkyl-3-aryl-2-phenylpropynamides (Chapter II), we serendipitously discovered the dimerization of **1a**, using only Cs_2CO_3 with no palladium and no DPPF ligand present, gave a 96% yield of **3a** (Figure 1.2) and only a 4% yield of (Z)-**2a** (Scheme 1.1 and Table 1.1, entry 9). Here, we now describe development of a new synthetic route to construct 6-substituted uracils by the dimerization of N-alkyl-3-substituted-2-propynamides.



Scheme 1.1 (a) Palladium-catalyzed, (b) Cs_2CO_3 -promoted dimerization of **1a**

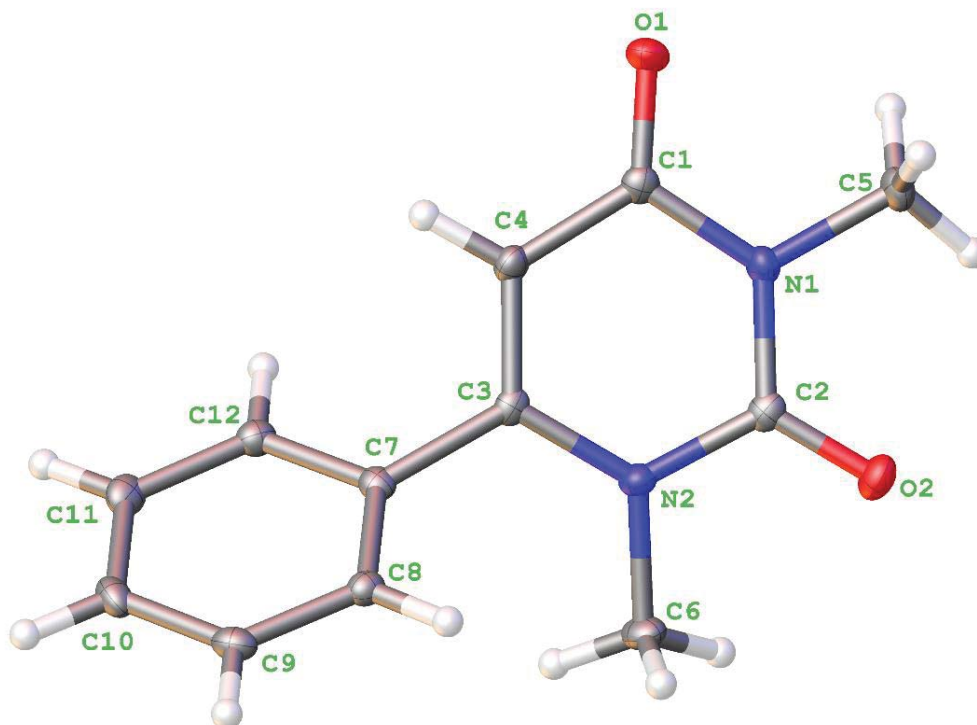
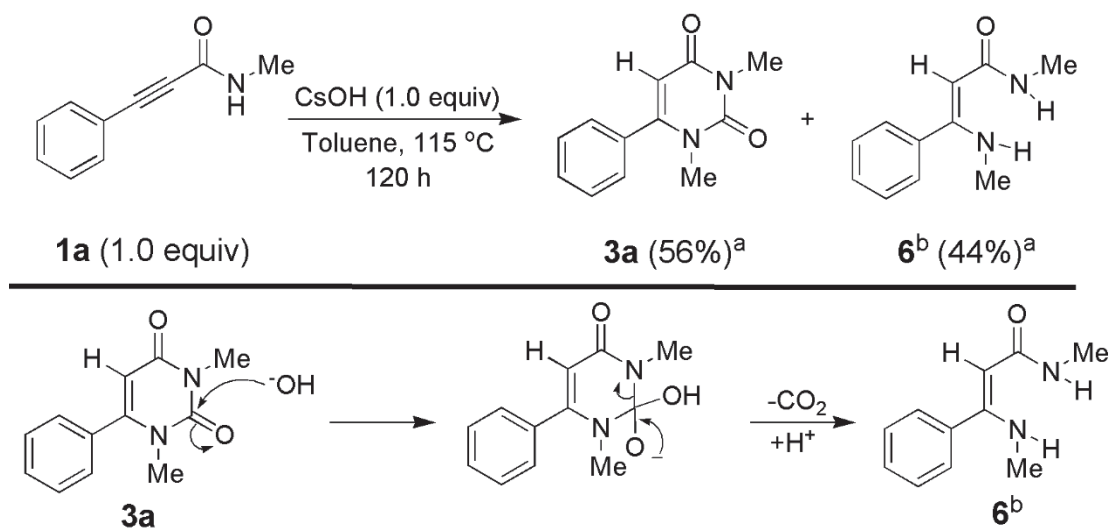


Figure 1.2 Molecular structure of 1,3-dimethyl-6-phenylpyrimidine-2,4(1H,3H)-dione, **3a**. Thermal ellipsoids are shown at 50% probability.

A variety of bases, cesium salts, and solvents were then tested with **1a** to prepare uracil **3a** (Table 1.1). Neither (*Z*)-**2a** nor **3a** formed in the absence of base in both polar and non-polar solvents (Table 1.1, entries 1 and 2). A small amount of **3a** was formed when either K_2CO_3 or $CaCO_3$ was used in toluene (Table 1.1, entries 3 and 4). Employing either KOH or K^tOBu as the base, gave conversions of **1a** of over 97%. However, KOH gave only 70% of **3a** while K^tOBu gave 80% of **3a** (Table 1.1, entries 5 and 6). In both entries a large number of other byproducts were also observed by GC-MS. Apparently, strong bases like KOH and K^tOBu can also induce side reactions along the path to uracils. Cs_2CO_3 in sharp contrast to the other bases provided very high yields and high selectivity to uracil derivative **3a** (Table 1.1, entries 7-13). Varying the amount of

Cs₂CO₃ from 0.1 to 1.0 equivalents increased the yields of **3a** from 89% to 96% (Table 1.1, entries 7-9). In contrast, when the amounts of Cs₂CO₃ used were increased from 1.0 to 2.0 equivalents, no further increase in **3a** formation occurred (Table 1.1, entry 9 vs 10). Hence 1.0 equivalent of Cs₂CO₃ was used as the standard amount.

Reactions employing Cs₂CO₃ always proceeded smoothly and in high yields in both non-polar (Table 1.1, entries 7-11) and polar aprotic (Table 1.1, entries 12-13) organic solvents. After 100% conversion of **1a** within 6 h in the polar protic solvent, ethanol, only a 14% yield of **3a** was achieved (Table 1.1, entry 14). A variety of cesium salts were also tested for the **1a** dimerizations in toluene (Table 1.1, entries 15-18). No **3a** was formed with CsNO₃. CsOAc gave poor yields of **3a**, while CsF gave a fair yield (67%) (Table 1.1, entries 16 and 17). When CsOH was used (Table 1.1, entry 18), complete conversion of **1a** generated only a 56 % yield of **3a** because hydroxide also attacked uracil **3a**. Hydroxide opened the **3a** ring by nucleophilic attack on the C-2 carbonyl carbon, followed by decarboxylation to produce (*Z*)-*N*-methyl-3-(methylamino)-3-phenylacrylamide, **6** (Scheme 1.2). High yields of **3a** were given by Cs₂CO₃ because both cesium and carbonate ions play crucial acid and base roles. Likewise, acetate, fluoride, and hydroxide act as bases in entries 16, 17, and 18. Surprisingly, when K₃PO₄ was used as a base, complete consumption of **1a** gave a 96% yield of **3a** (Table 1.1, entry 19) and reaction composition was similar to that of the Cs₂CO₃-promoted reaction (Table 1.1, entry 19 vs 9). Therefore, to further examine the reaction scope, both K₃PO₄ and Cs₂CO₃ were selected to test with a variety of substrates (Tables 1.2 and 1.3).



Scheme 1.2 Dimerization of **1a** with CsOH. ^aGC yield.

^bThe structure of **6** was assigned based on the molecular ion and its fragmentation pattern obtained using GC-MS.

Table 1.1 Optimization of reaction conditions for the dimerization of *N*-methyl-3-phenyl-2-propynamide to *N,N*-dimethyl-6-phenyluracil.^a

Reaction scheme: **1a** (1.0 equiv) $\xrightarrow[115\text{ }^\circ\text{C, 120 h}]{\text{Base, Solvent}}$ **(Z)-2a** + **3a**

Entry	Base (1.0 equiv)	Solvent	Conversion of 1a (%) ^b	Yield (%) ^b	
				(Z)-2a	3a
1	No base	Toluene	0	0	0
2	No base	THF	0	0	0
3	K ₂ CO ₃	Toluene	7	2	5
4	CaCO ₃	Toluene	3	1	2
5	KOH	Toluene	97	1	70
6	K ^t OBu	Toluene	98	1	80
7	Cs ₂ CO ₃ (0.1 equiv)	Toluene	100	10	89
8	Cs ₂ CO ₃ (0.5 equiv)	Toluene	100	9	90
9	Cs ₂ CO ₃ (1.0 equiv)	Toluene	100	4	96
10	Cs ₂ CO ₃ (2.0 equiv)	Toluene	100	6	94
11	Cs ₂ CO ₃	Benzene	100	6	94
12	Cs ₂ CO ₃	1,4-Dioxane	100	6	94
13	Cs ₂ CO ₃	THF	100	4	96
14	Cs ₂ CO ₃	EtOH	100	0	14 ^c
15	CsNO ₃	Toluene	0	0	0
16	CsOAc	Toluene	38	4	34
17	CsF	Toluene	73	6	67
18	CsOH	Toluene	100	0	56
19	K ₃ PO ₄	Toluene	100	4	96

^aReaction conditions: **1a** (0.4 mmol, 1.0 equiv), base (0.4 mmol, 1.0 equiv), solvent (2.5 mL), at 115 °C for 120 h. ^bGC Yield. ^cReaction time 6 h.

Although there was no difference in **3a** yields in either THF and toluene after complete consumption of **1a** (Table 1.1, entries 9 and 13), the reaction rates were different (Figure 1.3). About 90% conversion of **1a** was observed within 12 h and **1a** was

totally consumed after 50 h in THF at 115 °C. This compared to 80% conversion within 12 h and complete conversion within 96 h in toluene.

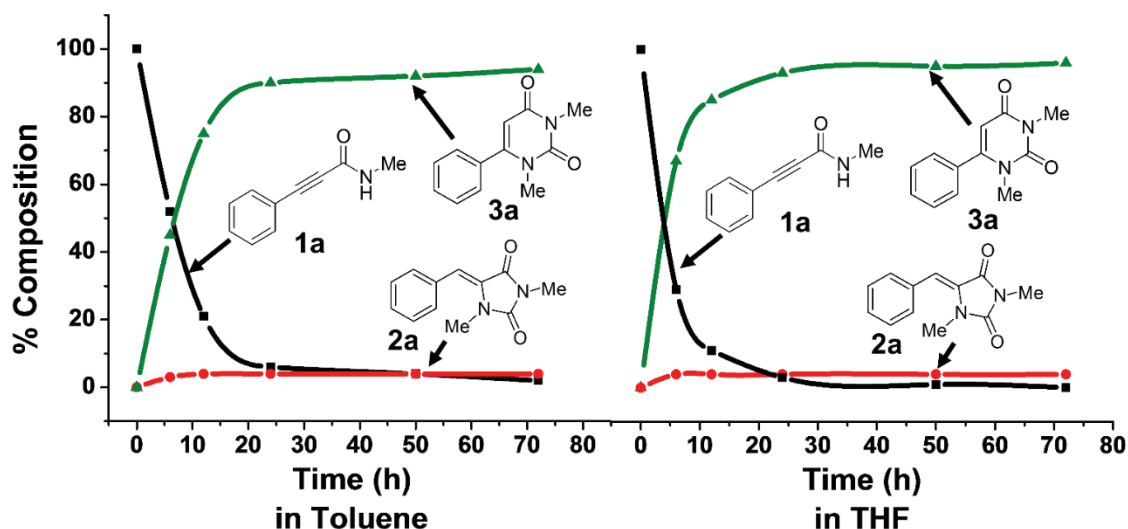


Figure 1.3 Reaction composition versus time in THF and toluene.^a

^aReaction conditions: *N*-methyl-3-phenyl-2-propynamide (1.0 equiv), Cs₂CO₃ (1.0 equiv), 115 °C, solvent (2.0 mL), time (h).

A variety of *N*-R₁-3-R₂-2-propynamides, **1a-m**, were used to explore this reaction's scope with both Cs₂CO₃ and K₃PO₄. Substituents R₂ included both electron-rich and electron-deficient 3-aryl substrates and an alkyl example (R₂ = propyl). In addition, the *N*-methyl, ethyl, and hydrogen substituents were selected as R₁. Each substrate **1a-m** was reacted under the selected conditions mentioned above to prepare 6-aryl or 6-propyluracil derivatives (Table 1.2). Excellent yields were achieved using both electron-rich and electron-deficient aryl substrates when R₁ was -CH₃ (Table 1.2, entries 1-6). The *N*-ethyl examples again favored the 6-aryluracil over the benzylidene-hydantoin but in lower selectivity than the corresponding *N*-methyl analogs (Table 1.2, entries 7 and 8 vs 1 and 2, respectively). Unfortunately, the reaction failed to give either

the corresponding uracil or hydantoin derivatives when R₁ was -H. Instead, a large number of byproducts were observed by GC-MS after complete consumption of the starting amide (Table 1.2, entries 9-12). These complex product mixtures were not further characterized. The use of a primary amide allows side reactions limiting the scope of this dimerization/cyclization reaction of secondary 3-substituted-2-propynamides.

Surprisingly, when R₂ was the alkyl group, n-propyl, all starting amide was consumed, generating 6-propyluracil derivative **3m** in only 40 % yield while substituted hydantoin (*Z*)-**2m** was not observed by GC-MS (Table 1.2, entry 13).

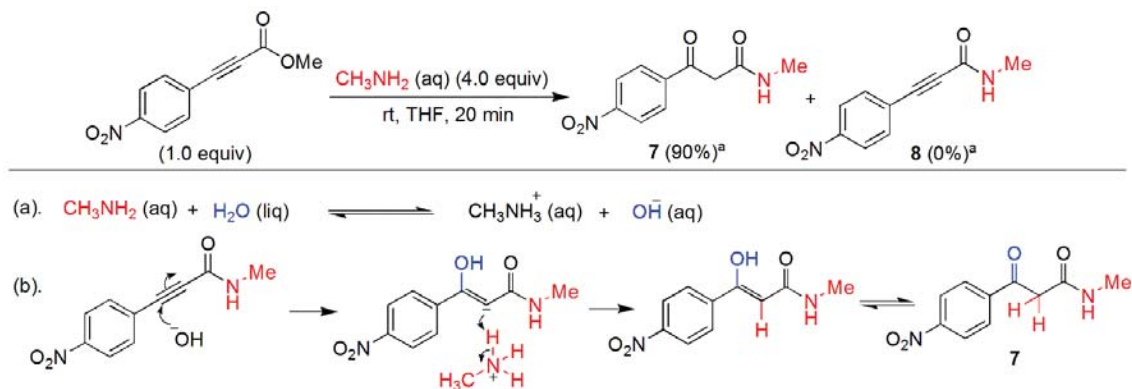
Table 1.2 Cs₂CO₃-promoted dimerizations of **1a-m** under optimized conditions^a

Entry	Amide 1	Hydantoin 2 (Yield%) ^b [%] ^c	Uracil 3 (Yield%) ^b [%] ^c	Entry	Amide 1	Hydantoin 2 (Yield%) ^b [%] ^c	Uracil 3 (Yield%) ^b [%] ^c
1.		 (Z - 2a (2) [4])	 3a (93) [96]	7. ^e		 (Z - 2g (-) ^d [14])	 3g (80) [84]
2.		 (Z - 2b (4))	 3b (94)	8. ^e		 (Z - 2h (15) [18])	 3h (73) [75]
3.		 (Z - 2c (2) [4])	 3c (93) [96]	9.		 (Z - 2i (-) ^f)	 3i (-) ^f
4.		 (Z - 2d (-) ^d [3])	 3d (94) [97]	10.		 (Z - 2j (-) ^f)	 3j (-) ^f
5.		 (Z - 2e (-) ^d [2])	 3e (94) [98]	11.		 (Z - 2k (-) ^f)	 3k (-) ^f
6. ^e		 (Z - 2f (-) ^d)	 3f (96)	12.		 (Z - 2l (-) ^f)	 3l (-) ^f
				13.		 (Z - 2m (-) ^f)	 3m (32) [40]

^aReaction conditions: Amide **1** (1.0 equiv), Cs₂CO₃ (1.0 equiv), dry toluene, at 115 °C for 96 h. **1a** was also converted to **3a** in 96% GC yield and (**Z**)-**2a** in 4% GC yield when refluxed at 110.6 °C at 1 atm with exposure to air. ^bIsolated yield. ^cGC Yield. ^dProduct was not isolated. ^eReaction time 120 h. ^fProduct was not observed by GC-MS.

The synthesis of the desired dimerization reagent, *N*-methyl-3-(4-nitrophenyl)-2-propynamide **8**, was unsuccessful due to a side reaction (Scheme 1.3). Nucleophilic

addition across the triple bond by OH^- present in aqueous methylamine, followed by keto-enol tautomerization gave **7** as the only product from the reaction and no **8** was observed as a product.



Scheme 1.3 Unsuccessful attempt to synthesize of **8**. ^aIsolated yield.

Surprisingly, substrates **1a-h** were successfully dimerized to its corresponding uracil analogues, similar to Cs_2CO_3 promoted dimerization, when K_3PO_4 was used as the catalyst. Similarly, no uracil products were observed with substrates in which R_1 is $-\text{H}$ (Table 1.3). Dimerization of **1m** with K_3PO_4 was not successful as it was with Cs_2CO_3 . The dimerization of **1a** was also performed in a round bottom flask equipped with a condenser under toluene reflux and exposure to air. No change in reaction composition was observed compared to performing the reaction in air tight culture tubes at $115\text{ }^\circ\text{C}$.

Table 1.3 K_3PO_4 -promoted dimerizations of **1a-m** under optimized conditions^a

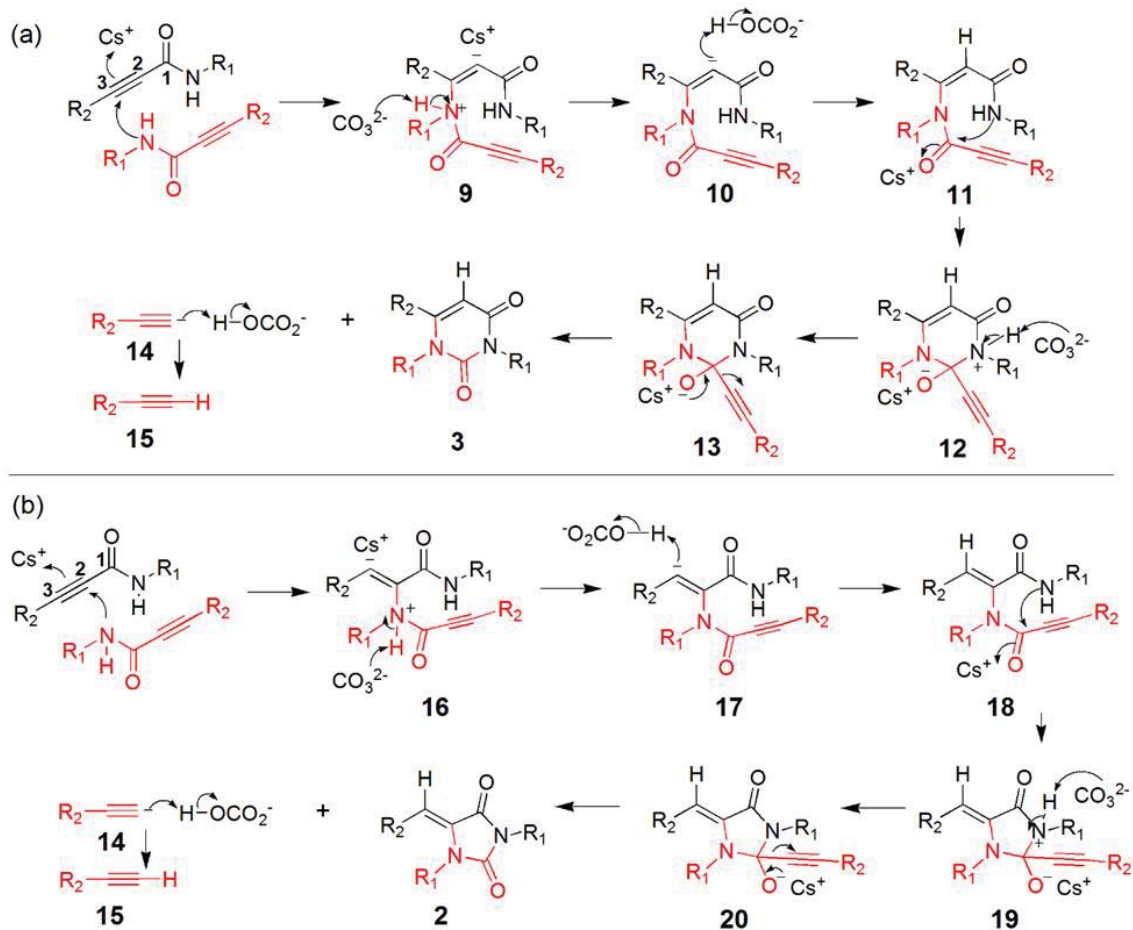
$R_2-C\equiv C-C(=O)NHR_1 \xrightarrow[\text{Toluene, 115 } ^\circ\text{C, 96 h}]{K_3PO_4 (1.0 \text{ equiv})} (Z)-2a-m + 3a-m$

Entry	Amide 1	Hydantoin 2 [%] ^b	Uracil 3 [%] ^b	Entry	Amide 1	Hydantoin 2 [%] ^b	Uracil 3 [%] ^b
1. ^d				7.			
2.				8.			
3.				9.			
4.				10.			
5.				11.			
6.				12.			
				13.			

^aReaction conditions: Amide **1** (1.0 equiv), K_3PO_4 (1.0 equiv), dry toluene, at 115 °C for 96 h. ^bGC Yield. ^cProduct was not observed by GC-MS. ^dReaction was also performed in refluxing toluene (110.6 °C) in a 25 mL round bottomed flask connected to a water cooling condenser for 120 h.

1.3.1 Insights into the dimerization mechanism:

Two mechanisms were proposed based on the dimerization results (Scheme 1.4a, b). Intermolecular nucleophilic attack by secondary amide nitrogen should occur on (β)-carbon (C-3) followed by intramolecular ring-closing nucleophilic attack on the carbonyl carbon to generate the six-membered uracil ring (Scheme 1.4a). Similarly, if nucleophilic amide nitrogen attack took place on the (α)-carbon (C-2) was followed by ring-closing intramolecular nucleophilic attack on the carbonyl carbon, this would produce the five-membered hydantoin ring (Scheme 1.4b). Cyclization of the R₁-substituted amide nitrogen at alkynyl amide carbonyl, as shown in **11** (Scheme 1.4a), is also represented here as promoted by Cs⁺. Displacement of the relatively good aryl acetylene leaving group **15** must occur from **13** and this corresponding terminal acetylene was detected during each GC-MS analysis of the products. This route is further suggested based on related literature reports.^{56,60,62,66}

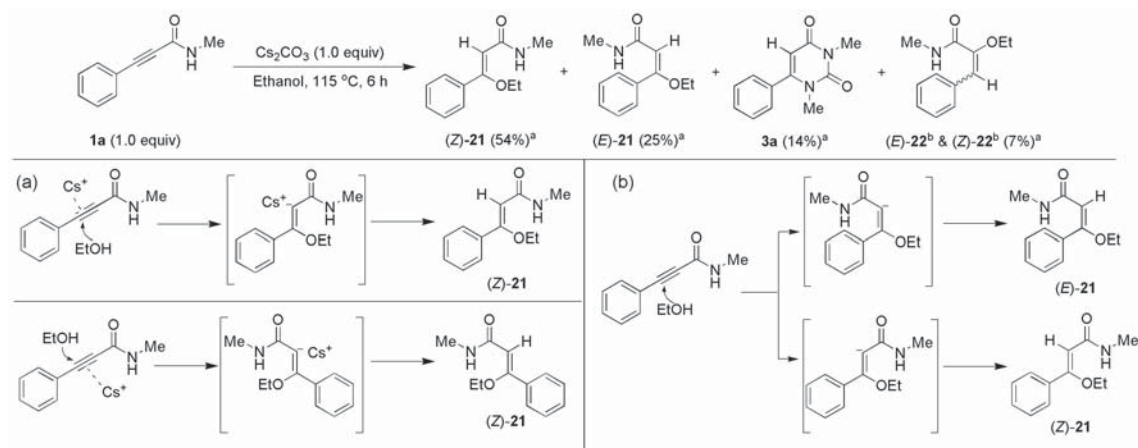


Scheme 1.4 Proposed mechanism for the regioselective synthesis of (a) 6-alkyl and 6-arylluracils and (b) (*Z*)-5-benzylidene-hydantoin promoted by Cs₂CO₃.

1.3.1.1 Evidence to support the proposed reaction mechanism (Scheme 1.4a).

Important clues regarding the reaction mechanism were collected when the dimerization of **1a** was performed using ethanol as a solvent. Two ethanol adducts were collected, including a 54% yield of (*Z*)-**21** and 25% yield of (*E*)-**21** (Scheme 1.5). Since ethanol is a competing nucleophile, major products of the reaction were (*Z*)-**21** and (*E*)-**21**. Self-dimerization of **1a** gave **3a** as only a minor product because amide **1a** is a weaker nucleophile than ethanol. A 93% overall predominance C-3 addition was

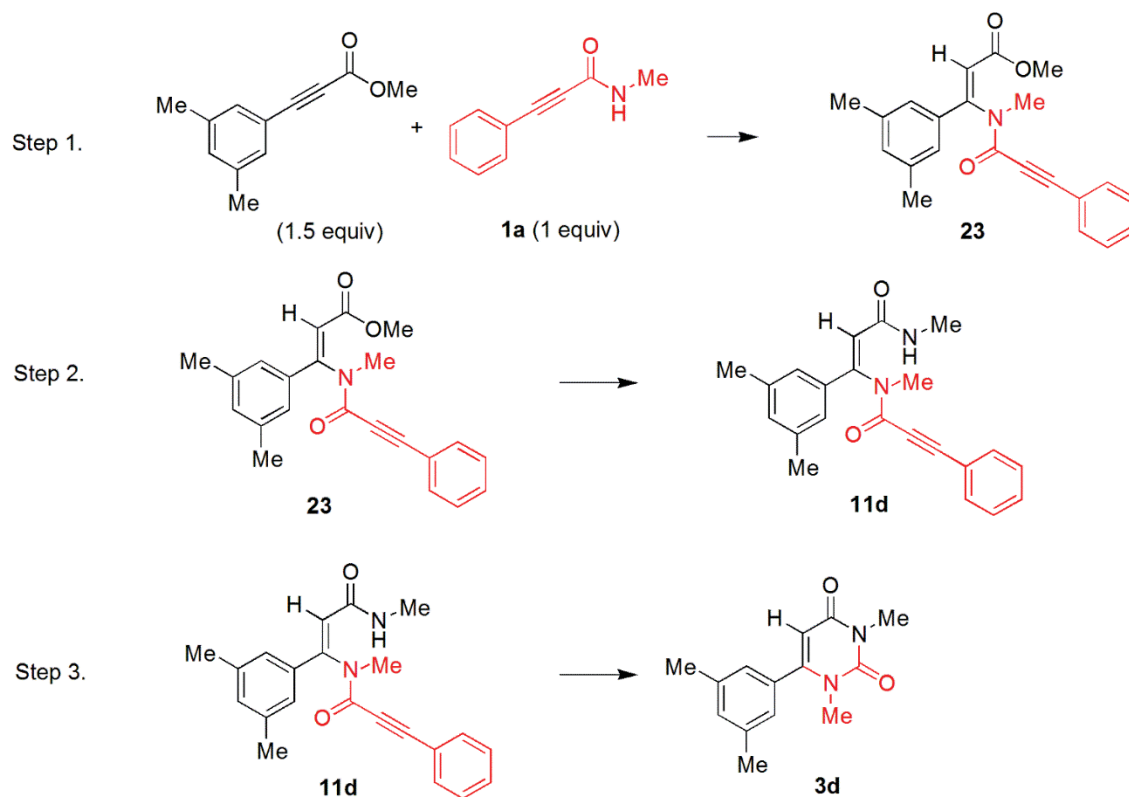
observed with nucleophilic attack on amide **1a**, when comparing the sum of products (*Z*)-**21**, (*E*)-**21**, and **3a** versus (*E*)-**22** and (*Z*)-**22** (Scheme 1.5).



Scheme 1.5 Conversion of **1a** to (*Z*)-**21** and (*E*)-**21** in ethanol

^aGC yield. ^bNeither (*E*)-**22** nor (*Z*)-**22** was isolated and fully characterized by ^1H NMR and ^{13}C NMR. However, **22** were identified by their mass spectra obtained using GC-MS.

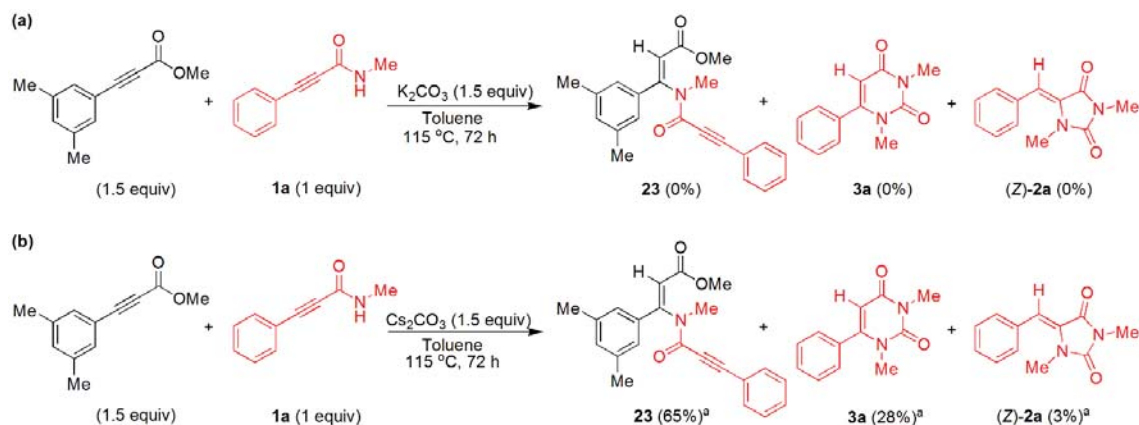
In order to provide strong experimental evidence to proof the proposed mechanism, synthesis of uracil **3d** was proposed via isolating intermediates and converting them in to uracil **3d** (Scheme 1.6).



Scheme 1.6 Proposed synthesis of **3d** via intermediates.

The crucial role of the Cs_2CO_3 was investigated while trying to construct intermediate **23** (Scheme 1.7). No intermolecular nucleophilic addition was observed when the reaction was performed with K_2CO_3 (Scheme 1.7a). On the other hand, the reaction proceeded to the expected intermediate **23** in a 65% yield, to **3a** in 32% yield, and to (*Z*)-**2a** in 3% yield using Cs_2CO_3 (Scheme 1.7b). These results support coordination of the “soft” Lewis acid Cs^+ to the triple bond, activating it to nucleophilic attack by the amide nitrogen of a second molecule of **1a**. During the dimerization to **3a-h**, **m** and to (*Z*)-**2a-h**, this same Cs^+ coordination also activates the triple bond to intermolecular nucleophilic attack by the amide nitrogen of a second secondary amide. Since secondary amide nitrogens are such weak nucleophiles, Cs^+ activation of the triple

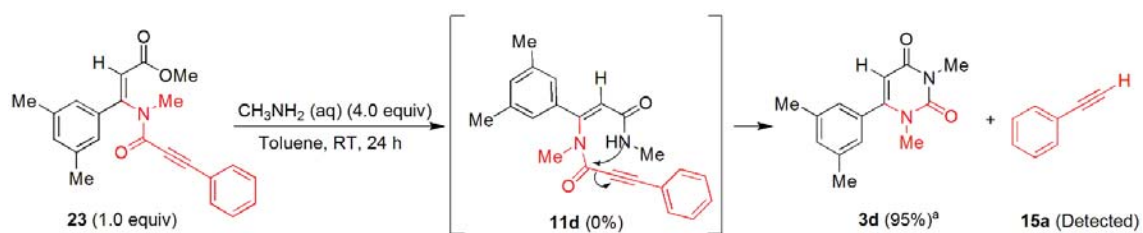
bond must occur (Scheme 1.7a vs 1.7b). The carbonyl group of the amide also polarizes the triple bond leaving C-3 (β -carbon) as the most electrophilic carbon.



Scheme 1.7 Synthesis of intermediate **23**. ^aIsolated yield.

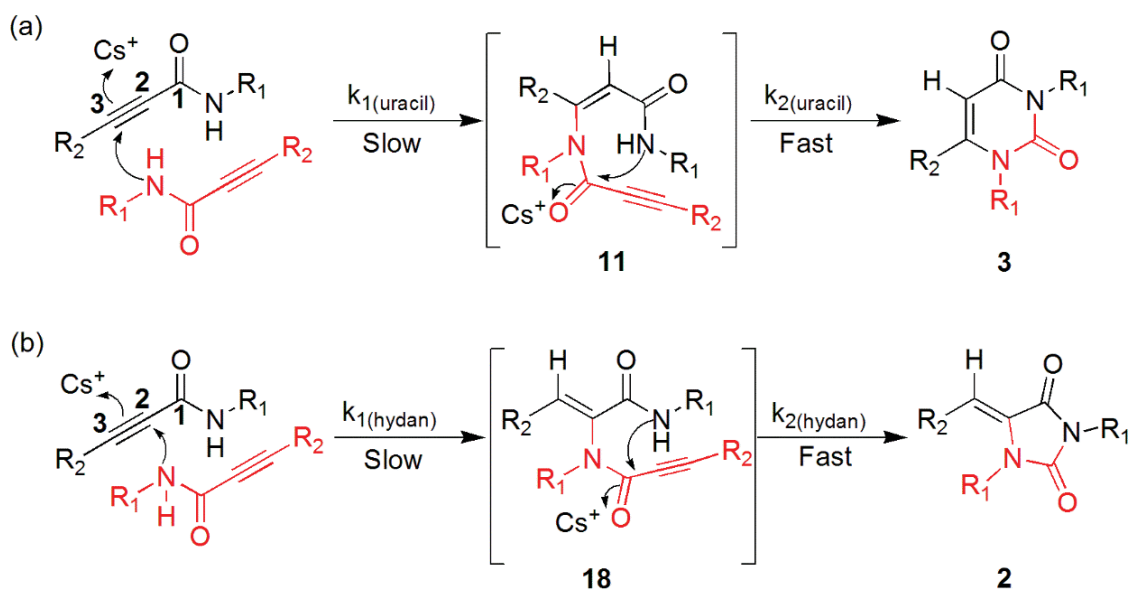
Synthesis of **11d** from intermediate **23** was attempted by reacting intermediate **23** with aqueous methyl amine solution at room temperature. Surprisingly, 100% conversion of intermediate **23** within 24 h was observed by GC-MS analysis, but no **11d** was detected. Instead, uracil **3d** was isolated in 95% yield, and 1-ethynylbenzene **10a** was formed (Scheme 1.8). Formation of **3d** at room temperature supports the rapid facile cyclization of **11d** as proposed in Scheme 1.4. This cyclization could be catalyzed by Cs^+ (see **11** in Scheme 1.4). The formation of **23** (Scheme 1.7) supports Cs^+ activation of the triple bond to nucleophilic attack by the amide nitrogen of a second secondary amide, as proposed in Scheme 1.4. The intramolecular cyclization step of the **11d** secondary amide nitrogen at the amide carbonyl carbon (Scheme 1.8) occurred without any Cs^+ present. Since Cs^+ polarization of the carbonyl oxygen is not required for the cyclization, it's role in cyclization of **11** in Scheme 1.4 and 1.8 may not be required. Alternatively carbonate

deprotonation of the amide function of **11** and **18** may occur instead to facilitate the cyclization.



Scheme 1.8 Attempted synthesis of **11d** via intermediate **23**

Since neither intermediate **11** nor **18** were ever observed in samples taken during the course of these reactions, step one (bimolecular nucleophilic attack at C-2 or C-3) should be rate determining (Scheme 1.9).



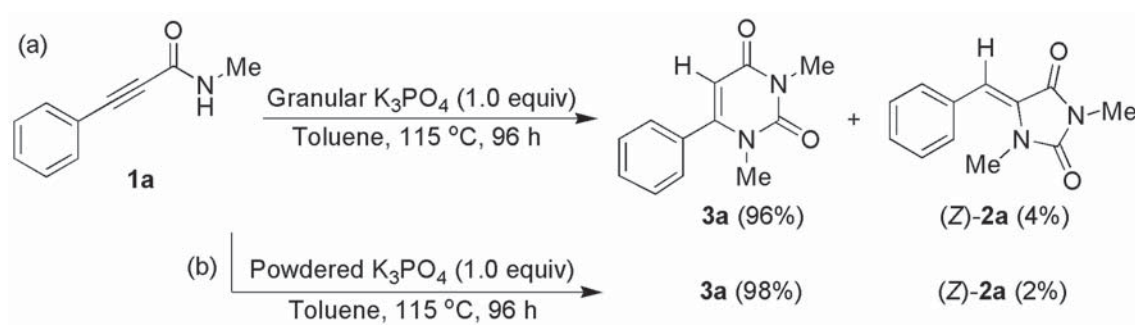
Scheme 1.9 Possible rate determining steps for dimerization of secondary 3-alkyl- and 3-aryl-2-propynamides, (a) to **3**, and (b) to (*Z*)-**2**

Since significant amounts of Cs_2CO_3 dissolve in toluene at $115\text{ }^\circ\text{C}$, Cs^+ is available as a soft Lewis acid in the solution to promote the dimerization reactions. On the other hand, K_3PO_4 solubility was very low (940 ppm) in toluene at $\sim 115\text{ }^\circ\text{C}$. The behavior of K_3PO_4 versus Cs_2CO_3 catalysis was investigated during Buchwald's CuI-promoted amidation of aryl halides.⁶⁷ The particle size of K_3PO_4 was found to be a critical factor. These amidations proceeded best when granular K_3PO_4 was used, but they were inhibited when powdered form K_3PO_4 was used. These results were explained in the following words "We believe that these observations are best explained by variable kinetic basicity of different K_3PO_4 samples, which should be heavily influenced by the particle size of this heterogeneous base".⁶⁷

In our study, the role of K_3PO_4 does not simply act as a base, but it plays a critical role of determining the regioselectivity. We suggest that K_3PO_4 might serve as a solid phase heterogeneous catalyst, where K^+ ions are influenced by PO_4^{3-} ions in the solid's

lattice structure. If dissolved K_3PO_4 is the actual catalyst, PO_4^{3-} ions in the toluene solution might be expected to be closely associated with K^+ , thereby weakening its hard Lewis acid character. Therefore, no change of reaction product composition would be expected upon switching from granular K_3PO_4 to powder K_3PO_4 . To test this hypothesis, since the granular form K_3PO_4 was also used in our experiments, granular K_3PO_4 was ground to a fine powder with a mortar and pestle. Then, this powdered K_3PO_4 was used in the **1a** dimerization and the product composition was determined (Scheme 1.10).

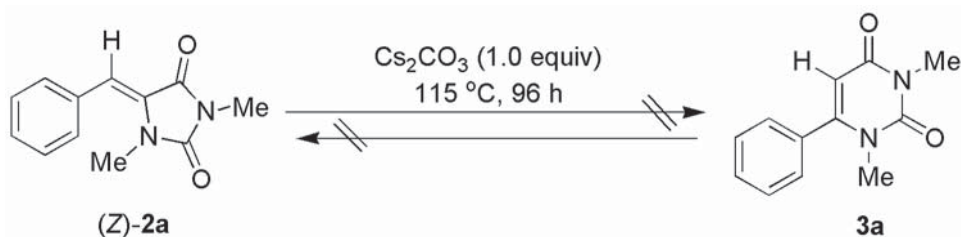
Granular K_3PO_4 use gave 96% of **3a** with 4% of (*Z*)-**2a** (Scheme 1.10a), while powdered K_3PO_4 gave 98% of **3a** and 2% of (*Z*)-**2a** (Scheme 1.10b). Neither reaction inhibition nor lower product yields were observed using powdered K_3PO_4 . In fact, the **3a** yield was slightly increased from 96% to 98% when powdered K_3PO_4 was used. These observations are consistent with similar reactivity displayed by such bifunctional solids such as CePO_4 , which acts both as a base and also as a heterogeneous catalyst.⁶⁸



Scheme 1.10 Dimerization of **1a** with, (a) granular K_3PO_4 , (b) powdered K_3PO_4 .

The possible interconversion of (*Z*)-**2a** into **3a** or, alternatively **3a** into (*Z*)-**2a**, was investigated at 115 °C in the presence of Cs_2CO_3 to determine whether the proposed mechanisms (Scheme 1.4a, b) might involve ring-opening of 6-substituted uracils **3** or

(*Z*)-5-arylidenehydantoin)s like **11** or **18** (Scheme 1.4). If this occurred the reaction could be under thermodynamic control. However, absolutely no conversion of (*Z*)-**2a** to **3a** or **3a** to (*Z*)-**2a** occurred, ruling out any equilibrium occurring between **2** and **3**. These results confirm the formation of (*Z*)-**2a** and **3a** are kinetically controlled under these reaction conditions (Scheme 1.11).



Scheme 1.11 Attempted interconversion of, (*Z*)-**2a** to **3a** and **3a** to (*Z*)-**2a**.

1.4 Conclusions

This study reports a novel one-pot synthesis of 6-substituted uracil derivatives from readily available *N*-substituted-3-alkyl- and 3-aryl-2-propynamides. Both Cs_2CO_3 and K_3PO_4 successfully promoted the regioselective synthesis of 6-aryl- and 6-alkyl-substituted uracils. The starting substituted 2-propynamide are easily constructed with a wide structural diversity. The scope of reactions can be further extended to obtain many uracil analogs. The atom efficiency is reduced by the displacement of one aryl (or alkyl) acetylide function from one of the two dimerizing *N*-substituted-3-substituted-2-propynamides. The observation that Cs_2CO_3 can catalyze the addition of alcohols to C-2 or C-3 of 2-propynamides, in addition to secondary amide nitrogens, suggests a host of other such additions might be successful. Thus, additions of alcohols, phenols, thiols,

amines, hydroxyl amines, etc to electron-deficient alkynes should be explored. The facile syntheses herein of **21**, and **23** suggest other useful synthetic procedures could result from extensions of this work.

1.5 References

- (1) La Motta, C.; Sartini, S.; Mugnaini, L.; Simorini, F.; Taliani, S.; Salerno, S.; Marini, A. M.; Da Settimo, F.; Lavecchia, A.; Novellino, E.; Cantore, M.; Failli, P.; Ciuffi, M. *J. Med. Chem.* **2007**, *50*, 4917.
- (2) Yoshida, K. I.; Nakayama, K.; Yokomizo, Y.; Ohtsuka, M.; Takemura, M.; Hoshino, K.; Kanda, H.; Namba, K.; Nitandai, H.; Zhang, J. Z.; Lee, V. J.; Watkins, W. J. *Bioorg. Med. Chem.* **2006**, *14*, 8506.
- (3) Peng, L.; Gao, X.; Duan, L.; Ren, X.; Wu, D.; Ding, K. *J. Med. Chem.* **2011**, *54*, 7729.
- (4) Guo, Z.; Chen, Y.; Huang, C. Q.; Gross, T. D.; Pontillo, J.; Rowbottom, M. W.; Saunders, J.; Struthers, S.; Tucci, F. C.; Xie, Q.; Wade, W.; Zhu, Y.-F.; Wu, D.; Chen, C. *Bioorg. Med. Chem. Lett.* **2005**, *15*, 2519.
- (5) Chen, C.; Wu, D.; Guo, Z.; Xie, Q.; Reinhart, G. J.; Madan, A.; Wen, J.; Chen, T.; Huang, C. Q.; Chen, M.; Chen, Y.; Tucci, F. C.; Rowbottom, M.; Pontillo, J.; Zhu, Y. F.; Wade, W.; Saunders, J.; Bozigian, H.; Struthers, R. S. *J. Med. Chem.* **2008**, *51*, 7478.
- (6) Regan, C. F.; Guo, Z.; Chen, Y.; Huang, C. Q.; Chen, M.; Jiang, W.; Rueter, J. K.; Coon, T.; Chen, C.; Saunders, J.; Brown, M. S.; Betz, S. F.; Struthers, R. S.; Yang, C.; Wen, J.; Madan, A.; Zhu, Y. F. *Bioorg. Med. Chem. Lett.* **2008**, *18*, 4503.
- (7) Medda, F.; Russell, R. J. M.; Higgins, M.; McCarthy, A. R.; Campbell, J.; Slawin, A. M. Z.; Lane, D. P.; Lain, S.; Westwood, N. J. *J. Med. Chem.* **2009**, *52*, 2673.
- (8) Zhang, Z.; Wallace, M. B.; Feng, J.; Stafford, J. A.; Skene, R. J.; Shi, L.; Lee, B.; Aertgeerts, K.; Jennings, A.; Xu, R.; Kassel, D. B.; Kaldor, S. W.; Navre, M.; Webb, D. R.; Gwaltney, S. L. *J. Med. Chem.* **2011**, *54*, 510.
- (9) Wang, X.; Zhang, J.; Huang, Y.; Wang, R.; Zhang, L.; Qiao, K.; Li, L.; Liu, C.; Ouyang, Y.; Xu, W.; Zhang, Z.; Zhang, L.; Shao, Y.; Jiang, S.; Ma, L.; Liu, J. *J. Med. Chem.* **2012**, *55*, 2242.
- (10) Taher, A. T.; Abou-Seri, S. M. *Molecules* **2012**, *17*, 9868.
- (11) Haouz, A.; Vanheusden, V.; Munier-Lehmann, H.; Froeyen, M.; Herdewijn, P.; Van Calenbergh, S.; Delarue, M. *J. Biol. Chem.* **2003**, *278*, 4963.
- (12) Rozners, E.; Smicius, R.; Uchiyama, C. *Chem. Commun.* **2005**, 5778.
- (13) Srivatsan, S. G.; Tor, Y. *J. Am. Chem. Soc.* **2007**, *129*, 2044.

- (14) Ding, Y.; Girardet, J. L.; Smith, K. L.; Larson, G.; Prigaro, B.; Wu, J. Z.; Yao, N. *Bioorg. Chem.* **2006**, *34*, 26.
- (15) Greco, N. J.; Tor, Y. *J. Am. Chem. Soc.* **2005**, *127*, 10784.
- (16) Fukuda, M.; Nakamura, M.; Takada, T.; Yamana, K. *Tetrahedron Lett.* **2010**, *51*, 1732.
- (17) Okamoto, A.; Tainaka, K.; Unzai, T.; Saito, I. *Tetrahedron* **2007**, *63*, 3465.
- (18) Wanninger-Weiß, C.; Wagenknecht, H.-A. *Eur. J. Org. Chem.* **2008**, *2008*, 64.
- (19) Kögler, M.; De Jonghe, S.; Herdewijn, P. *Tetrahedron Lett.* **2012**, *53*, 253.
- (20) Herdewijn, P.; Kerremans, L.; Wigerinck, P.; Vandendriessche, F.; Van Aerschot, A. *Tetrahedron Lett.* **1991**, *32*, 4397.
- (21) Galal, S. A.; Abdelsamie, A. S.; Tokuda, H.; Suzuki, N.; Lida, A.; ElHefnawi, M. M.; Ramadan, R. A.; Atta, M. H. E.; El Diwani, H. I. *Eur. J. Med. Chem.* **2011**, *46*, 327.
- (22) Palmisano, G.; Santagostino, M. *Tetrahedron* **1993**, *49*, 2533.
- (23) Tapolicsányi, P.; Krajsovsky, G.; Andó, R.; Lipcsey, P.; Horváth, G.; Mátyus, P.; Riedl, Z.; Hajós, G.; Maes, B. U. W.; Lemièrre, G. L. F. *Tetrahedron* **2002**, *58*, 10137.
- (24) Pomeisl, K.; Holý, A.; Pohl, R. *Tetrahedron Lett.* **2007**, *48*, 3065.
- (25) Bardagi, J. I.; Rossi, R. A. *J. Org. Chem.* **2008**, *73*, 4491.
- (26) Pomeisl, K.; Holý, A.; Pohl, R.; Horská, K. *Tetrahedron* **2009**, *65*, 8486.
- (27) Nencka, R.; Sinnaeve, D.; Karalic, I.; Martins, J. C.; Van Calenbergh, S. *Org. Biomol. Chem.* **2010**, *8*, 5234.
- (28) Shih, Y. C.; Chien, T.-C. *Tetrahedron* **2011**, *67*, 3915.
- (29) Bello, A. M.; Poduch, E.; Fujihashi, M.; Amani, M.; Li, Y.; Crandall, I.; Hui, R.; Lee, P. I.; Kain, K. C.; Pai, E. F.; Kotra, L. P. *J. Med. Chem.* **2007**, *50*, 915.
- (30) Tanaka, H.; Hayakawa, H.; Iijima, S.; Haraguchi, K.; Miyasaka, T. *Tetrahedron* **1985**, *41*, 861.
- (31) Čerňová, M.; Pohl, R.; Hocek, M. *Eur. J. Org. Chem.* **2009**, *2009*, 3698.
- (32) Kim, K. H.; Lee, H. S.; Kim, J. N. *Tetrahedron Lett.* **2011**, *52*, 6228.

- (33) Čerňová, M.; Čerňa, I.; Pohl, R.; Hocek, M. *J. Org. Chem.* **2011**, *76*, 5309.
- (34) Cheng, C.; Shih, Y.-C.; Chen, H. T.; Chien, T.-C. *Tetrahedron* **2013**, *69*, 1387.
- (35) Mondal, B.; Hazra, S.; Roy, B. *Tetrahedron Lett.* **2014**, *55*, 1077.
- (36) Klier, L.; Aranzamendi, E.; Ziegler, D.; Nickel, J.; Karaghiosoff, K.; Carell, T.; Knochel, P. *Organic Lett.* **2016**, *18*, 1068.
- (37) Guchhait, S. K.; Priyadarshani, G. *J. Org. Chem.* **2015**, *80*, 6342.
- (38) Ikehira, H.; Matsuura, T.; Saito, I. *Tetrahedron Lett.* **1985**, *26*, 1743.
- (39) Davidson, D.; Baudisch, O. *J. Am. Chem. Soc.* **1926**, *48*, 2379.
- (40) Schwartz, A. W.; Chittenden, G. J. F. *Biosystems* **1977**, *9*, 87.
- (41) Palacios, F.; Aparicio, D.; Ochoa de Retana, A. M.; de los Santos, J. M.; García, J.; Oyarzabal, J. *Tetrahedron* **1999**, *55*, 3105.
- (42) Fustero, S.; Salavert, E.; Sanz-Cervera, J. F.; Piera, J.; Asensio, A. *Chem. Commun.* **2003**, 844.
- (43) Kondo, T.; Nomura, M.; Ura, Y.; Wada, K.; Mitsudo, T.-a. *Tetrahedron Lett.* **2006**, *47*, 7107.
- (44) Sala, G. D.; Artillo, A.; Ricart, S.; Spinella, A. *J. Organomet. Chem.* **2007**, *692*, 1623.
- (45) Chichetti, S. M.; Ahearn, S. P.; Rivkin, A. *Tetrahedron Lett.* **2008**, *49*, 6081.
- (46) Perrone, S.; Capua, M.; Salomone, A.; Troisi, L. *J. Org. Chem.* **2015**, *80*, 8189.
- (47) Polo, R.; Moretó, J. M.; Schick, U.; Ricart, S. *Organometallics* **1998**, *17*, 2135.
- (48) Krajewska, E.; Shugar, D. *Biochem. Pharmacol.* **1982**, *31*, 1097.
- (49) Felczak, K.; Drabikowska, A. K.; Vilpo, J. A.; Kulikowski, T.; Shugar, D. *J. Med. Chem.* **1996**, *39*, 1720.
- (50) Zhang, X.; Bernet, B.; Vasella, A. *Helv. Chim. Acta* **2007**, *90*, 891.
- (51) Bello, A. M.; Konforte, D.; Poduch, E.; Furlonger, C.; Wei, L.; Liu, Y.; Lewis, M.; Pai, E. F.; Paige, C. J.; Kotra, L. P. *J. Med. Chem.* **2009**, *52*, 1648.
- (52) Nguyen, N. H.; Len, C.; Castanet, A. S.; Mortier, J. *Beilstein J. Org. Chem.* **2011**, *7*, 1228.

- (53) Tanaka, H.; Nasu, I.; Miyasaka, T. *Tetrahedron Lett.* **1979**, *20*, 4755.
- (54) Shih, Y. C.; Yang, Y.-Y.; Lin, C. C.; Chien, T.-C. *J. Org. Chem.* **2013**, *78*, 4027.
- (55) Senda, S.; Hirota, K.; Asao, T. *J. Org. Chem.* **1975**, *40*, 353.
- (56) Dijkstra, G.; Kruizinga, W. H.; Kellogg, R. M. *J. Org. Chem.* **1987**, *52*, 4230.
- (57) Galli, C. *Org. Prep. Proced. Int.* **1992**, *24*, 285.
- (58) Tzalis, D.; Knochel, P. *Angew. Chem. Int. Ed.* **1999**, *38*, 1463.
- (59) Cohen, R. J.; Fox, D. L.; Salvatore, R. N. *J. Org. Chem.* **2004**, *69*, 4265.
- (60) Kondoh, A.; Takami, K.; Yorimitsu, H.; Oshima, K. *J. Org. Chem.* **2005**, *70*, 6468.
- (61) Zou, K. B.; Qiu, R. H.; Fang, D. W.; Liu, X. Y.; Xu, X. H. *Synth. Commun.* **2008**, *38*, 2237.
- (62) Zou, K. B.; Yin, X. H.; Liu, W. Q.; Qiu, R. H.; Li, R. X.; Shao, L. L.; Li, Y. H.; Xu, X. H.; Yang, R. H. *Synth. Commun.* **2009**, *39*, 2464.
- (63) Surry, D. S.; Buchwald, S. L. *Chem. Sci.* **2011**, *2*, 27.
- (64) Hicks, J. D.; Hyde, A. M.; Cuezva, A. M.; Buchwald, S. L. *J. Am. Chem. Soc.* **2009**, *131*, 16720.
- (65) Jiang, T. S.; Tang, R. Y.; Zhang, X. G.; Li, X. H.; Li, J. H. *J. Org. Chem.* **2009**, *74*, 8834.
- (66) Salvatore, R. N.; Smith, R. A.; Nischwitz, A. K.; Gavin, T. *Tetrahedron Lett.* **2005**, *46*, 8931.
- (67) Klapars, A.; Huang, X.; Buchwald, S. L. *J. Am. Chem. Soc.* **2002**, *124*, 7421.
- (68) Kanai, S.; Nagahara, I.; Kita, Y.; Kamata, K.; Hara, M. *Chem. Sci.* **2017**.

CHAPTER II

A SYNTHESIS OF ARYLIDENEHYDANTOINS BY PALLADIUM-CATALYZED DIMERIZATION OF 3-ARYL-2-PROPYNAMIDES

2.1 Abstract

A synthetic route to prepare arylidenehydantoins was developed using the Pd-catalyzed dimerization of 3-aryl-2-propynamides. Both electron rich and electron deficient 3-aryl-2-propynamides were dimerized successfully to produce the desired arylidenehydantoins in moderate to excellent yields. When either Cs_2CO_3 or K_3PO_4 was the base, the reaction proceeded to give the corresponding dimerized products with *Z*-selectivity. Conversely, using K_2CO_3 as the base cause this dimerization to proceed with *E*-selectivity.

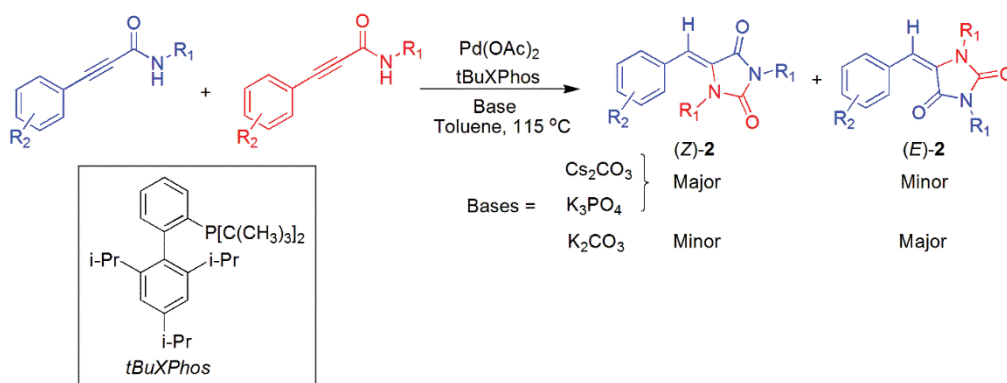


Figure 2.1 Pd-catalyzed dimerizations of 3-aryl-2-propynamides

2.2 Introduction

Synthesis of arylidenehydantoin skeletons is of a great interest because this important class of heterocycles exhibits diverse biological activities.¹⁻¹⁶ Many have antimicrobial,¹⁻⁴ anticonvulsant,⁵ antiproliferative,⁶⁻¹⁰ and antidiabetic activities.¹¹ Recently, arylidenehydantoins were reported to be molecular photo-switches.¹⁷ Several arylidenehydantoin photoactivated molecular switches can be completely turned on or off.¹⁷ Herein, we report a novel strategy to synthesize arylidenehydantoins from readily prepared secondary 3-aryl-2-propynamides in single step.

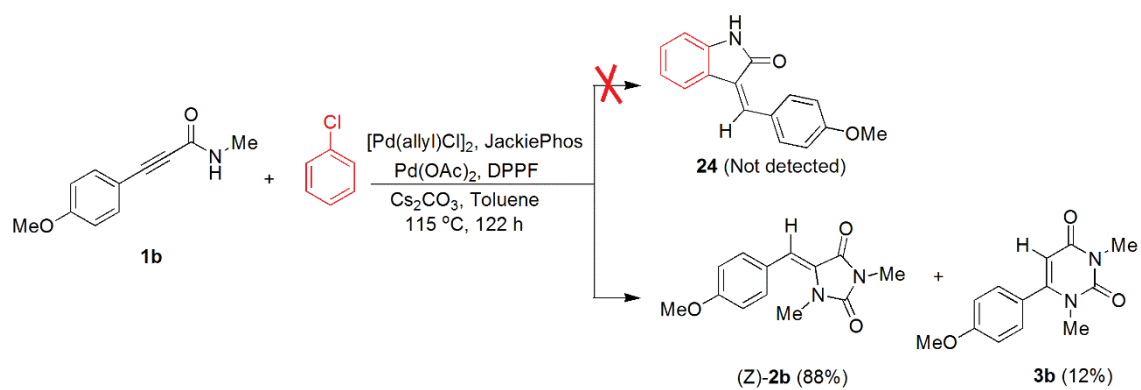
A variety of synthetic methods are already known to prepare hydantoin derivatives. Palladium-catalyzed carbonylation of aldehydes with urea derivatives,¹⁸ condensation of unsaturated ketoacids with urea derivatives,¹⁹ reacting *N*-substituted amino acids or their esters with isocyanates,²⁰⁻²² transition metal catalyzed reactions with isocyanates,²³⁻²⁶ multicomponent condensation reactions,^{27,28} the reaction of carboxylic acids with carbodiimide,^{29,30} and the reaction of imidazolidine-2,4-dione with aldehyde are known.^{1-3,5,17,31} Recently, the reaction of imidazolidine-2,4-diones with aldehydes has been successfully used to prepare arylidenehydantoin derivatives to use as molecular photoswitches.¹⁷

However, these synthetic routes required more than three steps to prepare arylidenehydantoins. In this study, palladium-catalyzed dimerizations of 3-aryl-2-propynamides are described, providing a new strategy to prepare arylidenehydantoin derivatives on one step. The application of phosphine ligands in palladium-catalyzed aminations were described by Buchwald.³² Herein, to the best of our knowledge,

application of these phosphine ligands to the first Pd-catalyzed dimerization of secondary 3-aryl-2-propynamides to prepare arylidenehydantoin derivatives is now described.

2.3 Results and discussion

The dimerization of *N*-methyl-3-(4-methoxyphenyl)-2-propynamide **1b** to benzylidene hydantoin **2b** was surprisingly observed while attempting to construct the oxindole skeleton **24** in a one-pot reaction. In this one pot reaction, [Pd(allyl)Cl]₂ and JackiePhos system was employed for *N*-arylation³³, while Pd(OAc)₂ and DPPF system was used for ring closing reaction (Scheme 2.1).³⁴ Although none of the desired oxindole **24** was detected, the major product of this one-pot reaction was (*Z*)-5-(4-methoxybenzylidene)-1,3-dimethylimidazolidine-2,4-dione (*Z*)-**2b**¹⁷ while the minor product was 6-(4-methoxyphenyl)-1,3-dimethylpyrimidine-2,4-dione (**3b**)^{35,36} (Scheme 2.1). The geometry of (*Z*)-**2b** was established by X-ray crystallography (Figure 2.2). Herein, we extended this finding to a new synthetic route to construct arylidenehydantoin derivatives.



Scheme 2.1 Unsuccessful attempt to prepare oxindole derivative **24**.

Reagents and conditions: **1b** (2.0 equiv), 4-chlorobenzene (1.0 equiv), $[\text{Pd}(\text{allyl})\text{Cl}]_2$ (1.0 mol%), JackiePhos (5.0 mol%), $\text{Pd}(\text{OAc})_2$ (5.0 mol%), DPPF (5.0 mol%), Cs_2CO_3 (2.0 equiv), toluene, 115°C , 112 h.

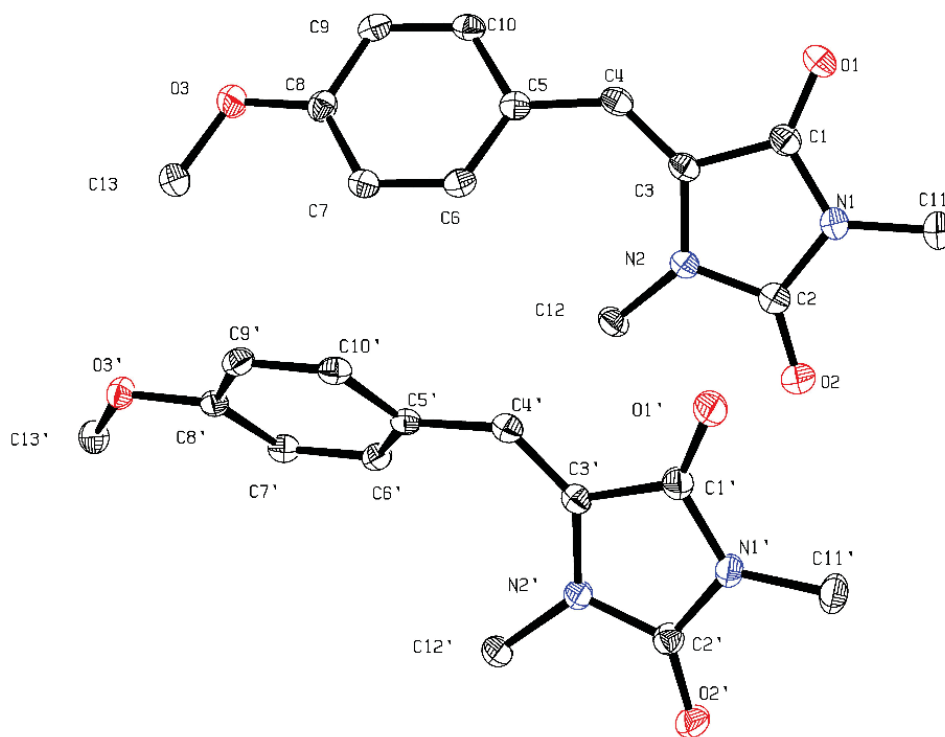


Figure 2.2 Molecular structure of **(Z)-5-(4-methoxybenzylidene)-1,3-dimethylimidazolidine-2,4-dione, (Z)-2b**.

The hydrogens are omitted for clarity. Thermal ellipsoids are shown at 50% probability.

Various phosphine ligands (Figure 2.3), Pd sources, and bases were screened in model dimerizations of *N*-methyl-3-phenyl-2-propynamide **1a** (Table 2.1). First, [Pd(allyl)Cl]₂ was used with ligands from **L**₁ to **L**₁₃ (Table 2.1, entries 1-13). Dimerizations of **1a** were observed with all ligands from **L**₁ to **L**₁₃. However, only the sterically crowded phosphine tBuXPhos, **L**₄, was able to give desired (*Z*)-**2a** in high yields when either Cs₂CO₃ or K₃PO₄ was the base (Table 2.1, entries 4A and 4B). When the base was changed to K₂CO₃ using tBuXPhos, the selectivity of the reaction switched from (*Z*)-**2a** towards (*E*)-**2a** (Table 2.1, entry 4C). Surprisingly, when the highly sterically crowded phosphines, **L**₅-**L**₇, and **L**₉, were employed with either Cs₂CO₃ or K₃PO₄, uracil formation was favored due to either Cs₂CO₃- or K₃PO₄-promoted dimerization of **1a** to uracil **3a**. These results indicate the importance of **L**₄ in efficiently forming the active catalyst.

Possible reasons for the selectivity change when base was switched from either Cs₂CO₃ or K₃PO₄ to K₂CO₃ are considered to propose a possible reaction mechanism. Employing Pd(0) sources such as Pd₂(dba)₃ and Pd(PPh₃)₄ in this dimerization led to loss of activity (Table 2.1, entries 14 and 15). However, using Pd(OAc)₂ with **L**₄ and either Cs₂CO₃ or K₃PO₄ gave the expected hydantoin products in excellent yields with higher (*Z*)- to (*E*)-selectivity compared to that of with [Pd(allyl)Cl]₂ (Table 2.1, entry 4 vs 16). Employing Pd(OAc)₂ with K₂CO₃ and **L**₄ again favored high (*E*) vs (*Z*) selectivity and this (*E*)-selectivity was higher than with [Pd(allyl)Cl]₂ (Table 2.1, entry 16). Triphenylphosphine **L**₁₄ with Pd(OAc)₂ gave complete consumption of **1a** and the expected hydantoins in moderate yield (Table 2.1, entry 17). When no Pd catalyst or phosphine ligand was present, **1a** still dimerized to give uracil **3a** as the major product in

excellent yields (Table 2.1 entry 18), when dimerization was promoted by C_2CO_3 or K_3PO_4 (*Z*)-**2a** was formed only in trace amounts (Table 2.1, entries 18A and 18B). This finding was further extended to develop the new synthetic route to uracils from 3-aryl-2-propynamides, which is described in Chapter one.

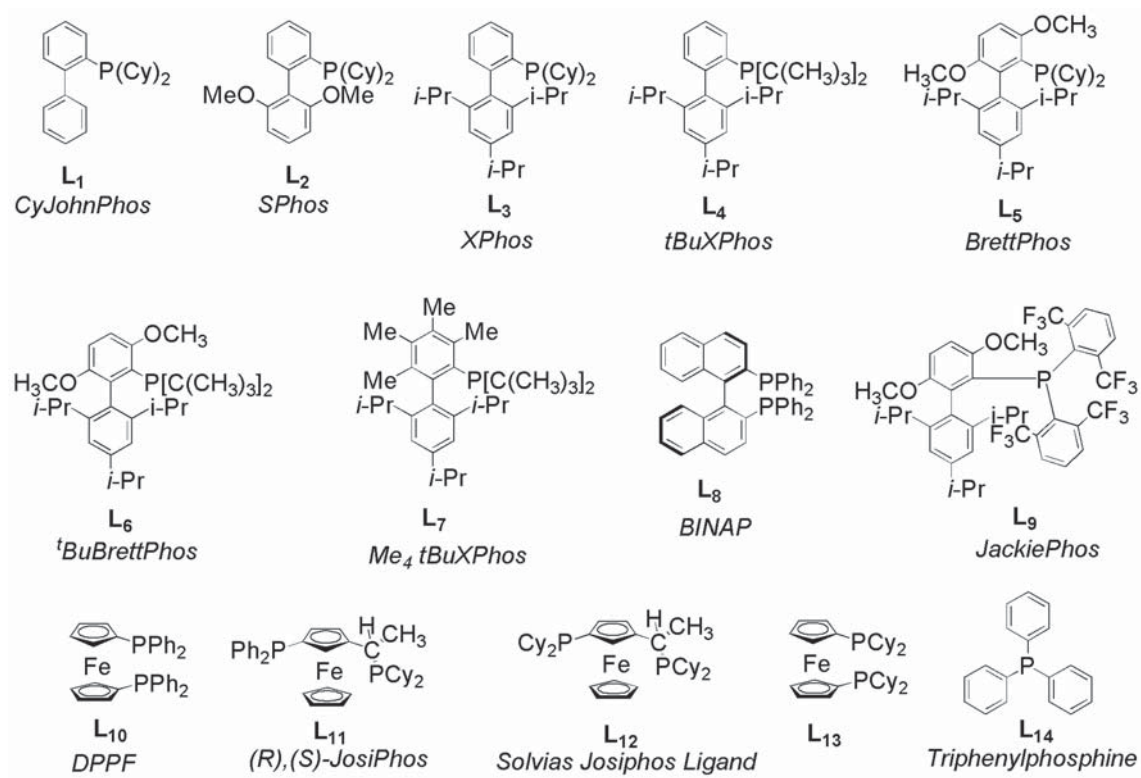


Figure 2.3 Phosphine ligands employed

Table 2.1 Screening palladium sources, ligands, and bases for the synthesis of hydantoin derivatives (*Z*-**2a** and (*E*)-**2a**.



Entry	Pd-source	Ligand	% Yield ^a											
			A (Base = Cs ₂ CO ₃)			B (Base = K ₃ PO ₄)			C (Base = K ₂ CO ₃)					
			1a ^b	(<i>Z</i>)- 2a	(<i>E</i>)- 2a	3a	1a ^b	(<i>Z</i>)- 2a	(<i>E</i>)- 2a	3a	1a ^b	(<i>Z</i>)- 2a	(<i>E</i>)- 2a	3a
01.	[Pd(allyl)Cl] ₂ (1 mol%)	L ₁ (5 mol%)	100	35	2	63	100	12	3	84	7	6	1	... ^c
02.	[Pd(allyl)Cl] ₂ (1 mol%)	L ₂ (5 mol%)	100	30	5	64	100	18	5	77	25	14	11	... ^c
03.	[Pd(allyl)Cl] ₂ (1 mol%)	L ₃ (5 mol%)	100	49	4	6	100	42	13	12	18	11	7	... ^c
04.	[Pd(allyl)Cl] ₂ (1 mol%)	L ₄ (5 mol%)	100	82	12	5	100	76	18	6	100	18	70	... ^c
05.	[Pd(allyl)Cl] ₂ (1 mol%)	L ₅ (5 mol%)	100	27	6	61	100	20	1	48	7	5	2	... ^c
06.	[Pd(allyl)Cl] ₂ (1 mol%)	L ₆ (5 mol%)	100	17	3	71	100	12	2	86	8	6	2	... ^c
07.	[Pd(allyl)Cl] ₂ (1 mol%)	L ₇ (5 mol%)	100	14	3	81	100	7	1	83	10	6	1	3
08.	[Pd(allyl)Cl] ₂ (1 mol%)	L ₈ (5 mol%)	100	3	6	65	100	4	4	65	15	... ^c	... ^c	... ^c
09.	[Pd(allyl)Cl] ₂ (1 mol%)	L ₉ (5 mol%)	100	3	6	65	100	4	4	65	15	... ^c	... ^c	... ^c
10.	[Pd(allyl)Cl] ₂ (1 mol%)	L ₁₀ (5 mol%)	100	16	3	79	100	11	3	83	1	... ^c	... ^c	... ^c
11.	[Pd(allyl)Cl] ₂ (1 mol%)	L ₁₁ (5 mol%)	100	27	4	67	100	58	13	29	43	22	21	... ^c
12.	[Pd(allyl)Cl] ₂ (1 mol%)	L ₁₂ (5 mol%)	100	23	2	74	100	8	1	91	86	35	47	... ^c
13.	[Pd(allyl)Cl] ₂ (1 mol%)	L ₁₃ (5 mol%)	100	17	3	78	100	10	1	89	2	1	... ^c	... ^c
14.	Pd ₂ (dba) ₃ (1 mol%)	L ₄ (5 mol%)	100	15	6	75	100	12	5	83	18	4	... ^c	... ^c
15.	Pd(PPh ₃) ₄ (2 mol%)	--No ligand--	100	17	1	79	100	13	1	81	100	24	22	... ^c
16.	Pd(OAc) ₂ (2.5 mol%)	L ₄ (5 mol%)	100	87	6	7	100	89	9	2	100	11	89	... ^c
17.	Pd(OAc) ₂ (2.5 mol%)	L ₁₄ (5 mol%)	100	42	3	55	100	68	12	... ^c	100	20	53	... ^c
18.	--No catalyst--	--No ligand--	100	4	... ^c	96	100	4	... ^c	96	7	2	... ^c	5

^aGC yield. ^bConversion of **1a**. ^cProduct was not detected. ^dReaction was not performed.

The Pd(OAc)₂/L₄ catalyst system was selected to further investigate the preparation of arylidenehydantoin. Product distribution as a function of conversion was determined using each of the three bases, K₃PO₄, Cs₂CO₃ and K₂CO₃. Using either Cs₂CO₃ or K₃PO₄ as the base gave 100% conversion of reactant within 12 h (Figures 2.4A and 2.4B). However, using K₂CO₃ as the base required about 72 h to achieve 100% conversion (Figure 2.4C).

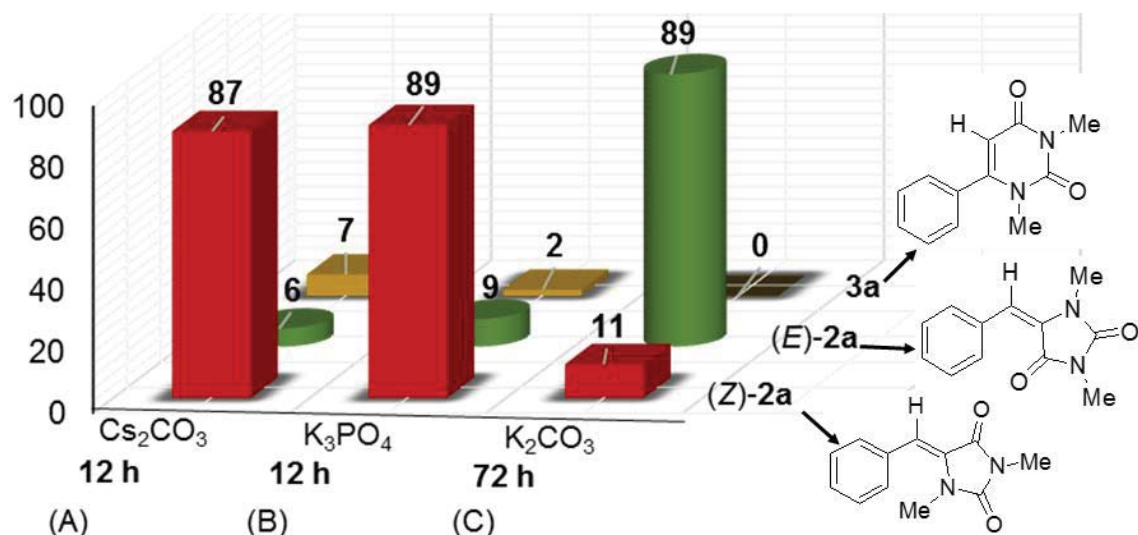


Figure 2.4 Product distribution in the dimerization of **1a** catalyzed by Pd(OAc)₂/L₄ system in toluene at 115 °C with (A). Cs₂CO₃, (B). K₃PO₄ and (C). K₂CO₃.

The scope of this Pd(OAc)₂/L₄ catalyzed dimerization was explored (Table 2.2 and Table 2.3). Both electron-neutral and electron-rich *N*-methyl-3-aryl-2-propynamides were completely consumed in 12 h at 115 °C in toluene to give desired (*Z*)-hydantoin in excellent yields when either Cs₂CO₃ or K₃PO₄ was used as the base (Table 2.2, entries 1-6). (*E*)-Hydantoin were produced in high yields (65-91 % yields) when K₂CO₃ was the base (Table 2.3, entries 1-6). Electron-deficient *N*-methyl-3-(3-nitrophenyl)-2-propynamide **1f** also proved to be an efficient substrate in this reaction with the same (*Z*) vs (*E*) selectivities as the base was varied from Cs₂CO₃ or K₃PO₄ to K₂CO₃ (Table 2.2 vs Table 2.3, entry 6). *N*-Ethyl-3-aryl-2-propynamides were also efficiently dimerized into corresponding (*Z*)-hydantoin in excellent yields with Cs₂CO₃ and K₃PO₄ (Table 2.2, entries 7 and 8) and (*E*)-hydantoin in moderate yields using K₂CO₃ (Table 2.3, entries 7 and 8). The corresponding uracil derivatives **3a-3h** were obtained in very small amounts using either Cs₂CO₃ or K₃PO₄ as the base in this 3-aryl-2-propynamide dimerization

(Table 2.2, entries 1-8). No uracil products **3a-3h** were detected when K_2CO_3 was employed as the base (Table 2.3, entries 1-8).

Table 2.2 Pd(OAc)₂/L₄-catalyzed dimerization of *N*-methyl- and *N*-ethyl-3-aryl-2-propynamides promoted by either Cs₂CO₃ or K₃PO₄.

Entry	1	(Z)-2 Yield ^a (%) ^b [%] ^c	(E)-2 Yield (%) ^a	3 Yield (%) ^a
1.		 (Z)-2a (87) [89]	 (E)-2a (6) [9]	 3a (7) [2]
2.		 (Z)-2b (91) ^d [89] ^e	 (E)-2b (4) [7]	 3b (5) [4]
3. ^d		 (Z)-2c (84) [76]	 (E)-2c (7) [2]	 3c (9) [22]
4.		 (Z)-2d (97) [93]	 (E)-2d (2) [3]	 3d (1) [4]
5.		 (Z)-2e (95) [93]	 (E)-2e (1) [5]	 3e (4) [2]
6. ^e		 (Z)-2f (84) [80]	 (E)-2f (10) [8]	 3f (7) [12]
7.		 (Z)-2g (85) [93]	 (E)-2g (1) [3]	 3g (14) [4]
8.		 (Z)-2h (94) [97]	 (E)-2h (1) [1]	 3h (5) [2]

^aGC yield. ^bBase = Cs₂CO₃. ^cBase = K₃PO₄. ^dReaction time = 18 h. ^eReaction time = 24 h

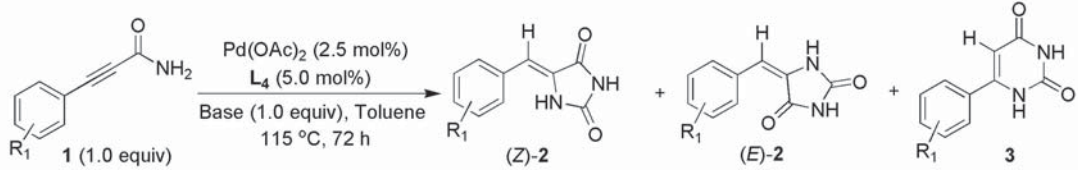
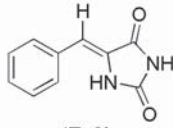
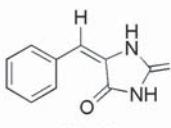
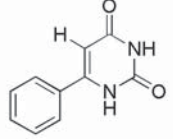
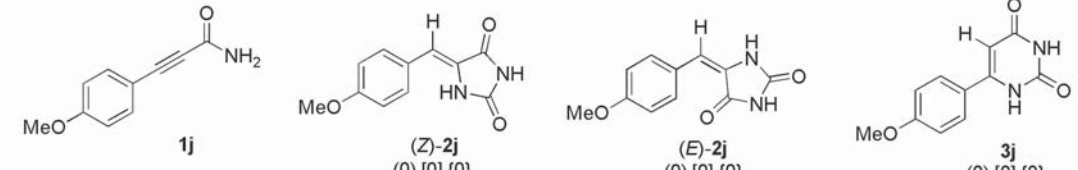
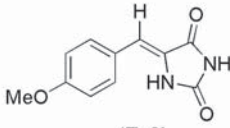
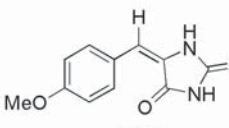
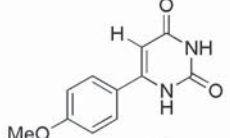
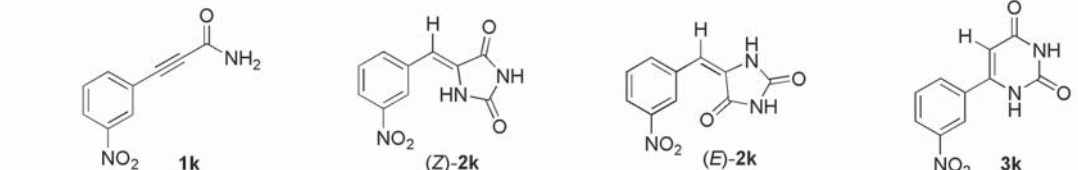
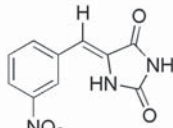
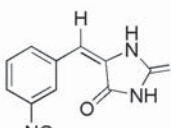
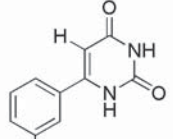
Table 2.3 Pd(OAc)₂/L₄-catalyzed dimerization of *N*-methyl- and *N*-ethyl-3-aryl-2-propynamides promoted by K₂CO₃.

Entry	1	(Z)-2 Yield (%) ^a	(E)-2 Yield (%) ^a	3 Yield (%) ^a
1.		 (Z)-2a (11)	 (E)-2a (89)	 3a (0)
2.		 (Z)-2b (8)	 (E)-2b (91)	 3b (0)
3.		 (Z)-2c (35)	 (E)-2c (65)	 3c (0)
4.		 (Z)-2d (22)	 (E)-2d (78)	 3d (0)
5.		 (Z)-2e (21)	 (E)-2e (73)	 3e (0)
6.		 (Z)-2f (17)	 (E)-2f (65)	 3f (0)
7.		 (Z)-2g (36)	 (E)-2g (61)	 3g (0)
8.		 (Z)-2h (35)	 (E)-2h (65)	 3h (0)

^aGC yield.

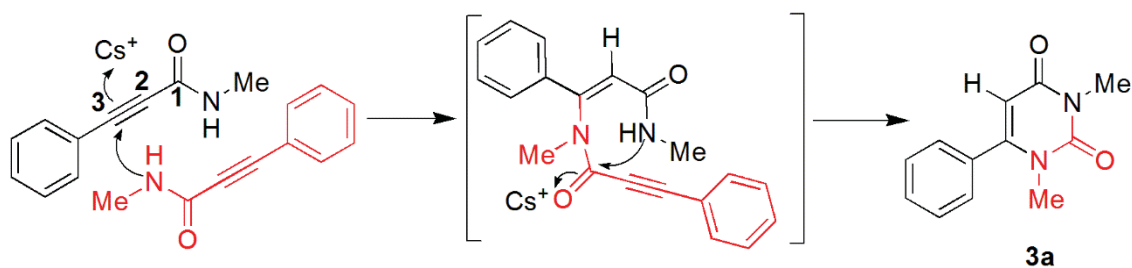
The dimerization of electron rich versus electron deficient primary 3-aryl-2-propynamides were also explored. Unfortunately, none of these primary amides dimerized into the corresponding hydantoin or to uracils with Pd(OAc)₂/L₄ using any of the three bases. These primary amides were completely consumed in this process giving a variety of products via GC which were not further explored (Table 2.4, entries 1-3).

Table 2.4 Pd-catalyzed self-dimerization of primary 3-aryl-2-propynamides

Entry	1	(Z)-2 Yield ^a (%) ^b [%] ^c {%} ^d	(E)-2 Yield ^a (%) ^b [%] ^c {%} ^d	3 Yield ^a (%) ^b [%] ^c {%} ^d
1.	 <chem>N#CC#Cc1ccccc1</chem> (1i)	 (Z)-2i (0) [0] {0}	 (E)-2i (0) [0] {0}	 3i (0) [0] {0}
2.	 <chem>N#CC#Cc1ccc(OC)cc1</chem> (1j)	 (Z)-2j (0) [0] {0}	 (E)-2j (0) [0] {0}	 3j (0) [0] {0}
3.	 <chem>N#CC#Cc1ccc([N+](=O)[O-])cc1</chem> (1k)	 (Z)-2k (0) [0] {0}	 (E)-2k (0) [0] {0}	 3k (0) [0] {0}

^aGC yield. ^bBase = Cs₂CO₃. ^cBase = K₃PO₄. ^dBase = K₂CO₃.

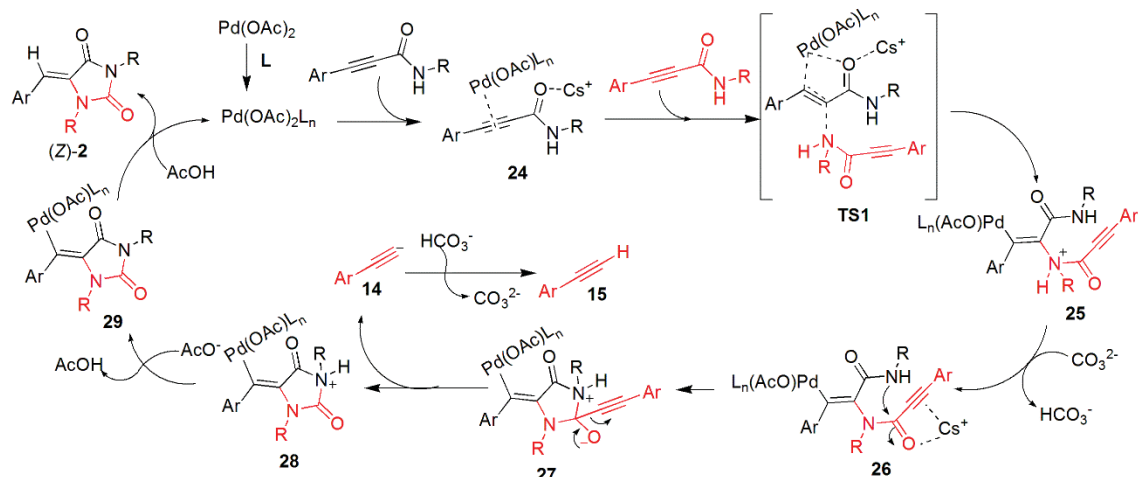
Two possible mechanisms are proposed for this arylidenehydantoin synthesis considering these results and literature^{34,37-46} evidence (Schemes 2.3 and 2.4). An important clue regarding crucial role of the palladium-catalyst was that Cs₂CO₃- or K₃PO₄-promoted dimerization of **1a** in the absence of palladium to give uracil derivative **3a** as the major product (Table 2.1, entry 18A and B). When **1a** dimerizes into uracil **3b**, the triple bond became sufficiently activated for the secondary amide nitrogen, a poor nucleophile, to attack β -carbon of amide **1a** as the first step to produce six-membered uracil ring **3b** (Scheme 2.2). However, to generate the five-membered hydantoin ring, the intermolecular nucleophilic amide attack on α -carbon must occur. The palladium catalyst plays a crucial role determining this regioselectivity in the arylidenehydantoin synthesis.



Scheme 2.2 Cs₂CO₃ promoted dimerization of **1a** to prepare uracil **3a**

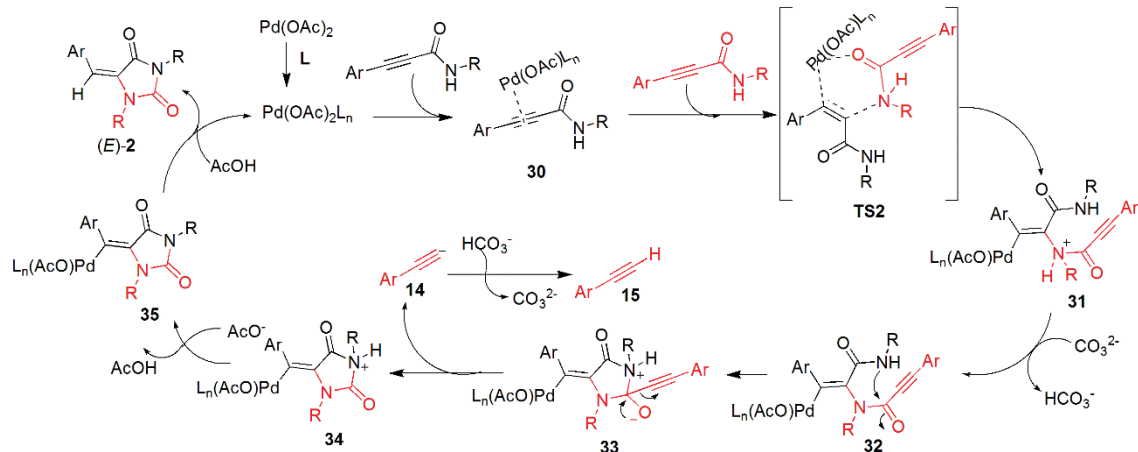
As reported in the literature, palladium can coordinate with the triple bond.^{37,40-46} The large, soft cesium cation may also be interacting with the carbonyl oxygen (Scheme 2.3, **24**). Intermolecular attack by the amide nitrogen from the opposite side of where palladium and cesium interact might form transition state **TS1**, where the Pd-C bond is *trans* to the new N-C bond that is forming (Scheme 2.3, **25**). The “Cesium Effect” is known to produce advantageous yields and improved reaction conditions compared to analogous routes without cesium ion.⁴⁷⁻⁵³ Amide attack at the α -position is in accord with

both experimental and relative energy calculations previously been reported³⁹ for palladium-catalysts where Pd might bond to either the α - or β -carbons of 3-phenyl-2-propynal. Such studies show that palladium catalysts insert on the β -carbons of 3-phenyl-2-propynal instead of α -carbon.³⁹ 3-Aryl-2-propynamides closely resemble 3-phenyl-2-propynal, so palladium should favor binding to the β -carbon of 3-aryl-2-propynamides, thereby directing the intermolecular amide nitrogen nucleophilic attack to the α -carbon (Scheme 2.3). Cyclization then occurs by an intramolecular secondary amide nitrogen nucleophilic acyl substitution at the second amide carbonyl carbon, possible promoted by Cs⁺ activation. This displaces the *sp*-hybridized anion **14**, a relatively good leaving group, and generates the five-membered hydantoin ring **27** (Scheme 2.3). Protonation of **14** gives terminal aryl-acetylene **15**, which was detected during each GC-MS analysis of the products. Protonolysis generates arylidenehydantoin (*Z*)-**2** and acetate re-coordinates with palladium, regenerating the active palladium species (Scheme 2.3).



Scheme 2.3 Proposed mechanism for palladium-catalyzed dimerization of *N*-methyl- and *N*-ethyl-3-aryl-2-propynamides to produce hydantoin with (*Z*)-selectivity in the presence of Cs_2CO_3 .

When K_2CO_3 was used as the base versus Cs_2CO_3 or K_3PO_4 , the regioselectivity switched from (*Z*) to (*E*). Since K^+ is not as bulky as Cs^+ , the nucleophilic amide attacks α -carbon on the same side of the palladium-catalyst interaction and from the opposite side of the carbonyl oxygen to generate possible transition state **TS2**, which gives (*E*)-selectivity (Scheme 2.4, **TS2**). Intramolecular cyclization of **32** creates the five-membered hydantoin ring **33** with *E*-selectivity. This cyclization generates same leaving group **14**, which produce the corresponding terminal aryl-acetylene **15** (Scheme 2.4). Similarly, the acetate ligand re-coordinates with palladium catalyst to regenerate the active palladium species and the major product arylidenehydantoin (*E*)-**2**.



Scheme 2.4 Possible mechanism for palladium-catalyzed dimerization of *N*-methyl- and *N*-ethyl-3-aryl-2-propynamides to produce with *E*-selectivity.

A possible reason for K_3PO_4 behaving similar to Cs_2CO_3 was provided in Chapter I. The same behavior of K_3PO_4 is expected in this synthesis.

2.4 Conclusion

A novel simple synthesis of (*Z*)-5-arylidenehydantoin derivatives by dimerization of 3-aryl-2-propynamides catalyzed by $\text{Pd}(\text{OAc})_2/\text{tBuXPhos}$ was demonstrated. This system allows dimerization of secondary electron-rich, electron-deficient *N*-methyl and *N*-ethyl-3-aryl-2-propynamides to (*Z*)-5-arylidenehydantoin in good yields. Dimerization of primary 3-aryl-2-propynamides were unsuccessful limiting the scope of the reaction to secondary 3-aryl-2-propynamides. Changing the base to K_2CO_3 resulted in the major product changing from the (*Z*)-geometry to give, instead, (*E*)-5-arylidenehydantoin. The starting substituted 2-propynamides can be easily constructed with a wide structural diversity. This should allow the scope of this dimerization reaction to be expanded.

2.5 References

- (1) Albuquerque, J. F. C.; Rocha Filho, J. A.; Brandao, S. S. F.; Lima, M. C. A.; Ximenes, E. A.; Galdino, S. L.; Pitta, I. R.; Chantegrel, J.; Perrissin, M.; Luu-Duc, C. *Il Farmaco* **1999**, *54*, 77.
- (2) Szymańska, E.; Kieć-Kononowicz, K. *Il Farmaco* **2002**, *57*, 355.
- (3) Szymańska, E.; Kieć-Kononowicz, K.; Białecka, A.; Kasprowicz, A. *Il Farmaco* **2002**, *57*, 39.
- (4) Kieć-Kononowicz, K.; Szymańska, E. *Il Farmaco* **2003**, *57*, 909.
- (5) Thenmozhiyal, J. C.; Wong, P. T. H.; Chui, W. K. *J. Med. Chem.* **2004**, *47*, 1527.
- (6) Carmi, C.; Cavazzoni, A.; Zuliani, V.; Lodola, A.; Bordi, F.; Plazzi, P. V.; Alfieri, R. R.; Petronini, P. G.; Mor, M. *Bioorg. Med. Chem. Lett.* **2006**, *16*, 4021.
- (7) Cavazzoni, A.; Alfieri, R. R.; Carmi, C.; Zuliani, V.; Galetti, M.; Fumarola, C.; Frazzi, R.; Bonelli, M.; Bordi, F.; Lodola, A.; Mor, M.; Petronini, P. G. *Mol. Cancer Ther.* **2008**, *7*, 361.
- (8) Zuliani, V.; Carmi, C.; Rivara, M.; Fantini, M.; Lodola, A.; Vacondio, F.; Bordi, F.; Plazzi, P. V.; Cavazzoni, A.; Galetti, M.; Alfieri, R. R.; Petronini, P. G.; Mor, M. *Eur. J. Med. Chem.* **2009**, *44*, 3471.
- (9) Mudit, M.; Khanfar, M.; Muralidharan, A.; Thomas, S.; Shah, G. V.; van Soest, R. W. M.; El Sayed, K. A. *Bioorg. Med. Chem.* **2009**, *17*, 1731.
- (10) Khanfar, M. A.; El Sayed, K. A. *Eur. J. Med. Chem.* **2010**, *45*, 5397.
- (11) Ceylan-Ünlüsoy, M.; Verspohl, E. J.; Ertan, R. *J. Enzyme Inhib. Med. Chem.* **2010**, *25*, 784.
- (12) Ha, Y. M.; Kim, J. A.; Park, Y. J.; Park, D.; Kim, J. M.; Chung, K. W.; Lee, E. K.; Park, J. Y.; Lee, J. Y.; Lee, H. J.; Yoon, J. H.; Moon, H. R.; Chung, H. Y. *Biochimica et Biophysica Acta (BBA) - General Subjects* **2011**, *1810*, 612.
- (13) Albers, H. M. H. G.; Hendrickx, L. J. D.; van Tol, R. J. P.; Hausmann, J.; Perrakis, A.; Ova, H. *J. Med. Chem.* **2011**, *54*, 4619.
- (14) Mendgen, T.; Steuer, C.; Klein, C. D. *J. Med. Chem.* **2012**, *55*, 743.
- (15) Nique, F.; Hebbe, S.; Triballeau, N.; Peixoto, C.; Lefrançois, J.-M.; Jary, H.; Alvey, L.; Manioc, M.; Housseman, C.; Klaassen, H.; Van Beeck, K.; Guédin, D.; Namour, F.; Minet, D.; Van der Aar, E.; Feyen, J.; Fletcher, S.; Blanqué, R.; Robin-Jagerschmidt, C.; Deprez, P. *J. Med. Chem.* **2012**, *55*, 8236.

- (16) Spicer, J. A.; Lena, G.; Lyons, D. M.; Huttunen, K. M.; Miller, C. K.; O'Connor, P. D.; Bull, M.; Helsby, N.; Jamieson, S. M. F.; Denny, W. A.; Ciccone, A.; Browne, K. A.; Lopez, J. A.; Rudd-Schmidt, J.; Voskoboinik, I.; Trapani, J. A. *J. Med. Chem.* **2013**, *56*, 9542.
- (17) Martínez-López, D.; Yu, M.-L.; García-Iriepa, C.; Campos, P. J.; Frutos, L. M.; Golen, J. A.; Rasapalli, S.; Sampedro, D. *J. Org. Chem.* **2015**, *80*, 3929.
- (18) Beller, M.; Eckert, M.; Moradi, W. A.; Neumann, H. *Angew. Chem. Int. Ed.* **1999**, *38*, 1454.
- (19) Gore, S.; Chinthapally, K.; Baskaran, S.; Konig, B. *Chem. Commun.* **2013**, *49*, 5052.
- (20) Matthews, J.; Rivero, R. A. *J. Org. Chem.* **1997**, *62*, 6090.
- (21) Boeijen, A.; Kruijtzter, J. A. W.; Liskamp, R. M. J. *Bioorg. Med. Chem. Lett.* **1998**, *8*, 2375.
- (22) Blagoeva, I. B.; Toteva, M. M.; Ouarti, N.; Ruasse, M.-F. *J. Org. Chem.* **2001**, *66*, 2123.
- (23) Alizadeh, A.; Sheikhi, E. *Tetrahedron Lett.* **2007**, *48*, 4887.
- (24) Kuninobu, Y.; Kikuchi, K.; Takai, K. *Chem. Lett.* **2008**, *37*, 740.
- (25) Miura, T.; Mikano, Y.; Murakami, M. *Org. Lett.* **2011**, *13*, 3560.
- (26) Hill, M. S.; Liptrot, D. J.; Mahon, M. F. *Angew. Chem. Int. Ed.* **2013**, *52*, 5364.
- (27) He, J.; Ouyang, G.; Yuan, Z.; Tong, R.; Shi, J.; Ouyang, L. *Molecules* **2013**, *18*, 5142.
- (28) Ignacio, J. M.; Macho, S.; Marcaccini, S.; Pepino, R.; Torroba, T. *Synlett* **2005**, *2005*, 3051.
- (29) Volonterio, A.; Ramirez de Arellano, C.; Zanda, M. *J. Org. Chem.* **2005**, *70*, 2161.
- (30) Cristina Bellucci, M.; Marcelli, T.; Scaglioni, L.; Volonterio, A. *RSC Adv.* **2011**, *1*, 1250.
- (31) Selič, L.; Jakše, R.; Lampič, K.; Golič, L.; Golič-Grdadolnik, S.; Stanovnik, B. *Helv. Chim. Acta* **2000**, *83*, 2802.
- (32) Surry, D. S.; Buchwald, S. L. *Chem. Sci.* **2011**, *2*, 27.

- (33) Hicks, J. D.; Hyde, A. M.; Cuezva, A. M.; Buchwald, S. L. *J. Am. Chem. Soc.* **2009**, *131*, 16720.
- (34) Jiang, T.-S.; Tang, R. Y.; Zhang, X.-G.; Li, X.-H.; Li, J.-H. *J. Org. Chem.* **2009**, *74*, 8834.
- (35) Čerňová, M.; Pohl, R.; Hocek, M. *Eur. J. Org. Chem.* **2009**, *2009*, 3698.
- (36) Kim, K. H.; Lee, H. S.; Kim, J. N. *Tetrahedron Lett.* **2011**, *52*, 6228.
- (37) Chernyak, N.; Gevorgyan, V. *J. Am. Chem. Soc.* **2008**, *130*, 5636.
- (38) Jensen, K. H.; Sigman, M. S. *Org. Biomol. Chem.* **2008**, *6*, 4083.
- (39) Ahlquist, M.; Fabrizi, G.; Cacchi, S.; Norrby, P. O. *J. Am. Chem. Soc.* **2006**, *128*, 12785.
- (40) Trost, B. M.; Toste, F. D.; Greenman, K. *J. Am. Chem. Soc.* **2003**, *125*, 4518.
- (41) Tunge, J. A.; Foresee, L. N. *Organometallics* **2005**, *24*, 6440.
- (42) Jia, C.; Kitamura, T.; Fujiwara, Y. *Acc. Chem. Res.* **2001**, *34*, 633.
- (43) Hatano, M.; Terada, M.; Mikami, K. *Angew. Chem. Int. Ed.* **2001**, *40*, 249.
- (44) Jia, C.; Lu, W.; Oyamada, J.; Kitamura, T.; Matsuda, K.; Irie, M.; Fujiwara, Y. *J. Am. Chem. Soc.* **2000**, *122*, 7252.
- (45) Jia, C.; Piao, D.; Kitamura, T.; Fujiwara, Y. *J. Org. Chem.* **2000**, *65*, 7516.
- (46) Lu, W.; Jia, C.; Kitamura, T.; Fujiwara, Y. *Org. Lett.* **2000**, *2*, 2927.
- (47) Dijkstra, G.; Kruizinga, W. H.; Kellogg, R. M. *J. Org. Chem.* **1987**, *52*, 4230.
- (48) Galli, C. *Org. Prep. Proced. Int.* **1992**, *24*, 285.
- (49) Tzalis, D.; Knochel, P. *Angew. Chem. Int. Ed.* **1999**, *38*, 1463.
- (50) Cohen, R. J.; Fox, D. L.; Salvatore, R. N. *J. Org. Chem.* **2004**, *69*, 4265.
- (51) Kondoh, A.; Takami, K.; Yorimitsu, H.; Oshima, K. *J. Org. Chem.* **2005**, *70*, 6468.
- (52) Zou, K. B.; Qiu, R. H.; Fang, D. W.; Liu, X. Y.; Xu, X. H. *Synth. Commun.* **2008**, *38*, 2237.
- (53) Zou, K. B.; Yin, X. H.; Liu, W. Q.; Qiu, R. H.; Li, R. X.; Shao, L. L.; Li, Y. H.; Xu, X. H.; Yang, R. H. *Synth. Commun.* **2009**, *39*, 2464.

CHAPTER III

ONE POT SYNTHESIS OF URACILS AND HYDANTOINS: EXPERIMENTAL

3.1 General Information

All commercial materials and solvents were used directly without further purification. Melting points were determined in open glass capillaries and were uncorrected (heating rates: 5 °C min⁻¹ from RT to 80 °C and 1-2 °C min⁻¹ above 80 °C). ¹H NMR chemical shifts (in ppm) were referenced to tetramethylsilane ($\delta = 0$ ppm) in CDCl₃ as an internal standard at room temperature. ¹³C NMR spectra were calibrated with CDCl₃ ($\delta = 77.16$ ppm). The IR spectra were recorded with a FT-IR spectrophotometer, and only major peaks were reported in cm⁻¹. A high-resolution mass spectrometer equipped with an ESI source (positive mode) and a TOF detector was used to obtain spectra (HRMS). Column chromatography was performed on silica gel (70–230 mesh ASTM) using the reported eluents. Thin layer chromatography (TLC) was carried out on plates with a layer thickness of 250 μ m (silica gel 60 F254). Gas chromatography coupled with a mass detector was used to performed GC-MS analysis, employing a 60 m \times 320 μ m \times 1 μ m, 100 % dimethylpolysiloxane capillary column. Unless otherwise noted, reactions were carried out with constant stirring in oven-dried glassware.

Methyl 3-aryl-2-propynoates were prepared according to the method reported by Negishi et al.¹ A procedure reported by Strübing et al.² was modified to prepare *N*-substituted-3-alkyl and 3-aryl-2-propynamides **1a-m**. A methyl or ethyl amine solution

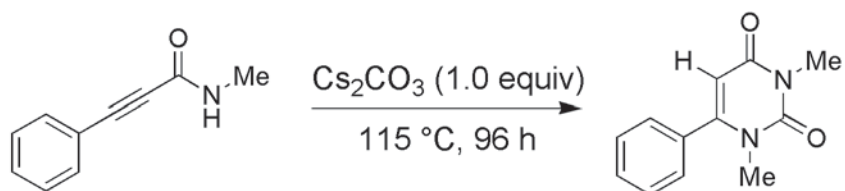
(4.0 equiv) was added to a methyl acrylate solution (1.0 equiv in THF) at room temperature. The reaction mixture was stirred for 15-90 min at room temperature. Then, the reaction mixture was concentrated under reduced pressure to remove remaining volatile amines. The product was collected by the flash column chromatography using a silica gel column with ethyl acetate and hexane as eluting solvents. It should be noted that these syntheses went smoothly except in the case of the desired reagent, *N*-methyl-3-(4-nitrophenyl)-2-propynamide. Repeated attempts were unsuccessful due to a side reaction in which hydroxide nucleophilic addition occurred across the triple bond of the desired *N*-methyl-3-(4-nitrophenyl)-2-propynamide. Hydroxyl addition was followed by keto-enol tautomerization, which generated 90% isolated yields of *N*-methyl-3-(4-nitrophenyl)-3-oxopropanamide as the only observed product.⁶⁶

3.2 General Procedure for the Cs₂CO₃-promoted dimerizations of **1a-h, m** to 6-substituted-uracils

All reactions were performed under air in airtight screw head reaction tubes with constant stirring on a Cole-Parmer aluminum metal block on a hot plate at 115 °C for 96-120 h. *N*-R₁-3-R₂-2-propynamides **1a-h, m** (0.4 mmol, 1.0 equiv), Cs₂CO₃ (0.4 mmol, 1.0 equiv), and anhydrous toluene (2.5 mL) were placed in the reaction tube. After the reaction, the contents were cooled to room temperature, and solvent was removed under reduced pressure. This crude product was then purified by flash column chromatography using a silica gel column with ethyl acetate and hexane as eluting solvents.

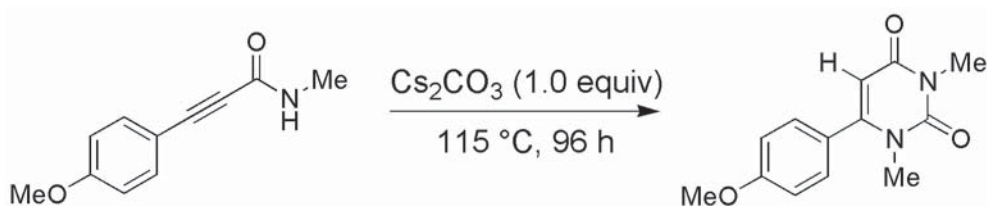
Uracils **3a**,³⁻⁷ **3b**,^{6,7} **3c**,^{6,7} **3d**,^{5,6} **3e**,^{5,6} and **3g**³ are known, and their characterization data (1H NMR, 13C NMR, HRMS, IR and mp) matched those reported in the literature.

Complete analytical characterization data for the uracil analogues **3a-h**, and **3m** are reported below.



Scheme 3.1 Synthesis of 1,3-dimethyl-6-phenylpyrimidine-2,4(1H,3H)-dione (**3a**)

1,3-Dimethyl-6-phenylpyrimidine-2,4(1H,3H)-dione (3a).³⁻⁷ Purification was carried out by flash column chromatography to obtain **3a** as a white solid (40 mg, 93% isolated yield); mp 98-100 °C; ¹H NMR (CDCl₃, 300 MHz) δ 7.51-7.47 (m, 3H), 7.35-7.32 (m, 2H), 5.70 (s, 1H), 3.41 (s, 3H), 2.23 (s, 3H); ¹³C NMR (CDCl₃, 150 MHz) δ 162.5, 154.7, 152.7, 133.4, 130.2, 129.0, 127.8, 102.5, 34.6, 28.1; FT-IR was recorded using the solid: 3103, 3057, 2930, 1689, 1637, 1602, 1447, 1429 cm⁻¹; HRMS (ESI) m/z; calcd for C₁₂H₁₂N₂NaO₂ [M+Na]⁺ 239.0791, found 239.0792.

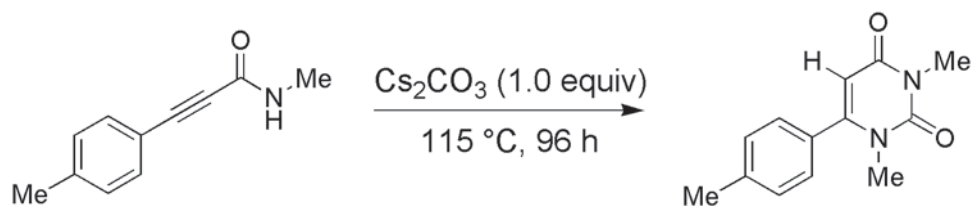


Scheme 3.2 Synthesis of 6-(4-methoxyphenyl)-1,3-dimethylpyrimidine-2,4(1H,3H)-dione (**3b**)

6-(4-Methoxyphenyl)-1,3-dimethylpyrimidine-2,4(1H,3H)-dione (3b).^{6,7}

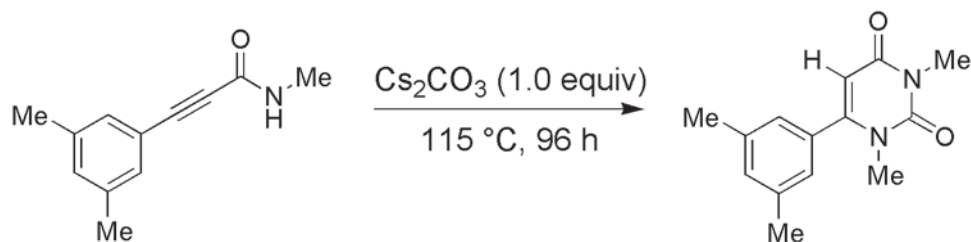
Purification was carried out by flash column chromatography to obtain **3b** as a white solid (46 mg, 94% isolated yield); mp 105-107 °C; ¹H NMR (CDCl₃, 600 MHz) δ 7.27-

2.26 (m, 2H), 6.99 (d, 2H, $J = 9.0$ Hz), 5.68 (s, 1H), 3.87 (s, 3H), 3.40 (s, 3H), 3.25 (s, 3H); ^{13}C NMR (CDCl_3 , 150 MHz) δ 162.7, 161.1, 154.7, 153.0, 129.4, 125.7, 114.5, 102.5, 55.6, 34.8, 28.2; FT-IR was recorded using the solid: 3074, 3010, 2942, 2840, 1688, 1643, 1603, 1430, 1251, 1027 cm^{-1} ; HRMS (ESI) m/z ; calcd for $\text{C}_{13}\text{H}_{14}\text{N}_2\text{NaO}_3$ $[\text{M}+\text{Na}]^+$ 269.0897, found 269.0898.



Scheme 3.3 Synthesis of 6-(4-methylphenyl)-1,3-dimethylpyrimidine-2,4(1H,3H)-dione (**3c**)

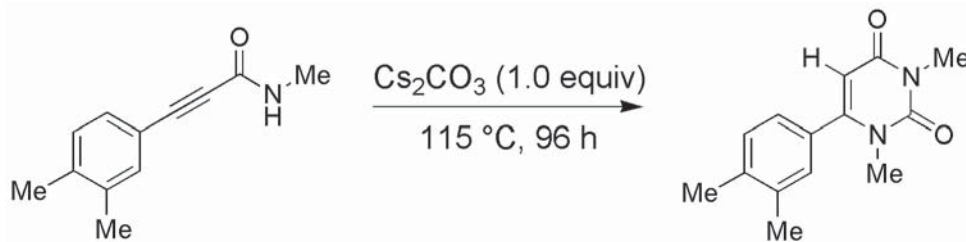
6-(4-Methylphenyl)-1,3-dimethylpyrimidine-2,4(1H,3H)-dione (**3c**).^{6,7} Purification was carried out by flash column chromatography to obtain **3c** as a white solid (43 mg, 93% isolated yield); mp 108-110 $^\circ\text{C}$; ^1H NMR (CDCl_3 , 600 MHz) δ 7.28 (d, 2H, $J = 7.2$ Hz), 7.21 (d, 2H, $J = 7.2$ Hz), 5.68 (s, 1H), 3.41 (s, 3H), 3.23 (s, 3H), 1.54 (s, 3H); ^{13}C NMR (CDCl_3 , 150 MHz) δ 162.7, 154.9, 152.9, 140.6, 130.7, 129.8, 127.8, 102.5, 34.7, 28.2, 21.5; FT-IR was recorded using the solid: 3094, 2947, 2923, 1697, 1648, 1618, 1430 cm^{-1} ; HRMS (ESI) m/z ; calcd for $\text{C}_{13}\text{H}_{14}\text{N}_2\text{NaO}_2$ $[\text{M}+\text{Na}]^+$ 253.0947, found 253.0948.



Scheme 3.4 Synthesis of 6-(3,5-dimethylphenyl)-1,3-dimethylpyrimidine-2,4(1H,3H)-dione (**3d**)

6-(3,5-Dimethylphenyl)-1,3-dimethylpyrimidine-2,4(1H,3H)-dione (3d).^{5,6}

Purification was carried out by flash column chromatography to obtain **3d** as a white solid (46 mg, 94% isolated yield); mp 174-176 °C; ¹H NMR (CDCl₃, 600 MHz) δ 7.12 (s, 1H), 6.93 (s, 2H), 5.67 (s, 1H), 3.40 (s, 3H), 3.22 (s, 3H), 2.37 (s, 6H); ¹³C NMR (CDCl₃, 150 MHz) δ 162.6, 155.1, 152.8, 138.8, 133.4, 131.8, 125.4, 102.2, 34.6, 28.0, 21.3; FT-IR was recorded using the solid: 2956, 2919, 1698, 1647, 1614, 1433 cm⁻¹; HRMS (ESI) m/z; calcd for C₁₄H₁₆N₂NaO₂ [M+Na]⁺ 267.1104, found 267.1106.

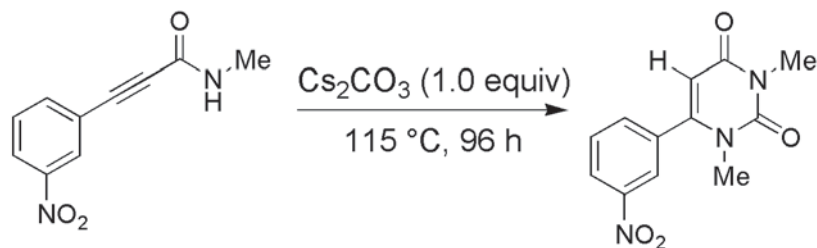


Scheme 3.5 Synthesis of 6-(3,4-dimethylphenyl)-1,3-dimethylpyrimidine-2,4(1H,3H)-dione (**3e**)

6-(3,4-Dimethylphenyl)-1,3-dimethylpyrimidine-2,4(1H,3H)-dione (3e).^{5,6}

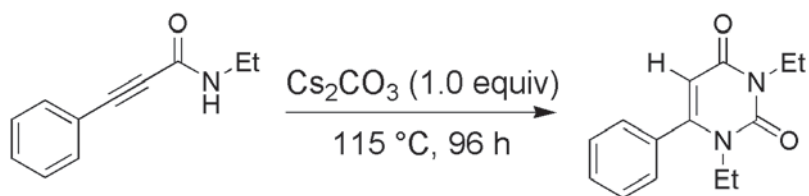
Purification was carried out by flash column chromatography to obtain **3e** as a white solid (46 mg, 94% isolated yield); mp 112-114 °C; ¹H NMR (CDCl₃, 600 MHz) δ 7.23 (d, 1H, *J* = 7.2 Hz), 7.09 (s, 1H), 7.05 (d, 1H, *J* = 7.2 Hz), 5.67 (s, 1H), 3.40 (s, 3H), 3.23 (s, 3H),

2.32 (s, 6H, broad singlet overlap of 2CH₃ signals); ¹³C NMR (CDCl₃, 150 MHz) δ 162.6, 155.0, 152.8, 139.1, 137.5, 131.0, 130.1, 128.8, 125.2, 102.3, 34.6, 28.0, 19.9, 19.7; FT-IR was recorded using the solid: 3053, 2944, 1698, 1644, 1617, 1478, 1433 cm⁻¹; HRMS (ESI) m/z; calcd for C₁₄H₁₆N₂NaO₂ [M+Na]⁺ 267.1104, found 267.1105.



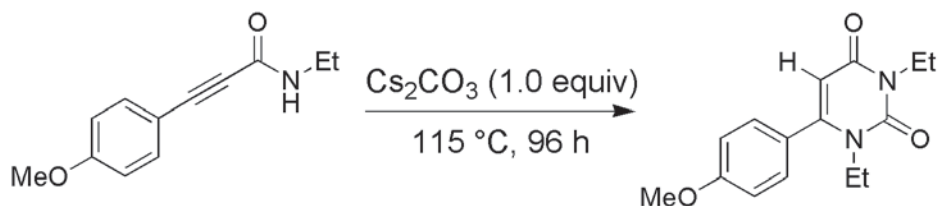
Scheme 3.6 Synthesis of 1,3-dimethyl-6-(3-nitrophenyl)pyrimidine-2,4(1H,3H)-dione (**3f**)

1,3-Dimethyl-6-(3-nitrophenyl)pyrimidine-2,4(1H,3H)-dione (3f). Purification was carried out by flash column chromatography to obtain **3f** as a yellow solid (50 mg, 96% isolated yield); mp 161-162 °C; ¹H NMR (CDCl₃, 600 MHz) δ 8.39 (d, 1H, *J* = 7.8 Hz), 8.26 (s, 1H), 7.76-7.70 (m, 2H), 5.74 (s, 1H), 3.42 (s, 3H), 3.24 (s, 3H); ¹³C NMR (CDCl₃, 150 MHz) δ 162.0, 152.4, 151.9, 148.5, 134.9, 133.8, 130.6, 125.2, 123.1, 103.5, 34.7, 28.3; FT-IR was recorded using the solid: 3069, 2959, 1693, 1651, 1623, 1525, 1430, 1349 cm⁻¹; HRMS (ESI) m/z; calcd for C₁₂H₁₁N₃NaO₄ [M+Na]⁺ 284.0642, found 284.0643.



Scheme 3.7 Synthesis of 1,3-diethyl-6-phenylpyrimidine-2,4(1H,3H)-dione (**3g**)

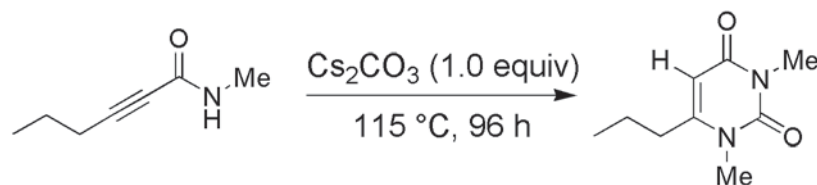
1,3-Diethyl-6-phenylpyrimidine-2,4(1H,3H)-dione (3g).³ Purification was carried out by flash column chromatography to obtain **3g** as a white solid (39 mg, 80 % isolated yield); mp 119-121 °C; ¹H NMR (CDCl₃, 300 MHz) δ 7.51-7.46 (m, 3H), 7.36-7.32 (m, 2H), 5.62 (s, 1H), 4.07 (q, 2H, *J* = 6.9 Hz), 3.73 (q, 2H, *J* = 7.2 Hz), 1.29 (t, 3H, *J* = 7.2 Hz), 1.11 (t, 3H, *J* = 6.9 Hz); ¹³C NMR (CDCl₃, 75 MHz) δ 162.1, 154.5, 151.7, 133.6, 130.0, 128.9, 127.8, 103.2, 41.7, 36.6, 14.3, 12.9; FT-IR was recorded using the solid: 3094, 3077, 2973, 2931, 2871, 1695, 1646, 1619, 1447, 1423 cm⁻¹; HRMS (ESI) *m/z*; calcd for C₁₄H₁₆N₂NaO₂ [M+Na]⁺ 267.1104, found 267.1106.



Scheme 3.8 Synthesis of 1,3-diethyl-6-(4-methoxyphenyl)pyrimidine-2,4(1H,3H)-dione (**3h**)

1,3-Diethyl-6-(4-methoxyphenyl)pyrimidine-2,4(1H,3H)-dione (3h). Purification was carried out by flash column chromatography to obtain **3h** as a white solid (40 mg, 73% isolated yield); mp 135-136 °C; ¹H NMR (CDCl₃, 600 MHz) δ 7.27-7.26 (m, 2H), 6.98 (d, 2H, *J* = 8.4 Hz), 5.60 (s, 1H), 4.06 (q, 2H, *J* = 7.2 Hz), 3.87 (s, 3H), 3.75 (q, 2H, *J* = 7.2 Hz), 1.28 (t, 3H, *J* = 7.2 Hz), 1.11 (t, 3H, *J* = 7.2 Hz); ¹³C NMR (CDCl₃, 150

MHz) δ 162.2, 160.8, 154.5, 151.9, 129.3, 125.8, 114.3, 103.3, 55.5, 41.7, 36.6, 14.3, 13.0; FT-IR was recorded using the solid: 3095, 3008, 2982, 2938, 1696, 1647, 1618, 1604, 1432, 1250, 1027 cm^{-1} ; HRMS (ESI) m/z ; calcd for $\text{C}_{15}\text{H}_{18}\text{N}_2\text{NaO}_3$ $[\text{M}+\text{Na}]^+$ 297.1210, found 297.1211.



Scheme 3.9 Synthesis of 1,3-dimethyl-6-propylpyrimidine-2,4(1H,3H)-dione (**3m**)

1,3-Dimethyl-6-propylpyrimidine-2,4(1H,3H)-dione (3m). Purification was carried out by flash column chromatography to obtain **3m** as a white solid (12 mg, 32% isolated yield); mp (heating rate: $1\text{-}2\text{ }^\circ\text{C min}^{-1}$) $52\text{-}53\text{ }^\circ\text{C}$; $^1\text{H NMR}$ (CDCl_3 , 600 MHz) δ 5.61 (s, 1H), 3.41 (s, 3H), 3.34 (s, 3H), 2.45 (t, 2H, $J = 7.8\text{ Hz}$), 1.65 (sextet, 2H, $J = 7.8\text{ Hz}$), 1.05 (t, 3H, $J = 7.8\text{ Hz}$); $^{13}\text{C NMR}$ (CDCl_3 , 150 MHz) δ 162.7, 154.9, 152.9, 100.3, 34.6, 31.4, 28.0, 20.5, 13.7; FT-IR was recorded using solid: 3117, 2967, 2938, 2880, 1692, 1651, 1626, 1435 cm^{-1} ; HRMS (ESI) m/z ; calcd for $\text{C}_9\text{H}_{14}\text{N}_2\text{NaO}_2$ $[\text{M}+\text{Na}]^+$ 205.0947, found 205.0950.

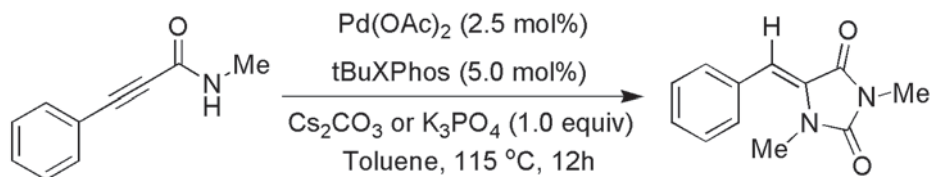
3.3 General Procedure for the K_3PO_4 -promoted dimerizations of **1a-m** to 6-substituted-uracils.

All reactions were performed under air in airtight screw head reaction tubes with constant stirring on a Cole-Parmer Aluminum metal block on a hot plate at $115\text{ }^\circ\text{C}$ for 96 hrs. *N*- R_1 -3- R_2 -2-propynamides **1a-m** (0.1 mmol, 1.0 equiv), K_3PO_4 (0.1 mmol, 1.0 equiv), and anhydrous toluene (2.0 mL) were placed in the reaction tube. The reaction

under reflux was performed in a 25 mL round bottomed flask connected to a water cooling condenser. **1a** (0.6 mmol, 1.0 equiv), K₃PO₄ (0.6 mmol, 1.0 equiv), and anhydrous toluene (10.0 mL) at 115 °C for 120 h were used.

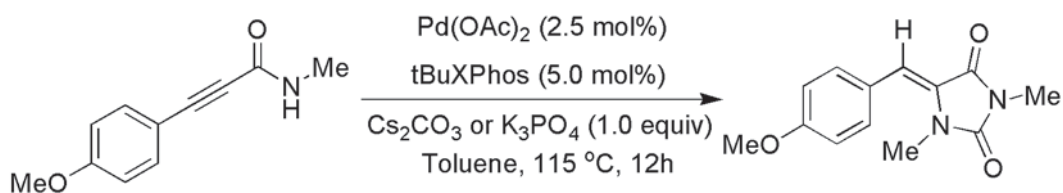
3.4 General procedure for Pd(OAc)₂/tBuXPhos-catalyzed dimerization of *N*-methyl- and *N*-ethyl-3-aryl-2-propynamides promoted by either Cs₂CO₃ or K₃PO₄.

All reactions were performed under the Ar gas in airtight screw head reaction tubes with constant stirring on a Cole-Parmer aluminum metal block on a hot plate at 115 °C for 12-18 h. 3-Aryl-2-propynamides (0.4 mmol, 1.0 equiv) and K₃PO₄ or Cs₂CO₃ (0.4 mmol, 1.0 equiv) were placed in the reaction tubes. Reaction tubes were evacuated and refilled with Ar gas. Finally, 1.0 mL of 0.01 M Pd(OAc)₂ (2.5 mol%), 1.0 mL of 0.02 M tBuXPhos (5.0 mol%), and 2 mL of anhydrous toluene were added to reaction tubes under Ar gas. After the reaction time, reactions were filtered through a plug of silica gel and solution were prepared for GC-MS analysis. Finally, products were purified by flash column chromatography using a silica gel column with ethyl acetate and hexane as eluting solvents. All hydantoin, (*Z*) and (*E*)-**2a-h** were isolated and characterized by ¹H NMR, ¹³C-NMR, HRMS, and NOESY. Characterization data for the uracil analogues (*Z*)-**2a-h** are reported below.



Scheme 3.10 Synthesis of (Z)-5-benzylidene-1,3-dimethylimidazolidine-2,4-dione [(Z)-**2a**]

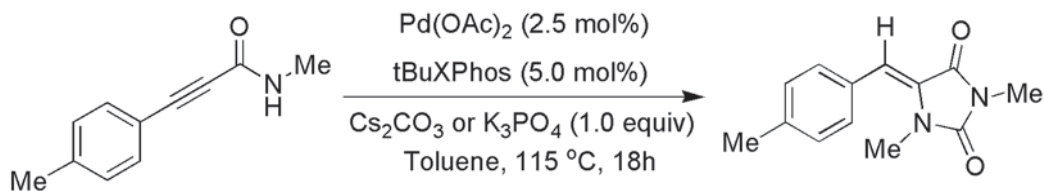
(Z)-5-Benzylidene-1,3-dimethylimidazolidine-2,4-dione [(Z)-**2a**]. Purification was carried out by flash column chromatography to obtain **2a** as a pale yellow color amorphous solid (36 mg, 83% isolated yield); ¹H NMR (CDCl₃, 600 MHz) δ 7.39-7.29 (m, 5H), 6.95 (s, 1H), 3.14 (s, 3H), 2.95 (s, 3H); ¹³C-NMR (CDCl₃, 150 MHz) δ 163.9, 156.1, 132.8, 129.9, 129.6, 128.5, 128.4, 112.5, 30.5, 25.2; HRMS (ESI) m/z; calcd for C₁₂H₁₂N₂NaO₂ [M+Na]⁺ 239.0791, found 239.0794.



Scheme 3.11 Synthesis of (Z)-5-(4-methoxybenzylidene)-1,3-dimethylimidazolidine-2,4-dione [(Z)-**2b**].

(Z)-5-(4-Methoxybenzylidene)-1,3-dimethylimidazolidine-2,4-dione [(Z)-**2b**].⁸

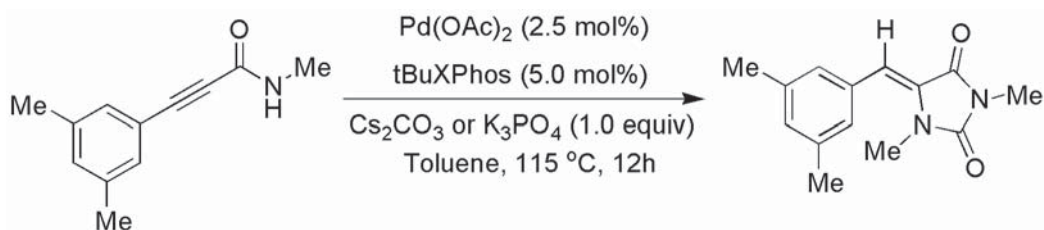
Purification was carried out by flash column chromatography to obtain **2b** as a pale yellow color amorphous solid (43 mg, 87% isolated yield); ¹H NMR (CDCl₃, 600 MHz) δ 7.24 (d, 2H, *J* = 8.4 Hz), 6.92 (d, 2H, *J* = 8.4 Hz), 6.90 (s, 1H), 3.84 (s, 3H), 3.14 (s, 3H), 3.00 (s, 3H); ¹³C NMR (CDCl₃, 150 MHz) δ 164.0, 159.8, 156.2, 131.1, 128.8, 124.8, 113.8, 112.8, 55.4, 30.7, 25.2; HRMS (ESI) m/z; calcd for C₁₃H₁₄N₂NaO₃ [M+Na]⁺ 269.0897, found 269.0895.



Scheme 3.12 Synthesis of (Z)-5-(4-methylbenzylidene)-1,3-dimethylimidazolidine-2,4-dione [(Z)-**2c**]

*(Z)-5-(4-Methylbenzylidene)-1,3-dimethylimidazolidine-2,4-dione [(Z)-**2c**].*

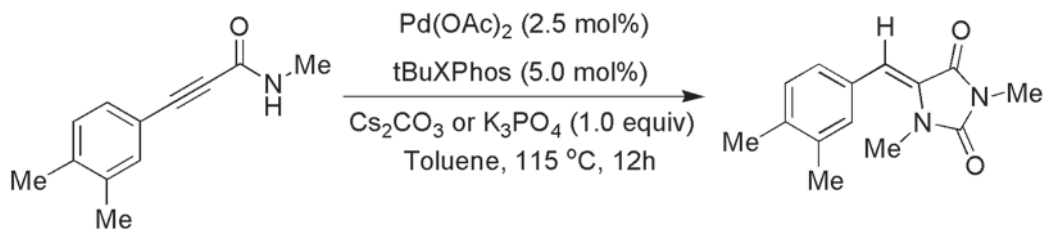
Purification was carried out by flash column chromatography to obtain **2c** as a pale yellow color amorphous solid (32 mg, 70% isolated yield); ¹H NMR (CDCl₃, 600 MHz) δ 7.21-7.19 (m, 4H), 6.92 (s, 1H), 3.13 (s, 3H), 2.97 (s, 3H), 2.38 (s, 3H); ¹³C NMR (CDCl₃, 150 MHz) δ 164.0, 156.1, 138.6, 129.8, 129.6, 129.5, 129.1, 112.8, 30.6, 25.2, 21.5; HRMS (ESI) m/z; calcd for C₁₃H₁₄N₂NaO₂ [M+Na]⁺ 253.0947, found 253.0946.



Scheme 3.13 Synthesis of (Z)-5-(3,5-dimethylbenzylidene)-1,3-dimethylimidazolidine-2,4-dione [(Z)-**2d**]

*(Z)-5-(3,5-Dimethylbenzylidene)-1,3-dimethylimidazolidine-2,4-dione [(Z)-**2d**].*

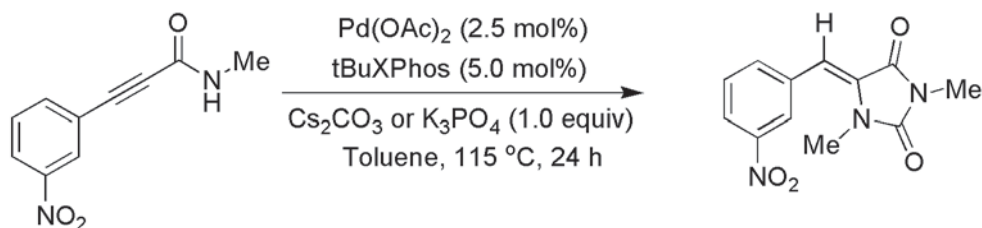
Purification was carried out by flash column chromatography to obtain **2d** as a pale yellow color amorphous solid (44 mg, 90% isolated yield); ¹H NMR (CDCl₃, 600 MHz) δ 6.97 (s, 1H), 6.90 (m, 3H), 3.14 (s, 3H), 2.96 (s, 3H), 2.33 (s, 6H); ¹³C NMR (CDCl₃, 150 MHz) δ 164.0, 156.1, 137.9, 132.6, 130.2, 129.6, 127.4, 113.0, 30.6, 25.2, 21.4; HRMS (ESI) m/z; calcd for C₁₄H₁₆N₂NaO₂ [M+Na]⁺ 267.1104, found 267.1103.



Scheme 3.14 Synthesis of (Z)-5-(3,4-dimethylbenzylidene)-1,3-dimethylimidazolidine-2,4-dione [(Z)-**2e**]

(Z)-5-(3,4-Dimethylbenzylidene)-1,3-dimethylimidazolidine-2,4-dione [(Z)-**2e**].

Purification was carried out by flash column chromatography to obtain **2e** as a pale yellow color amorphous solid (41 mg, 84% isolated yield); ¹H NMR (CDCl₃, 600 MHz) δ 7.14 (d, 1H, *J* = 7.2 Hz), 7.06-7.02 (m, 2H), 6.91 (s, 1H), 3.13 (s, 3H), 2.98 (s, 3H), 2.28 (s, 6H); ¹³C NMR (CDCl₃, 150 MHz) δ 164.1, 156.2, 137.4, 136.6, 130.8, 130.2, 129.6, 129.3, 127.1, 113.1, 30.6, 25.2, 19.9, 19.8; MS (EI) *m/z*; 244.2, 229.1, 159.1, 144.1, 129.1, 115.1; HRMS (ESI) *m/z*; calcd for C₁₄H₁₆N₂NaO₂ [M+Na]⁺ 267.1104, found 267.1102.

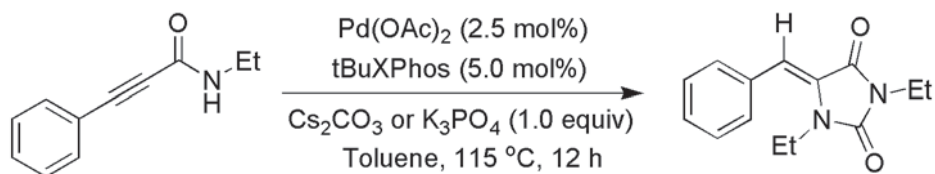


Scheme 3.15 Synthesis of (Z)-5-(3-nitrophenyl)-1,3-dimethylimidazolidine-2,4-dione [(Z)-**2f**]

(Z)-5-(3-Nitrophenyl)-1,3-dimethylimidazolidine-2,4-dione [(Z)-**2f**]. Purification

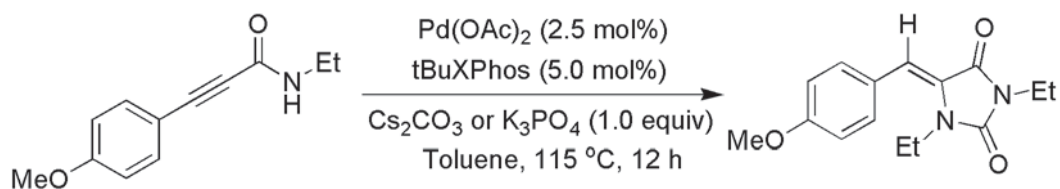
was carried out by flash column chromatography to obtain **2f** as a pale yellow color

amorphous solid (41 mg, 78% isolated yield); ¹H NMR (CDCl₃, 600 MHz) δ 8.20 (d, 1H, *J* = 9 Hz), 8.16 (s, 1H), 7.63-7.57 (m, 2H), 6.88 (s, 1H), 3.16 (s, 3H), 2.96 (s, 3H); ¹³C NMR (CDCl₃, 150 MHz) δ 163.4, 155.8, 148.3, 135.3, 134.8, 131.6, 129.5, 124.3, 123.2, 108.5, 30.6, 25.4; MS (EI) *m/z*; 161, 215, 176, 130, 103, 89; HRMS (ESI) *m/z*; calcd for C₁₂H₁₁N₃NaO₄ [M+Na]⁺ 284.0642, found 284.0641.



Scheme 3.16 Synthesis of (Z)-5-benzylidene-1,3-diethylimidazolidine-2,4-dione [(Z)-**2g**]

(Z)-5-Benzylidene-1,3-diethylimidazolidine-2,4-dione [(Z)-**2g**]; Purification was carried out by flash column chromatography to obtain **2g** as a pale yellow color amorphous solid (39 mg, 80% isolated yield); ¹H NMR (CDCl₃, 600 MHz) δ 7.40-7.30 (m, 5H), 6.94 (s, 1H), 3.68 (q, 2H, *J* = 7.2 Hz), 3.58 (q, 2H, *J* = 7.2 Hz), 1.28 (t, 3H, *J* = 7.2 Hz), 0.77 (t, 3H, *J* = 7.2 Hz); ¹³C NMR (CDCl₃, 150 MHz) δ 164.0, 155.4, 133.2, 129.2, 128.5, 128.4, 128.4, 112.1, 36.8, 34.3, 13.7, 13.0; MS (EI) *m/z*; 244, 215, 158, 130, 177; HRMS (ESI) *m/z*; calcd for C₁₄H₁₆N₂NaO₂ [M+Na]⁺ 267.1104, found 267.1102.



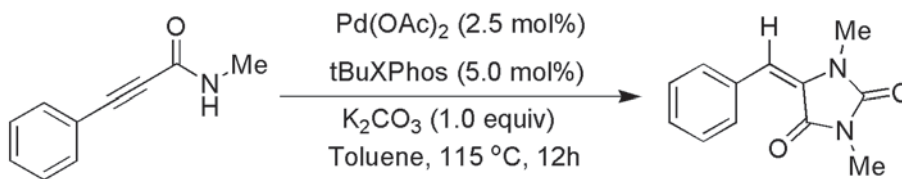
Scheme 3.17 Synthesis of (*Z*)-5-(4-methoxybenzylidene)-1,3-diethylimidazolidine-2,4-dione [(*Z*)-**2h**].

(Z)-5-(4-Methoxybenzylidene)-1,3-diethylimidazolidine-2,4-dione [(*Z*)-**2h**].

Purification was carried out by flash column chromatography to obtain **2h** as a pale yellow color amorphous solid (50 mg, 91% isolated yield); ¹H NMR (CDCl₃, 600 MHz) δ 7.24 (d, 2H, *J* = 8.4 Hz), 6.92-6.89 (m, 3H), 3.84 (s, 3H), 3.69-3.61 (m, 4H), 1.27 (t, 3H, *J* = 7.2 Hz), 0.80 (t, 3H, *J* = 7.2 Hz); ¹³C NMR (CDCl₃, 150 MHz) δ 164.1, 159.8, 155.6, 130.7, 127.6, 125.4, 113.9, 112.5, 55.5, 36.9, 34.2, 13.7, 13.0; HRMS (ESI) *m/z*; calcd for C₁₅H₁₈N₂NaO₃ [M+Na]⁺ 297.1210, found 297.1208.

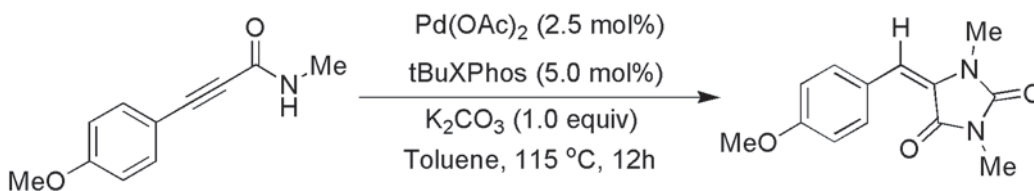
3.5 General procedure for Pd(OAc)₂/tBuXPhos-catalyzed dimerization of *N*-methyl- and *N*-ethyl-3-aryl-2-propynamides promoted by K₂CO₃.

The synthesis procedure was exactly to similar to the Pd(OAc)₂/tBuXPhos-catalyzed dimerization of *N*-methyl- and *N*-ethyl-3-aryl-2-propynamides promoted by either Cs₂CO₃ or K₃PO₄. K₂CO₃ was used instead of Cs₂CO₃ or K₃PO₄. Reactions were performed for at least 72 h. The *E*-hydantoin, (*E*)-**2a-c**, **e-g** were isolated and characterized by ¹H NMR, ¹³C-NMR, HRMS, and NOESY. Characterization data for the uracil analogues (*E*)-**2a-h** are reported below.



Scheme 3.18 Synthesis of (*E*)-5-benzylidene-1,3-dimethylimidazolidine-2,4-dione [(*E*)-**2a**]

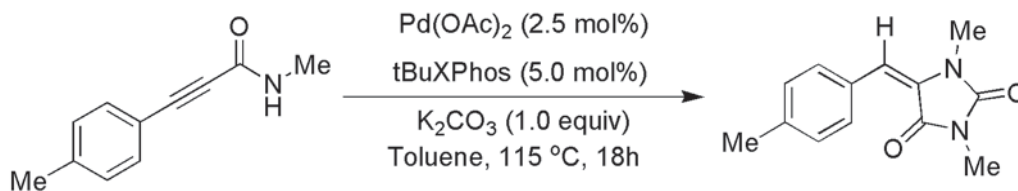
(*E*)-5-Benzylidene-1,3-dimethylimidazolidine-2,4-dione [(*E*)-**2a**]. Purification was carried out by flash column chromatography to obtain **2a** as a pale yellow color amorphous solid (37 mg, 85% isolated yield); ¹H NMR (CDCl₃, 600 MHz) δ 7.89 (s, 3H, *J*=7.2 Hz), 7.40-7.33 (m, 3H), 6.24 (s, 1H), 3.25 (s, 3H), 3.12 (s, 3H); ¹³C-NMR (CDCl₃, 150 MHz) δ 161.8, 153.9, 132.5, 130.3, 129.4, 129.1, 128.4, 117.2, 26.5, 24.8; HRMS (ESI) *m/z*; calcd for C₁₂H₁₂N₂NaO₂ [M+Na]⁺ 239.0791, found 239.0789.



Scheme 3.19 Synthesis of (*E*)-5-(4-methoxybenzylidene)-1,3-dimethylimidazolidine-2,4-dione [(*E*)-**2b**].

(*E*)-5-(4-Methoxybenzylidene)-1,3-dimethylimidazolidine-2,4-dione [(*E*)-**2b**].⁸

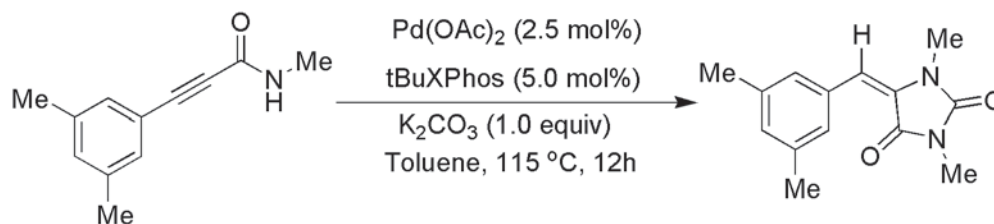
Purification was carried out by flash column chromatography to obtain **2b** as a pale yellow color amorphous solid (42 mg, 85% isolated yield); ¹H NMR (CDCl₃, 600 MHz) δ 7.94 (d, 2H, *J* = 8.4 Hz), 6.91 (d, 2H, *J* = 8.4 Hz), 6.19 (s, 1H), 3.84 (s, 3H), 3.22 (s, 3H), 3.12 (s, 3H); ¹³C NMR (CDCl₃, 150 MHz) δ 162.0, 160.4, 153.8, 132.2, 127.7, 125.3, 117.6, 113.8, 55.4, 26.5, 24.8; HRMS (ESI) *m/z*; calcd for C₁₃H₁₄N₂NaO₃ [M+Na]⁺ 269.0897, found 269.0896.



Scheme 3.20 Synthesis of (*E*)-5-(4-methylbenzylidene)-1,3-dimethylimidazolidine-2,4-dione [(*E*)-**2c**]

(*E*)-5-(4-Methylbenzylidene)-1,3-dimethylimidazolidine-2,4-dione [(*E*)-**2c**].

Purification was carried out by flash column chromatography to obtain **2c** as a pale yellow color amorphous solid (27 mg, 58% isolated yield); ¹H NMR (CDCl₃, 600 MHz) δ 7.82 (d, 2H, *J* = 8.4 Hz), 7.19 (d, 2H, *J* = 8.4 Hz), 6.22 (s, 1H), 3.23 (s, 3H), 3.12 (s, 3H), 2.37 (s, 3H); ¹³C NMR (CDCl₃, 150 MHz) δ 161.9, 153.8, 139.5, 130.4, 129.8, 129.2, 128.7, 117.6, 26.5, 24.5, 21.6; HRMS (ESI) *m/z*; calcd for C₁₃H₁₄N₂NaO₂ [M+Na]⁺ 253.0947, found 253.0945.

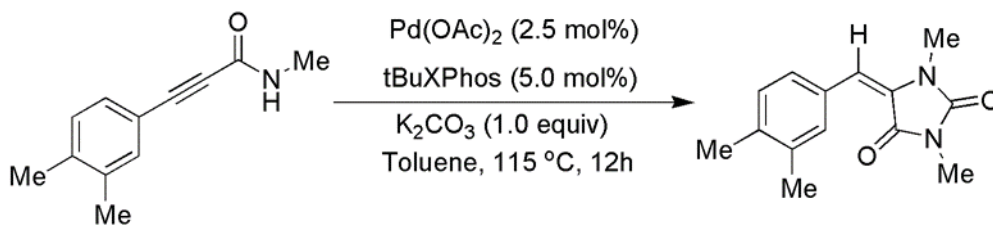


Scheme 3.21 Synthesis of (*E*)-5-(3,5-dimethylbenzylidene)-1,3-dimethylimidazolidine-2,4-dione [(*E*)-**2d**]

(*E*)-5-(3,5-Dimethylbenzylidene)-1,3-dimethylimidazolidine-2,4-dione [(*E*)-**2d**].

Purification was carried out by flash column chromatography to obtain **2d** as a pale yellow color amorphous solid (34 mg, 70% isolated yield); ¹H NMR (CDCl₃, 600 MHz) δ 7.55 (s, 2H), 6.99 (s, 1H), 6.19 (s, 1H), 3.22 (s, 3H), 3.12 (s, 3H), 2.37 (s, 3H); MS (EI)

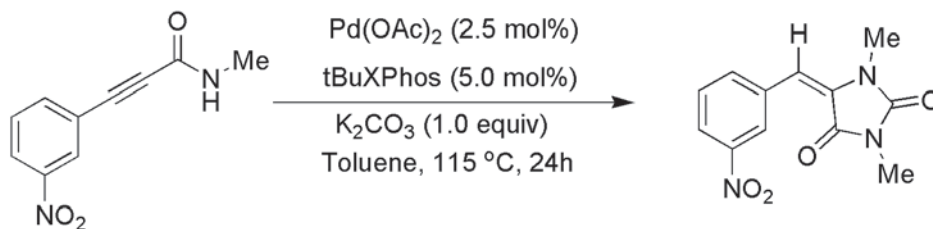
m/z; 244.2, 229.1, 159.1, 144.1, 129.1, 115.1, 91.0, 77.1; HRMS (ESI) m/z; calcd for C₁₄H₁₆N₂NaO₂ [M+Na]⁺ 267.1104, found 267.1110.



Scheme 3.22 Synthesis of (*E*)-5-(3,4-dimethylbenzylidene)-1,3-dimethylimidazolidine-2,4-dione [(*E*)-**2e**]

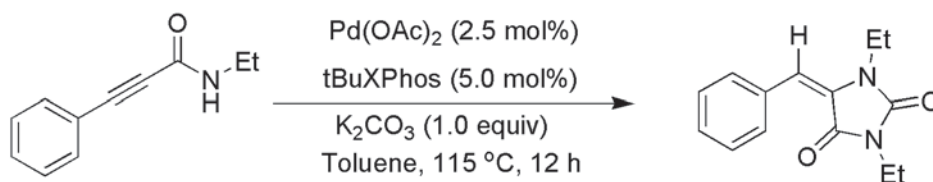
(E)-5-(3,4-Dimethylbenzylidene)-1,3-dimethylimidazolidine-2,4-dione [(*E*)-**2e**].

Purification was carried out by flash column chromatography to obtain **2e** as a pale yellow color amorphous solid (32 mg, 65% isolated yield); ¹H NMR (CDCl₃, 600 MHz) δ 7.70-7.69 (m, 2H), 7.16-7.14 (m, 1H), 6.20 (s, 1H), 3.22 (s, 3H), 3.12 (s, 3H), 2.29 (s, 6H); ¹³C NMR (CDCl₃, 150 MHz) δ 161.9, 153.9, 138.3, 136.6, 131.6, 130.1, 129.8, 128.0, 128.6, 117.8, 26.5, 24.8, 19.9; HRMS (ESI) m/z; calcd for C₁₄H₁₆N₂NaO₂ [M+Na]⁺ 267.1104, found 267.1107.



Scheme 3.23 Synthesis of *(E)*-5-(3-nitrophenyl)-1,3-dimethylimidazolidine-2,4-dione [(*E*)-**2f**]

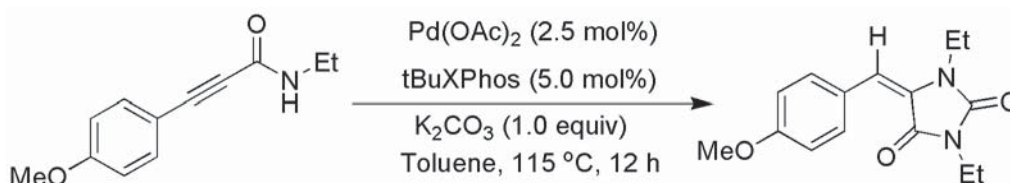
(E)-5-(3-Nitrophenyl)-1,3-dimethylimidazolidine-2,4-dione [(*E*)-**2f**]. Purification was carried out by flash column chromatography to obtain **2f** as a pale yellow color amorphous solid (30 mg, 57% isolated yield); ¹H NMR (CDCl₃, 600 MHz) δ 8.72 (s, 1H), 8.20-8.15 (m, 2H), 7.54 (t, 1H, *J* = 7.8 Hz), 6.21 (s, 1H), 3.26 (s, 3H), 3.13 (s, 3H); ¹³C NMR (CDCl₃, 150 MHz) δ 161.7, 153.8, 148.4, 135.8, 134.3, 131.6, 129.2, 125.1, 123.4, 113.3, 26.6, 25.0; calcd for C₁₂H₁₁N₃NaO₄ [M+Na]⁺ 284.0642, found 284.0639.



Scheme 3.24 Synthesis of *(E)*-5-benzylidene-1,3-diethylimidazolidine-2,4-dione [(*E*)-**2g**]

(E)-5-Benzylidene-1,3-diethylimidazolidine-2,4-dione [(*E*)-**2g**]; Purification was carried out by flash column chromatography to obtain **2g** as a pale yellow color amorphous solid (26 mg, 53% isolated yield); ¹H NMR (CDCl₃, 600 MHz) δ 7.87 (d, 2H, *J* = 7.8 Hz), 7.38 (d, 2H, *J* = 7.8 Hz), 7.33 (d, 1H, *J* = 7.8 Hz), 6.27 (s, 1H), 3.79 (q, 2H, *J* = 7.2 Hz), 3.66 (q, 2H, *J* = 7.2 Hz), 1.30-1.22 (m, 6H); ¹³C NMR (CDCl₃, 150 MHz) δ

161.7, 153.3, 132.6, 130.3, 129.0, 128.3, 128.0, 116.6, 34.7, 33.9, 13.7, 12.9; HRMS (ESI) m/z; calcd for C₁₄H₁₆N₂NaO₂ [M+Na]⁺ 267.1104, found 267.1102.



Scheme 3.25 Synthesis of (*E*)-5-(4-methoxybenzylidene)-1,3-diethylimidazolidine-2,4-dione [(*E*)-**2h**]

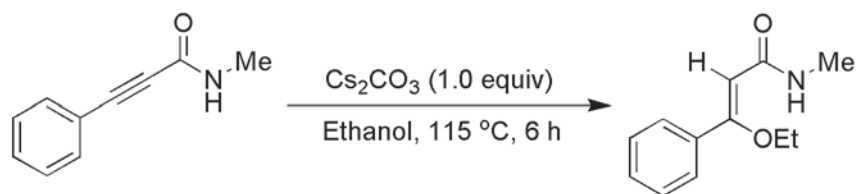
(*E*)-5-(4-Methoxybenzylidene)-1,3-diethylimidazolidine-2,4-dione [(*E*)-**2h**].

Purification was carried out by flash column chromatography to obtain **2h** as a pale yellow color amorphous solid (32 mg, 58% isolated yield); ¹H NMR (CDCl₃, 600 MHz) δ 7.93 (d, 2H, *J* = 8.4 Hz), 6.91 (d, 2H, *J* = 8.4 Hz), 6.22 (s, 1H), 3.84 (s, 3H), 3.77 (q, 2H, *J* = 7.8 Hz), 3.66 (q, 2H, *J* = 7.2 Hz), 1.29-1.25 (m, 6H); ¹³C NMR (CDCl₃, 150 MHz) δ 161.9, 160.3, 153.2, 132.2, 126.3, 125.4, 117.1, 113.8, 55.5, 34.6, 33.8, 13.7, 13.0; HRMS (ESI) m/z; calcd for C₁₅H₁₈N₂NaO₃ [M+Na]⁺ 297.1210, found 297.1215.

3.6 General procedure for the dimerization of **1a** in ethanol

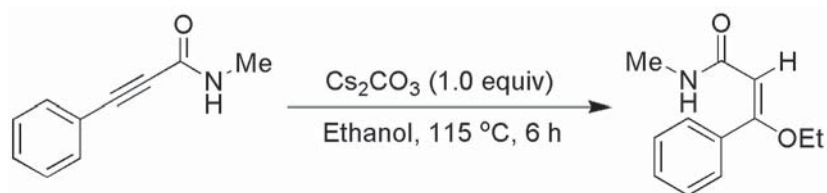
This reaction was conducted under air in airtight screw head reaction tube with constant stirring on a Cole-Parmer aluminum metal block on a hot plate at 115 °C for 6 h. **1a** (0.4 mmol, 1.0 equiv) and Cs₂CO₃ (0.4 mmol, 1.0 equiv) in ethanol (2.5 mL) were placed in the reaction tube. After 6 h, the reaction mixture was cooled to room temperature, and solvent was removed under reduced pressure to give a crude mixture. This crude reaction mixture could not be successfully separated by column chromatography after several tries, so the products were purified by TLC separation and

removing silica from the TLC plates. Analytical characterization data for the uracil analogues (*Z*)-**21** and (*E*)-**21** are reported below.



Scheme 3.26 Synthesis of (*Z*)-3-ethoxy-*N*-methyl-3-phenyl-2-propenamide [(*Z*)-**21**].

(*Z*)-3-Ethoxy-*N*-methyl-3-phenyl-2-propenamide [(*Z*)-**21**]. The compound was isolated by removing silica from TLC plates after development to obtain (*Z*)-**21** as a colorless liquid (33 mg, 40 % isolated yield); $R_f = 0.63$ (ethyl acetate/hexane 99:1); ^1H NMR (CDCl_3 , 600 MHz) δ 7.54 (s, 1H, N-H), 7.45-7.40 (m, 5H), 5.52 (s, 1H), 3.89 (q, 2H, $J = 7.2$ Hz), 2.93 (d, 3H), 1.31 (t, 3H, $J = 7.2$ Hz); ^{13}C NMR (CDCl_3 , 150 MHz) δ 166.8, 161.8, 134.4, 130.0, 128.8, 127.5, 108.8, 67.2, 26.1, 15.4; FT-IR recorded in DCM: 3419, 3056, 2982, 1653, 1611, 1265, 1054 cm^{-1} ; HRMS (ESI) m/z ; calcd for $\text{C}_{12}\text{H}_{15}\text{N}_1\text{NaO}_2$ [$\text{M}+\text{Na}$] $^+$ 228.0995, found 228.0996.



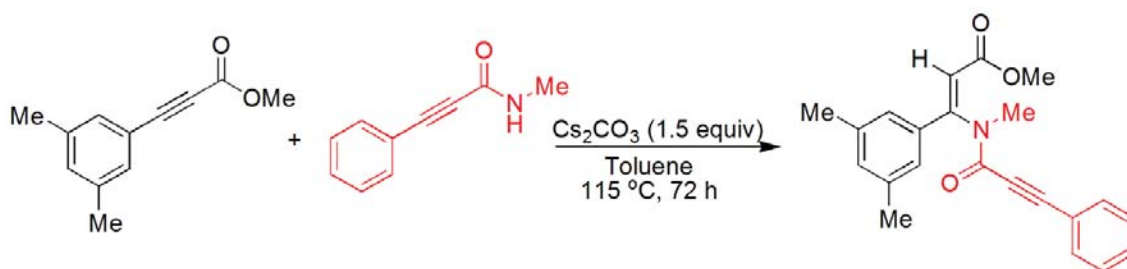
Scheme 3.27 Synthesis of (*E*)-3-ethoxy-*N*-methyl-3-phenyl-2-propenamide [(*E*)-**21**].

(*E*)-3-Ethoxy-*N*-methyl-3-phenyl-2-propenamide [(*E*)-**21**]. The compound was isolated by removing silica from TLC plates after development to obtain (*E*)-**21** as a

colorless liquid (15 mg, 18 % isolated yield); $R_f = 0.54$ (ethyl acetate/hexane 99:1); ^1H NMR (CDCl_3 , 600 MHz) δ 7.46-7.38 (m, 5H), 5.23 (s, 1H), 5.03 (s, 1H, N-H), 3.93 (q, 2H, $J = 7.2$ Hz), 2.63 (d, 3H), 1.40 (t, 3H, $J = 7.2$ Hz); ^{13}C NMR (CDCl_3 , 150 MHz) δ 168.0, 164.1, 135.3, 129.9, 128.8, 128.4, 97.6, 64.4, 26.4, 14.5; FT-IR recorded in DCM: 3457, 3056, 2984, 1645, 1619, 1264, 1076 cm^{-1} ; HRMS (ESI) m/z ; calcd for $\text{C}_{12}\text{H}_{15}\text{N}_1\text{NaO}_2$ $[\text{M}+\text{Na}]^+$ 228.0995, found 228.0993.

3.7 General procedure for the synthesis of intermediate **23**

Reaction was conducted under air in airtight screw head reaction tube with constant stirring on a Cole-Parmer aluminum metal block on a hot plate at 115 °C for 72 hrs. Methyl 3-(3,5-dimethylphenyl)-2-propynate (0.75 mmol, 1.5 equiv), *N*-methyl-3-phenyl-2-propynamide **1a** (0.5 mmol, 1.0 equiv), Cs_2CO_3 (0.75 mmol, 1.5 equiv), and 5 mL of toluene were placed in the reaction tube. Crude mixture was purified using a silica gel column using hexane and ethyl acetate (1:1) as eluting solvent mixture. Analytical characterization data are given below.



Scheme 3.28 (Z)-Methyl 3-(3,5-dimethylphenyl)-3-(*N*-methyl-3-phenyl-2-propynamido)acrylate, **23**

(Z)-Methyl 3-(3,5-dimethylphenyl)-3-(*N*-methyl-3-phenyl-2-propynamido)acrylate, **23**. Purification was carried out by flash column chromatography

to obtain **23** as a pale yellow color liquid (108 mg, 65% isolated yield); ¹H NMR (CDCl₃, 600 MHz) δ 7.35-7.27 (m, 5H), 7.13-7.10 (m, 3H), 6.35 (s, 1H), 3.77 (s, 3H), 3.14 (s, 3H), 2.35 (s, 3H); ¹³C NMR (CDCl₃, 150 MHz) δ 165.1, 154.4, 152.8, 140.0, 135.2, 132.9, 132.6, 130.1, 128.5, 125.3, 120.6, 115.8, 88.9, 82.0, 52.0, 34.5, 21.4; HRMS (ESI) m/z; calcd for C₂₂H₂₁NNaO₃ [M+Na]⁺ 370.1414, found 370.1410.

3.8 Determination of concentration of the K₃PO₄ in toluene at 115 °C.

K₃PO₄ (0.5198 g) was added to 5 mL of toluene in screwhead cultural tube. It was stirred for 1 h at 115 °C. After 1 h, the solution was immediately filtered hot and the K₃PO₄ solid on the filter was dried before recording the mass (0.5151 g). The concentration of K₃PO₄ in toluene at 115 °C was back-calculated to be 940 ppm.

3.9 References

- (1) Anastasia, L.; Negishi, E.-i. *Org. Lett.* **2001**, *3*, 3111.
- (2) Strübing, D.; Neumann, H.; Klaus, S.; Hübner, S.; Beller, M. *Tetrahedron* **2005**, *61*, 11333.
- (3) Mondal, B.; Hazra, S.; Roy, B. *Tetrahedron Lett.* **2014**, *55*, 1077.
- (4) Shih, Y.-C.; Chien, T.-C. *Tetrahedron* **2011**, *67*, 3915.
- (5) Kim, K. H.; Lee, H. S.; Kim, S. H.; Kim, J. N. *Tetrahedron Lett.* **2012**, *53*, 1323.
- (6) Kim, K. H.; Lee, H. S.; Kim, J. N. *Tetrahedron Lett.* **2011**, *52*, 6228.
- (7) Čerňová, M.; Pohl, R.; Hocek, M. *Eur. J. Org. Chem.* **2009**, *2009*, 3698.
- (8) Martínez-López, D.; Yu, M.-L.; García-Iriepa, C.; Campos, P. J.; Frutos, L. M.; Golen, J. A.; Rasapalli, S.; Sampedro, D. *J. Org. Chem.* **2015**, *80*, 3929.

CHAPTER IV

EXTRACTION AND QUANTIFICATION OF XYLITOL IN SUGAR FREE GUM SAMPLES BY DIRECT AQUEOUS INJECTION GC-MS

4.1 Abstract

A reliable low-cost method to determine amounts of xylitol in sugar free gum samples has been developed to predict dangerous exposure levels for dogs. Xylitol is generally considered safe for human consumption and is frequently used in sugar free gum, however, it is extremely toxic to dogs. It is unknown if partially consumed chewing gum is also dangerous. A method to determine xylitol content of these sugar free gum samples employing GC-MS with direct aqueous injection (DAI) is presented. This method was successfully applied to over 120 samples including, fresh gum, 5 min, 15 min, and 30 min chewed gum samples. An average of 179.2 mg, 7.8 mg, and 1.1 mg was of xylitol found in the fresh, 5 min and 15 min chewed samples while the 30 min samples were below limits of detection. These results indicate that there is very little danger of xylitol poisoning, even for the smallest of dogs, who consume discarded gum that has been chewed for at least five minutes. Further extension of this work resulted in the development of an undergraduate laboratory experiment (Chapter 5) for upper-level undergraduate chemistry students which teaches calibration methods, xylitol extraction, sample preparation for GC-MS analysis, and data analysis.

4.2 Introduction

Xylitol can be found naturally in low concentrations in fruits, vegetables, mushrooms and sugar cane. It is a sugar alcohol,¹ commonly used as an artificial sweetener or sugar substitute in many “reduced-calorie” foods. D-xylitol is industrially produced in large scale from D-xylose, which is derived from hemicellulose, by either chemical reduction or biosynthesis (Figure 4.1).² The chemical reduction of D-xylose to D-xylitol involves catalytic hydrogenation in the presence of a nickel catalyst at high temperature and pressure. D-xylitol can also be biosynthesized through the microbial conversion of D-xylose by various bacteria, fungi, and yeasts.³

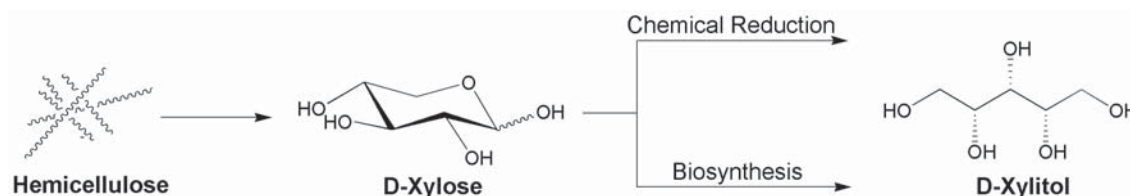


Figure 4.1 Commercial production of xylitol

In food, the primary role of artificial sugar alcohols are to act as sweeteners, but they also influence product texture, preservation, moisture maintenance, and the cooling sensations in the mouth upon consumption.¹ For these many reasons xylitol is extensively utilized in chewing gum and consumers favor xylitol-containing products because of perceived reduction in energy intake which can produce weight loss.^{4,5} Xylitol is safe for diabetics because it stimulates much less insulin release than a comparable quantity of table sugar.¹ Xylitol also helps to prevent dental caries.⁶⁻¹⁰ Diet is a major etiological factor in dental health and limiting the consumption of fermentable carbohydrates and sugars is an effective strategy to control dental caries. Therefore, there is interest in

replacing sucrose in chewing gum with non-fermentable sugars such as xylitol, which prevent the lactic acid production that can result in cavities.⁶⁻¹⁰

Xylitol has a varied safety margin in mammals. The LD₅₀ of xylitol in mice is 20g of xylitol per kilogram¹¹ while it is nontoxic for both cats and humans. While xylitol consumption has been proven to be beneficial to humans, it can be fatal to dogs. Xylitol is rapidly absorbed in dogs, increasing insulin levels within 15 min of ingestion.¹² Hypoglycemia occurs when intracellular transfer of potassium ions is activated by insulin.¹³ A dose of 0.1 g of xylitol per kg of dog has been reported to cause hypoglycemia in dogs within 30-60 minutes of ingestion and some veterinary clinicians have reported liver failure in dogs after 8-12 h.¹² Generally, xylitol ingestion by dogs causes hyperinsulinemia, which can result in vomiting, ataxia, lethargy, weakness, seizures, hypoglycemia, hepatotoxicity, coma, and death.¹¹⁻¹⁶ Thus, ingestion of xylitol containing products such as chewing gum can result in xylitol poisoning in dogs if enough of the product is consumed. Table 4.1 shows the minimum number of gum sticks to provide a toxic dose of xylitol (0.1g of xylitol per kilogram of dog) to cause hypoglycemia.^{15,17,18}

Table 4.1 The amount of xylitol and number of fresh gum sticks that can cause hypoglycemia in dogs.^{15,17,18}

Dog Size	Amount of xylitol to cause hypoglycemia in dog (Dose, 0.1 g of xylitol / kg of dog)	Required gum sticks		
		Ice Breakers, 1.5 g of xylitol/ piece	Stride, 0.2 g of xylitol/piece	Trident, 0.2 g of xylitol/piece
2 kg Chihuahua	0.2 g	1	1	1
4 kg Yorkie	0.4 g	1	2	2
6 kg Jack Russell Terrier	0.6 g	1	3	3
12 kg Border Collie	1.2 g	1	6	6
25 kg Golden Retriever	2.5 g	2	12	12

Xylitol’s presence in chewing gum and other consumer products makes it readily available to dogs with detrimental effects often requiring veterinary care. This study was inspired by many such incidences including this comment posted on the Mother Nature Network (MNN):¹⁹

Direct Quote:¹⁹ *“Please listen, this warning is not nearly as urgent as it needs to be! I never buy low calorie chewing gum, but one day, on a whim, I did. The gum was individually wrapped, inside their box, inside my purse, which I put on my bedroom night table. I went to my home office, and an hour later, when I went back to my bedroom, I found that my lovely girl Sandy (a rescue), had smelled the gum, gotten on top of the bed, then the night table, then taken the pack out of my purse, and eaten at least four pieces of gum. Not knowing anything about Xylitol, I did nothing. She died in my arms a little over 24 hours later. Four pieces of chiclet-sized gum killed my 30lb dog. A week later, I come to find information on Xylitol, and I checked the package, and sure enough, it was an*

ingredient. Had this information been widespread, I would not have bought the gum, or if I had, and she had eaten it, I would have immediately taken her to the vet to have her stomach pumped, which is the ONLY way to save the pup once the Xylitol has been ingested. Please spread this information, so your beloved pet does not die like mine did.”

Today, many dog-owning customers are aware of the risks associate with xylitol containing chewing gums. However, there remains some uncertainty as to whether or not these chewing gums are still dangerous to dogs after they have been partially consumed. The primary goal of this study was to provide conclusive evidence of the toxicity of xylitol containing chewing gums after partial consumption.

Numerous methods are commonly employed for the analysis of polyols^{20,21} including those that utilize HPLC,²²⁻²⁴ GC-MS²⁵ with sample derivatization, Over-Pressured Layer Chromatography (OPLC),²⁶ and High Performance Anion-exchange Chromatography (HPAEC).²⁷ HPLC seems to be the obvious choice in this analysis, however, separation can be complicated because gum samples often have multiple polyols with overlapping retention times. Consequently, HPLC separation often requires specialty, high cost columns that may not be available in many analytical laboratories. Herein, a reliable low-cost method to determine amounts of xylitol in sugar free gum samples has been developed.

A direct aqueous injection GC-MS method utilizing an Agilent 7890A GC/5975C MS has been developed. Direct aqueous injection (DAI) is key to this analysis because polyols are more soluble in water than any other common solvent.²⁸ Employing DAI with GC-MS analysis has important advantages including high speed analysis, simplicity, and the elimination of the lengthy sample derivatization steps that are often required.^{29,30}

Direct aqueous GC injection has been successfully used to analyze polar compounds such as carboxylic acids, ethers, fuel oxygenates and other fuel components.³¹⁻³⁵ To the best of our knowledge, the method described here is the first to explore the use of GC-MS direct aqueous injection to determine xylitol content of chewing gum samples. An undergraduate teaching laboratory experiment was also developed as an extension of this work.

4.3 Materials and Method

4.3.1 Reagents and Materials

Glycerol (CAS-56-81-5, assay 99.5%, MW-92.09 g mol⁻¹), xylitol (CAS-87-99-0, assay 99%, MW- 152.15 g mol⁻¹), DL-threitol (CAS-7493-90-5, assay-97%, MW- 122.12 g mol⁻¹), and sorbitol (CAS-50-70-4, assay 99%, MW-182.17 g mol⁻¹) were purchased from Sigma Aldrich. Xylitol containing Trident sugar free gum was purchased from Walmart (regular 0.17-0.20 mg of xylitol/piece). DI-water was used to prepare all samples and standard stock solutions. Similar weight gum pieces were chosen for analysis.

4.3.2 GC-MS Analysis

An Agilent 7890A-5975C gas chromatograph with a mass detector (GC-MS) was used with a water resistant 60 m × 320 μm × 1 μm, 100 % dimethylpolysiloxane, Agilent *J&W DB-1* column.³⁶ The GC oven was programmed to heat as follows; temperature at injection was 216 °C, followed by heating from 216 to 230 °C at 1 °C min⁻¹, from 230 to 290 °C at 30 °C min⁻¹, and then holding at 290 °C for 3 min. The total program time is 20 min. The carrier gas was He at a pressure of 60 kPa. Using a 10 μL syringe, 1 μL

injections were done in split mode (30:1) at 280 °C. The Agilent 5975C mass spectrometer was operated under scan mode with an electron impact ion source operated at 70 eV. The ion source temperature was 250 °C and the interface temperature was 280 °C.

4.3.3 Method overview

A flow diagram of the method is shown in Figure 4.2 which includes sample collection, xylitol extractions by grinding gum pieces using a mortar and pestle, and centrifugation to remove any particulates before preparing solutions for GC-MS analysis. A fresh sample contains a large quantity of xylitol, so sample concentration before analysis was not required (Figure 4.2, **a**). However, the chewed gum samples contain very small amounts of xylitol and extracts must be concentrated for accurate GC-MS analysis (Figure 4.2, **b**). Typically, a nitrogen evaporator is used to concentrate samples. However, in this study, a large amount of water needed to be evaporated which required 2-3 h per sample using the nitrogen evaporator with a bath temperature of 60-70 °C. The rotary evaporator proved to be more efficient. With a bath temperature of 40 °C, the vacuum (water aspirator) rotary evaporator shortened the concentration step from hours to minutes (maximum 30 min).

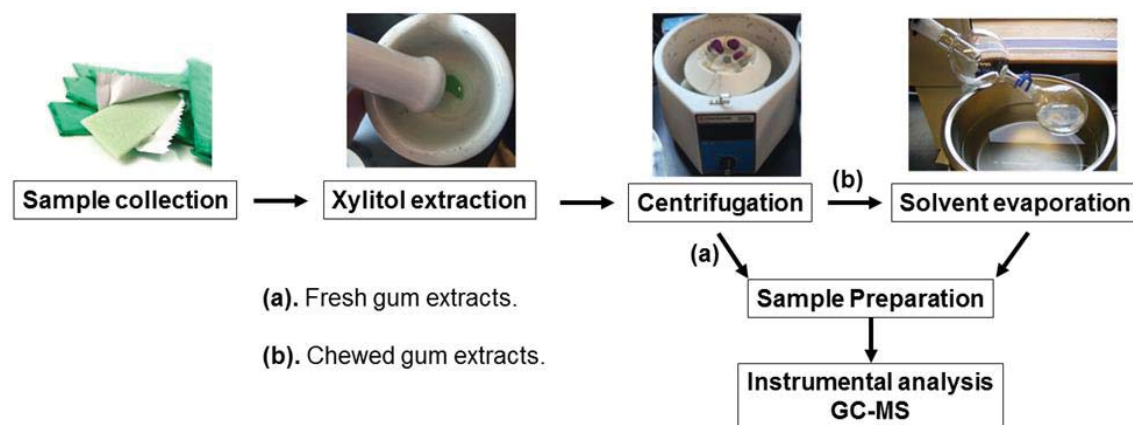


Figure 4.2 A flow diagram of xylitol analysis method.

4.3.3.1 Extraction of xylitol from Fresh Gum samples

Sample collection: 4 gum packs, each containing 18 gum sticks, were randomly selected from a commercial package containing 14 packs. A total of 12 fresh gum sticks were collected from the gum packs including the 1st, 9th, and 18th gum sticks of each pack to determine xylitol content.

A fresh gum stick was carefully cut into about 6-7 small pieces. Gum pieces were ground for 5 min with 10 mL of DI-water. This extraction step was repeated 9 times requiring a total of 90 mL DI-water and 45 min to extract xylitol completely from a single gum piece (Figure 4.3). Nine extractions are recommended to account for differences in an extractor's grinding technique. Gum extracts were centrifuged to remove any particulate and the supernatant was transferred to a 100 mL volumetric flask. DI-water was then added to the 100 mL mark. Exactly 20.0 mL from the gum extraction was transferred to a 50 mL volumetric flask along with 5.0 mL of 5.0 mg mL⁻¹ of DL-theritol solution as an internal standard. 1 µL from the solution was injected to the GC inlet. Another, 10th extraction (10 mL × 5 min) was performed to confirm that no xylitol

was still trapped in the gum. This extraction was centrifuged and concentrated into 1 mL before 1 uL was injected for GCMS analysis.

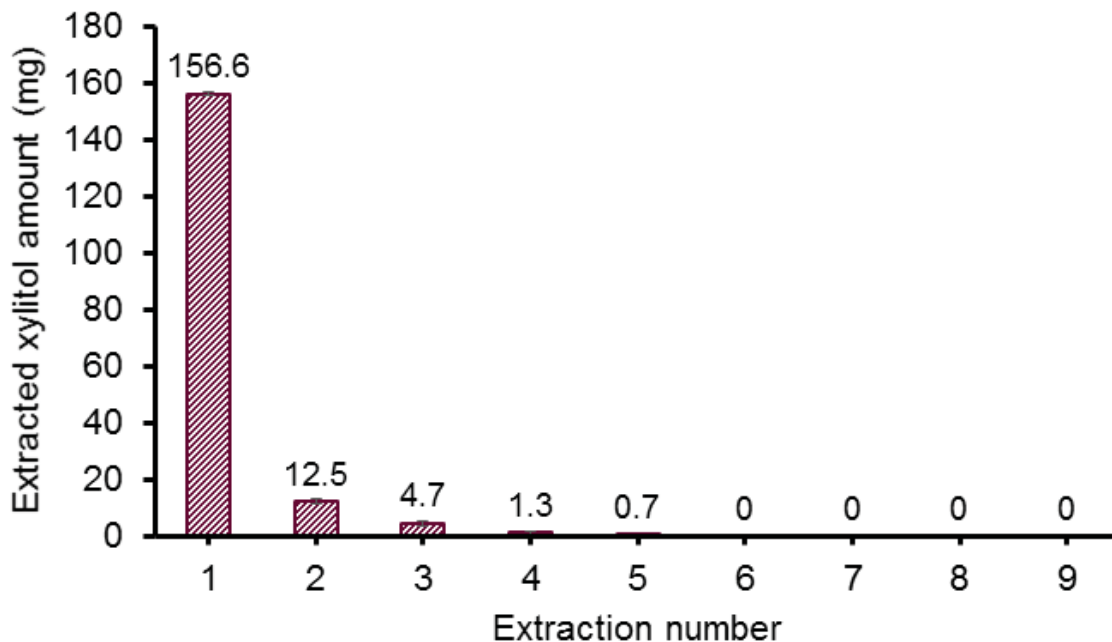


Figure 4.3 Amount of xylitol extracted after each extraction.

4.3.3.2 Extraction of xylitol from 5 min chewed gum samples

Sample collection: 12 volunteers, between 20 to 40 years old participated in this study. Participants were asked to wash their mouth with water before they chewed a gum stick. Participants chewed their gum pieces with similar starting masses ($1.724 \text{ g} \pm 0.008$) for 5 min before placing the chewed gum into a sterilized container. Three gum samples from each participant were collected within a 2-day interval (a total of 36 gum samples). The xylitol content of each 5 min chewed gum piece was determined as follows.

The gum stick was ground using a mortar and pestle for 5 min with 10 mL of DI-water. This extraction step was repeated **8 times** for a total of 80 mL of DI-water and 40

min to extract xylitol completely from the gum piece. The reduced xylitol content in the chewed samples required fewer extraction steps than the fresh gum. Gum extracts were centrifuged to remove any particulate and then the supernatant was carefully transferred to a 100 mL evaporation flask. The combined extract was concentrated down to 5 mL under reduced pressure using a water aspirated rotary evaporator with a water bath temperature of 40 °C. The concentrated sample was carefully transferred into the 10 mL volumetric flask. To ensure complete transfer, the evaporation flask was washed with another 3 mL of DI water. This washing was then transferred to the same 10 mL volumetric flask. 1.0 mL of a 5.0 mg mL⁻¹ of DL-theritol solution was added as an internal standard to the flask which was then filled to the 10 mL mark with DI-water. 1 µL from the solution was injected to the GC inlet for analysis. Another, 9th extraction (10 mL × 5 min) was performed using the same gum piece to confirm that no xylitol was still trapped in the gum. This extraction was centrifuged and concentrated into 1 mL, followed by a 1 µL injection into the GC-MS.

4.3.3.3 Extraction of xylitol from 15 min chewed gum samples

Sample collection: the same 12 volunteers who participated in the 5 min chewed gum sampling also participated in this study. A similar procedure was used as above. Participants washed their mouth with water before chewing gum pieces with almost identical masses (1.724 g ± 0.008), for 15 min. The chewed gum pieces were collected into sterilized containers before extraction. Three replicates were performed by each participant (total 36 gum samples).

A similar extraction method was used as above with the 5 min samples. However, with these 15 min samples, the 10 mL extraction step was repeated **6 times** with a total of

60 mL of DI-water and required 30 min to completely extract xylitol from the gum piece. As with the 5 min samples, the gum extracts were then centrifuged to remove any particulate and the supernatant was carefully transferred to 100 mL evaporation flask, and water was evaporated to dryness, under reduced pressure using a rotary evaporator. To the evaporation flask, 900 μL of DI water and 100 μL of 5.0 mg mL^{-1} DL-theritol solution was added and mixed. Then 1 μL of the solution was analyzed by DAI GC-MS. A final 7th extraction (10 mL \times 5 min) was performed using the same gum pieces to determine if xylitol remained in the extracted gum pieces. This extract was also centrifuged and concentrated to 1 mL. Then, 1 μL was injected to the GC-MS.

4.3.3.4 Extraction of xylitol from 30 min chewed gum samples

Sample collection: the same 12 volunteers who participated for both the 5 and 15 min chewed samples also participated in this study. An identical method was used with the exception being 30 min of chewing before extraction. Xylitol was then extracted and analyzed using an identical method as above for the 15 min samples.

4.4 Results and Discussion

4.4.1 GC-MS method development

Water is considered to be a poor solvent in GC analysis due to problems with backflash and chemical reactivity. Common GC solvents such as hexane, ethyl acetate, acetone, and dichloromethane have vapor-to-liquid volume ratios between 100-300.³⁶ However, the water vapor-to-liquid volume ratio is 1000. Hence, injecting 1 μL of liquid water into the GC liner creates 1000 μL of water vapor.³⁶ A typical volume of a liner is between 200-900 μL , solvent vapor that expands beyond the liner volume results in

backflash which can cause both sample and solvent to contaminate purge lines and the GC inlet. A laminar cup splitter (Figure 4.4), used in this study, is suitable for large volume injections of low volatile compounds. With a laminar cup inlet, liquid can trap at the liner base until vaporized ensuring complete vaporization. Chemical damage to the stationary phase is another problem associated with water injection GC. In order to avoid stationary phase degradation and enable high temperature analysis, a water resistant, 100 % dimethylpolysiloxane, low-bleed, cross-linked, and water rinsable column was used.³⁶



Figure 4.4 Laminar cup splitter design

Analysis of xylitol (boiling point 216 °C) in a complex mixture requires both high temperature injection and temperature programming to ensure chromatographic separation. The GC oven was programmed with an initial temperature at the boiling point of xylitol to facilitate high temperature analysis, while reducing column bleed and improving limits of detection (Figure 4.5). The mass detector was programmed to analyze mass fragments between 35-350 m/z from 4.5 min to 15 min in order to avoid detector saturation caused by volatile components of gum extracts which elute before 4.5 min. After 15 min, the GC was baked out for 5 min (a 2 min heating ramp from 230 °C to 290 °C followed by holding for 3 min at 290 °C) to remove residual sorbitol still trapped in the column. Following the fresh gum (high xylitol concentration) analysis, a blank run was performed to confirm no sorbitol remained trapped in the GC system before further analysis.

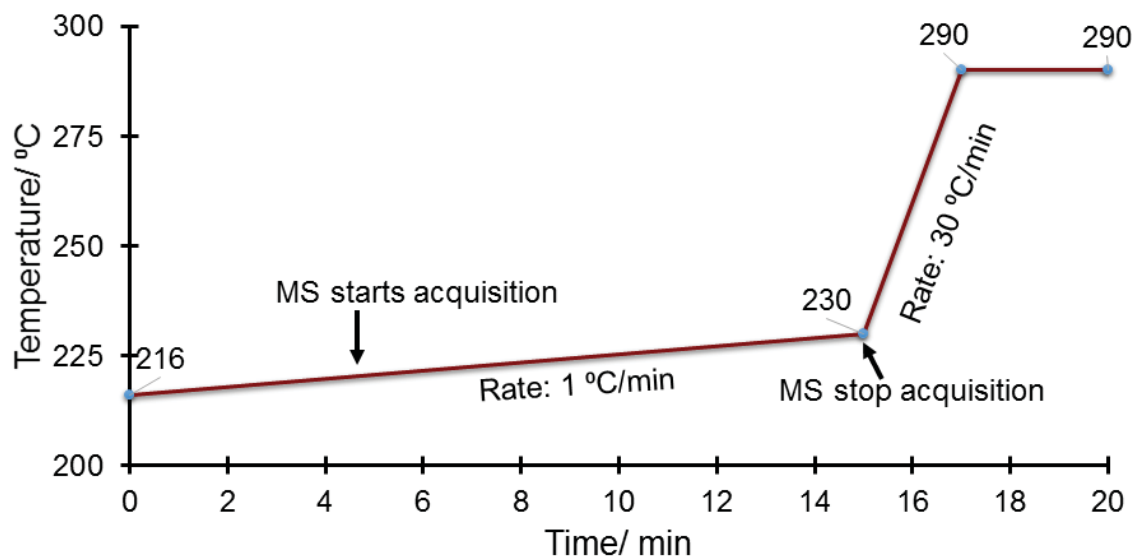


Figure 4.5 GC oven program

The effect of injection temperature was studied to facilitate complete vaporization of xylitol in the GC inlet. Raising the injection temperature from 200 °C to 280 °C increased xylitol peak area by a factor of 5. However, only a 5% increase was observed when the inlet temperature was increased from 280 °C to 300 °C (Figure 4.6). Operating the inlet at 300 °C may accelerate septum failure, therefore, 280 °C was selected as the optimum injection temperature.

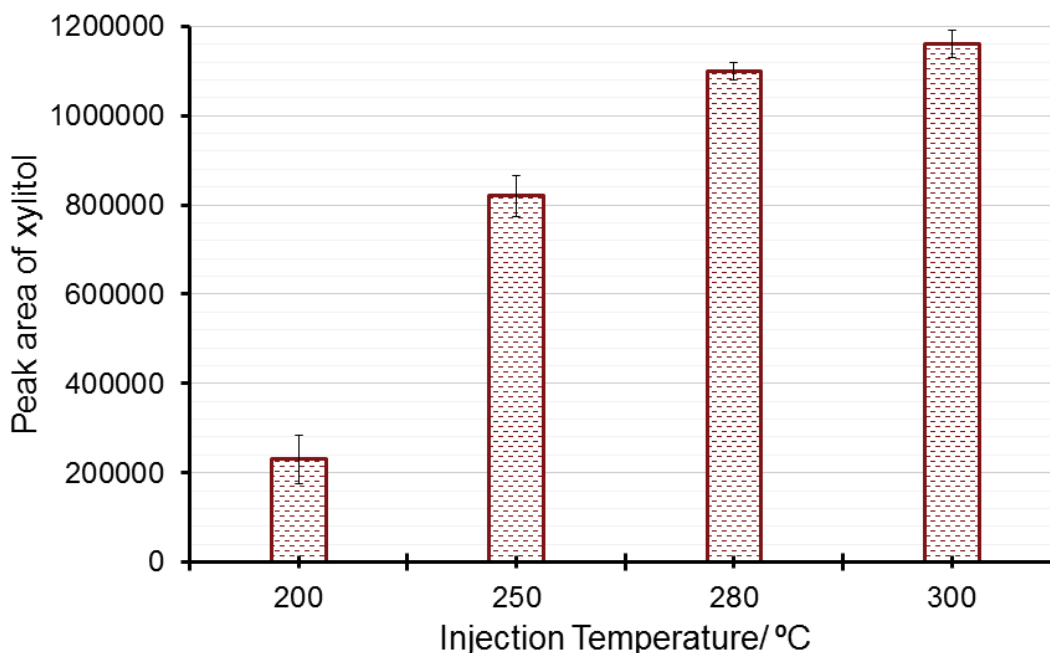


Figure 4.6 Effect of injection temperature on xylitol peak area. Note: Error bars indicate standard deviation ($n = 3$).

4.4.2 Selection of internal standard

Choosing a correct internal standard (IS) can improve a method's accuracy and precision. Method development for GC-MS often utilizes an internal standard to account for routine variation of the instrument response and injection volumes. An internal standard should be chemically similar to the analyte but it should not be naturally present in any of the samples to be analyzed. A Trident spearmint flavor gum piece contains three polyols in large quantities, xylitol, glycerol, and sorbitol. Mannitol is also present but at low concentrations compared to the xylitol and sorbitol content of the gum piece (Figure 4.7).

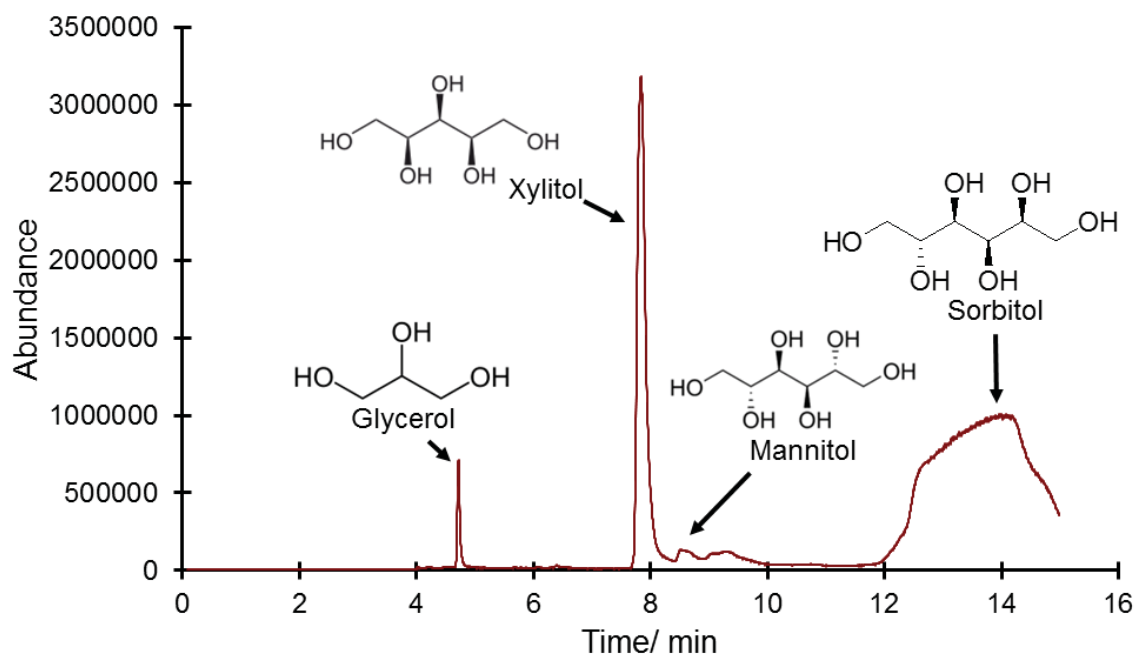


Figure 4.7 Total ion chromatogram (TIC) of Trident gum extract.

Various chemicals were tested as an internal standard for this study including, ethylene glycol, 3,5-dimethoxyphenol, 2-methoxyphenol, terpineol, 2-nonanol, and DL-threitol. Both 2-methoxyphenol and DL-threitol were found to be suitable for analysis in the terms of retention times, since they did not overlap with any peaks of the trident gum extract. However, DL-threitol was picked as the better internal standard because it has the same functional groups as xylitol. More importantly, glycerol, threitol, xylitol, and sorbitol are members of a series of compounds in which any two members in a sequence differ by one carbon atom, two hydrogen atoms, and one oxygen atom, CH–OH unit (Figure 4.8). Therefore, DL-threitol is a suitable internal standard in this analysis.

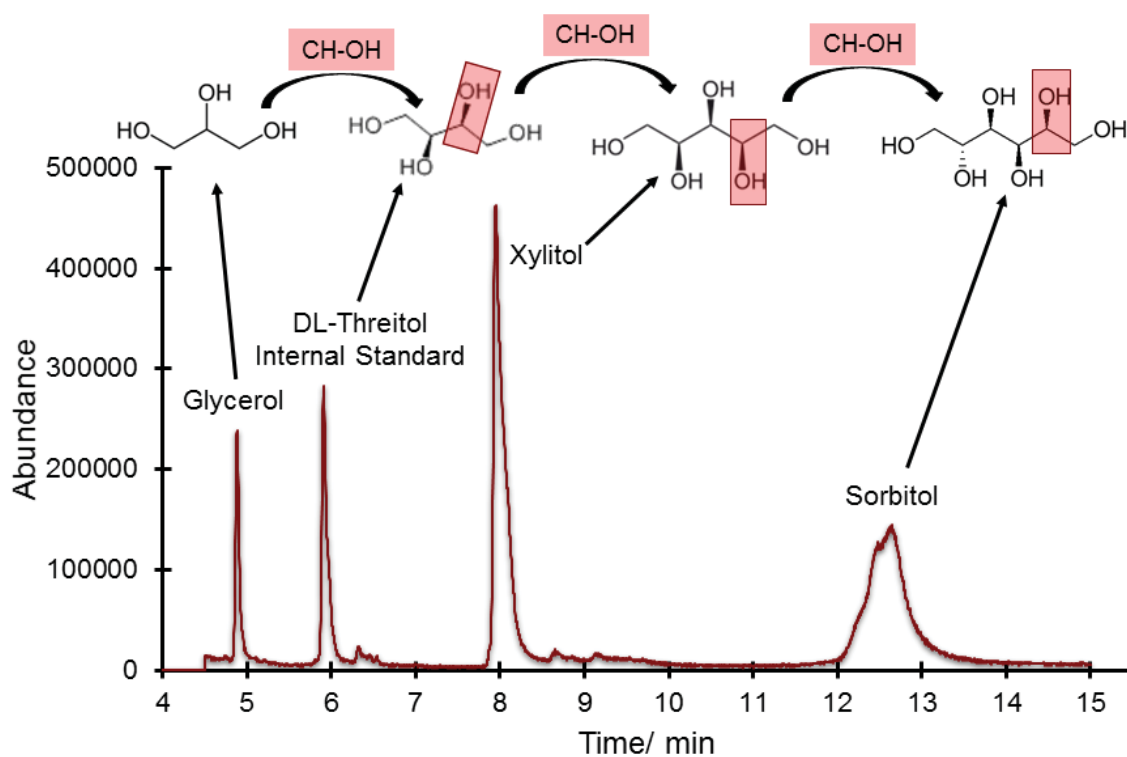


Figure 4.8 Total ion chromatogram (TIC) of Trident gum extract with internal standard.

4.4.3 Recovery

Recovery tests were performed to evaluate extraction efficiency. Gum base left after the 10th extraction was spiked with a known amount of solid xylitol (180.0 mg). The xylitol was thoroughly ground into the gum base using a mortar and pestle before extraction and DAI GC-MS analysis using the fresh gum method described above. This procedure was repeated for five gum-base samples (GB-1 through GB-5). Recovery values (Table 4.2) using the fresh gum extraction method were 95-99% with relative standard deviations of less than 1%. Acceptable recovery values and low standard deviations indicate high accuracy and precision of the method; thus reliable quantification is expected using this method.

Table 4.2 Precision and recovery of fresh gum analysis method ($n = 3$)

Gum base No:	Spiked (mg)	Measured (mg)	Recovery (%)	RSD%
GB-1	178.2	177.2	99.4	0.31
GB-2	180.3	178.4	98.9	0.18
GB-3	179.4	177.2	98.8	0.17
GB-4	180.6	176.6	97.8	0.24
GB-5	178.4	169.9	95.1	0.72

4.4.4 Detection limit

Limit of Detection (LOD) and Limit of Quantification (LOQ) were determined. An internal standard calibration graph was plotted using the ratio of peak areas of the internal standard (DL-threitol) versus the concentration of xylitol. Good linearity was observed, with a square of the correlation coefficient (r^2) of 0.9995 in the range of 0.7 to 2.0 mg mL⁻¹ xylitol. A signal-to-noise approach was selected to determine limits of detection and quantification. LOD was determined to be 0.1 mg/mL using a signal-to-noise (S/N) ratio of 3, while the LOQ was determined to be 0.7 mg/mL using a S/N approximately of 10.

4.4.5 Statistical analysis

Analysis of Variance with Tukey's honestly significant difference test ($P < 0.05$, IBM SPSS Statistics, Version 24) was performed to determine the significant differences in xylitol contents in fresh and chewed gums.

4.4.6 Determination effect of chewing rate on xylitol release from gum base

Effect of chewing rate on xylitol release was studied. Four volunteers were randomly selected for this experiment. Each participant was given three gum sticks with similar masses ($1.724 \text{ g} \pm 0.008$). Chewing rates were selected after considering general chewing habits. We observed, a person starts chewing a gum piece at a rate between 30 and 120 chews per minute for the first two-minutes due to the sugar taste. Chewing rates then decrease with time due to decreased sugar content of the gum. Three chewing rates 30, 60 and 120 chews per minute were selected. Participants were asked to chew gum pieces at the selected rates for 2 minutes. The method, which was used for the Fresh gum analysis, was used to determine the xylitol content of chewed gum samples in this experiment (Figure 4.9).

Results show that chewing rate had no significant effect on the remaining xylitol content in the 2 min chewed gums ($P < 0.05$). It should be noted that there appears to be a trend that more xylitol is released with more rapid chewing, however a larger sample size is required for proof.

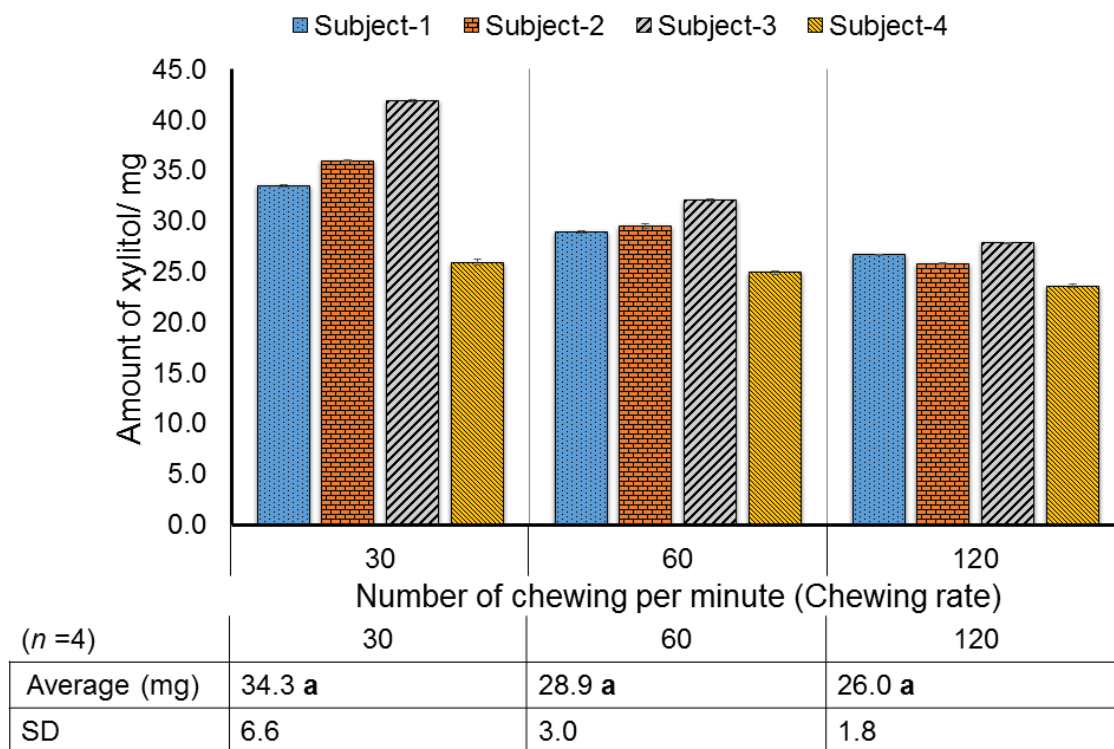


Figure 4.9 Amount of xylitol remaining in a gum piece chewed by four participants at three different rates.

Numbers sharing similar lower case letters indicate no significant difference.

4.4.7 Sample analysis

Trident spearmint flavor gum pieces were selected for this study. In order to determine the range of xylitol content in a gum stick, 4 gum packs were chosen randomly, each with 18 gum sticks. The 1st, 9th, and 18th sticks of each pack were selected for analysis. The amount of xylitol in the fresh gum pieces were determined using the fresh gum analysis method established above. Each sample was analyzed by DAI GC-MS three times and the results are summarized in Table 4.3 (P1-4 represent gum pack number, ST 1, 9, and 18 represent gum stick number). The xylitol content of the fresh gum samples ranged from 170.7 to 193.0 mg with average 179.2 mg of xylitol per piece.

There were no significant differences in the xylitol contents in fresh gum packs, which were used in this study ($P < 0.05$).

Table 4.3 Determination xylitol content of Trident spearmint gum flavor (regular care)

Gum piece ID	Xylitol content (mg)	SD ($n = 3$)	Gum piece ID	Xylitol content (mg)	SD ($n = 3$)
P1-ST1	180.8	0.8	P3-ST1	187.8	0.5
P1-ST9	179.1	0.2	P3-ST9	179.8	0.6
P1-ST18	179.7	0.3	P3-T18	171.3	0.2
P2-ST1	193.0	0.3	P4-ST1	170.7	0.4
P2-ST9	187.8	0.6	P4-ST9	172.4	0.4
P2-ST18	174.0	0.4	P4-ST18	181.1	0.2

A total of 36 samples (3 each for the 12 participants) were analyzed to determine the amount of xylitol in 5 min chewed gum samples and results are summarized in Figure 4.10. The mass of xylitol ranged from 5.3 to 10.3 mg with an average of 7.8 mg per piece. Although there were significant differences among the xylitol content in gum samples, samples collected from a single participant were not significantly different ($P < 0.05$) (Table 4.4). On average, the 5 min chewed gum samples retain about 4% of the original xylitol in a fresh gum stick.

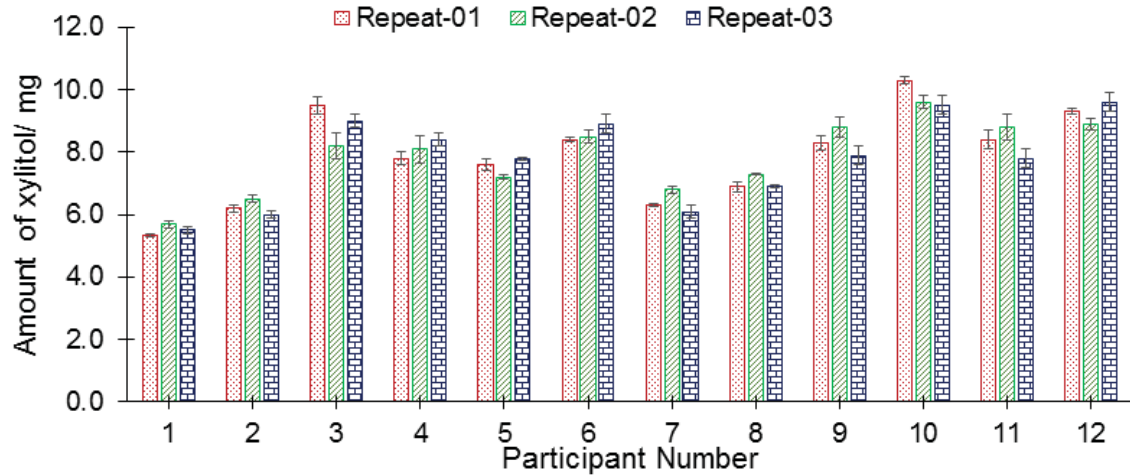


Figure 4.10 Determination of xylitol content in 5 min chewed gum samples

A total of 36 (3 from each participant) of the 15 minutes chewed gum samples were also analyzed (Figure 4.11). The amount of xylitol found in these samples ranged from 0.7 mg to 1.8 mg with an average of 1.1 mg per piece. This represents about 0.6% of the original xylitol. As shown in Figure 4.11, the amount of xylitol remaining in gum after 15 min of chewing varies significantly from person to person ($P < 0.05$) (Table 4.4).

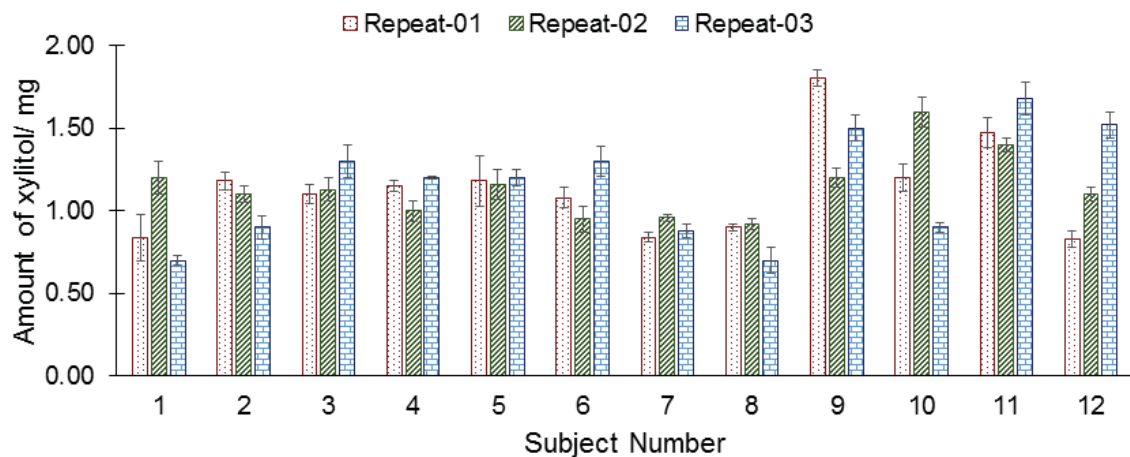


Figure 4.11 Determination of xylitol content in 15 min chewed gum samples

There was no xylitol above the LOD in any of the 36 samples collected after a 30 min chewing period. Approximately 99.4% of xylitol is removed from the gum within the first 15 min, another 15 min of chewing time reduced the xylitol content below the method limits to detect.

Table 4.4 Statistical analysis of xylitol content of chewed gum samples

Participant #	Chewing time		
	5 min	15 min	30 min
1	5.5 a	0.91 abc	ND
2	6.2 ab	1.06 abc	ND
3	8.9 ef	1.18 abc	ND
4	8.1 cde	1.12 abc	ND
5	7.5 cd	1.18 abc	ND
6	8.6 def	1.11 abc	ND
7	6.4 ab	0.89 ab	ND
8	7.0 bc	0.84 a	ND
9	8.3 def	1.50 bc	ND
10	9.8 fg	1.23 abc	ND
11	8.3 def	1.51 c	ND
12	9.3 efg	1.15 abc	ND
Mean	7.8 C	1.14 B	0 A

Numbers in the same column sharing similar lowercase letters or mean values sharing similar uppercase letters are not significantly different. ND = Not Detected

Table 4.5 was generated to demonstrate the number of gum sticks (fresh, 5 and 15 min chewed) required to deliver a toxic dose to each dog size resulting in hypoglycemia. Although a large number of 5 and 15 min chewed gum pieces are required to cause hyperglycemia in a 2 kg Chihuahua, chewed gum samples should not be neglected because they still pose a threat, particularly to smaller dogs. In general, a dog's size affects its tolerance to xylitol poisoning: the smaller the dog, the less tolerant and vice versa. While a large dog may have little to fear after eating 5 min chewed samples, a small dog is very much at risk to the dangers of ingesting xylitol. Eating several 30 min chewed gum sticks are not likely to result in xylitol poisoning, however, digestion issues could occur.

Table 4.5 Amount of gum sticks required to supply toxic dose to make a dog sick

Size of the dog	Amount of xylitol to cause hyperglycemia (g)	Number of gum pieces required to supply toxic dose (Dose: 0.1 g of xylitol per kg of dog)		
		Fresh (Xylitol = 179 mg)	5 min chewed (Xylitol = 7.8 mg)	15 min chewed (Xylitol = 1.1 mg)
2 kg Chihuahua	0.2	1	26	182
4 kg of Yorkie	0.4	2	51	364
6 kg of Jack Russel Terrier	0.6	3	77	545
12 kg of Border Collie	1.2	7	154	1091
25 kg of Golden Retriever	2.5	14	320	2273

4.5 Conclusions

A method for the determination of xylitol in sugar gum samples was successfully developed using GC-MS with direct aqueous injection. Additional cleanup steps and sample derivatization were not required for the analysis, resulting in short analysis times. Spiked recoveries of the sample ranged from 95 to 99% while RSD ranged from 0.17 to

0.72% ($n=3$) supporting that this is a reliable quantification method, with high accuracy and precision. Thus, this method possesses advantages in terms of efficiency, selectivity, and accuracy.

4.6 References

- (1) Grembecka, M. *Eur. Food. Res. Technol.* **2015**, *241*, 1.
- (2) Chen, X.; Jiang, Z.-H.; Chen, S.; Qin, W. *Int. J. Biol. Sci.* **2010**, *6*, 834.
- (3) Dhar, K. S.; Wendisch, V. F.; Nampoothiri, K. M. *J. Biotechnol.* **2016**, *230*, 63.
- (4) Grabitske, H. A.; Slavin, J. L. *J. Am. Diet. Assoc.* **2008**, *108*, 1677.
- (5) Livesey, G. *Nutr. Res. Rev.* **2003**, *16*, 163.
- (6) Antonio, A. G.; Pierro, V. S. d. S.; Maia, L. C. *J. Public. Health Dent.* **2011**, *71*, 117.
- (7) Twetman, S. *Evid-based Dent.* **2008**, *10*, 10.
- (8) Hayes, C. *J. Dent. Educ.* **2001**, *65*, 1106.
- (9) Deshpande, A.; Jadad, A. R. *J. Am. Dent. Assoc.* **2008**, *139*, 1602.
- (10) Burt, B. A. *J. Am. Dent. Assoc.* **2006**, *137*, 190.
- (11) Dunayer, E. K. *Vet. Med.* **2006**.
- (12) Todd, J. M.; Powell, L. L. *J. Vet. Emerg. Crit. Care* **2007**, *17*, 286.
- (13) Peterson, M. E. *T. Companion. Anim. Med.* **2013**, *28*, 18.
- (14) Dunayer, E. K.; Gwaltney-Brant, S. M. *J. Am. Vet. Med. Asso.* **2006**, *229*, 1113.
- (15) Xia, Z.; He, Y.; Yu, J. *J. Vet. Pharmacol. Ther.* **2009**, *32*, 465.
- (16) Murphy, L. A.; Coleman, A. E. *Vet. Clin. North Am. Small Anim. Practice* **2012**, *42*, 307.
- (17) Campbell, A.; Bates, N. *Vet. Rec.* **2010**, *167*, 108.
- (18) Campbell, A.; Bates, N. *Vet. Rec.* **2008**, *162*, 254.
- (19) Mother Nature Network. Don't let your dog eat xylitol:
<http://www.mnn.com/family/pets/blogs/dont-let-your-dog-eat-peanut-butter-with-xylitol>. (Accessed on 2-15-2017).
- (20) Martínez Montero, C.; Rodríguez Dodero, M. C.; Guillén Sánchez, D. A.; Barroso, C. G. *Chromatographia* **2004**, *59*, 15.
- (21) Molnár-Perl, I. *J. Chromatogr. A* **2000**, *891*, 1.

- (22) Pomata, D.; Di Filippo, P.; Riccardi, C.; Buiarelli, F.; Gallo, V. *Atmos. Environ.* **2014**, *48*, 332.
- (23) Wamelink, M. M. C.; Smith, D. E. C.; Jakobs, C.; Verhoeven, N. M. *J. Inherit. Metab. Dis.* **2005**, *28*, 951.
- (24) Bernal, J. L.; Del Nozal, M. J.; Toribio, L.; Del Alamo, M. *J. Agric. Food Chem.* **1996**, *44*, 507.
- (25) Roessner, U.; Wagner, C.; Kopka, J.; Trethewey, R. N.; Willmitzer, L. *Plant. J.* **2000**, *23*, 131.
- (26) Tamburini, E.; Bernardi, T.; Granini, M.; Vaccari, G. *J. Planar Chromat.* **2006**, *19*, 10.
- (27) Cataldi, T. R. I.; Margiotta, G.; Zambonin, C. G. *Food Chem.* **1998**, *62*, 109.
- (28) Wang, S.; Li, Q.-S.; Li, Z.; Su, M.-G. *J. Chem. Eng. Data* **2007**, *52*, 186.
- (29) Ruiz-Matute, A. I.; Hernández-Hernández, O.; Rodríguez-Sánchez, S.; Sanz, M. L.; Martínez-Castro, I. *J. Chromatogr. B* **2011**, *879*, 1226.
- (30) Schummer, C.; Delhomme, O.; Appenzeller, B. M. R.; Wennig, R.; Millet, M. *Talanta* **2009**, *77*, 1473.
- (31) Wortberg, M.; Ziemer, W.; Kugel, M.; Müller, H.; Neu, H.-J. *Anal. Bioanal. Chem.* **2006**, *384*, 1113.
- (32) Zwank, L.; Schmidt, T. C.; Haderlein, S. B.; Berg, M. *Environ. Sci. Technol.* **2002**, *36*, 2054.
- (33) Hong, S.; Duttweiler, C. M.; Lemley, A. T. *J. Chromatogr. A* **1999**, *857*, 205.
- (34) Wolska, L.; Olszewska, C.; Turska, M.; Zygmunt, B.; Namieśnik, J. *Chemosphere* **1998**, *37*, 2645.
- (35) H. Jurdáková, A. K., W. Lorenz, R. Kubinec, Ž. Krkošová, J. Blaško, I. Ostrovský, L. Soják, V. Pacáková; Ciszkowski, N. A. *Petroleum & Coal* **2005**, *47*, 49.
- (36) Kuhn, E. R. *LCGC ASIA PACIFIC* **2002**, *5*, 30.

CHAPTER V
ANALYSIS OF XYLITOL IN SUGAR FREE GUM BY GC-MS WITH DIRECT
AQUEOUS INJECTION: A LABORATORY EXPERIMENT FOR
CHEMISTRY STUDENTS

5.1 Abstract

Proficiency with GC-MS instrumental analysis is an important skill for chemistry students. The application of analytical techniques and fundamental theoretical principles to real world problems can be valuable learning exercises for undergraduates while improving their analytical thinking skills. Xylitol is generally considered safe for human consumption and is frequently used in sugar free gum, however, it is extremely toxic to dogs. In this laboratory experiment, upper-level undergraduate chemistry students extract xylitol from both fresh and chewed gum sticks followed by direct aqueous injection GC-MS analysis. Students learn the proper steps and techniques required for sample extraction and preparation, GC-MS analysis, and compute levels of xylitol present in gum samples. Identification of the chemical components in gum extract occurs via GC-MS peak areas with students comparing external and internal standard calibration methods for xylitol quantification. Upon quantification of xylitol in chewed and unchewed gum samples, students are able to calculate the level of hazard for dogs upon ingestion.

5.2 Introduction

Xylitol is a sugar alcohol, commonly used as an artificial sweetener or sugar substitute in many “reduced-calorie” foods (Figure 5.1). Xylitol is extensively utilized in chewing gum because it helps prevent dental caries.¹⁻⁵ Although xylitol consumption has proven beneficial to humans, dogs find it hazardous. Xylitol ingestion by dogs causes vomiting, ataxia, seizures, hypoglycemia, and hepatotoxicity in the animal.⁶⁻¹¹

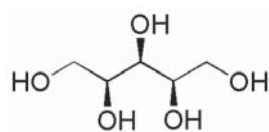


Figure 5.1 Xylitol

Ingestion of xylitol containing products such as chewing gum can result in xylitol poisoning for dogs if enough product is consumed (Table 5.1).^{7,12,13} This undergraduate experiment uses a reliable low-cost method to determine amounts of xylitol in sugar free gum sticks to predict dangerous exposure levels for dogs. An aqueous extraction technique and water-based GC-MS analysis method allows students to calculate levels of hazardous xylitol in selected gum samples.

Table 5.1 Amounts of xylitol required to cause hypoglycemia in dogs.

Dog Size	Amount of xylitol to cause hypoglycemia in dog <i>(Dose, 0.1 g of xylitol / kg of dog)</i>	Required gum sticks		
		Ice Breakers, 1.5 g of xylitol/ piece	Stride, 0.2 g of xylitol/piece	Trident, 0.2 g of xylitol/piece
2 kg Chihuahua	0.2 g	1	1	1
4 kg Yorkie	0.4 g	1	2	2
6 kg Jack Russell Terrier	0.6 g	1	3	3
12 kg Border Collie	1.2 g	1	6	6
25 kg Golden Retriever	2.5 g	2	12	12

Learning objectives for this experiment include sample injection techniques, quantification of xylitol using GC-MS and a comparison of external versus internal standard techniques while allowing students to explore a topic that has direct impact to animal safety. Previous undergraduate laboratory experiments have been developed which utilize GC-MS to analyze and quantify components of diverse samples including gasoline, plasticizers, food, water, urine, perfume, beverages and others.¹⁴⁻²⁸ GC-MS experiments have also been utilized within the organic chemistry curriculum, since it provides a great opportunity for students to analyze organic reactions such as nucleophilic substitution²⁹ and elimination reactions.³⁰ This experiment is designed for upper level undergraduate students enrolled in organic or instrumental analysis courses. Fundamental theoretical principles and practical quantification techniques underlying this experiment present opportunities for undergraduates to apply textbook information to a real world situation.

5.3 Experimental overview

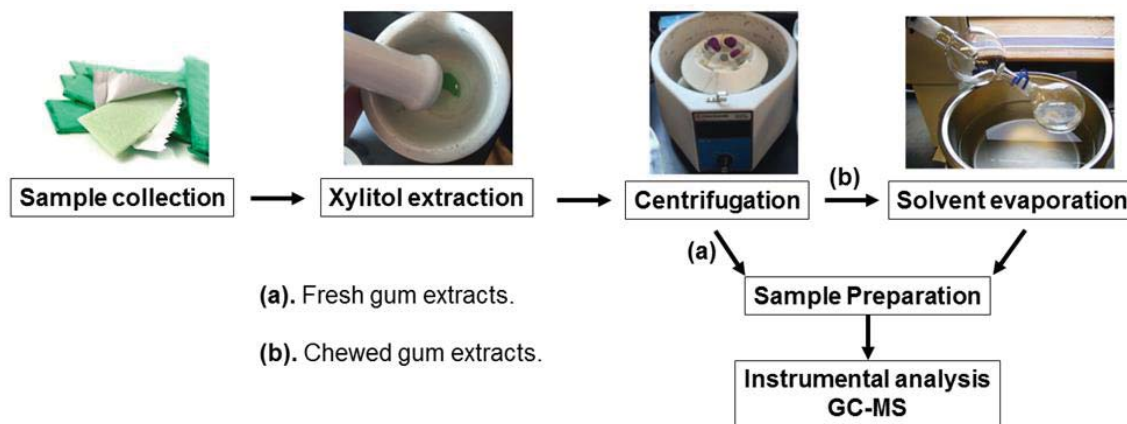


Figure 5.2 Overview of xylitol analysis laboratory procedure

(a). Fresh gum and 1 minute chewed gum extractions require no sample concentration,
(b). Five minute chewed gum extractions require concentration.

The procedure of this experiment has four parts, including preparation of DL-threitol standard solutions to generate a calibration curve, extractions of xylitol from fresh, 1 minute chewed, and 5 minutes chewed gum sticks, sample preparation of each extract for GC-MS analysis, and analysis of samples (Figure 5.2). Students were directed to chew gum sticks outside of the laboratory environment due to safety concerns. Multiple extractions were performed for each gum sample by grinding chewed or fresh gum pieces with 10 mL of DI-water for 5 minutes, three times, using a mortar and pestle. All extractions were centrifuged to remove any particulates before preparing solutions for GC-MS analysis. Both fresh and 1 minute chewed gum samples contained a large quantity of xylitol, so sample concentration before the analysis was not required. The 5-minutes chewed gum samples contained very small amounts of xylitol and were concentrated via Roto-vap before GC-MS analysis. Sample preparation included addition of an internal standard (DL-threitol) for quantification of xylitol.

Students were given detailed instructions on GC-MS including the instrument operation and proper injection technique. The instrument, an Agilent 7890A-5975C gas chromatograph with a mass detector (GC-MS) and helium carrier gas was used with a water resistant 60 m × 320 μm × 1 μm, 100 % dimethylpolysiloxane column with a temperature profile that includes oven programming starting at 216 °C, followed by thermal ramp and 3 min bake out. The total program time was 20 min. Using a 10 μL syringe, 1 μL injections were done in split mode (30:1) at 280 °C. The Agilent 5975C mass spectrometer was operated under scan mode with an electron impact ion source operated at 70 eV. While the GC was running the first gum sample, students were given instruction on data processing steps to record the mass spectrum of each polyol and to determine peak areas. In addition, students use mass fragmentation patterns and the mass spectral data base to match each peak with the correct polyol structure.

5.4 Safety hazards

Gum sticks are weighed on a food scale in a clean, non-chemical environment prior to the lab experiment. Gum chewing should occur outside the laboratory environment before putting on any personal protective equipment or gloves. Students should wash hands with soap and water and carefully transfer chewed gum pieces back to the gum wrapper for transfer into the laboratory, or use a clean weighing boat to retain chewed samples. DI water is used for extraction in this experiment. Discarded gum pieces can be safely disposed in the trash can.

5.5 Results and discussion

A Trident gum sample has three polyols in large quantities, glycerol, xylitol, and sorbitol. Figure 5.3 illustrates a gas chromatograph of trident gum extraction after adding the internal standard DL-threitol for the analysis.

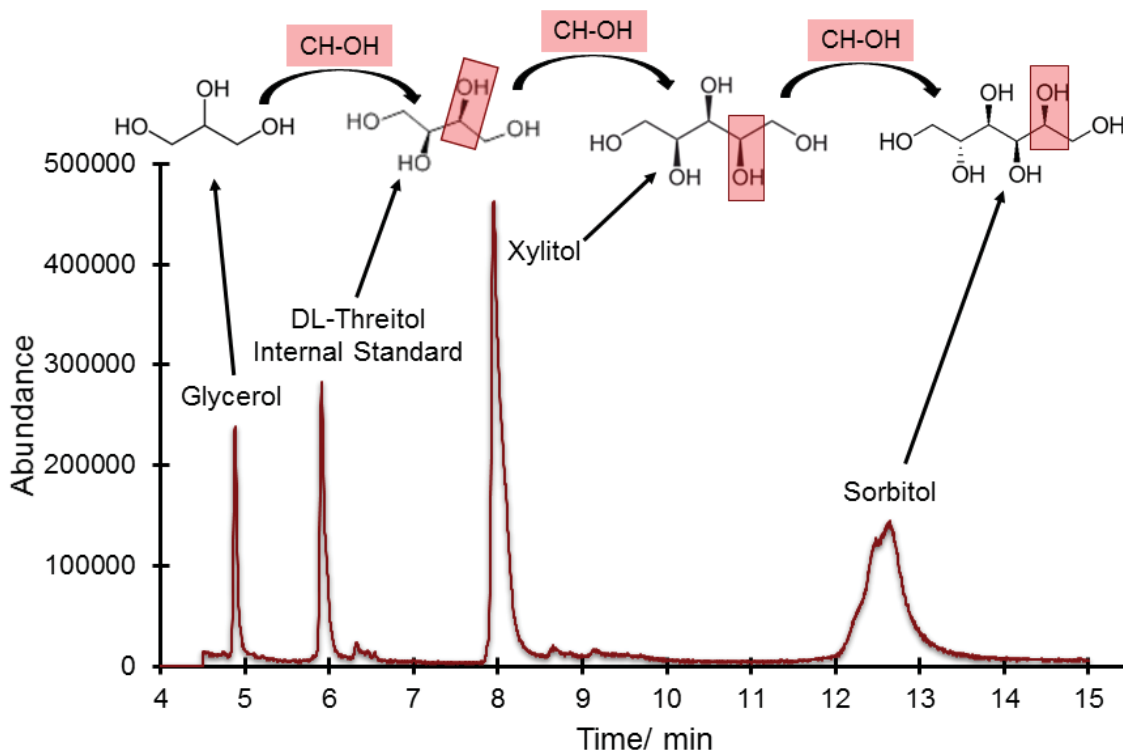


Figure 5.3 Total ion chromatogram (TIC) of Trident gum extraction with internal standard.

A G-C coupled to a mass analyzer operating under electron ionization (EI) mode, will produce a fragmentation pattern that plays a key role in compound identification. Glycerol, threitol, xylitol, and sorbitol are members of a series of compounds in which any two members in a sequence differ by one carbon atom, two hydrogen atoms, and one oxygen atom (CH–OH unit) (Figure 5.3). The molecular ion peaks of these polyols are extremely weak or not visible because cleavage of the C–C bond next to the oxygen atom

is common. Glycerol has a base peak of m/z 61 resulting from the loss of CH and H₂O. Loss of hydrogen atoms from hydroxyl groups, loss of multiple H₂O molecules, and multiple C–C bond cleavages result in peaks at m/z 61, 91, 103, and 117 common for threitol, xylitol and sorbitol, while peaks m/z 129 and 147 are common for both xylitol and sorbitol. A representative fragmentation pattern for xylitol is shown in Figure 5.4. Students use both retention time and mass spectra when identifying components of the gum extractions.

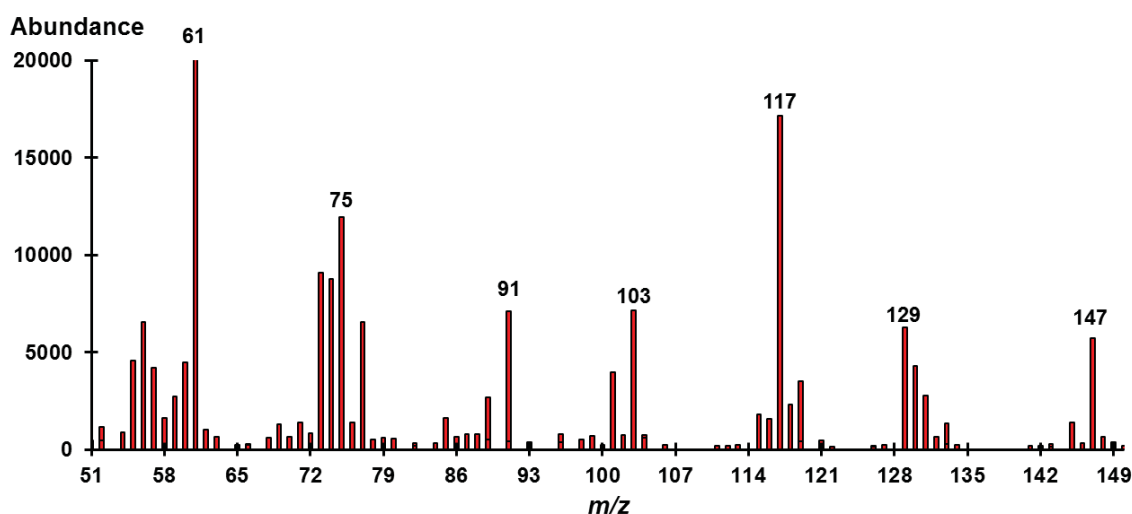


Figure 5.4 Low resolution mass spectrum collected from GC-MS for the xylitol peak.

Calibration methods can improve the accuracy and precision of GC-MS results. External standard calibration is commonly used to establish a linear relationship between signal magnitude and sample concentration. However, this method does not account for sample matrix chemicals, inconsistent injection volumes or instrument drift. An internal standard calibration method can be used to reduce these potential sources of error. When using an internal standard, a known substance is added to both gum samples and

calibration standards, and a calibration curve is produced by plotting the ratio of the analyte signal to the internal standard signal as a function of the analyte concentration. In this experiment, data from the standard xylitol samples is provided to the students to generate two calibration curves. One graph is produced according to the external calibration method and another created using the internal standard method. Students are tasked to compare the square of the correlation coefficient (r^2) for each method in order to determine the best calibration curve to analyze xylitol in the gum samples. A near perfect linear calibration curve is often obtained using the internal standard method providing high accuracy and precision ($r^2=0.9992$) (Figure 5.5). Conversely, poor linearity (Figure 5.6) is often observed with the external standard calibration ($r^2=0.9808$). Upon quantification of xylitol in samples, students calculate the xylitol concentration that causes hypoglycemia in dogs, with emphasis on determining the quantity of gum stick that would cause toxicity for dogs of varying weights.

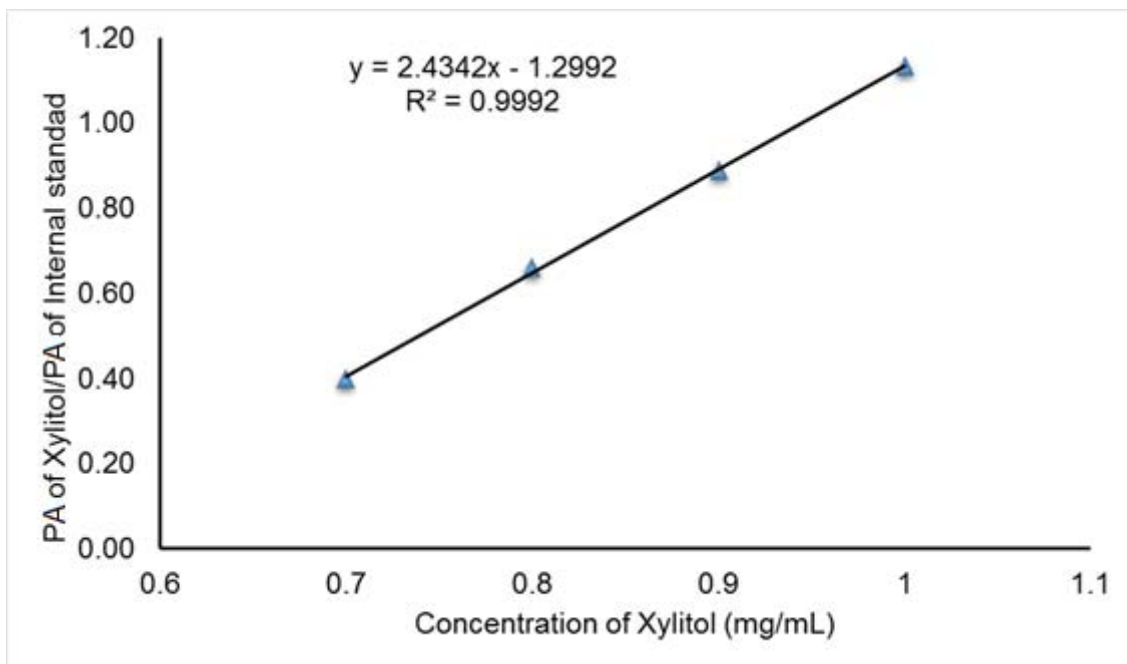


Figure 5.5 Calibration plot with internal standard.

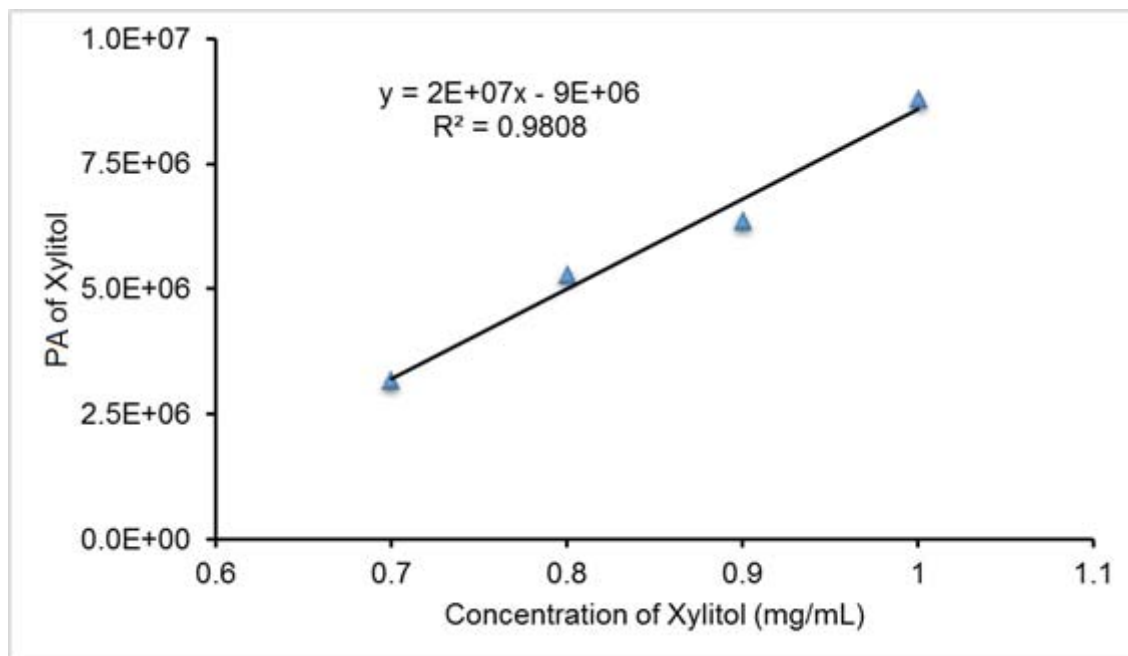


Figure 5.6 Calibration plot without internal standard

Where, PA = Peak Area and IS = Internal Standard

5.6 Evaluation of learning outcomes

This laboratory exercise was initially placed in front of 31 students in a second-semester organic laboratory course. Students were excited to find gum-chewing a part of the planned exercise and enthusiastically engaged in the extraction and analysis of xylitol from samples. Over 77% of surveyed students with this lab identified it as their favorite laboratory experiment of the semester.

Learning objectives included the comparison of internal versus external calibration techniques and the correct calculation of xylitol concentrations within each gum sample extract. We found that only 55% of our students could correctly calculate xylitol concentrations. Revised experimental protocol for the student procedure allowed us to clarify the extraction volumes for students to fix this difficulty. The revised procedure supported a second group of students (9 students; instrumental analysis course) to successfully calculate the xylitol concentrations (89%).

Laboratory reports for the experiment allowed students to practice mass spectral interpretation for peak identification in each chromatogram and encouraged students to understand splitting patterns for MS. The data analysis for each chromatogram honed student skills in critical thinking and supported their knowledge in spectral interpretation.

Students enjoyed the real- world application of identifying toxic concentrations of xylitol in sugar-free gums. In addition, the laboratory exercise allowed for analysis of organic compounds using water as the only extraction solvent and a method that avoided derivatives for GC-MS analysis. The laboratory experiment supports several of the 12 Principles of Green Chemistry³¹ including the use of safer solvents, the reduction of derivatives and the safer chemistry for accident prevention initiatives.

5.7 Conclusions

This laboratory experiment is excellent vehicle to explore the topics of extraction, solution preparation, calibration, and identification of components by mass spectrometry. The topic allows students to apply textbook knowledge as they work to address a real world situation. Challenging the students to choose a suitable calibration method for the analysis helps develop critical thinking while supporting a safe and green chemistry approach in the laboratory.

5.8 References

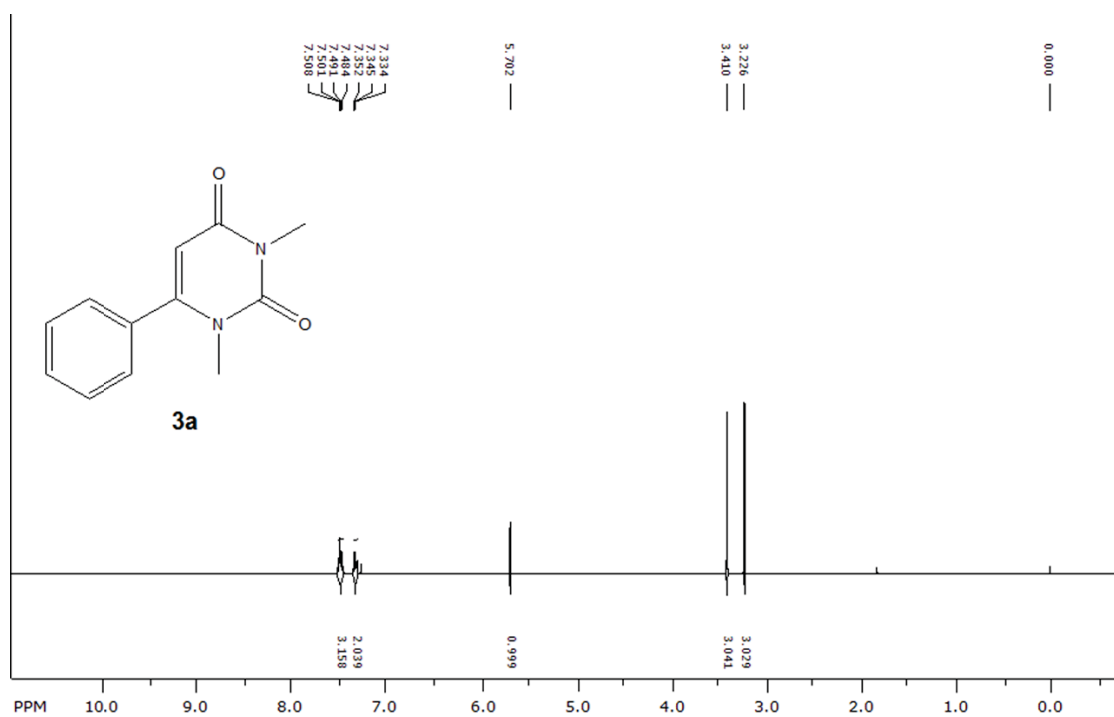
- (1) Antonio, A. G.; Pierro, V. S. d. S.; Maia, L. C. *J. Public. Health. Dent.* **2011**, *71*, 117.
- (2) Twetman, S. *Evid-based Dent* **2008**, *10*, 10.
- (3) Hayes, C. *J. Dent. Educ.* **2001**, *65*, 1106.
- (4) Deshpande, A.; Jadad, A. R. *J. Am. Dent. Assoc.* **2008**, *139*, 1602.
- (5) Burt, B. A. *J. Am. Dent. Assoc.* **2006**, *137*, 190.
- (6) Dunayer, E. K.; Gwaltney-Brant, S. M. *J. Am. Vet. Med. Assoc.* **2006**, *229*, 1113.
- (7) Xia, Z.; He, Y.; Yu, J. *J. Vet. Pharmacol. Ther.* **2009**, *32*, 465.
- (8) Peterson, M. E. *Top. Companion Anim. Med.* **2013**, *28*, 18.
- (9) Dunayer, E. K. *Vet. Med.* **2006**.
- (10) Todd, J. M.; Powell, L. L. *J. Vet. Emerg. Crit. Care* **2007**, *17*, 286.
- (11) Murphy, L. A.; Coleman, A. E. *Vet. Clin. North Am. Small Anim. Pract.* **2012**, *42*, 307.
- (12) Campbell, A.; Bates, N. *Vet. Rec.* **2010**, *167*, 108.
- (13) Campbell, A.; Bates, N. *Vet. Rec.* **2008**, *162*, 254.
- (14) Quach, D. T.; Ciszkowski, N. A.; Finlayson-Pitts, B. J. *J. Chem. Educ.* **1998**, *75*, 1595.
- (15) Pierce, K. M.; Schale, S. P.; Le, T. M.; Larson, J. C. *J. Chem. Educ.* **2011**, *88*, 806.
- (16) Guisto-Norkus, R.; Gounili, G.; Wisniecki, P.; Hubball, J. A.; Smith, S. R.; Stuart, J. D. *J. Chem. Educ.* **1996**, *73*, 1176.
- (17) Galipo, R. C.; Canhoto, A. J.; Walla, M. D.; Morgan, S. L. *J. Chem. Educ.* **1999**, *76*, 245.
- (18) Wilson, R. I.; Mathers, D. T.; Mabury, S. A.; Jorgensen, G. M. *J. Chem. Educ.* **2000**, *77*, 1619.
- (19) Mead, R. N.; Seaton, P. J. *J. Chem. Educ.* **2011**, *88*, 1130.
- (20) Rubinson, J. F.; Neyer-Hilvert, J. *J. Chem. Educ.* **1997**, *74*, 1106.

- (21) Mowery, K. A.; Blanchard, D. E.; Smith, S.; Betts, T. A. *J. Chem. Educ.* **2004**, *81*, 87.
- (22) Sobel, R. M.; Ballantine, D. S.; Ryzhov, V. *J. Chem. Educ.* **2005**, *82*, 601.
- (23) Pawliszyn, J.; Yang, M. J.; Orton, M. L. *J. Chem. Educ.* **1997**, *74*, 1130.
- (24) Fan, X.; Lam, M.; Mathers, D. T.; Mabury, S. A.; Witter, A. E.; Klinger, D. M. *J. Chem. Educ.* **2002**, *79*, 1257.
- (25) Hardee, J. R.; Long, J.; Otts, J. *J. Chem. Educ.* **2002**, *79*, 633.
- (26) Heimbeck, C. A.; Bower, N. W. *J. Chem. Educ.* **2002**, *79*, 1254.
- (27) O'Malley, R. M.; Lin, H. C. *J. Chem. Educ.* **1999**, *76*, 1547.
- (28) Hodgson, S. C.; Casey, R. J.; Orbell, J. D.; Bigger, S. W. *J. Chem. Educ.* **2000**, *77*, 1631.
- (29) Clennan, M. M.; Clennan, E. L. *J. Chem. Educ.* **2005**, *82*, 1676.
- (30) Novak, M.; Heinrich, J.; Martin, K. A.; Green, J.; Lytle, S. *J. Chem. Educ.* **1993**, *70*, A103.
- (31) ACS Green Chemistry Institute: 12 Principles of Green Chemistry. <https://www.acs.org/content/acs/en/greenchemistry/what-is-green-chemistry/principles/12-principles-of-green-chemistry.html> (Accessed Feb 24, **2017**).

APPENDIX A

^1H NMR, ^{13}C NMR AND 2D-NOESY OF ALL NEW COMPOUNDS

1,3-dimethyl-6-phenylpyrimidine-2,4(1H,3H)-dione (3a).

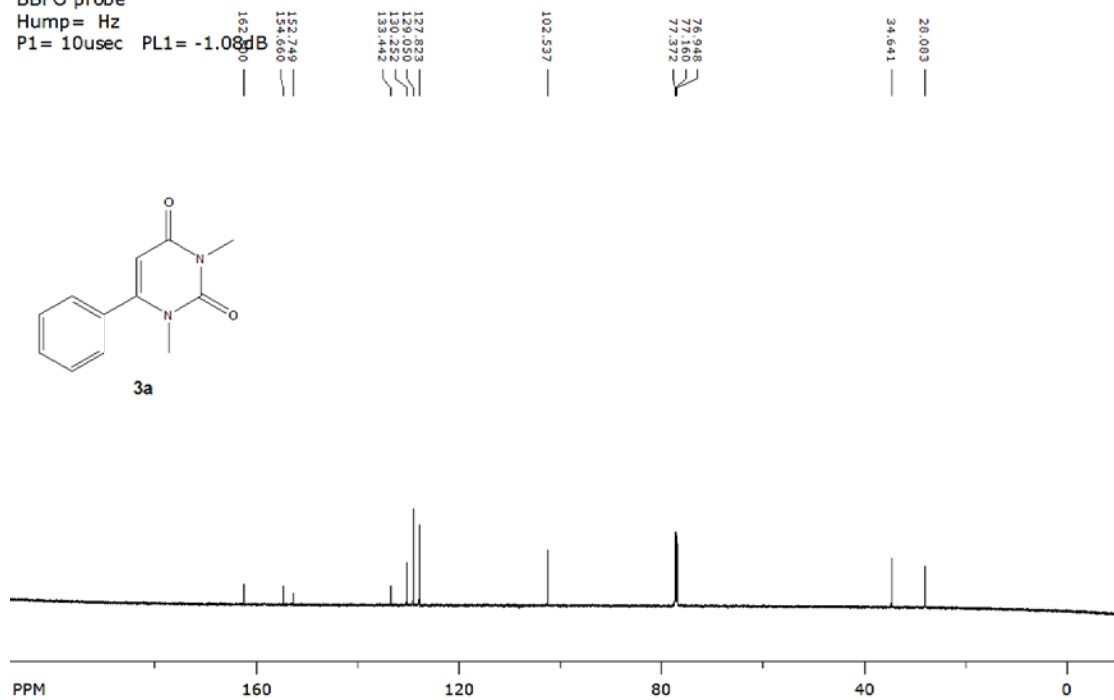


BBFO probe

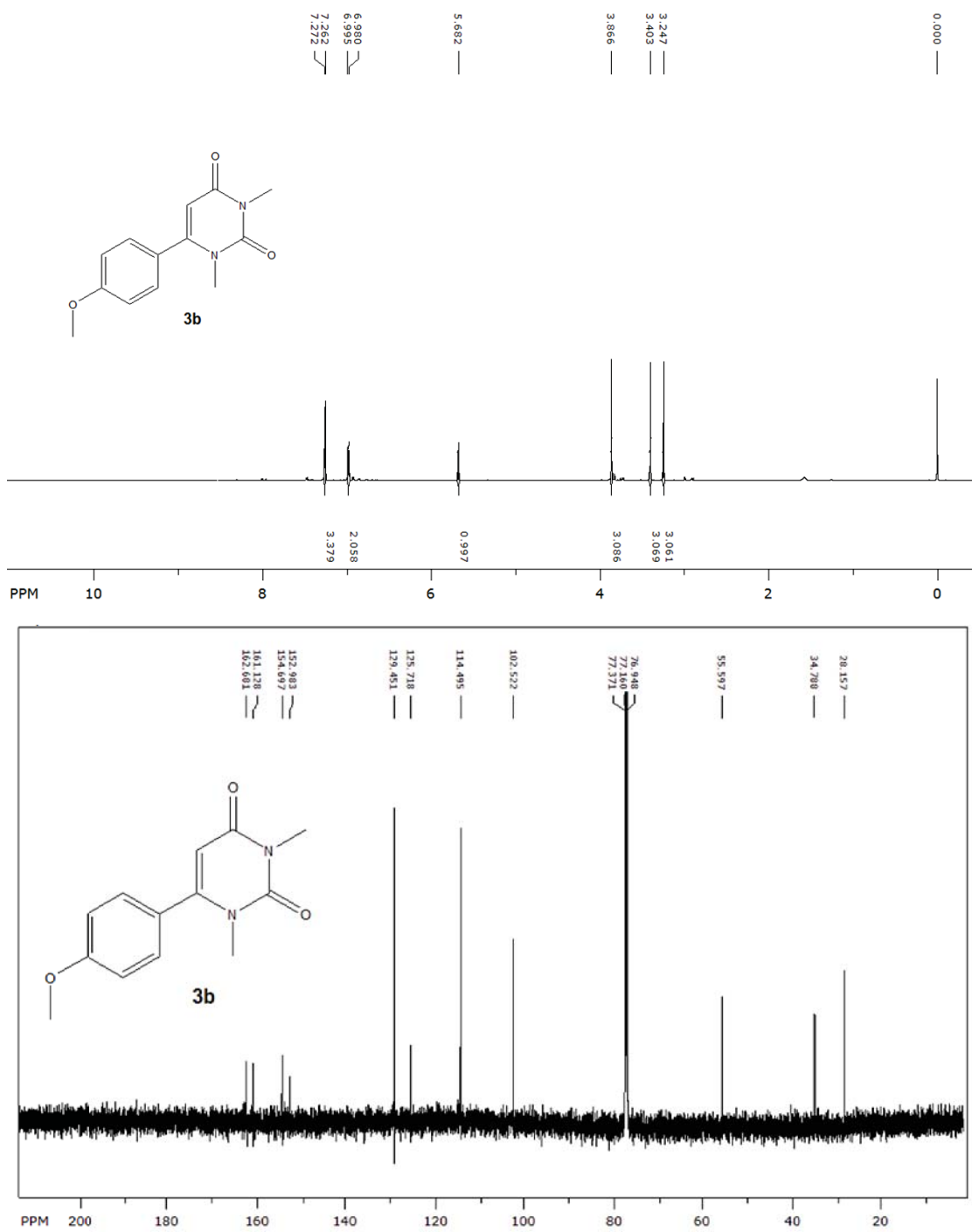
Hump = Hz

P1 = 10usec

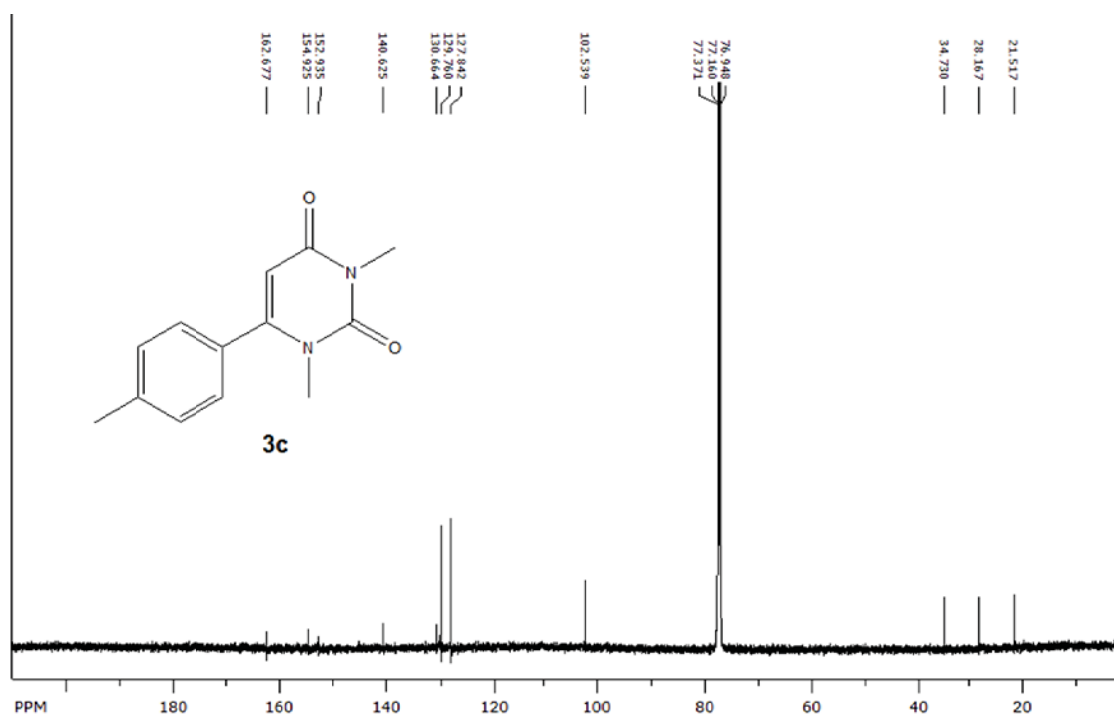
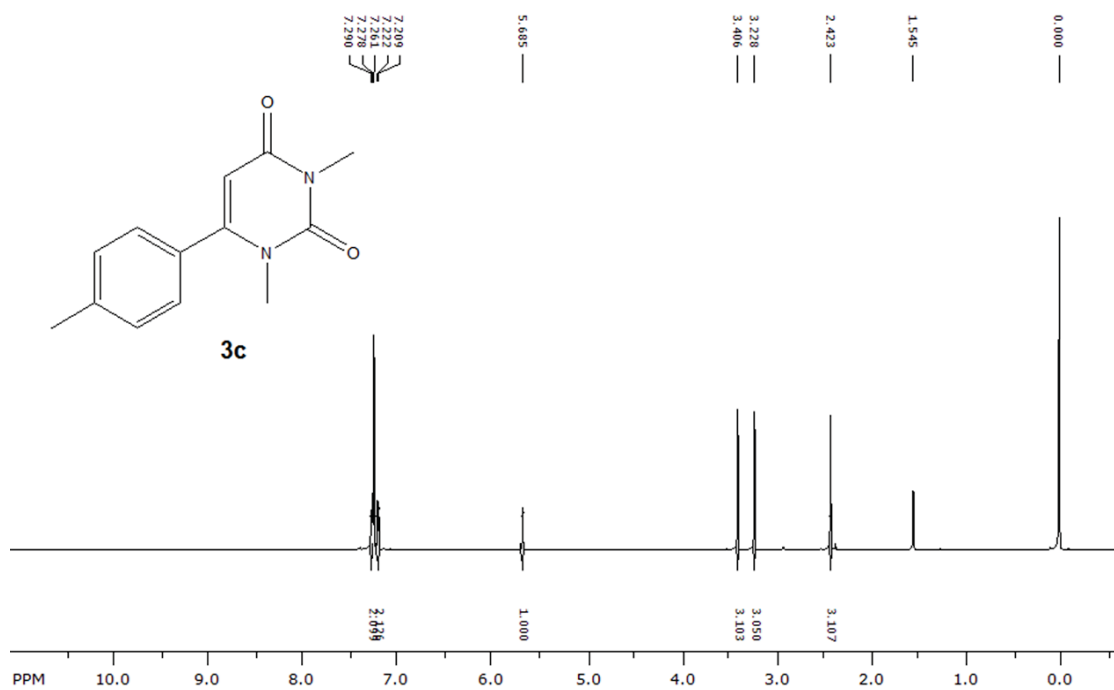
PL1 = -1.08dB



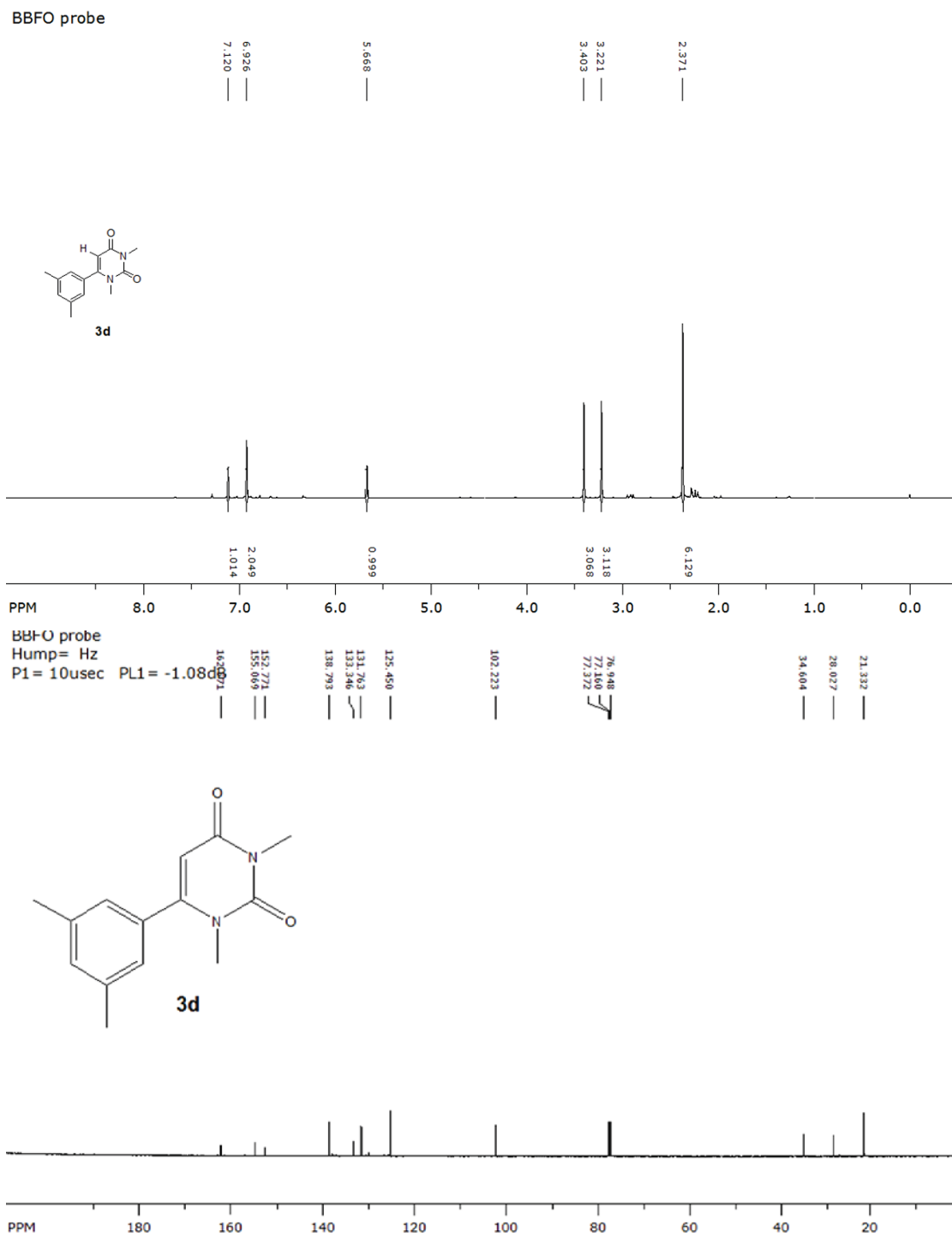
6-(4-Methoxyphenyl)-1,3-dimethylpyrimidine-2,4 (1H,3H)-dione (3b).



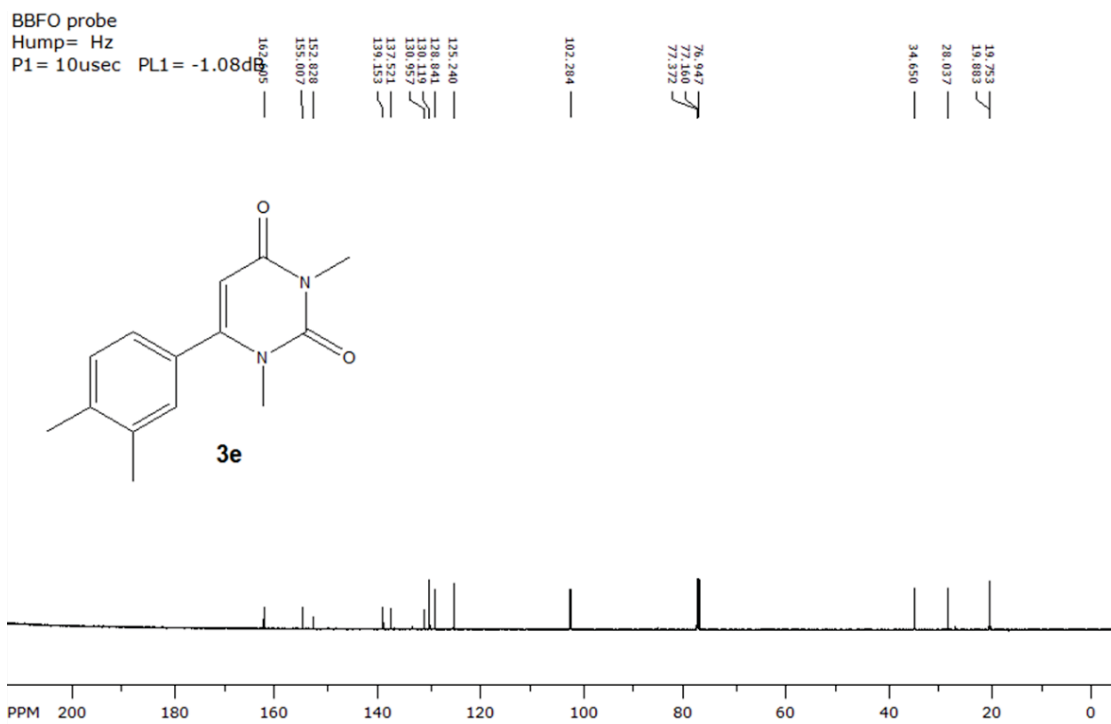
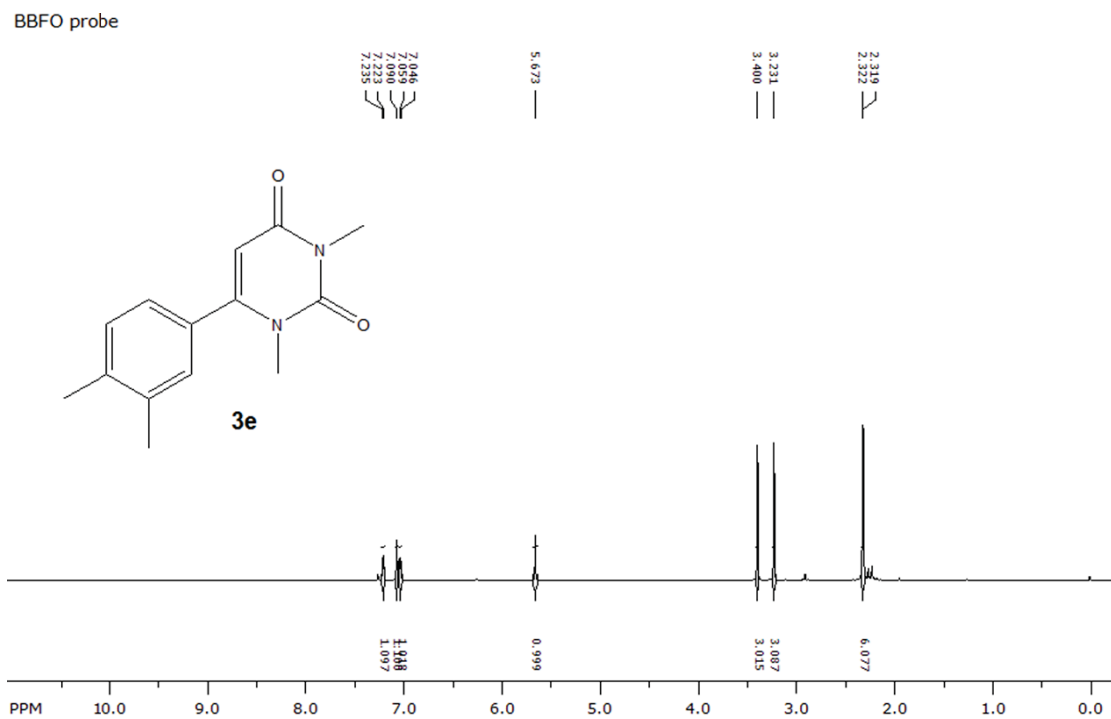
6-(4-Methylphenyl)-1,3-dimethylpyrimidine-2,4(1H,3H)-dione (3c).



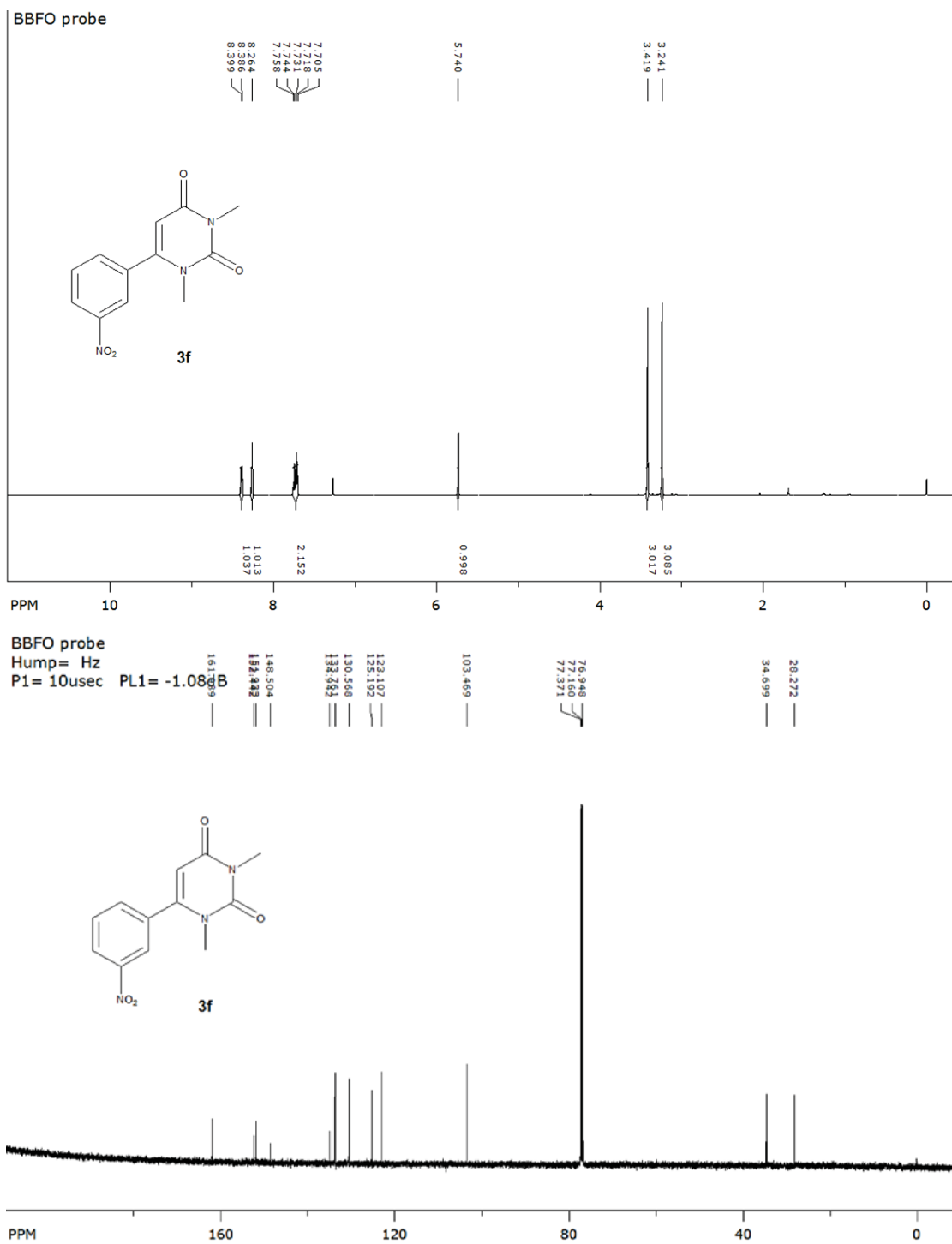
6-(3,5-Dimethylphenyl)-1,3-dimethylpyrimidine-2,4(1H,3H)-dione (3d).



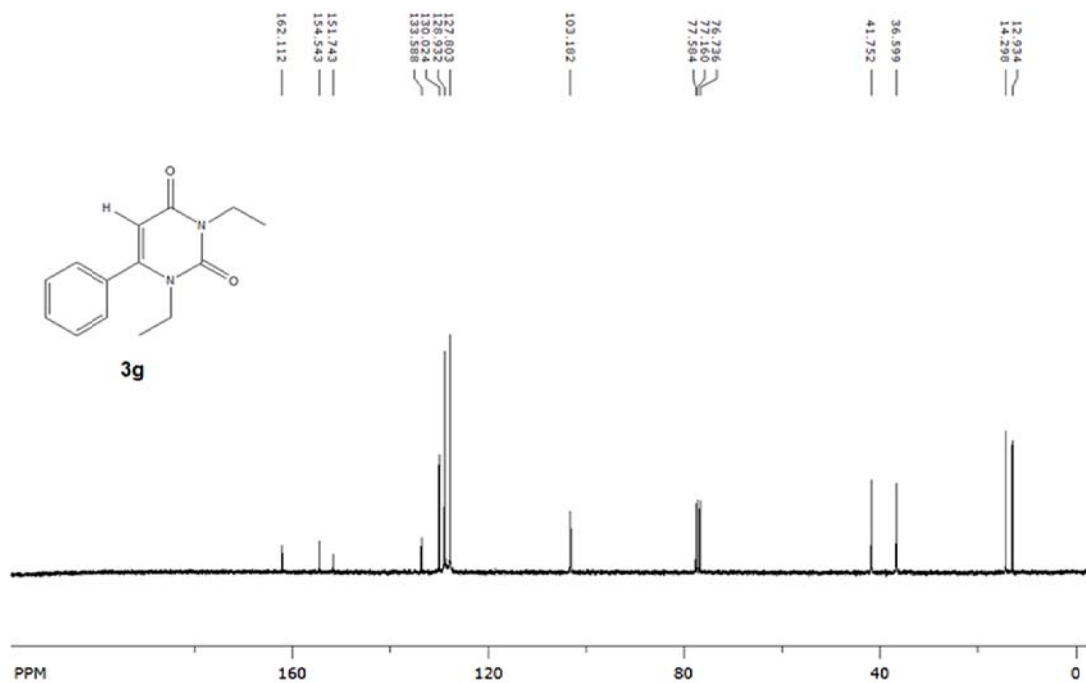
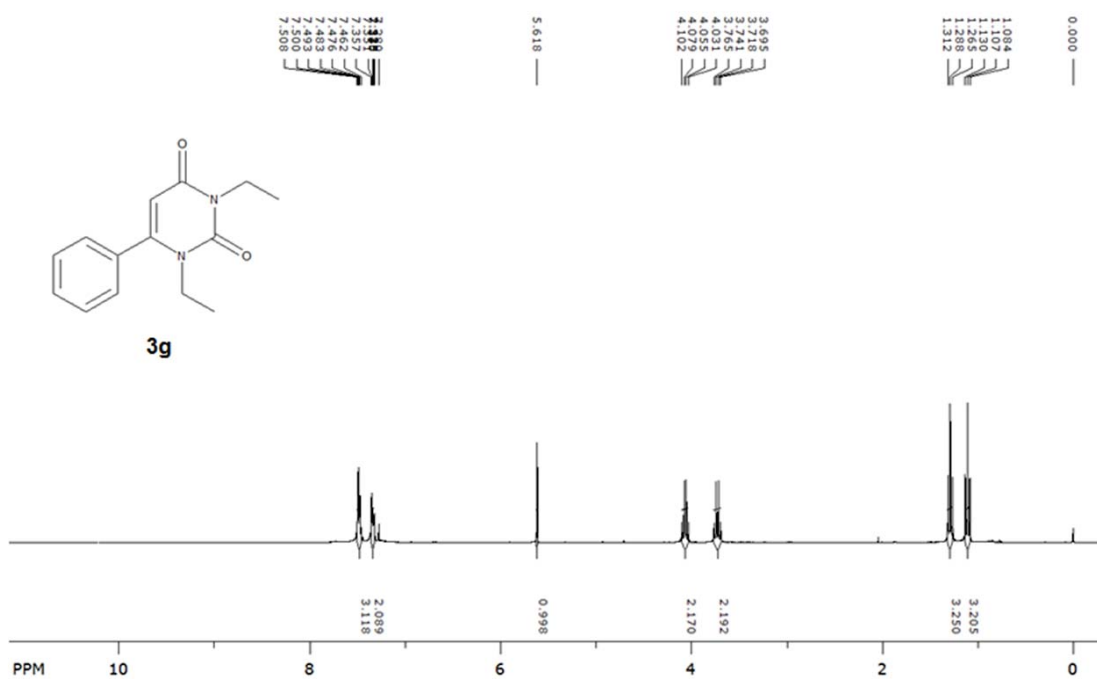
6-(3,4-Dimethylphenyl)-1,3-dimethylpyrimidine-2,4(1H,3H)-dione (3e).



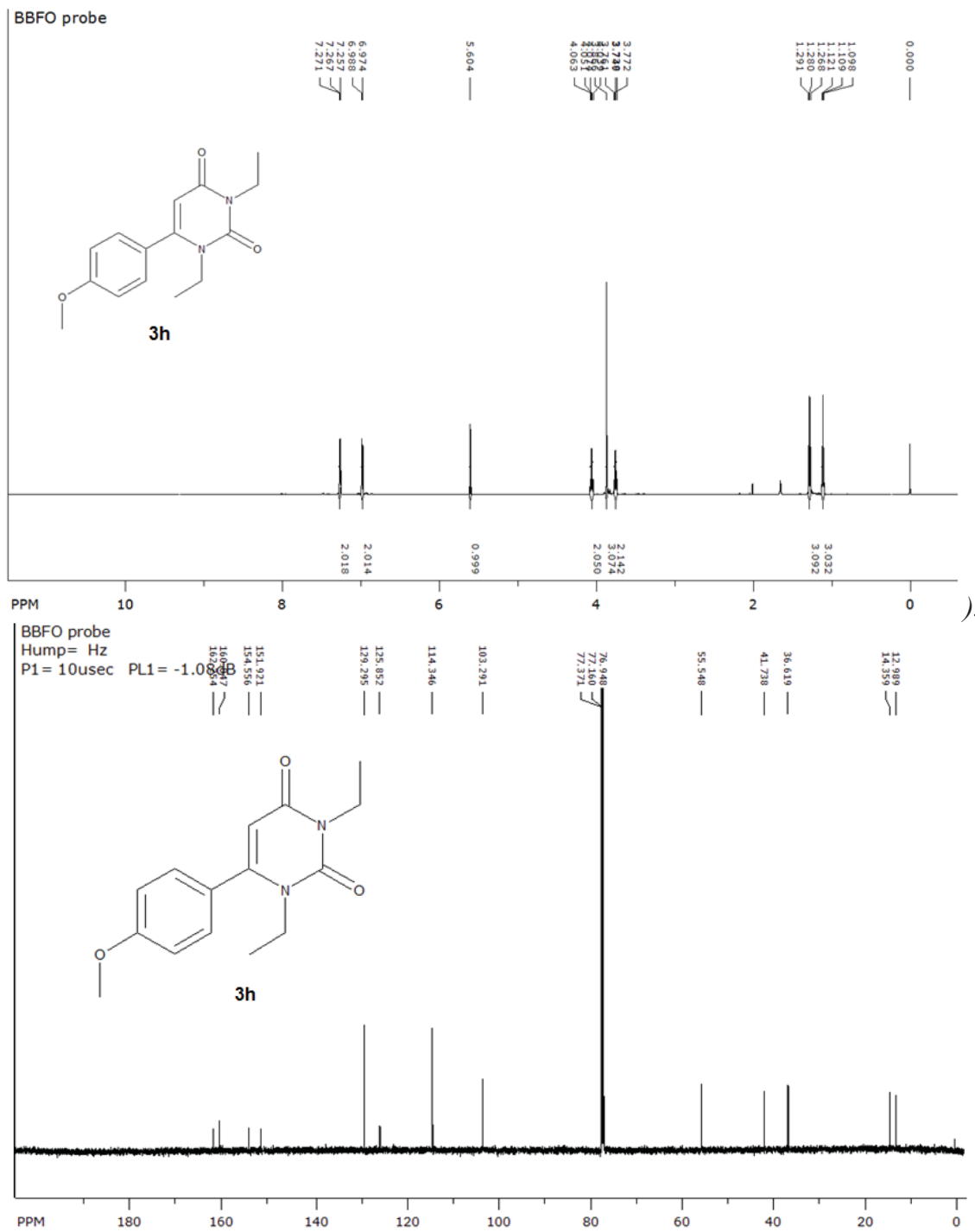
1,3-Dimethyl-6-(3-nitrophenyl)pyrimidine-2,4(1H,3H)-dione (3f).



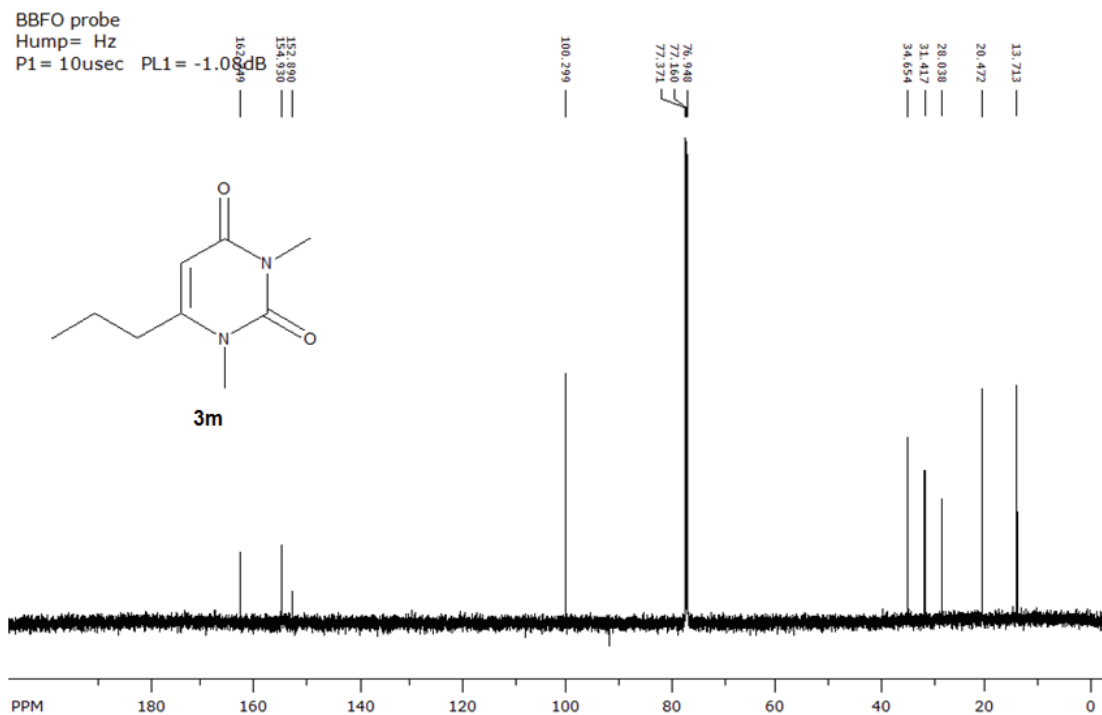
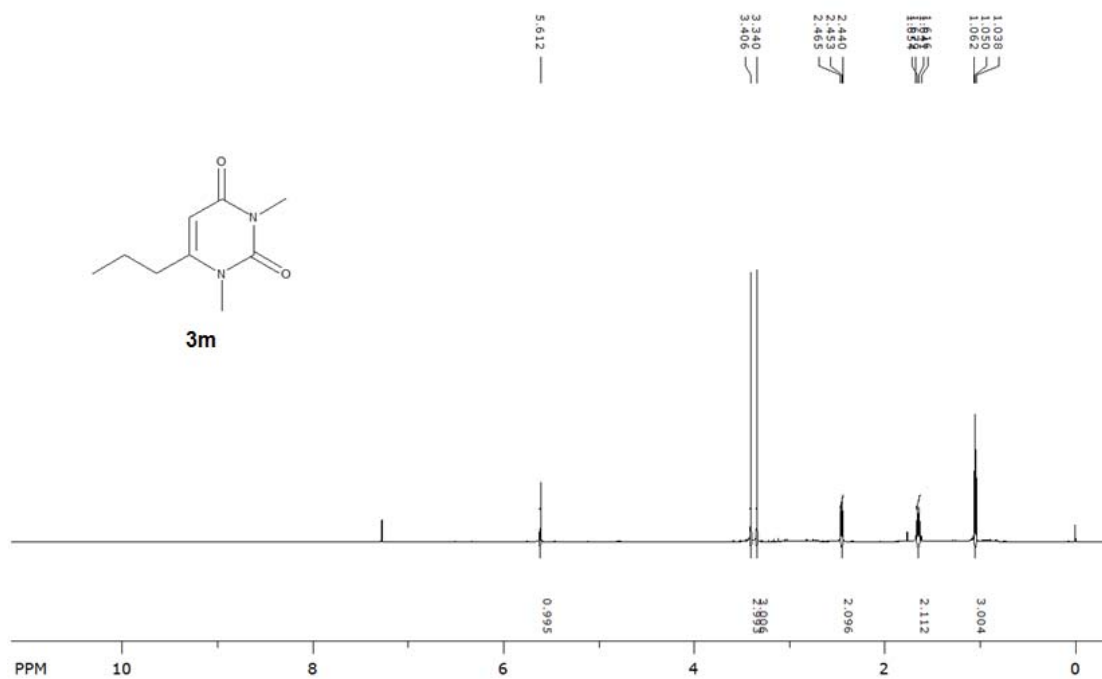
1,3-Diethyl-6-phenylpyrimidine-2,4(1H,3H)-dione (3g).



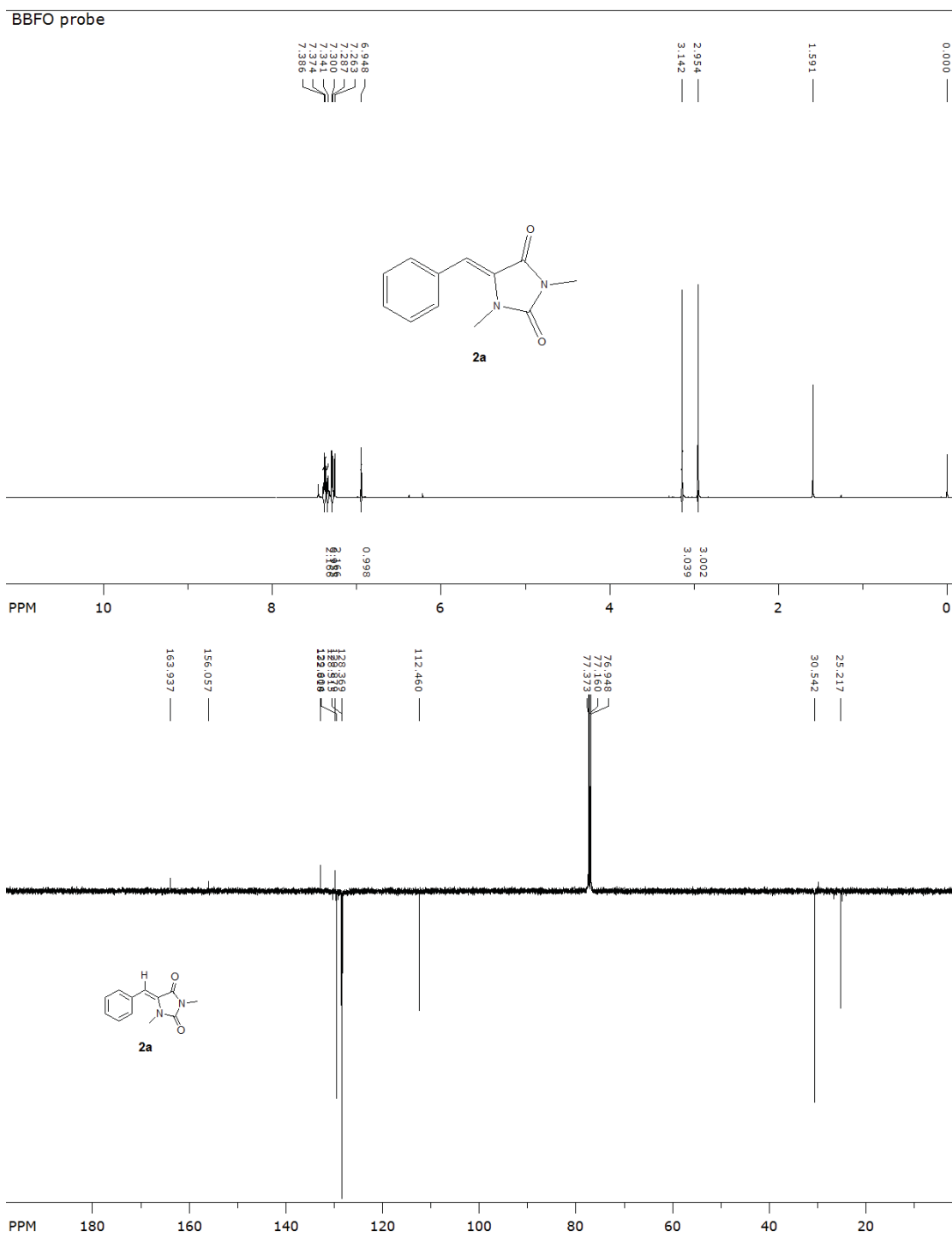
6-(4-Methoxyphenyl)-1,3-diethylpyrimidine-2,4(1H,3H)-dione (3h).

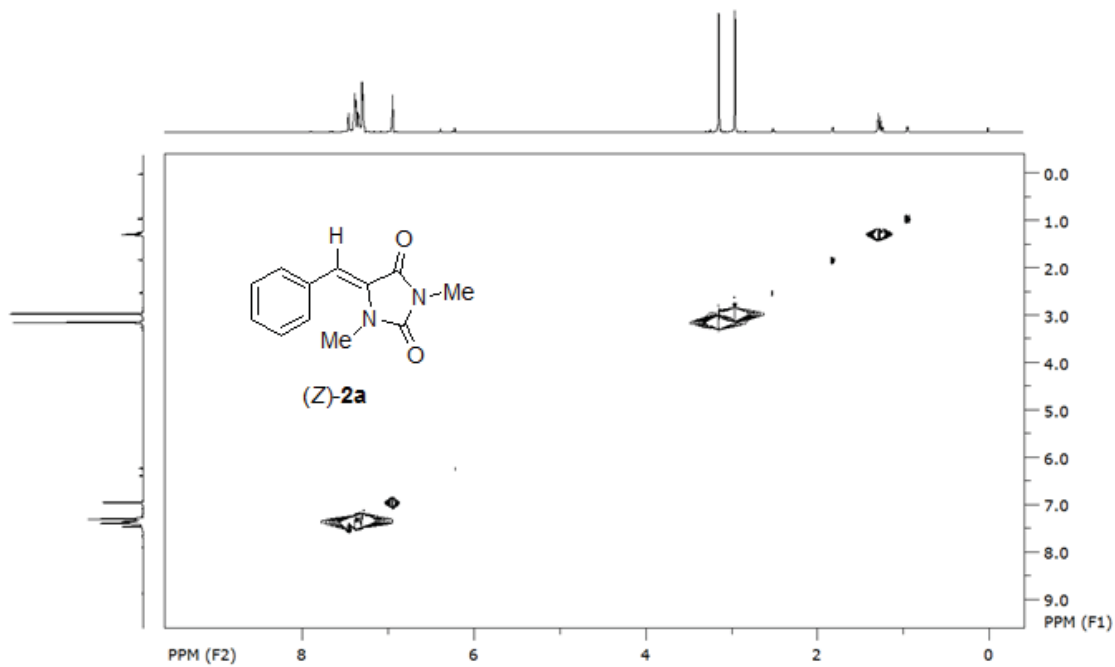


1,3-Dimethyl-6-propylpyrimidine-2,4(1H,3H)-dione (3m).

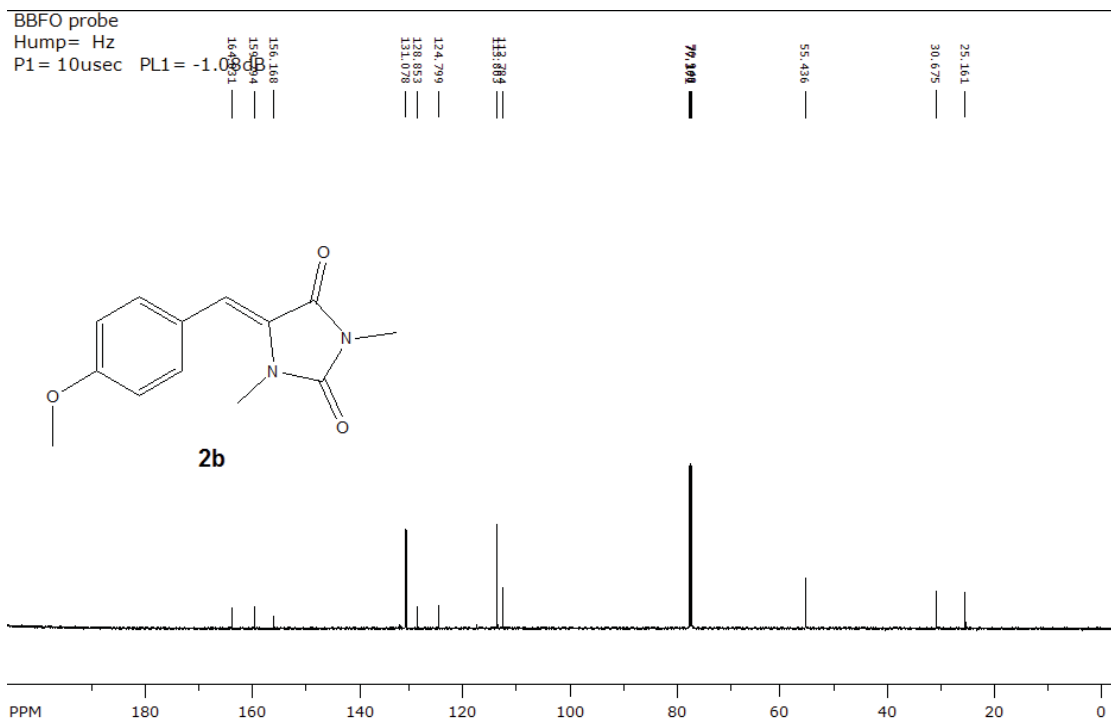
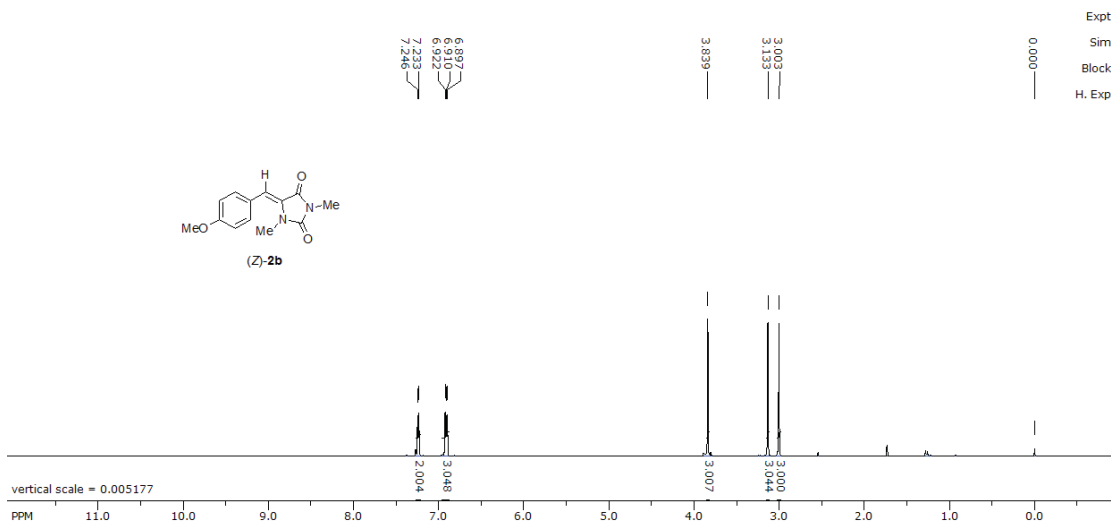


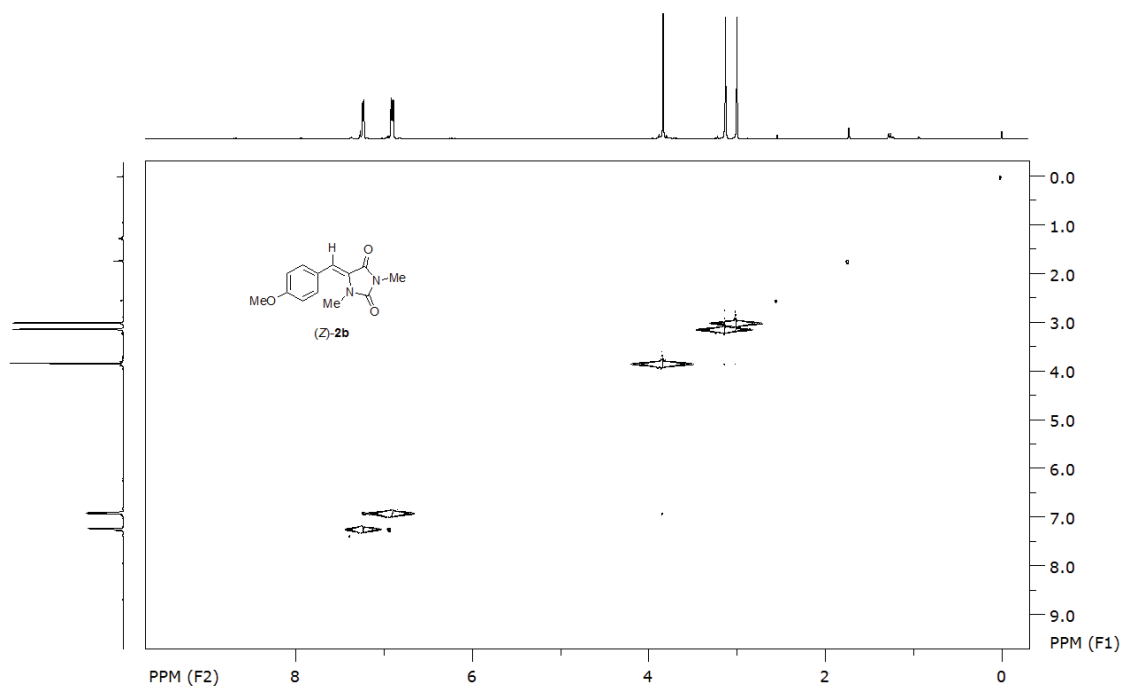
(Z)-5-Benzylidene-1,3-dimethylimidazolidine-2,4-dione [(Z)-2a].



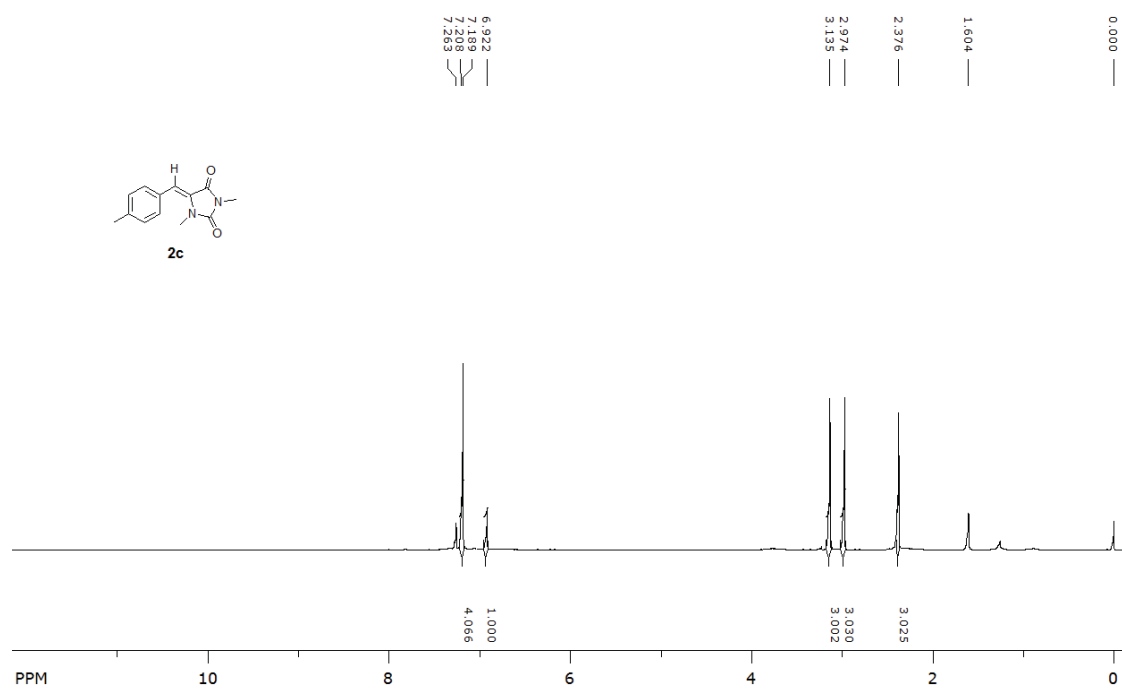


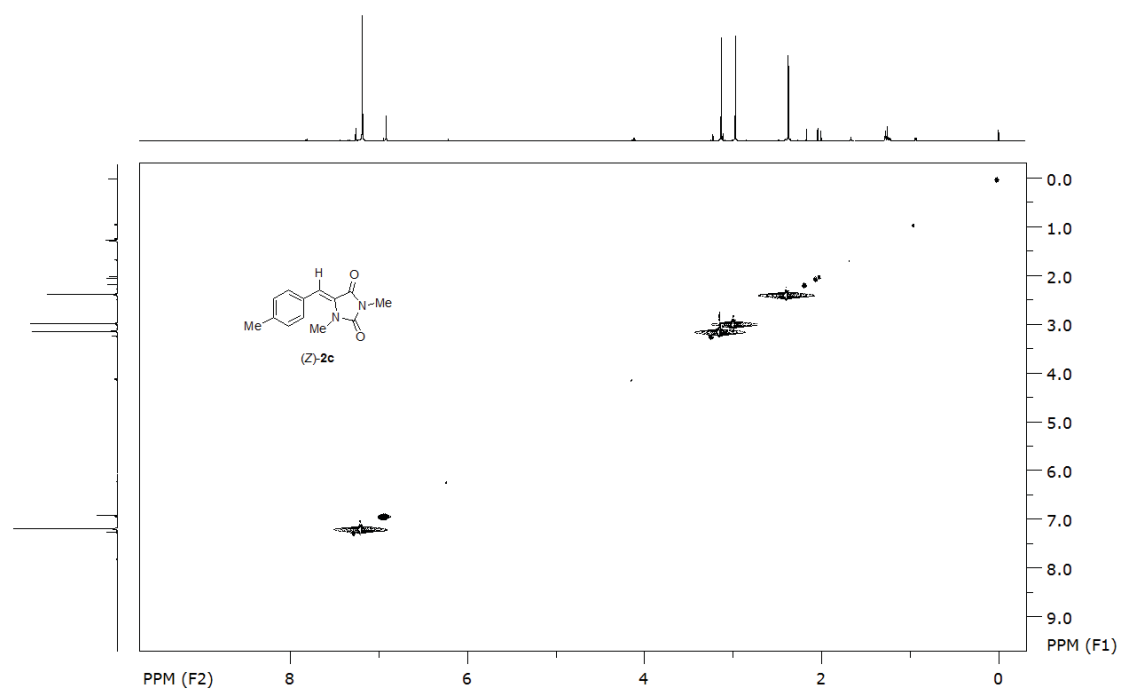
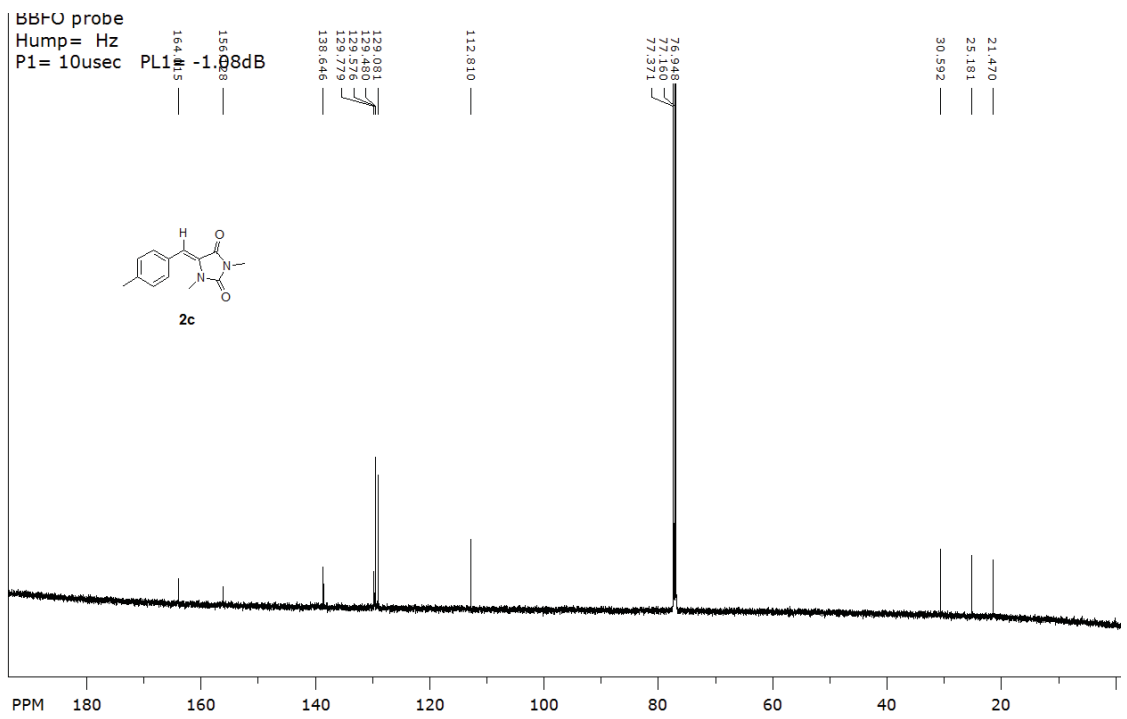
(Z)-5-(4-Methoxybenzylidene)-1,3-dimethylimidazolidine-2,4-dione [(Z)-2b].



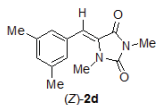
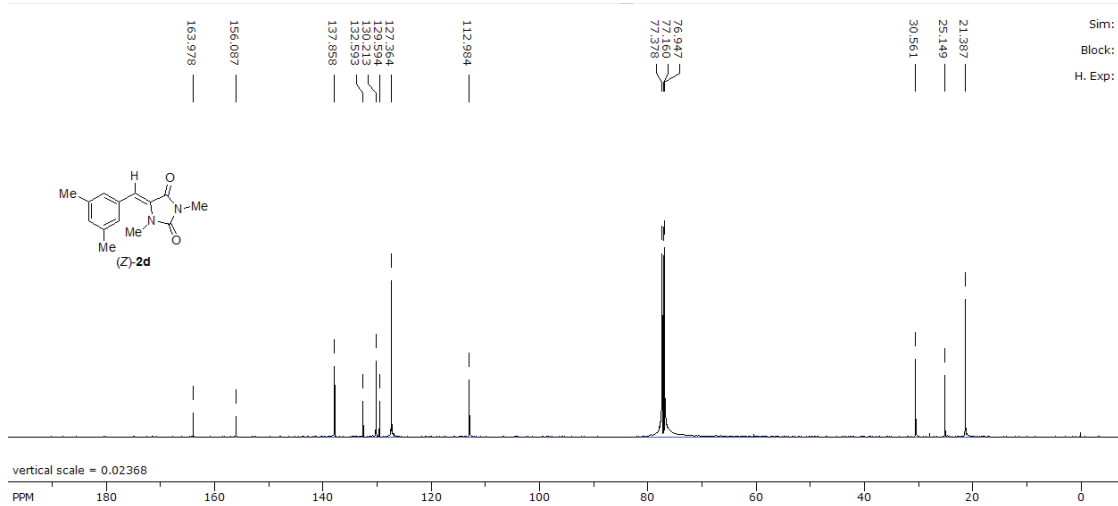
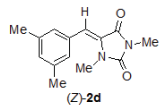
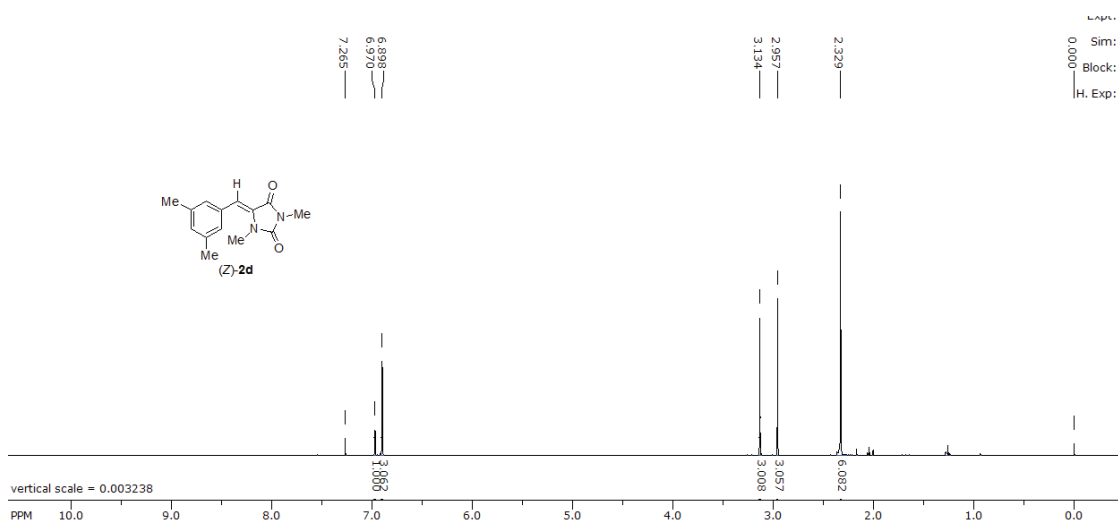


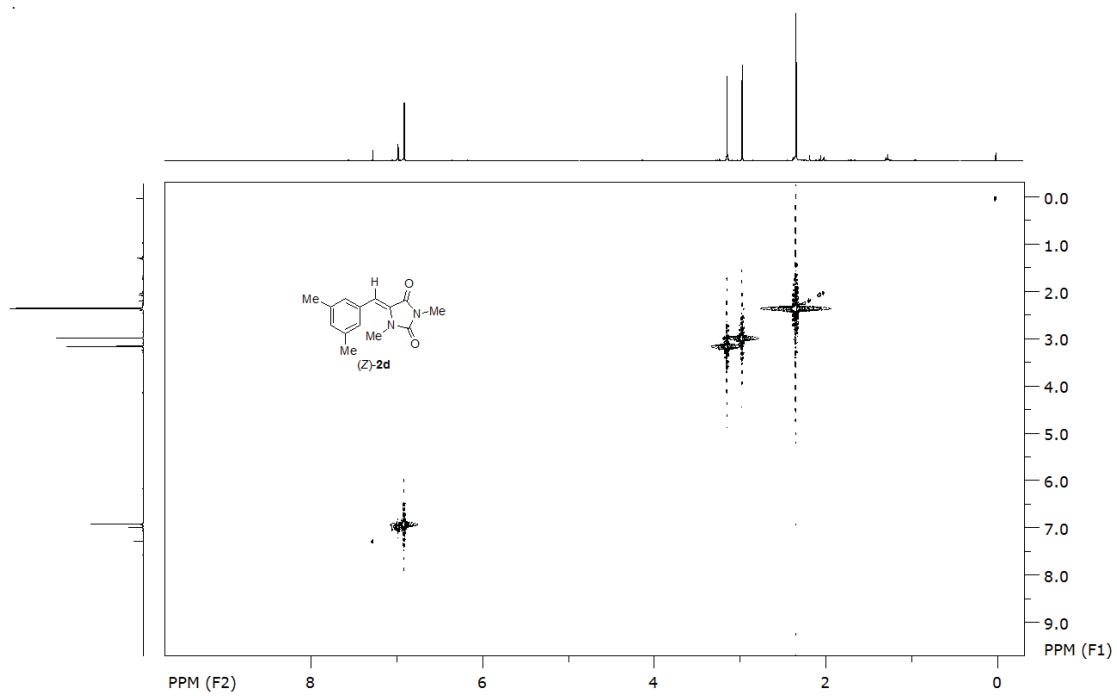
(Z)-5-(4-Methylbenzylidene)-1,3-dimethylimidazolidine-2,4-dione [(Z)-2c].



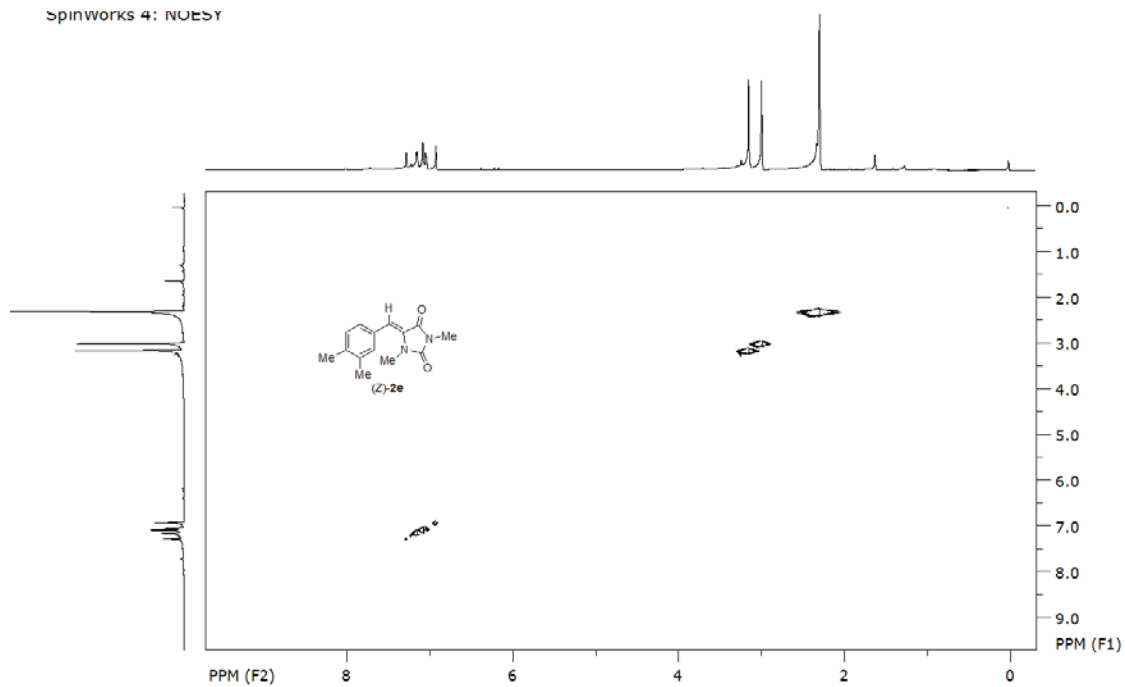


(Z)-5-(3,5-Dimethylbenzylidene)-1,3-dimethylimidazolidine-2,4-dione [(Z)-2d].

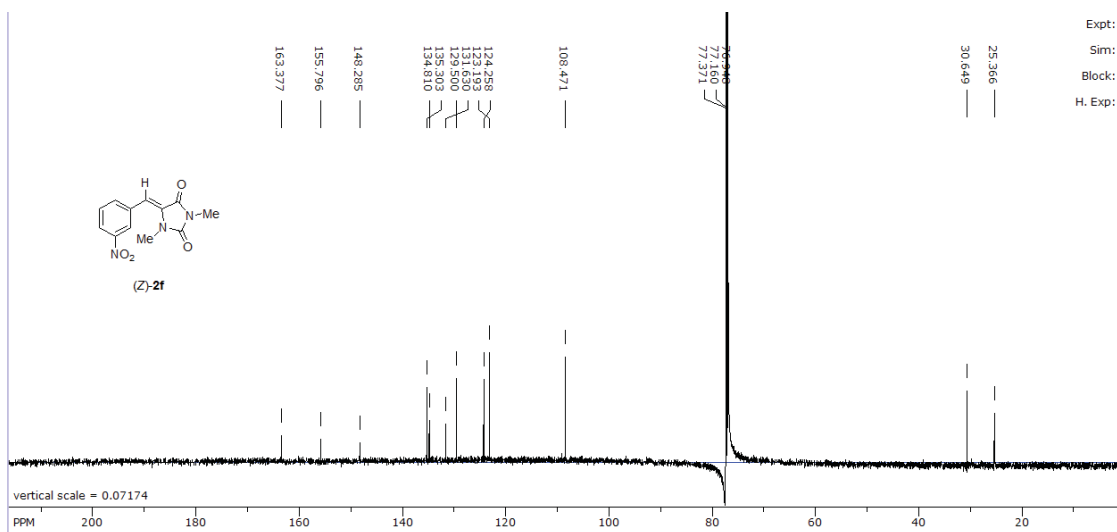
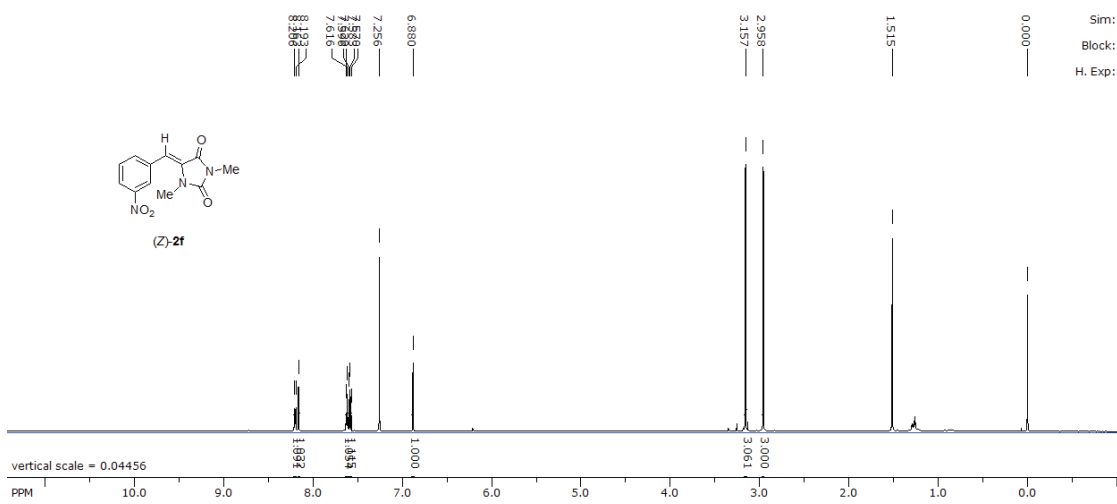




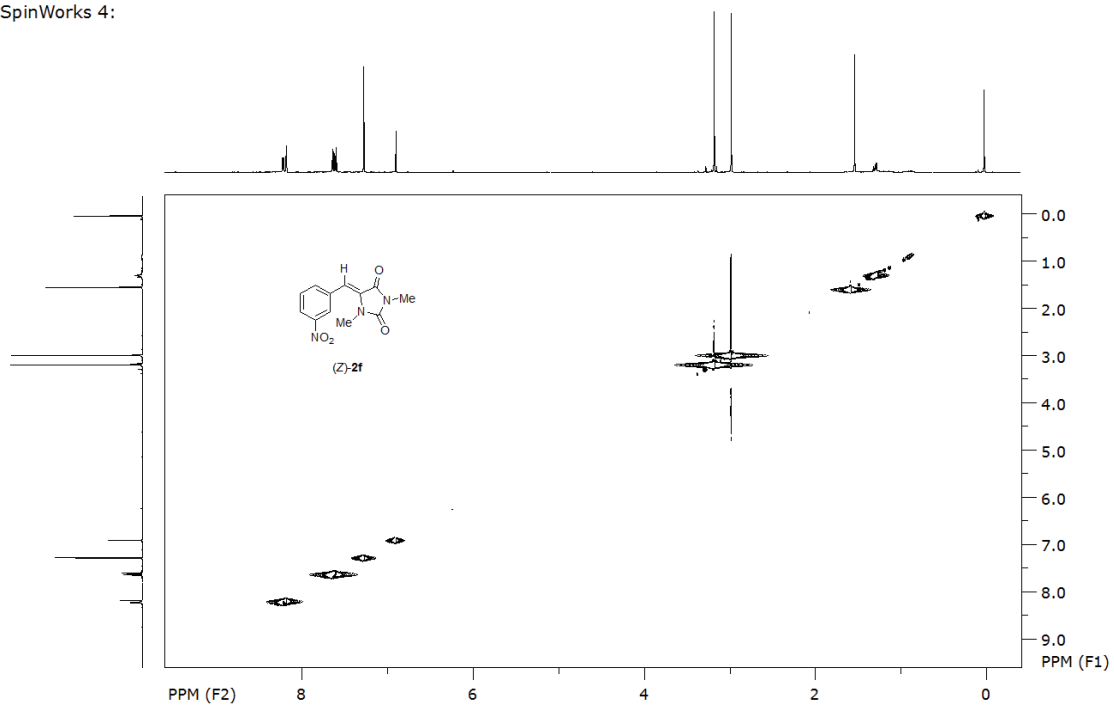
Spinworks 4: NOESY



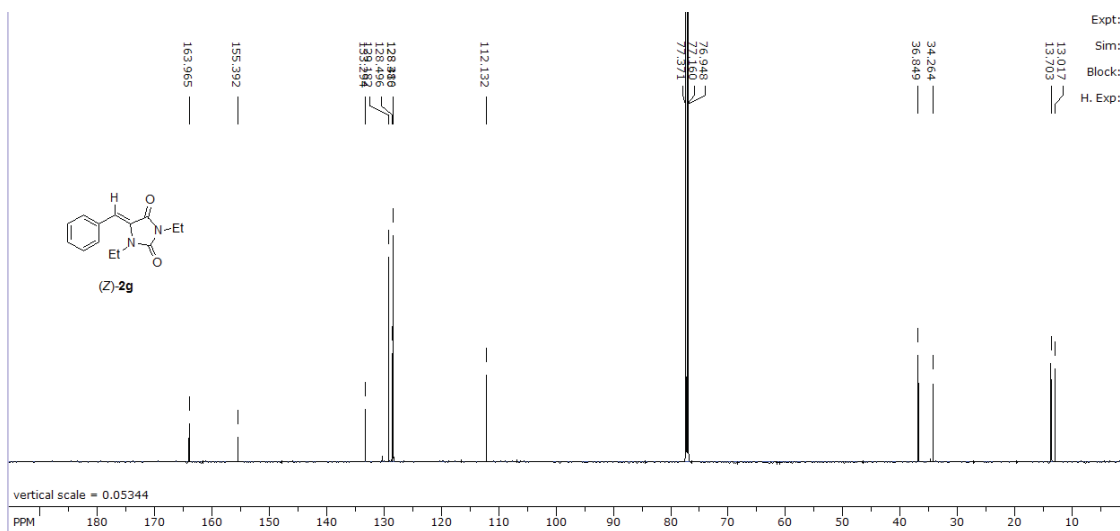
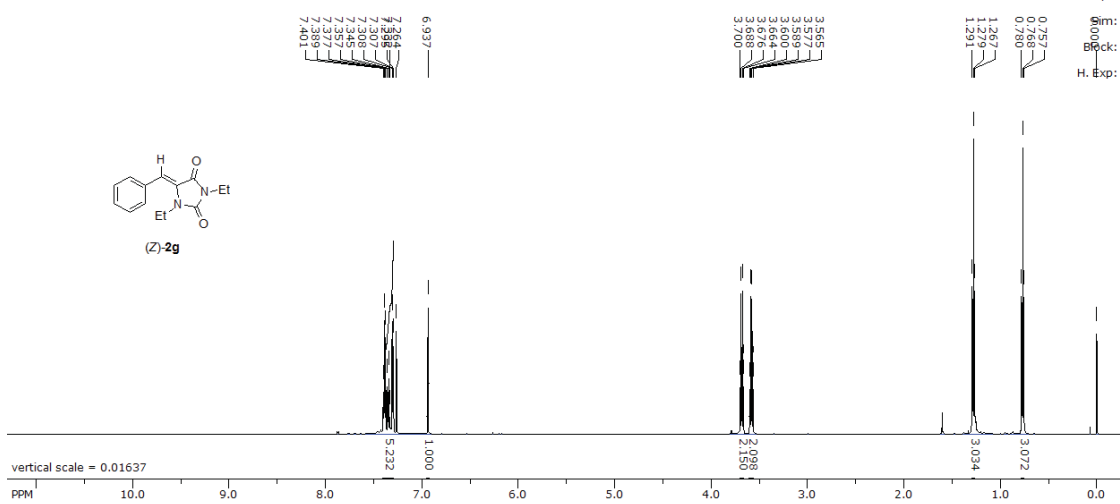
(Z)-5-(3-Nitrophenyl)-1,3-dimethylimidazolidine-2,4-dione [(Z)-2f].

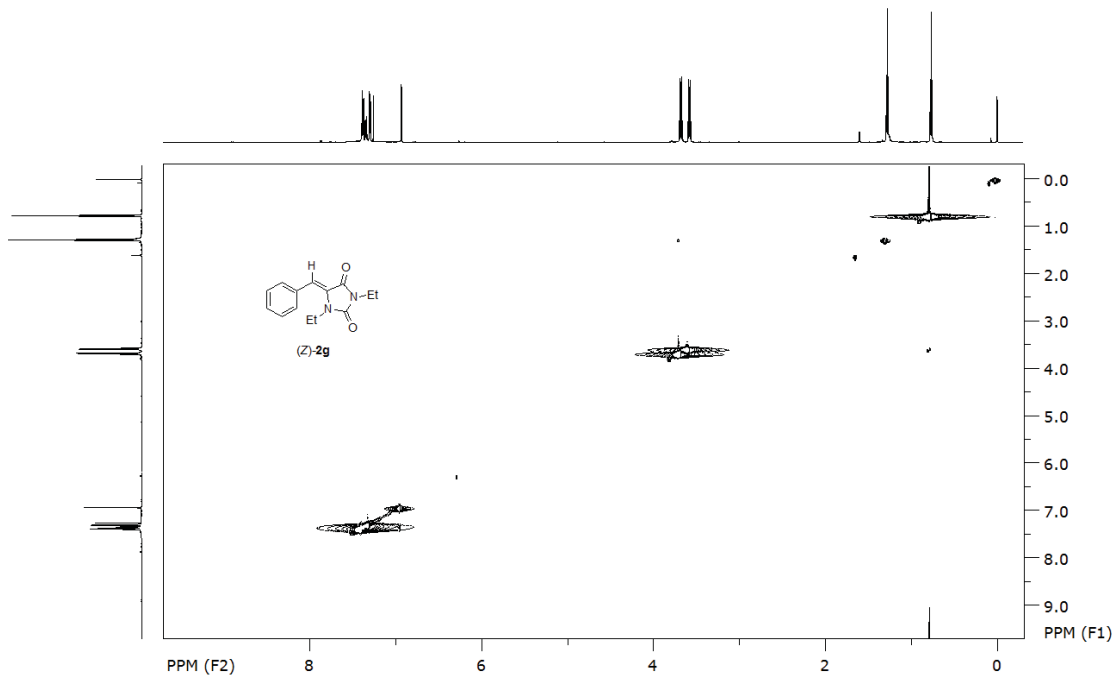


SpinWorks 4:

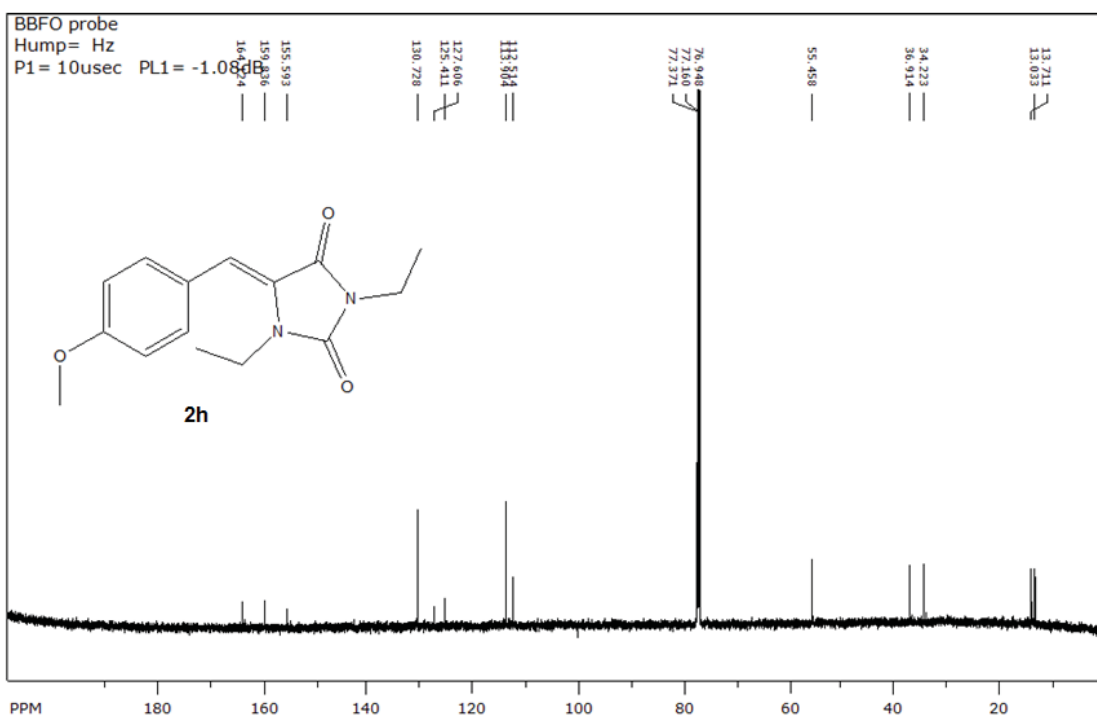
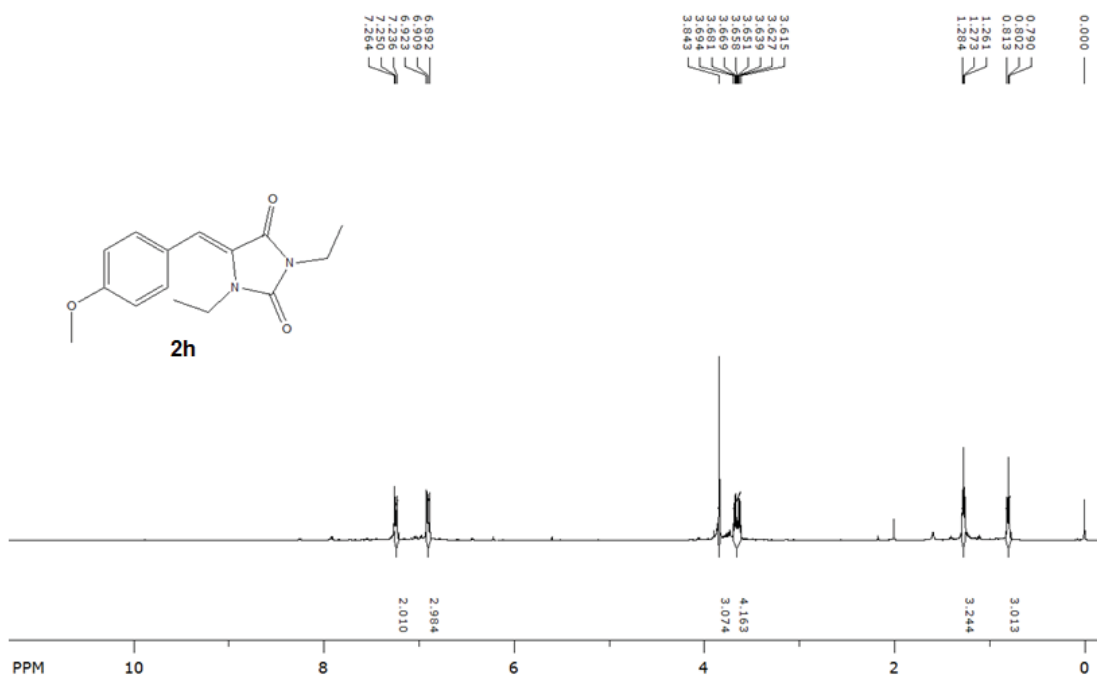


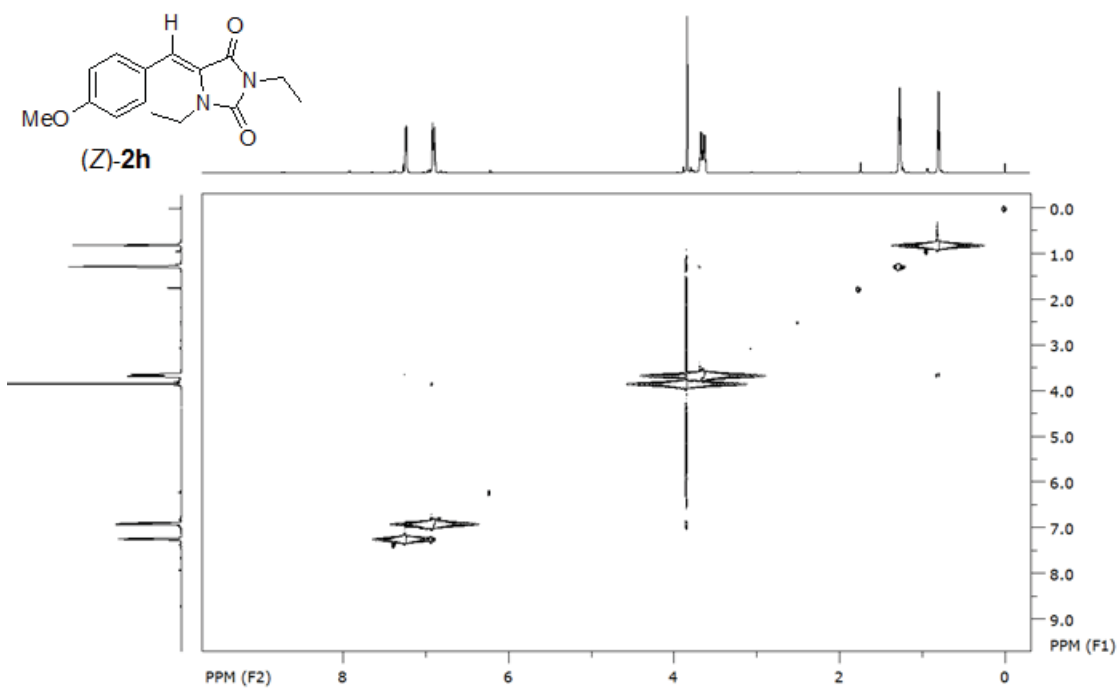
(Z)-5-Benzylidene-1,3-diethylimidazolidine-2,4-dione [(Z)-2g].



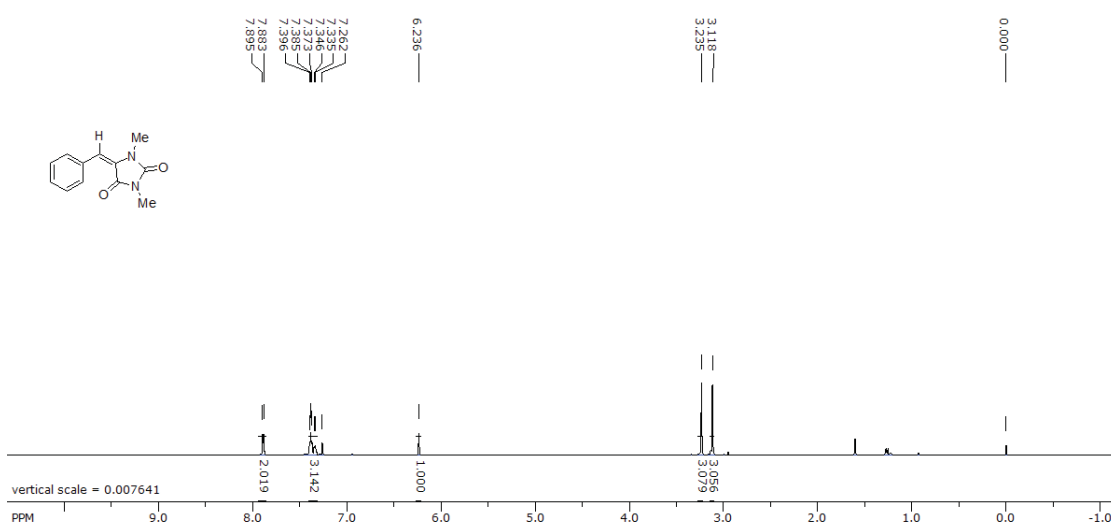
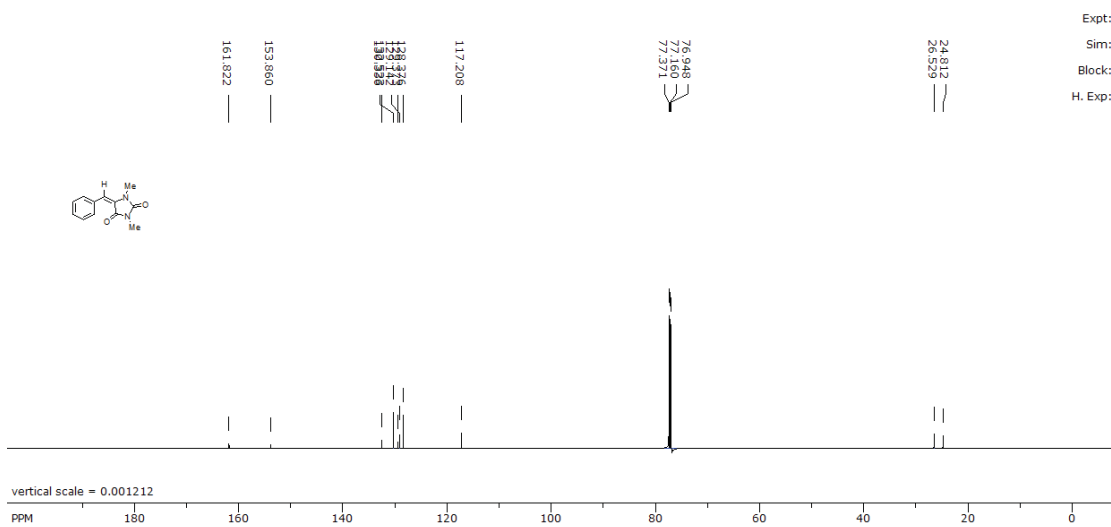


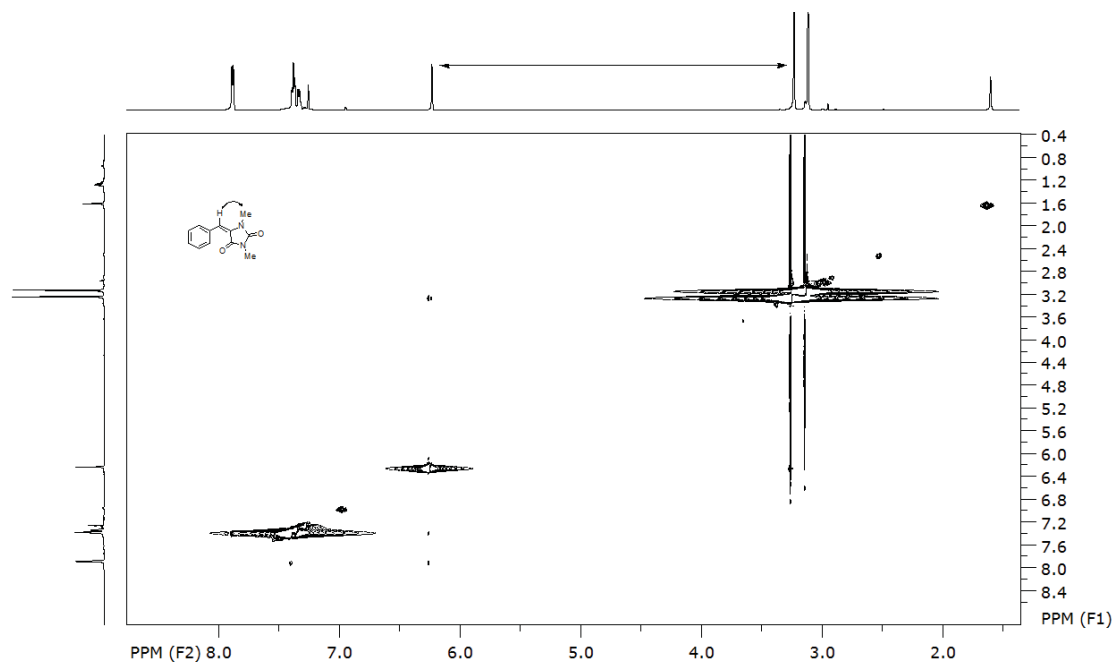
(Z)-5-(4-Methoxybenzylidene)-1,3-diethylimidazolidine-2,4-dione [(Z)-2h].



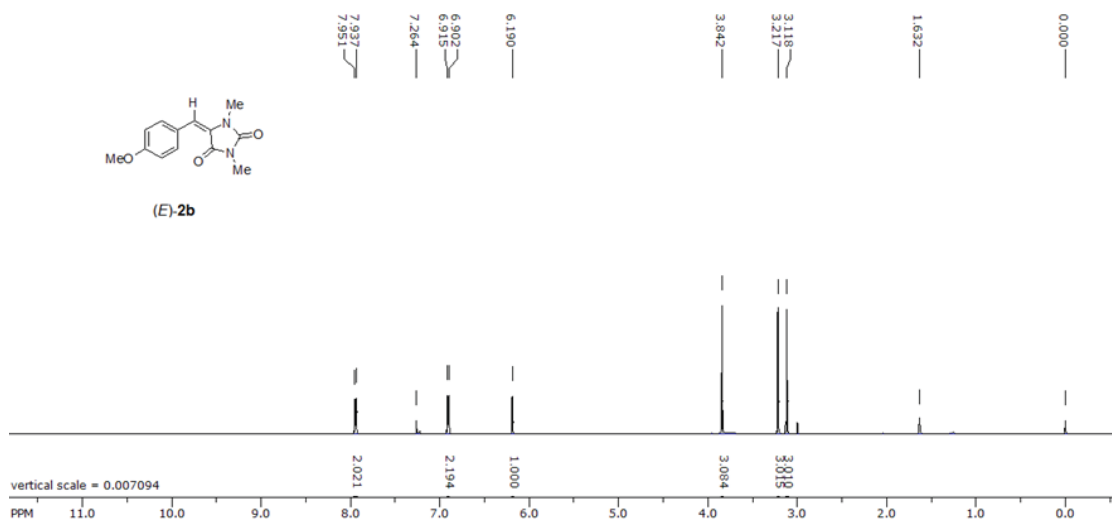


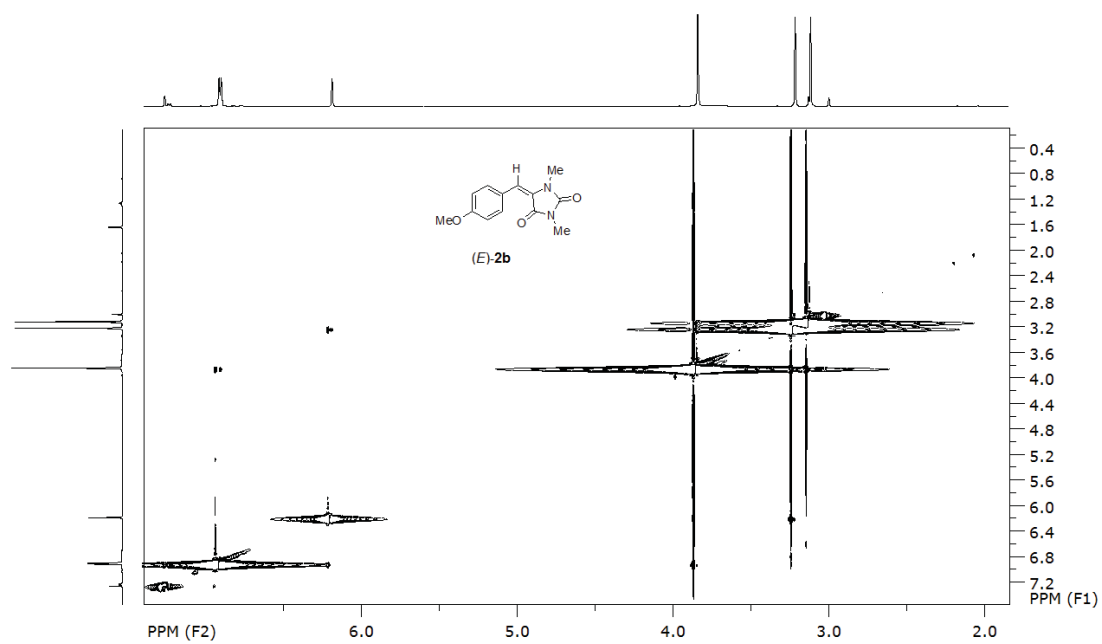
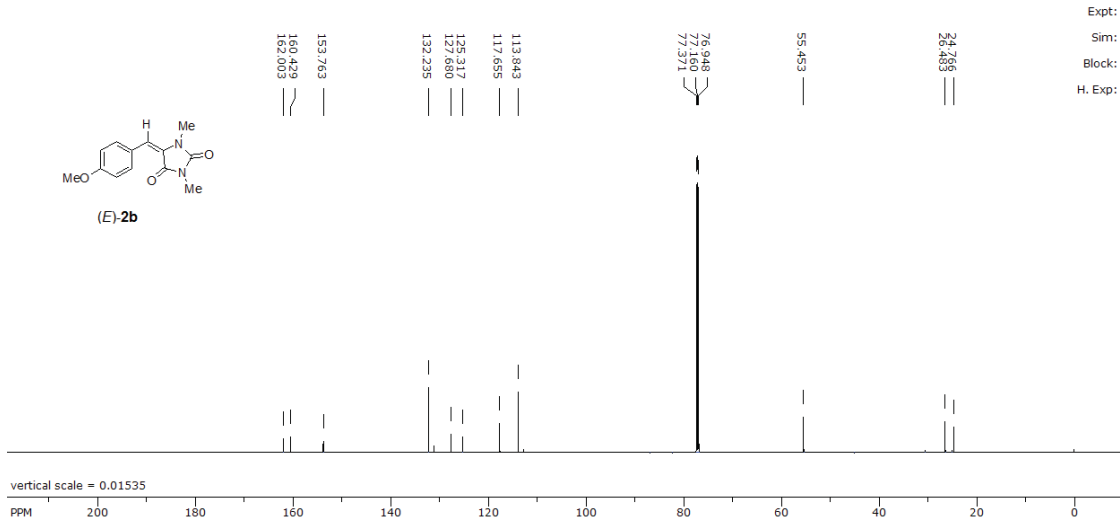
(E)-5-Benzylidene-1,3-dimethylimidazolidine-2,4-dione [(E)-2a].



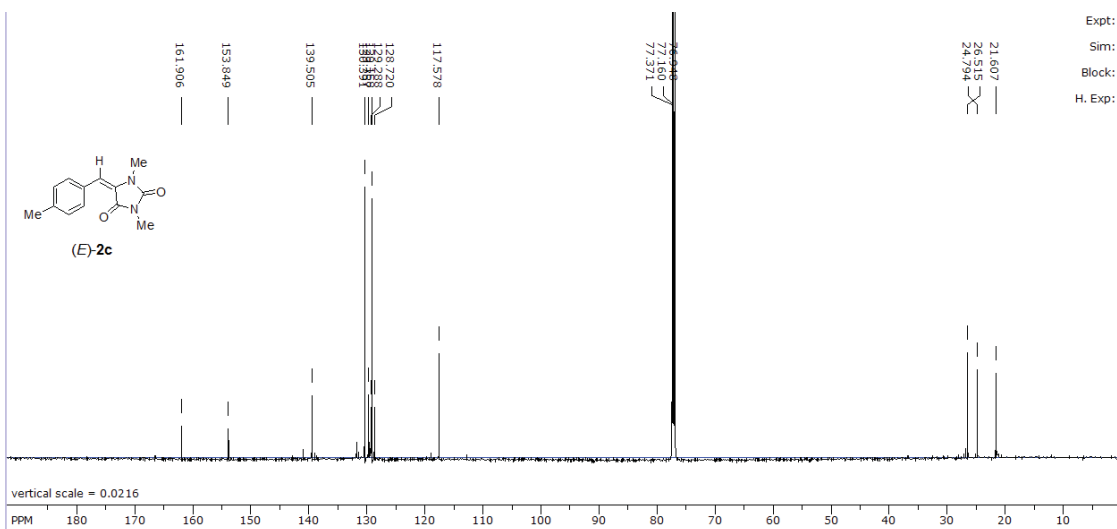
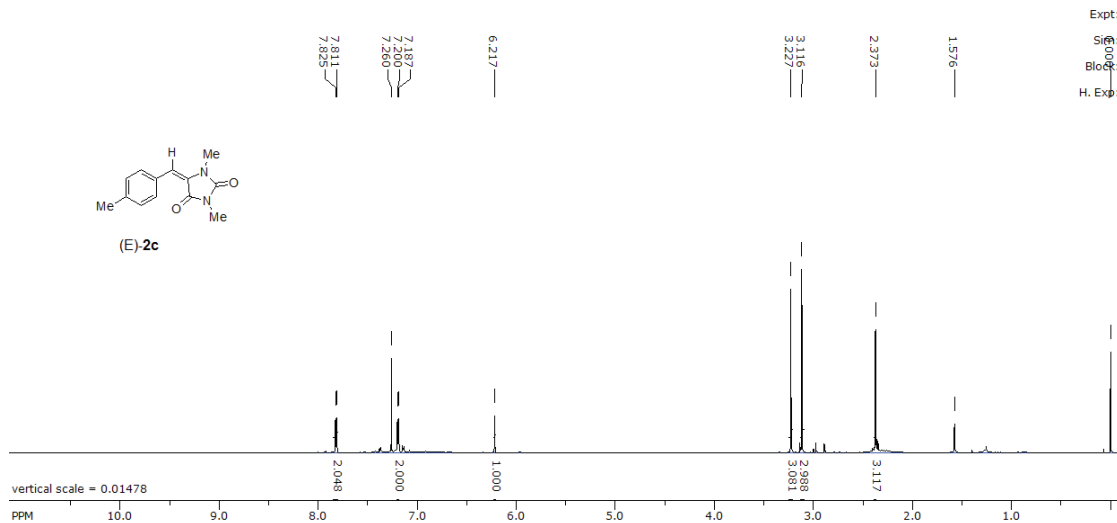


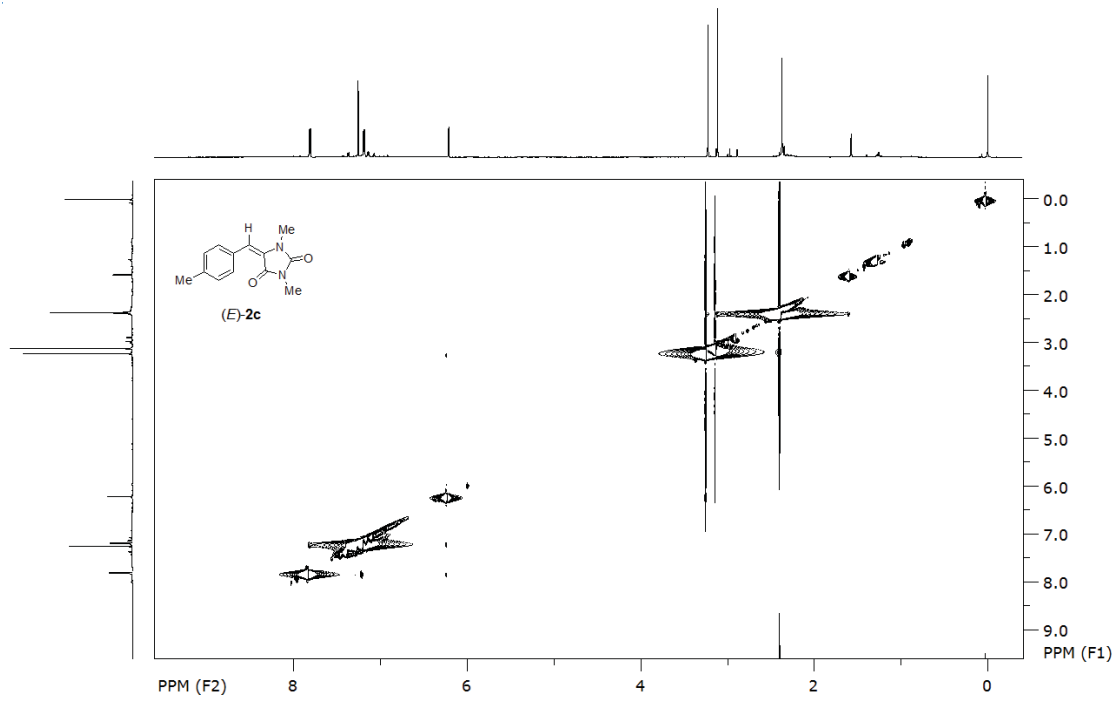
(E)-5-(4-Methoxybenzylidene)-1,3-dimethylimidazolidine-2,4-dione [(E)-2b].



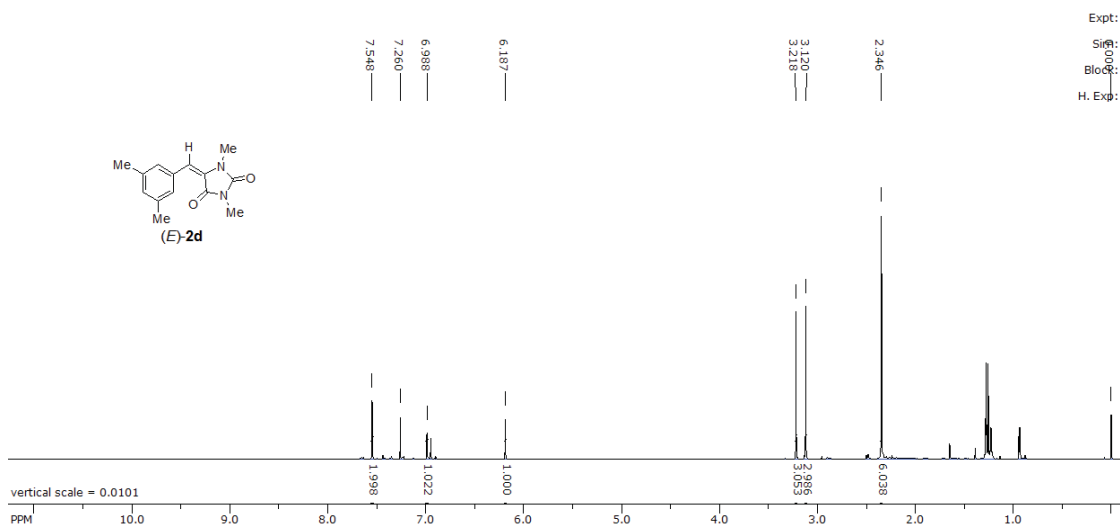


(E)-5-(4-Methylbenzylidene)-1,3-dimethylimidazolidine-2,4-dione [(E)-2c].

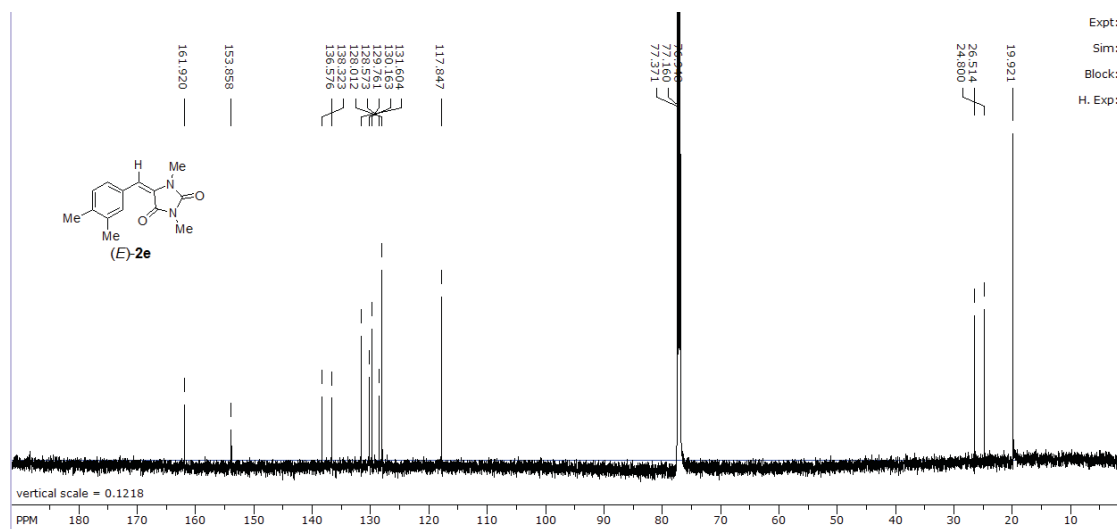
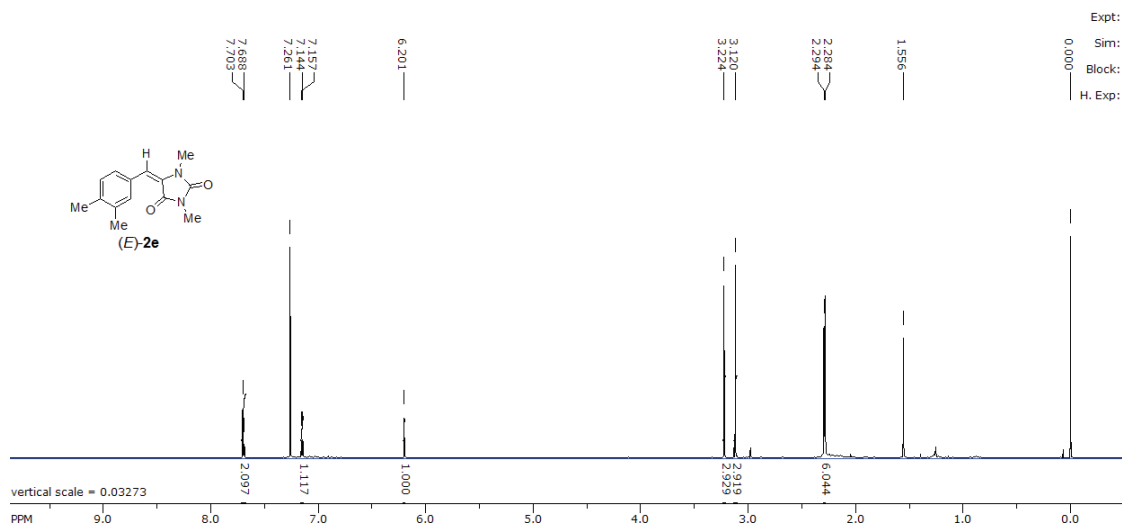


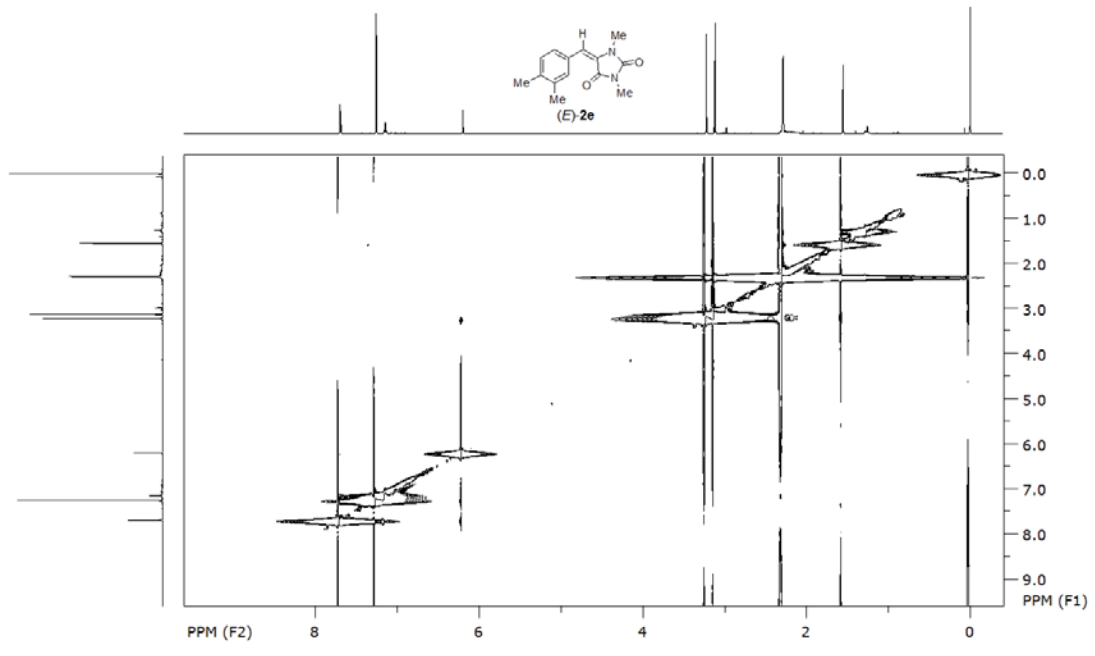


(E)-5-(3,5-Dimethylbenzylidene)-1,3-dimethylimidazolidine-2,4-dione [(E)-2d].

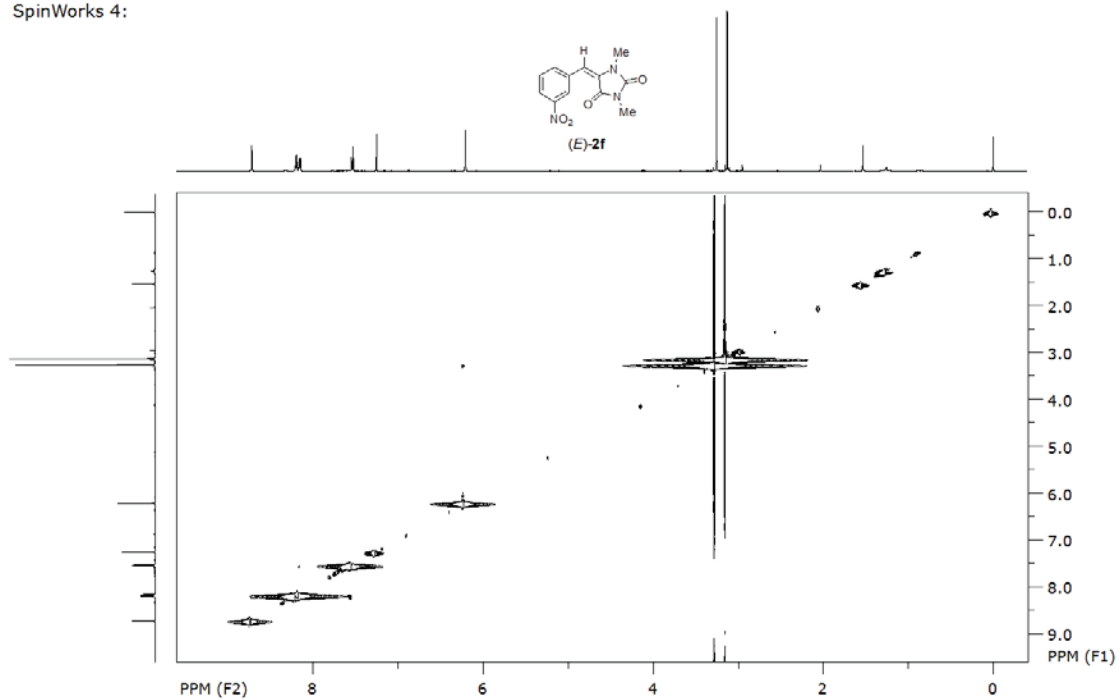


(E)-5-(3,4-Dimethylbenzylidene)-1,3-dimethylimidazolidine-2,4-dione [(E)-2e].

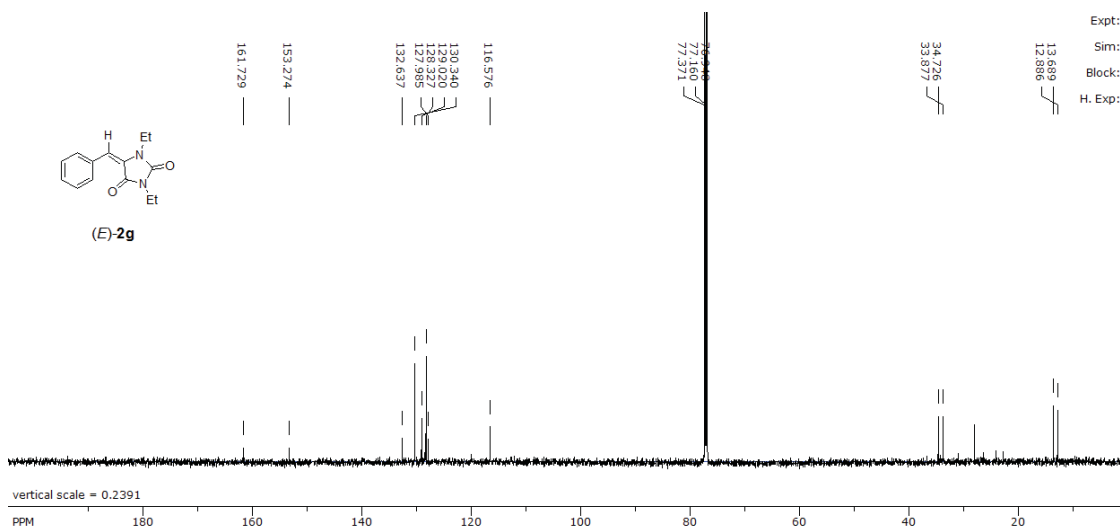
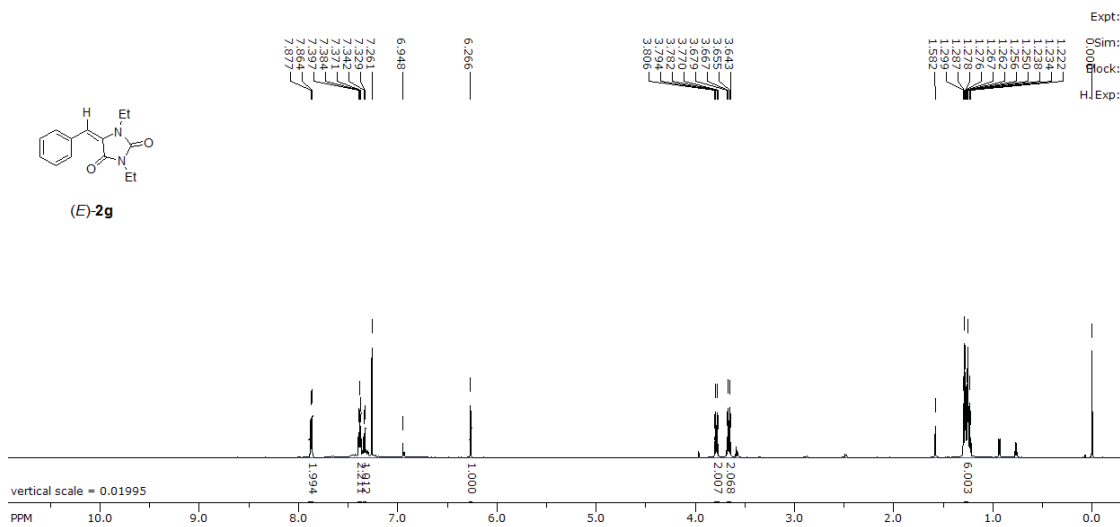


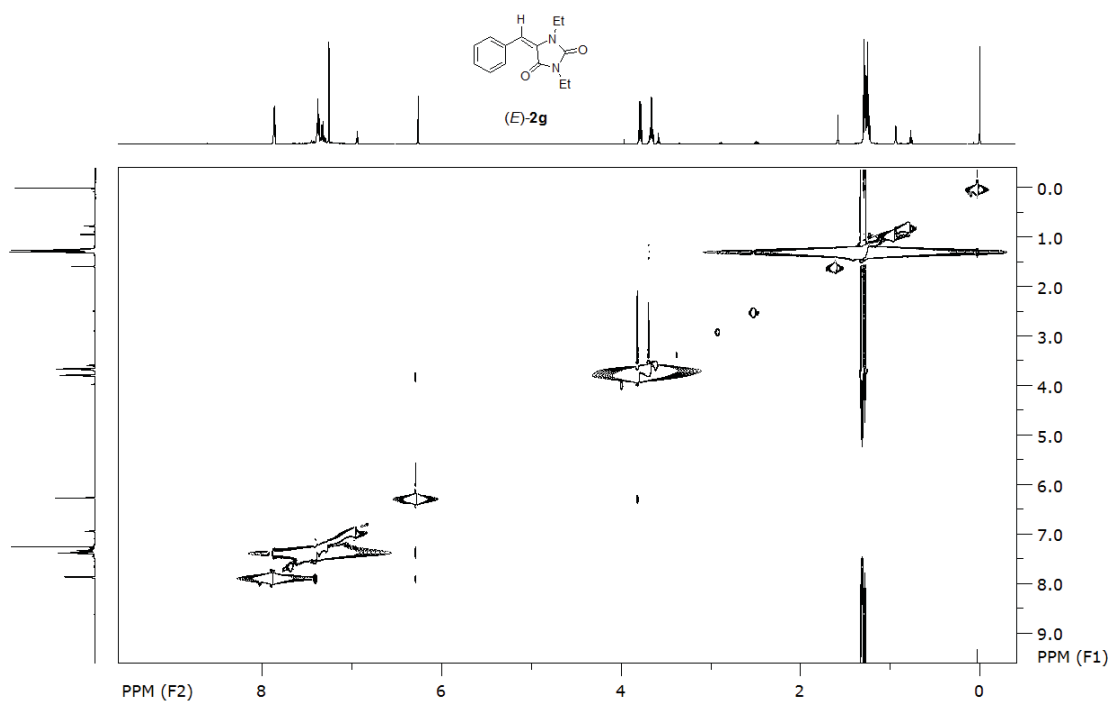


SpinWorks 4:

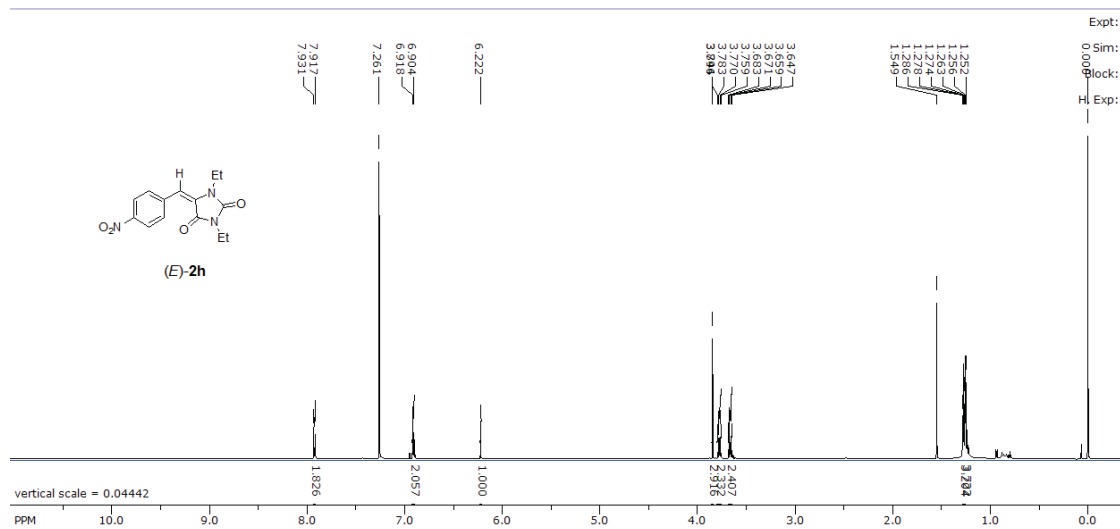
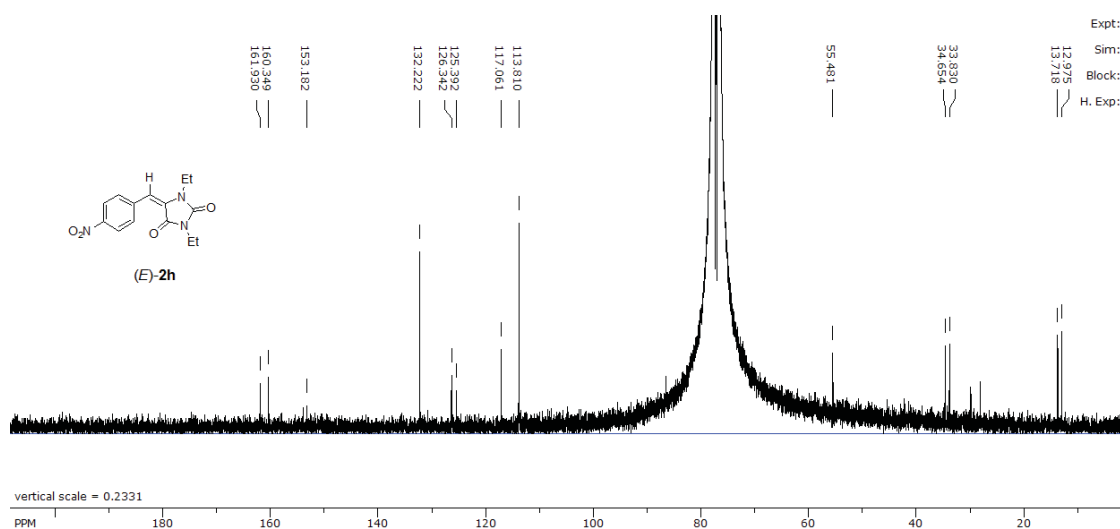


(E)-5-Benzylidene-1,3-diethylimidazolidine-2,4-dione [(E)-2g].

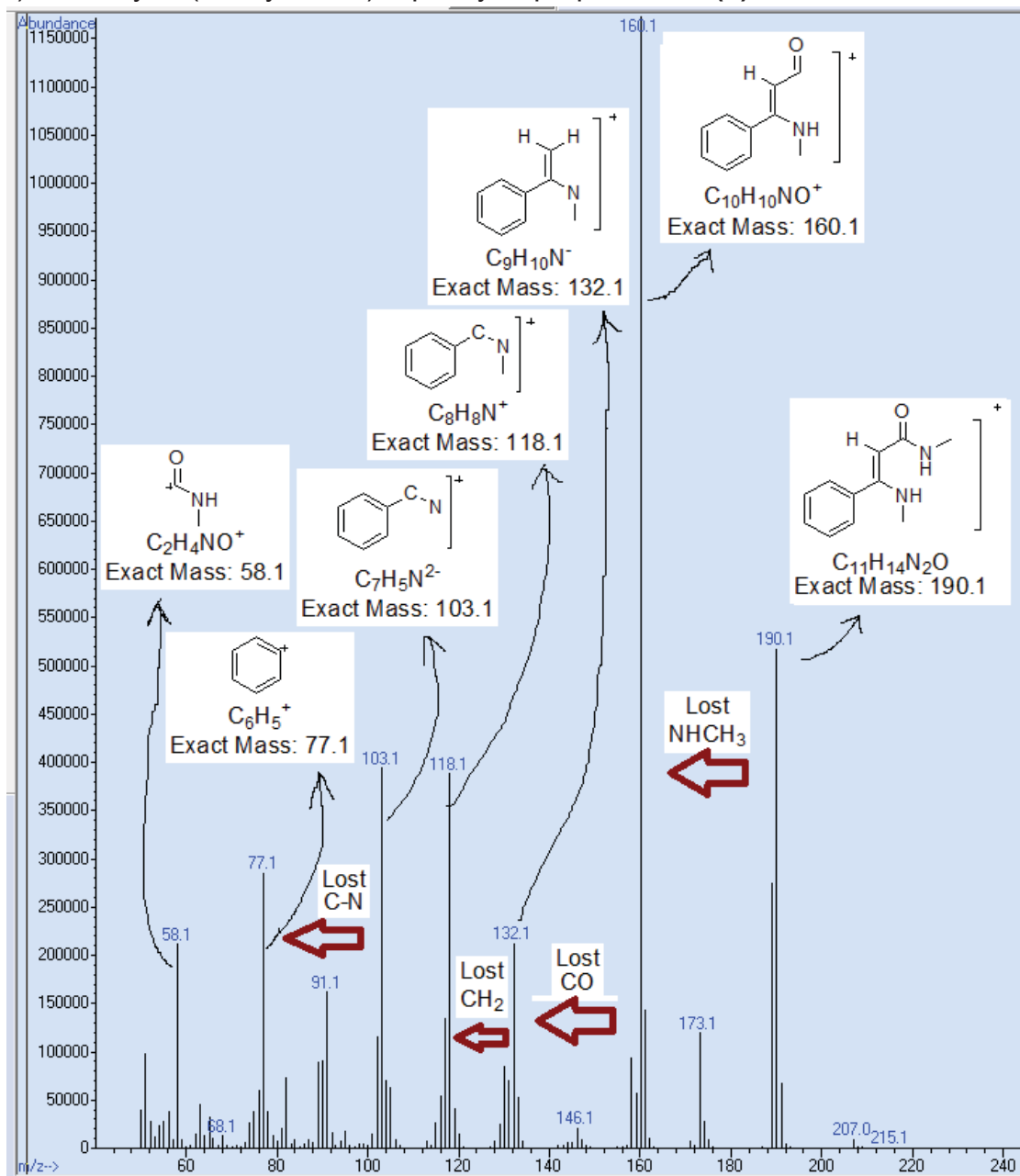




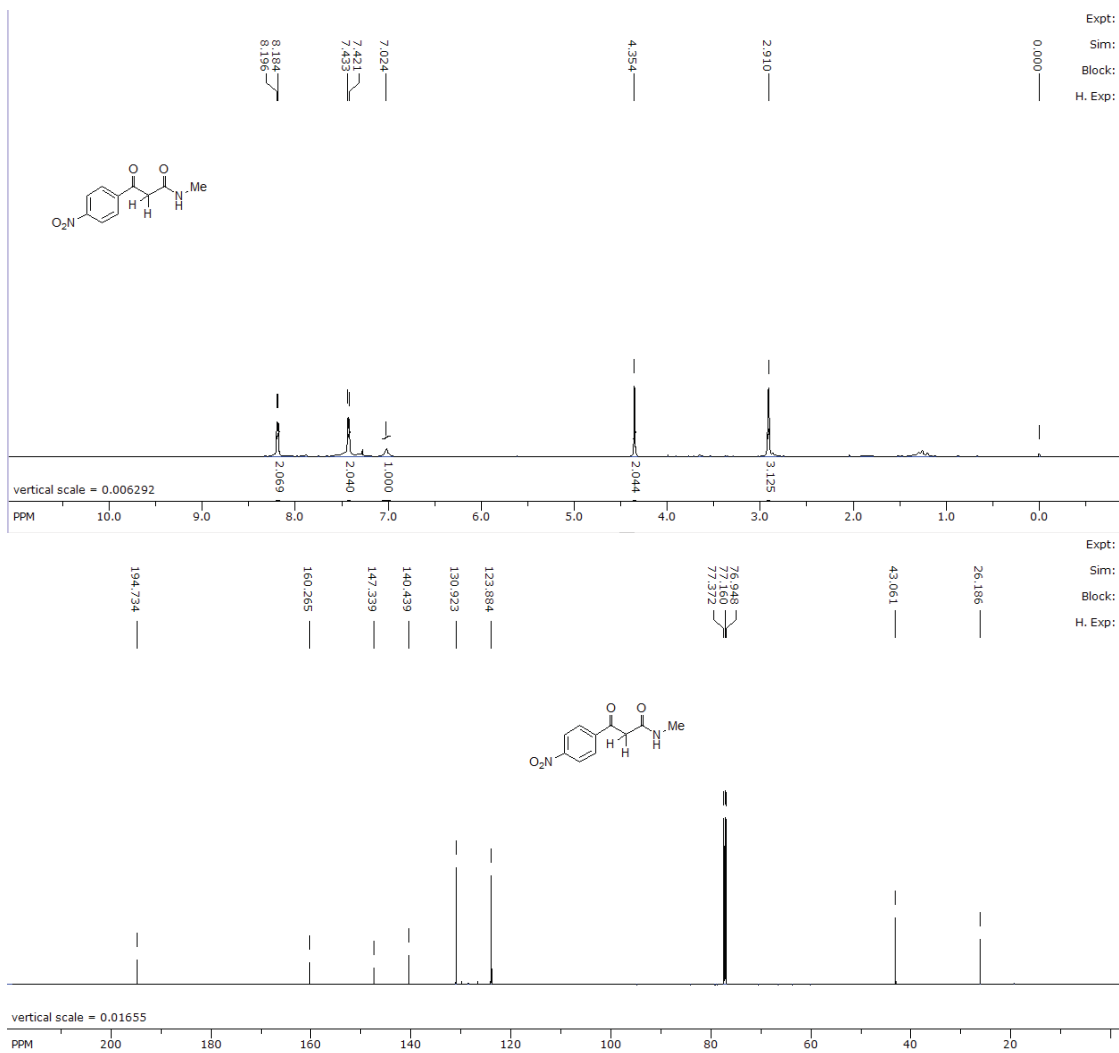
(E)-5-(4-Methoxybenzylidene)-1,3-diethylimidazolidine-2,4-dione [(E)-2h].



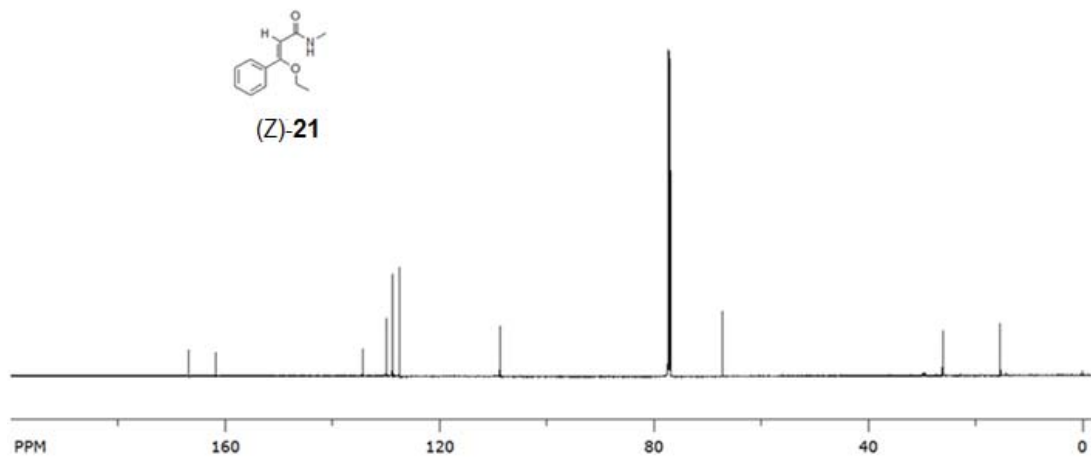
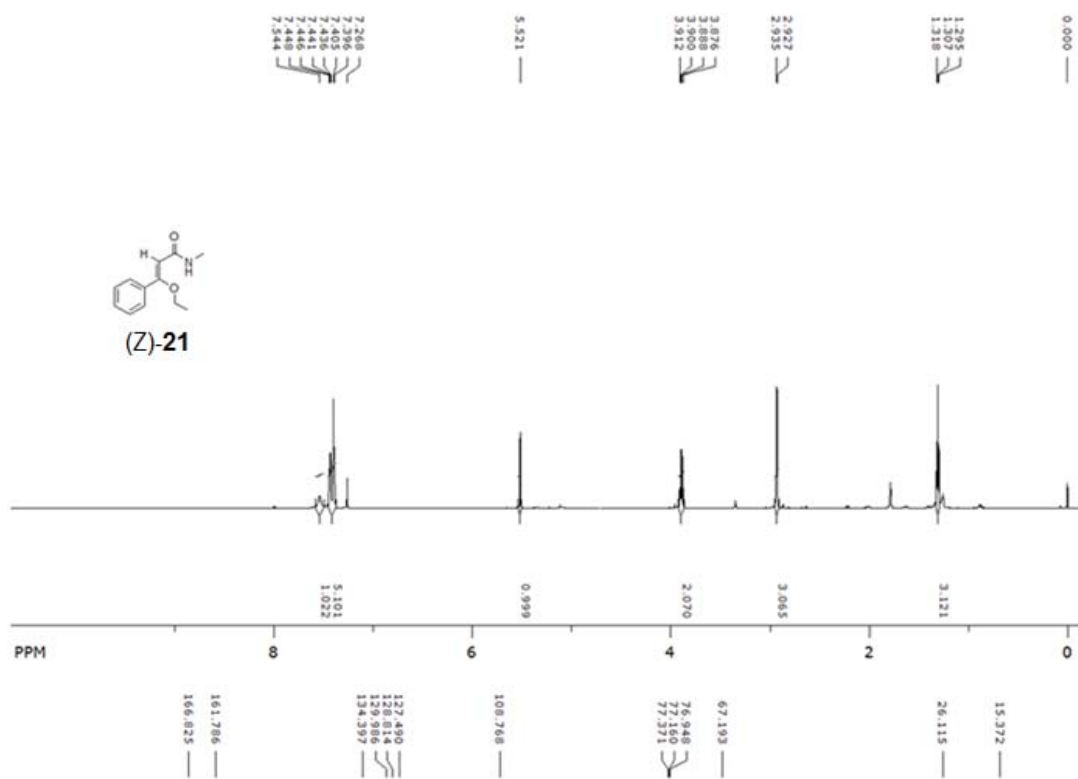
(Z)-N-methyl-3-(methylamino)-3-phenyl-2-propenamide (**6**).



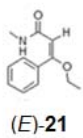
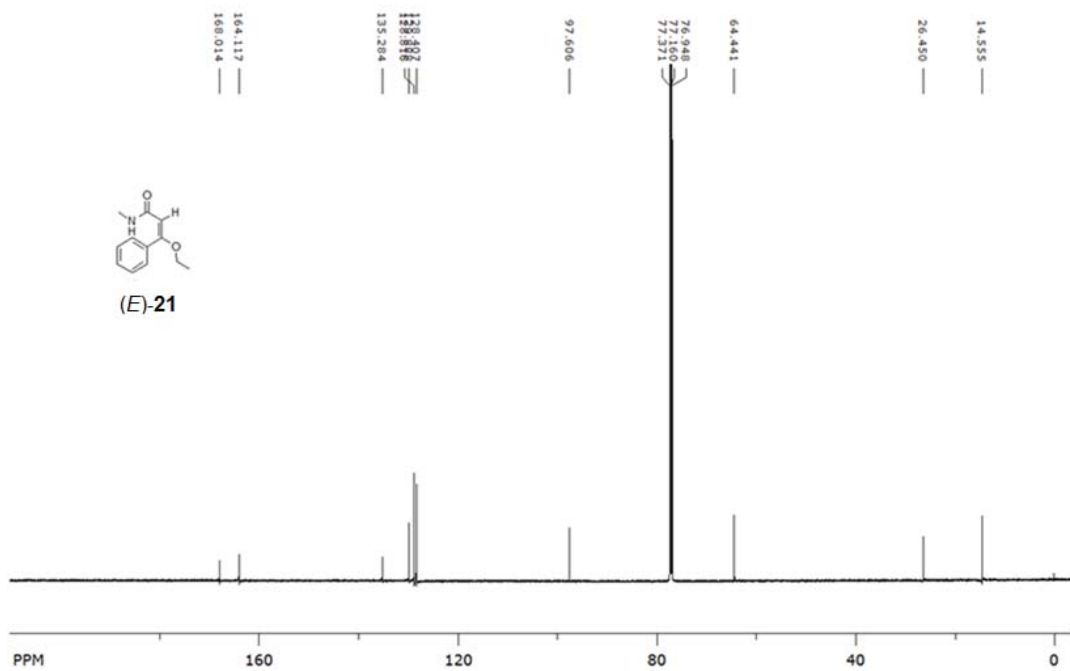
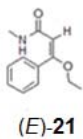
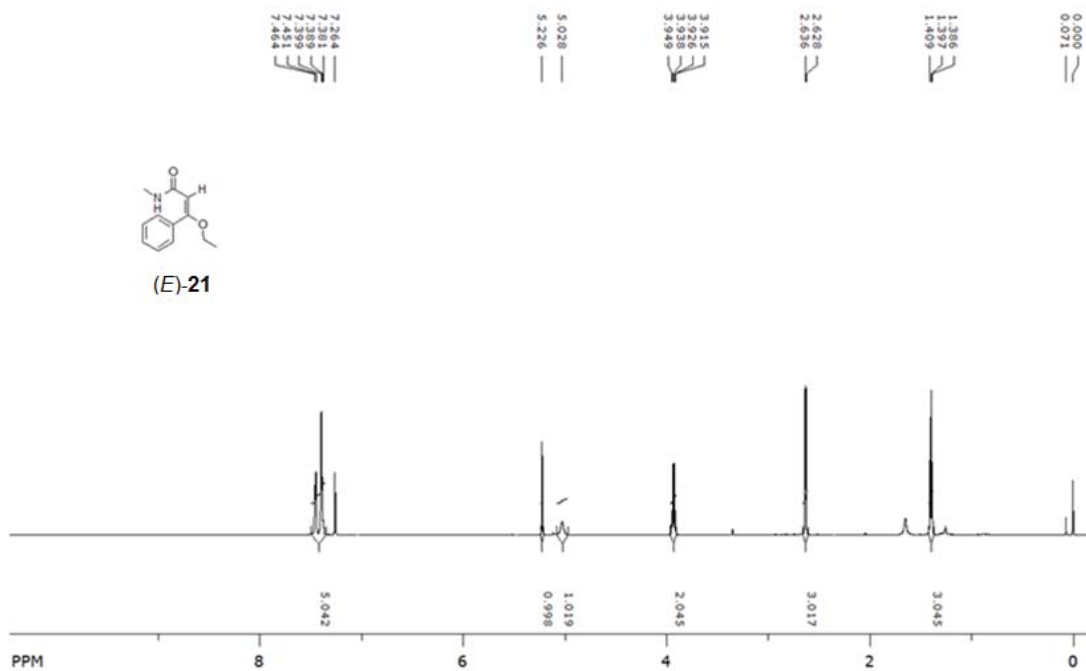
N-methyl-3-(4-nitrophenyl)-3-oxopropanamide (**7**).



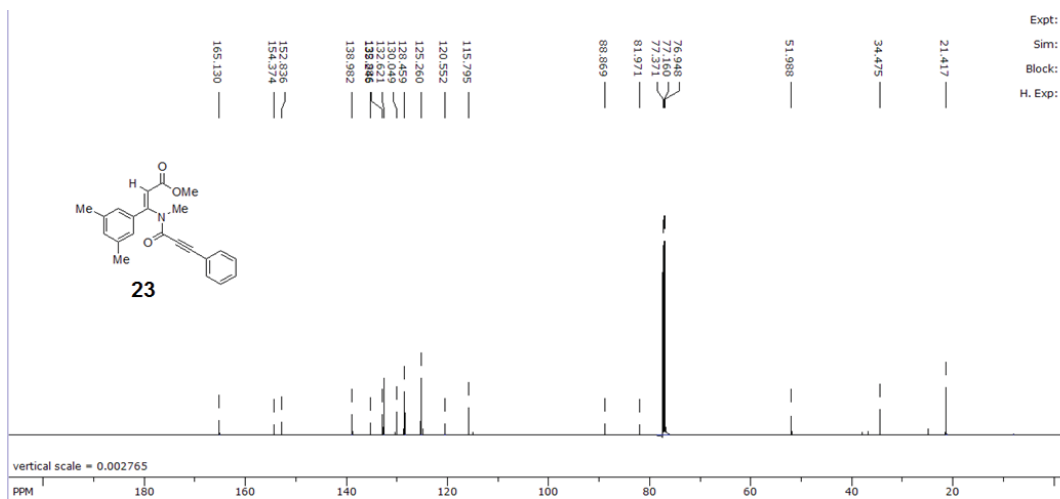
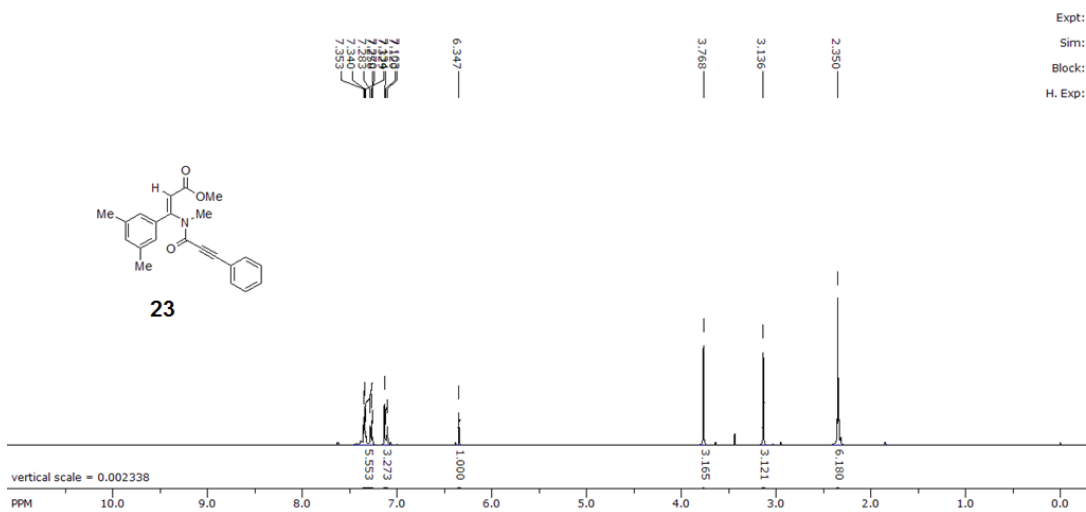
(Z)-3-Ethoxy-N-methyl-3-phenyl-2-propenamide [(Z)-21].

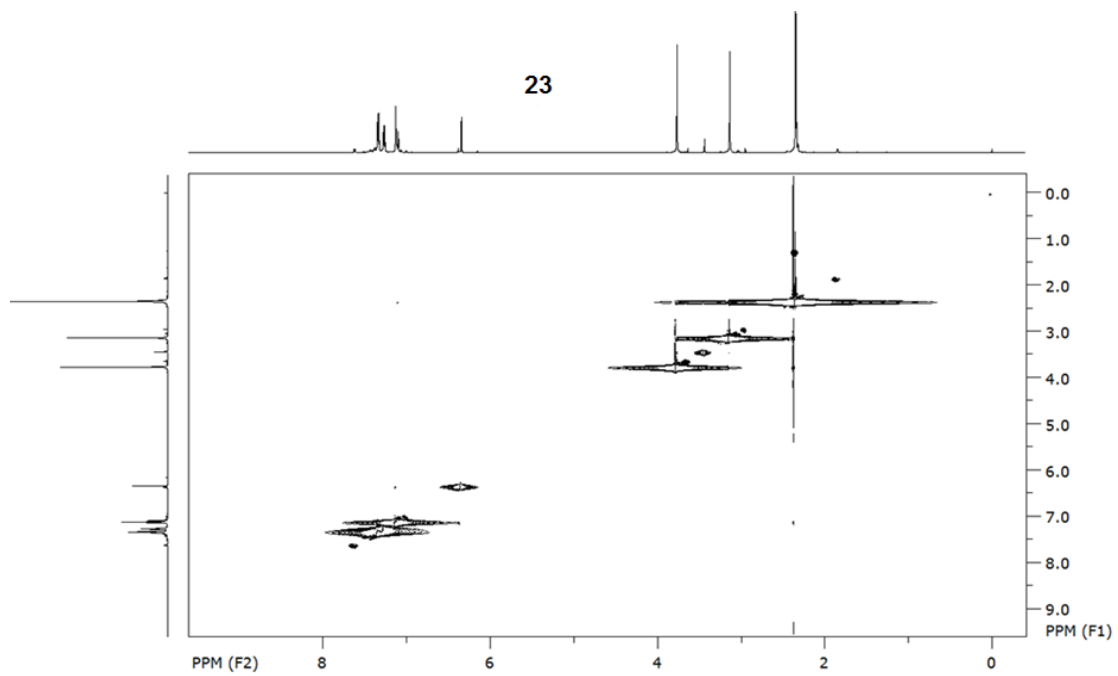


(E)-3-Ethoxy-N-methyl-3-phenyl-2-propenamide [(E)-21].



(Z)-methyl 3-(3,5-dimethylphenyl)-3-(N-methyl-3-phenyl-2-propynamido)acrylate, 23.





APPENDIX B
X-RAY CRYSTAL STRUCTURES

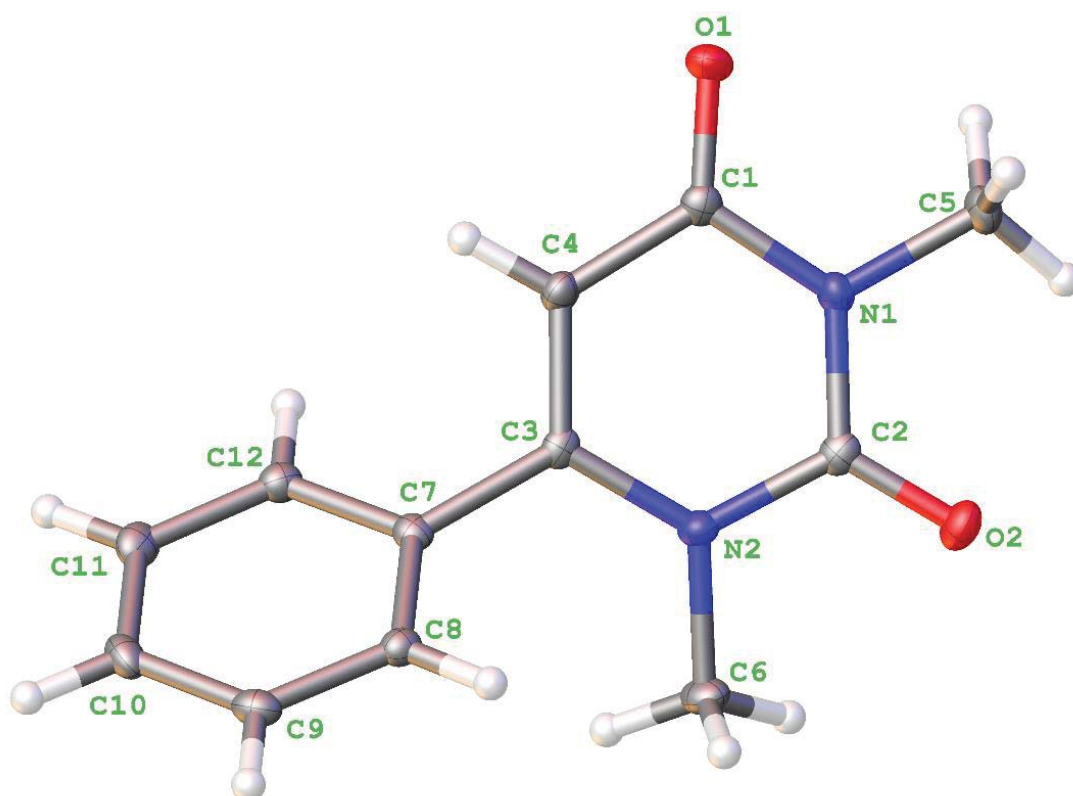


Table 1 Crystal data and structure refinement for 3a.

Identification code	MSU008D8
Empirical formula	C ₁₂ H ₁₂ N ₂ O ₂
Formula weight	216.24
Temperature/K	100.02
Crystal system	orthorhombic
Space group	Pna2 ₁
a/Å	12.1357(6)
b/Å	7.3640(4)
c/Å	11.6257(6)
α/°	90
β/°	90
γ/°	90
Volume/Å ³	1038.96(9)
Z	4
ρ _{calc} /cm ³	1.382
μ/mm ⁻¹	0.096
F(000)	456.0
Crystal size/mm ³	0.277 × 0.15 × 0.107

Radiation	MoK α ($\lambda = 0.71073$)
2 Θ range for data collection/ $^{\circ}$	6.55 to 54.304
Index ranges	$-15 \leq h \leq 15, -9 \leq k \leq 9, -14 \leq l \leq 14$
Reflections collected	30672
Independent reflections	2298 [$R_{\text{int}} = 0.0325, R_{\text{sigma}} = 0.0138$]
Data/restraints/parameters	2298/1/147
Goodness-of-fit on F^2	1.078
Final R indexes [$I \geq 2\sigma(I)$]	$R_1 = 0.0267, wR_2 = 0.0689$
Final R indexes [all data]	$R_1 = 0.0288, wR_2 = 0.0699$
Largest diff. peak/hole / $e \text{ \AA}^{-3}$	0.14/-0.19
Flack parameter	-0.1(2)

Table 2 Fractional Atomic Coordinates ($\times 10^4$) and Equivalent Isotropic Displacement Parameters ($\text{\AA}^2 \times 10^3$) for MSU008D8. U_{eq} is defined as 1/3 of of the trace of the orthogonalised U_{ij} tensor.

Atom	x	y	z	$U(\text{eq})$
O2	6224.6(10)	3282.5(16)	3125.5(10)	18.3(3)
O1	5364.4(10)	8124.4(15)	5394.5(11)	18.2(3)
N1	5769.0(11)	5750.1(19)	4217.4(12)	13.4(3)
N2	4641.5(11)	3143.7(17)	4172.8(12)	12.9(3)
C2	5594.1(13)	4005(2)	3805.1(14)	13.2(3)
C1	5117.4(13)	6603(2)	5043.2(15)	13.4(3)
C3	3985.5(13)	3878(2)	5031.3(14)	11.6(3)
C7	3099.8(13)	2769(2)	5571.7(14)	12.3(3)
C8	3302.6(13)	1000(2)	5960.0(13)	13.5(3)
C9	2515.0(14)	94(2)	6611.5(14)	15.5(3)
C12	2087.9(13)	3596(2)	5822.3(14)	14.2(3)
C4	4196.0(13)	5555(2)	5446.6(14)	13.7(3)
C10	1517.0(14)	932(2)	6866.7(14)	16.5(4)
C11	1302.5(13)	2673(2)	6464.5(15)	16.3(3)
C6	4337.7(15)	1488(2)	3532.0(15)	18.0(4)
C5	6739.6(14)	6744(2)	3799.0(15)	17.1(4)

Table 3 Anisotropic Displacement Parameters ($\text{\AA}^2 \times 10^3$) for MSU008D8. The Anisotropic displacement factor exponent takes the form: - $2\pi^2[h^2a^{*2}U_{11}+2hka^*b^*U_{12}+\dots]$.

Atom	U ₁₁	U ₂₂	U ₃₃	U ₂₃	U ₁₃	U ₁₂
O2	20.2(6)	19.6(6)	15.1(6)	-0.9(5)	5.1(5)	3.1(5)
O1	18.9(6)	12.0(5)	23.8(7)	-2.2(5)	1.8(5)	-2.4(4)
N1	13.6(6)	13.7(6)	13.0(6)	2.2(5)	1.7(5)	-0.8(5)
N2	15.4(7)	11.7(7)	11.5(7)	-1.3(5)	-0.1(6)	-0.3(5)
C2	15.3(8)	14.3(8)	9.9(8)	1.9(6)	-1.2(6)	2.9(6)
C1	13.9(7)	12.7(7)	13.7(8)	1.9(6)	-0.9(6)	2.1(6)
C3	11.0(7)	13.6(7)	10.3(7)	1.2(6)	-1.7(6)	3.2(6)
C7	12.9(7)	13.4(7)	10.6(7)	-0.5(6)	-2.1(6)	-1.2(6)
C8	13.0(7)	13.7(8)	13.9(8)	-1.9(6)	-1.3(6)	0.7(6)
C9	20.1(8)	12.1(7)	14.4(8)	0.2(6)	-3.0(6)	-2.2(6)
C12	14.1(8)	13.8(7)	14.5(8)	-0.9(7)	-2.0(6)	0.9(6)
C4	13.8(7)	13.1(7)	14.3(7)	-0.2(6)	1.7(6)	2.2(6)
C10	15.6(8)	20.4(9)	13.6(8)	-0.6(6)	0.6(6)	-6.8(6)
C11	11.4(7)	20.5(8)	17.0(8)	-3.0(7)	-2.8(6)	0.1(6)
C6	24.9(9)	14.6(8)	14.6(8)	-4.1(6)	1.4(7)	-2.9(6)
C5	16.2(8)	18.4(8)	16.6(8)	2.5(7)	4.5(6)	-2.6(6)

Table 4 Bond Lengths for MSU008D8.

Atom	Atom	Length/ \AA	Atom	Atom	Length/ \AA
O2	C2	1.222(2)	C3	C7	1.489(2)
O1	C1	1.230(2)	C3	C4	1.351(2)
N1	C2	1.388(2)	C7	C8	1.401(2)
N1	C1	1.393(2)	C7	C12	1.401(2)
N1	C5	1.469(2)	C8	C9	1.390(2)
N2	C2	1.386(2)	C9	C10	1.391(2)
N2	C3	1.386(2)	C12	C11	1.389(2)
N2	C6	1.476(2)	C10	C11	1.389(3)
C1	C4	1.437(2)			

Table 5 Bond Angles for MSU008D8.

Atom	Atom	Atom	Angle/°	Atom	Atom	Atom	Angle/°
C2	N1	C1	124.65(13)	N2	C3	C7	120.32(14)
C2	N1	C5	117.99(13)	C4	C3	N2	120.35(14)
C1	N1	C5	117.29(13)	C4	C3	C7	119.15(15)
C2	N2	C3	121.52(13)	C8	C7	C3	121.27(14)
C2	N2	C6	115.51(13)	C8	C7	C12	119.41(15)
C3	N2	C6	122.82(13)	C12	C7	C3	118.84(14)
O2	C2	N1	122.04(14)	C9	C8	C7	120.09(15)
O2	C2	N2	121.52(15)	C8	C9	C10	120.10(14)
N2	C2	N1	116.39(14)	C11	C12	C7	120.04(15)
O1	C1	N1	120.08(15)	C3	C4	C1	121.44(15)
O1	C1	C4	124.79(16)	C11	C10	C9	120.06(15)
N1	C1	C4	115.10(14)	C12	C11	C10	120.28(15)

Table 6 Torsion Angles for MSU008D8.

A	B	C	D	Angle/°	A	B	C	D	Angle/°
O1	C1 C4	C3		-178.98(15)	C7	C8	C9 C10		0.9(2)
N1	C1 C4	C3		-0.8(2)	C7	C12	C11 C10		0.4(2)
N2	C3 C7	C8		48.0(2)	C8	C7	C12 C11		0.9(2)
N2	C3 C7	C12		-139.95(16)	C8	C9	C10 C11		0.4(2)
N2	C3 C4	C1		-1.9(2)	C9	C10	C11 C12		-1.0(2)
C2	N1 C1	O1		176.74(14)	C12	C7	C8 C9		-1.5(2)
C2	N1 C1	C4		-1.5(2)	C4	C3	C7 C8		- 127.01(16)
C2	N2 C3	C7		-167.80(14)	C4	C3	C7 C12		45.0(2)
C2	N2 C3	C4		7.2(2)	C6	N2	C2 O2		-11.2(2)
C1	N1 C2	O2		-175.98(16)	C6	N2	C2 N1		166.53(13)
C1	N1 C2	N2		6.3(2)	C6	N2	C3 C7		16.9(2)
C3	N2 C2	O2		173.23(15)	C6	N2	C3 C4		- 168.08(15)
C3	N2 C2	N1		-9.1(2)	C5	N1	C2 O2		0.9(2)
C3	C7 C8	C9		170.46(15)	C5	N1	C2 N2		- 176.82(14)
C3	C7 C12	C11		-171.26(15)	C5	N1	C1 O1		-0.1(2)
C7	C3 C4	C1		173.09(14)	C5	N1	C1 C4		- 178.38(14)

Table 7 Hydrogen Atom Coordinates ($\text{\AA} \times 10^4$) and Isotropic Displacement Parameters ($\text{\AA}^2 \times 10^3$) for MSU008D8.

Atom	x	y	z	U(eq)
H8	3979	419	5778	16
H9	2658	-1100	6883	19
H12	1939	4789	5553	17
H4	3725	6053	6018	16
H10	982	314	7316	20
H11	616	3234	6629	20
H6A	4526	1642	2718	27
H6B	3544	1274	3607	27
H6C	4742	447	3845	27
H5A	7330	6671	4372	26
H5B	6544	8019	3671	26
H5C	6992	6204	3075	26

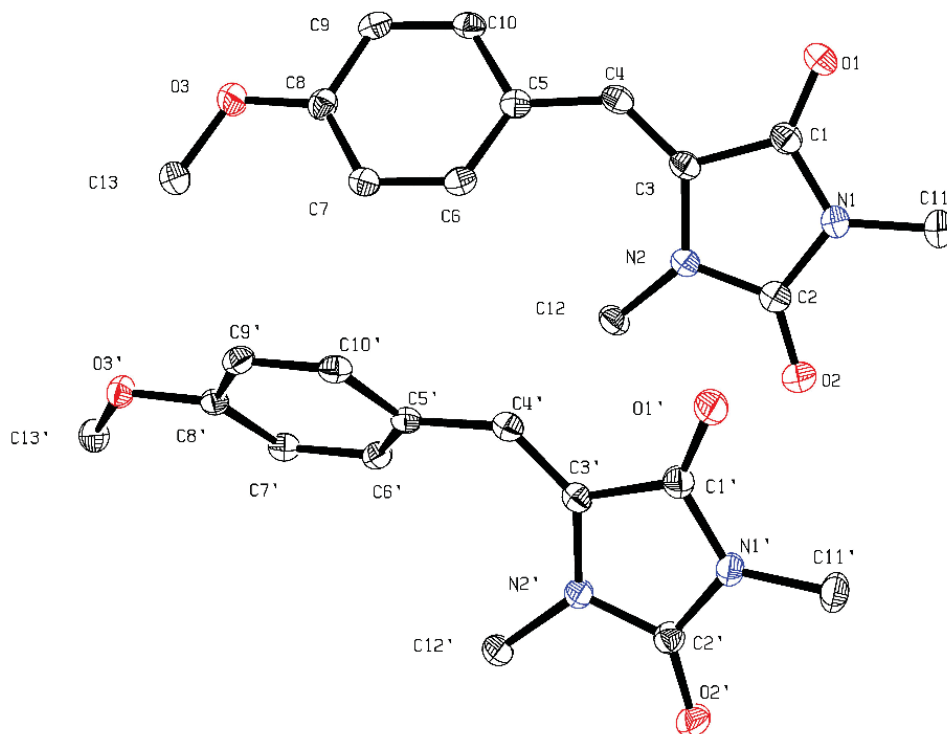


Table 1 Crystal data and structure refinement for (Z)-2b.

Identification code	MSU0012
Empirical formula	C ₂₆ H ₂₈ N ₄ O ₆
Formula weight	492.52
Temperature/K	100.0
Crystal system	monoclinic
Space group	P2 ₁ /n
a/Å	12.6530(3)
b/Å	7.2868(2)
c/Å	25.8912(7)
α/°	90
β/°	100.3798(12)
γ/°	90
Volume/Å ³	2348.10(11)
Z	4
ρ _{calc} /cm ³	1.393
μ/mm ⁻¹	0.100
F(000)	1040.0
Crystal size/mm ³	0.2 × 0.2 × 0.2
Radiation	MoKα (λ = 0.71073)
2θ range for data collection/°	3.198 to 50.932
Index ranges	-15 ≤ h ≤ 15, -8 ≤ k ≤ 8, -31 ≤ l ≤ 25

Reflections collected	27139
Independent reflections	4350 [$R_{\text{int}} = 0.0233$, $R_{\text{sigma}} = 0.0141$]
Data/restraints/parameters	4350/0/332
Goodness-of-fit on F^2	1.055
Final R indexes [$I \geq 2\sigma(I)$]	$R_1 = 0.0305$, $wR_2 = 0.0809$
Final R indexes [all data]	$R_1 = 0.0327$, $wR_2 = 0.0829$
Largest diff. peak/hole / $e \text{ \AA}^{-3}$	0.24/-0.18

Table 2 Fractional Atomic Coordinates ($\times 10^4$) and Equivalent Isotropic Displacement Parameters ($\text{\AA}^2 \times 10^3$) for MSU0012. U_{eq} is defined as 1/3 of the trace of the orthogonalised U_{ij} tensor.

Atom	x	y	z	$U(\text{eq})$
O1	1792.4(7)	8015.6(13)	-429.7(3)	26.1(2)
O2	1238.6(7)	6149.8(15)	1183.3(3)	35.0(2)
O3	8360.9(6)	6355.2(12)	962.2(3)	26.1(2)
N1	1217.8(8)	6986.3(15)	315.8(4)	23.5(2)
N2	2796.7(8)	6529.7(14)	843.8(4)	21.1(2)
C1	1975.6(9)	7446.7(16)	19.1(4)	20.3(2)
C2	1702.3(9)	6502.0(18)	822.4(5)	24.4(3)
C3	3037.6(9)	7079.2(15)	359.1(4)	18.4(2)
C4	3948.5(9)	7273.7(15)	167.0(4)	18.5(2)
C5	5077.4(9)	6909.2(15)	382.5(4)	17.5(2)
C6	5437.5(9)	5617.8(15)	772.9(4)	18.5(2)
C7	6521.5(9)	5381.9(16)	975.0(4)	19.0(2)
C8	7281.5(9)	6433.4(16)	780.2(4)	19.4(2)
C9	6949.7(9)	7652.3(16)	367.1(4)	20.7(2)
C10	5866.8(9)	7870.6(16)	172.5(4)	19.3(2)
C11	66.3(10)	7264(2)	151.9(5)	30.6(3)
C12	3504.4(9)	6479.3(17)	1356.2(4)	21.5(3)
C13	8734.4(9)	5084.1(18)	1376.0(5)	26.1(3)
O1'	1845.1(6)	1083.7(14)	739.3(3)	28.6(2)
O2'	1357.2(6)	226.7(12)	2427.8(3)	24.6(2)
O3'	8456.5(6)	1472.4(11)	2160.1(3)	18.79(18)
N1'	1300.4(7)	692.7(14)	1537.7(4)	20.8(2)
N2'	2888.1(7)	824.6(13)	2078.7(4)	17.9(2)
C1'	2036.6(9)	982.8(16)	1215.5(4)	20.2(2)
C2'	1802.3(9)	547.9(16)	2059.1(4)	18.7(2)
C3'	3103.8(9)	1107.2(15)	1573.0(4)	16.9(2)
C4'	4001.2(9)	1342.0(15)	1373.7(4)	17.9(2)
C5'	5146.8(9)	1471.2(15)	1608.4(4)	16.7(2)

C6'	5559.2(9)	2420.3(15)	2069.6(4)	17.2(2)
C7'	6659.6(9)	2456.2(15)	2267.3(4)	17.3(2)
C8'	7367.2(8)	1562.0(15)	1998.2(4)	16.0(2)
C9'	6977.7(9)	678.7(15)	1524.3(4)	17.7(2)
C10'	5887.2(9)	643.8(15)	1334.8(4)	17.6(2)
C11'	151.9(9)	375(2)	1359.1(5)	27.9(3)
C12'	3651.8(9)	481.9(17)	2561.5(4)	21.2(3)
C13'	8903.0(9)	2246.8(16)	2659.1(4)	20.6(2)

Table 3 Anisotropic Displacement Parameters ($\text{\AA}^2 \times 10^3$) for MSU0012. The Anisotropic displacement factor exponent takes the form: - $2\pi^2[h^2a^{*2}U_{11}+2hka^*b^*U_{12}+\dots]$.

Atom	U_{11}	U_{22}	U_{33}	U_{23}	U_{13}	U_{12}
O1	24.6(4)	35.1(5)	16.9(4)	3.5(4)	-0.7(3)	0.3(4)
O2	24.3(5)	56.1(6)	25.7(5)	12.7(4)	7.8(4)	2.1(4)
O3	17.9(4)	30.8(5)	29.0(5)	7.3(4)	2.7(3)	-1.7(3)
N1	17.3(5)	31.3(6)	20.9(5)	3.5(4)	0.4(4)	-0.7(4)
N2	18.7(5)	28.1(5)	15.8(5)	3.5(4)	1.6(4)	0.0(4)
C1	21.8(6)	20.2(6)	18.0(6)	-1.3(5)	1.2(4)	-0.9(4)
C2	21.7(6)	30.0(7)	21.3(6)	3.6(5)	3.4(5)	0.0(5)
C3	21.6(6)	17.7(6)	15.0(5)	0.0(4)	0.8(4)	-0.7(4)
C4	23.2(6)	17.3(6)	14.5(5)	-0.8(4)	1.6(4)	-0.5(4)
C5	20.8(6)	16.6(5)	15.1(5)	-3.8(4)	3.7(4)	-0.4(4)
C6	20.9(5)	16.6(5)	18.6(6)	-1.4(4)	5.8(4)	-2.3(4)
C7	22.4(6)	17.6(6)	17.3(5)	0.6(4)	4.3(4)	1.0(4)
C8	18.4(5)	20.8(6)	19.3(6)	-3.1(5)	4.5(4)	0.1(4)
C9	23.6(6)	19.9(6)	20.9(6)	0.3(5)	9.7(5)	-1.8(5)
C10	25.4(6)	18.3(6)	14.8(5)	0.3(4)	5.8(4)	1.2(4)
C11	18.6(6)	42.2(8)	29.5(7)	4.9(6)	0.5(5)	1.1(5)
C12	22.5(6)	25.1(6)	16.0(6)	2.0(5)	0.9(4)	2.6(5)
C13	20.3(6)	34.0(7)	23.1(6)	4.1(5)	1.4(5)	1.5(5)
O1'	20.8(4)	47.8(6)	16.5(4)	2.9(4)	1.6(3)	1.2(4)
O2'	20.6(4)	34.7(5)	19.8(4)	1.1(4)	7.3(3)	-0.7(4)
O3'	14.9(4)	22.3(4)	19.1(4)	-2.2(3)	2.7(3)	-0.2(3)
N1'	14.5(5)	29.8(6)	17.9(5)	1.2(4)	2.4(4)	0.8(4)
N2'	15.9(4)	22.7(5)	15.0(5)	0.5(4)	2.5(4)	0.1(4)
C1'	18.7(6)	23.3(6)	18.5(6)	0.6(5)	3.4(4)	2.1(4)
C2'	18.3(5)	19.4(6)	18.8(6)	-0.9(5)	4.4(4)	1.2(4)
C3'	18.5(5)	16.6(5)	15.2(5)	0.1(4)	2.1(4)	1.5(4)

C4'	19.8(6)	18.4(6)	15.3(5)	1.1(4)	2.5(4)	0.5(4)
C5'	17.8(5)	15.2(5)	17.3(5)	3.4(4)	4.1(4)	-1.1(4)
C6'	18.6(5)	15.1(5)	19.2(5)	0.6(4)	6.8(4)	0.5(4)
C7'	20.4(5)	14.9(5)	16.6(5)	-1.1(4)	3.6(4)	-2.2(4)
C8'	15.3(5)	14.3(5)	18.4(5)	3.4(4)	3.1(4)	-1.7(4)
C9'	19.2(5)	17.2(5)	18.4(5)	0.2(4)	7.7(4)	0.2(4)
C10'	20.8(5)	18.0(6)	14.3(5)	0.0(4)	3.6(4)	-2.5(4)
C11'	14.1(5)	45.4(8)	23.7(6)	0.3(6)	2.4(5)	1.5(5)
C12'	19.2(5)	28.1(6)	15.5(5)	2.2(5)	1.2(4)	0.4(5)
C13'	17.8(5)	22.1(6)	20.7(6)	-2.0(5)	0.0(4)	-1.8(4)

Table 4 Bond Lengths for MSU0012.

Atom	Atom	Length/Å	Atom	Atom	Length/Å
O1	C1	1.2160(14)	O1'	C1'	1.2151(14)
O2	C2	1.2168(15)	O2'	C2'	1.2152(14)
O3	C8	1.3633(13)	O3'	C8'	1.3680(13)
O3	C13	1.4306(15)	O3'	C13'	1.4296(13)
N1	C1	1.3740(15)	N1'	C1'	1.3741(15)
N1	C2	1.3896(15)	N1'	C2'	1.3886(14)
N1	C11	1.4564(15)	N1'	C11'	1.4619(14)
N2	C2	1.3759(15)	N2'	C2'	1.3805(14)
N2	C3	1.4023(15)	N2'	C3'	1.3998(14)
N2	C12	1.4611(14)	N2'	C12'	1.4572(14)
C1	C3	1.4920(15)	C1'	C3'	1.4961(15)
C3	C4	1.3425(16)	C3'	C4'	1.3402(16)
C4	C5	1.4612(15)	C4'	C5'	1.4703(15)
C5	C6	1.3960(16)	C5'	C6'	1.3971(16)
C5	C10	1.4070(16)	C5'	C10'	1.4080(16)
C6	C7	1.3879(16)	C6'	C7'	1.3944(15)
C7	C8	1.3932(16)	C7'	C8'	1.3916(16)
C8	C9	1.3955(16)	C8'	C9'	1.3945(15)
C9	C10	1.3812(16)	C9'	C10'	1.3789(15)

Table 5 Bond Angles for MSU0012.

Atom	Atom	Atom	Angle/ $^{\circ}$	Atom	Atom	Atom	Angle/ $^{\circ}$
C8	O3	C13	117.45(9)	C8'	O3'	C13'	118.07(8)
C1	N1	C2	110.87(9)	C1'	N1'	C2'	111.14(9)
C1	N1	C11	124.43(10)	C1'	N1'	C11'	125.19(10)
C2	N1	C11	123.94(10)	C2'	N1'	C11'	123.35(9)
C2	N2	C3	110.34(9)	C2'	N2'	C3'	110.35(9)
C2	N2	C12	118.94(9)	C2'	N2'	C12'	120.54(9)
C3	N2	C12	128.55(9)	C3'	N2'	C12'	128.07(9)
O1	C1	N1	125.84(10)	O1'	C1'	N1'	126.31(10)
O1	C1	C3	128.41(11)	O1'	C1'	C3'	128.09(10)
N1	C1	C3	105.74(9)	N1'	C1'	C3'	105.59(9)
O2	C2	N1	125.92(11)	O2'	C2'	N1'	125.66(10)
O2	C2	N2	126.38(11)	O2'	C2'	N2'	126.75(10)
N2	C2	N1	107.70(10)	N2'	C2'	N1'	107.59(9)
N2	C3	C1	105.15(9)	N2'	C3'	C1'	105.28(9)
C4	C3	N2	134.53(10)	C4'	C3'	N2'	134.46(10)
C4	C3	C1	120.30(10)	C4'	C3'	C1'	120.15(10)
C3	C4	C5	133.22(10)	C3'	C4'	C5'	133.59(10)
C6	C5	C4	124.62(10)	C6'	C5'	C4'	125.00(10)
C6	C5	C10	116.98(10)	C6'	C5'	C10'	117.52(10)
C10	C5	C4	118.37(10)	C10'	C5'	C4'	117.41(10)
C7	C6	C5	121.87(10)	C7'	C6'	C5'	121.16(10)
C6	C7	C8	119.68(10)	C8'	C7'	C6'	119.83(10)
O3	C8	C7	124.46(10)	O3'	C8'	C7'	124.92(10)
O3	C8	C9	115.83(10)	O3'	C8'	C9'	115.12(9)
C7	C8	C9	119.71(10)	C7'	C8'	C9'	119.96(10)
C10	C9	C8	119.64(10)	C10'	C9'	C8'	119.61(10)
C9	C10	C5	121.89(10)	C9'	C10'	C5'	121.80(10)

Table 6 Torsion Angles for MSU0012.

A	B	C	D	Angle/ $^{\circ}$	A	B	C	D	Angle/ $^{\circ}$
O1	C1	C3	N2	177.25(12)	O1'	C1'	C3'	N2'	-177.41(12)
O1	C1	C3	C4	-3.96(19)	O1'	C1'	C3'	C4'	-0.68(19)
O3	C8	C9	C10	-177.49(10)	O3'	C8'	C9'	C10'	178.11(9)
N1	C1	C3	N2	-3.46(12)	N1'	C1'	C3'	N2'	1.52(12)
N1	C1	C3	C4	175.34(11)	N1'	C1'	C3'	C4'	178.24(10)
N2	C3	C4	C5	3.2(2)	N2'	C3'	C4'	C5'	-2.8(2)
C1	N1	C2	O2	174.74(13)	C1'	N1'	C2'	O2'	-177.27(11)

C1 N1C2 N2	-4.07(14)	C1' N1'C2' N2'	2.43(13)
C1 C3C4 C5	-175.21(11)	C1' C3'C4' C5'	-178.32(11)
C2 N1C1 O1	-176.04(12)	C2' N1'C1' O1'	176.52(12)
C2 N1C1 C3	4.64(13)	C2' N1'C1' C3'	-2.43(13)
C2 N2C3 C1	1.11(13)	C2' N2'C3' C1'	-0.10(12)
C2 N2C3 C4	-177.44(13)	C2' N2'C3' C4'	-176.13(13)
C3 N2C2 O2	-177.14(13)	C3' N2'C2' O2'	178.34(11)
C3 N2C2 N1	1.66(14)	C3' N2'C2' N1'	-1.36(13)
C3 C4C5 C6	26.1(2)	C3' C4'C5' C6'	-40.74(19)
C3 C4C5 C10	-156.26(12)	C3' C4'C5' C10'	142.26(13)
C4 C5C6 C7	-177.62(10)	C4' C5'C6' C7'	179.38(10)
C4 C5C10C9	177.66(10)	C4' C5'C10'C9'	-179.53(10)
C5 C6C7 C8	-1.09(17)	C5' C6'C7' C8'	1.15(16)
C6 C5C10C9	-4.54(16)	C6' C5'C10'C9'	3.24(16)
C6 C7C8 O3	177.74(10)	C6' C7'C8' O3'	-178.54(10)
C6 C7C8 C9	-2.97(17)	C6' C7'C8' C9'	1.86(16)
C7 C8C9 C10	3.17(17)	C7' C8'C9' C10'	-2.25(16)
C8 C9C10C5	0.68(17)	C8' C9'C10'C5'	-0.35(16)
C10C5C6 C7	4.75(16)	C10'C5'C6' C7'	-3.62(16)
C11N1C1 O1	-5.7(2)	C11'N1'C1' O1'	2.7(2)
C11N1C1 C3	174.99(11)	C11'N1'C1' C3'	-176.21(11)
C11N1C2 O2	4.3(2)	C11'N1'C2' O2'	-3.36(19)
C11N1C2 N2	-174.47(11)	C11'N1'C2' N2'	176.34(11)
C12N2C2 O2	-12.44(19)	C12'N2'C2' O2'	9.13(18)
C12N2C2 N1	166.37(10)	C12'N2'C2' N1'	-170.57(10)
C12N2C3 C1	-161.72(11)	C12'N2'C3' C1'	168.08(11)
C12N2C3 C4	19.7(2)	C12'N2'C3' C4'	-7.9(2)
C13O3C8 C7	0.99(16)	C13'O3'C8' C7'	4.33(15)
C13O3C8 C9	-178.32(10)	C13'O3'C8' C9'	-176.05(9)

Table 7 Hydrogen Atom Coordinates ($\text{\AA}\times 10^4$) and Isotropic Displacement Parameters ($\text{\AA}^2\times 10^3$) for MSU0012.

Atom	<i>x</i>	<i>y</i>	<i>z</i>	U(eq)
H4	3836	7746	-181	22
H6	4926	4879	904	22
H7	6744	4508	1245	23
H9	7466	8328	221	25
H10	5649	8693	-111	23
H11A	-107	8561	194	46
H11B	-322	6508	369	46
H11C	-147	6912	-217	46
H12A	3105	6871	1628	32
H12B	4114	7308	1354	32
H12C	3769	5226	1430	32
H13A	8433	5410	1687	39
H13B	9520	5130	1462	39
H13C	8505	3841	1262	39
H4'	3869	1447	1002	22
H6'	5082	3052	2252	21
H7'	6925	3090	2585	21
H9'	7461	104	1333	21
H10'	5628	45	1011	21
H11D	-96	1081	1038	42
H11E	-244	765	1633	42
H11F	25	-935	1287	42
H12D	3277	-73	2822	32
H12E	3979	1644	2698	32
H12F	4213	-355	2489	32
H13D	8785	3576	2649	31
H13E	9676	1994	2739	31
H13F	8554	1701	2931	31